

NOTE TO USERS

This reproduction is the best copy available.

UMI[®]

A METHODOLOGY FOR INTEGRATED DAYLIGHTING AND THERMAL ANALYSIS OF BUILDINGS

Athanassios Tzempelikos

A Thesis in
the Department of
Building, Civil and Environmental Engineering

Presented in Partial Fulfillment of the Requirements
for the Degree of Doctor of Philosophy (Building Studies) at
Concordia University
Montreal, Quebec, Canada

July 2005

© Athanassios Tzempelikos, 2005



Library and
Archives Canada

Bibliothèque et
Archives Canada

Published Heritage
Branch

Direction du
Patrimoine de l'édition

395 Wellington Street
Ottawa ON K1A 0N4
Canada

395, rue Wellington
Ottawa ON K1A 0N4
Canada

Your file Votre référence

ISBN: 0-494-09962-3

Our file Notre référence

ISBN: 0-494-09962-3

NOTICE:

The author has granted a non-exclusive license allowing Library and Archives Canada to reproduce, publish, archive, preserve, conserve, communicate to the public by telecommunication or on the Internet, loan, distribute and sell theses worldwide, for commercial or non-commercial purposes, in microform, paper, electronic and/or any other formats.

The author retains copyright ownership and moral rights in this thesis. Neither the thesis nor substantial extracts from it may be printed or otherwise reproduced without the author's permission.

AVIS:

L'auteur a accordé une licence non exclusive permettant à la Bibliothèque et Archives Canada de reproduire, publier, archiver, sauvegarder, conserver, transmettre au public par télécommunication ou par l'Internet, prêter, distribuer et vendre des thèses partout dans le monde, à des fins commerciales ou autres, sur support microforme, papier, électronique et/ou autres formats.

L'auteur conserve la propriété du droit d'auteur et des droits moraux qui protègent cette thèse. Ni la thèse ni des extraits substantiels de celle-ci ne doivent être imprimés ou autrement reproduits sans son autorisation.

In compliance with the Canadian Privacy Act some supporting forms may have been removed from this thesis.

Conformément à la loi canadienne sur la protection de la vie privée, quelques formulaires secondaires ont été enlevés de cette thèse.

While these forms may be included in the document page count, their removal does not represent any loss of content from the thesis.

Bien que ces formulaires aient inclus dans la pagination, il n'y aura aucun contenu manquant.


Canada

ABSTRACT

During the conceptual design stage of a building, the design team often has to make critical decisions with significant impact on energy performance and indoor comfort conditions. The design and selection of fenestration systems and their control plays a key role in determining building performance, especially for perimeter spaces of commercial buildings. The domains of heating, cooling and lighting are closely related. An integrated thermal and daylighting approach is required for investigating the interactions between the different building systems. Advanced building simulation software can be used to evaluate overall building performance for specific fenestration schemes. However, these tools cannot provide information on how to select near-optimal design solutions from a large set of alternatives, since they require detailed input data which are not yet available at the early design stage. Therefore the selection of final design solutions concerning fenestration often involves many subjective factors.

In this Thesis, a general and systematic simulation-based methodology for integrated daylighting and thermal analysis of facades and perimeter spaces of commercial buildings during the early design stage is presented. Using a systems integration approach, major dynamic links between thermal and daylighting performance are identified and used as design variables in a coupled thermal and daylighting simulation program. Integrated performance-based indices, generated from the continuous interaction between daylighting and thermal simulation, are calculated as a function of key linking parameters for investigating the balance between daylighting benefits and energy performance. The variation of these measures allows extraction of critical information for selection of window-to-wall ratio, shading device properties and control

plus electric lighting control strategies. Maximization of daylight utilization, reduction in peak loads and energy demand for heating, cooling and lighting are used as criteria. The methodology is general and can be applied to any type of façade, location, orientation, glazing type and shading options. Results presented for perimeter offices in Montreal provide guidelines for selecting window-to-wall ratio for unobstructed facades, as well as recommendations for choosing shading device properties and control in conjunction with electric lighting operation.

ACKNOWLEDGMENTS

I would like to express my deepest gratitude to my supervisor, Professor Andreas K. Athienitis, for his continuous encouragement and excellent guidance throughout my graduate studies. His expertise as a researcher and his enthusiasm as a teacher were very important for me. He has an endless appetite for research and I hope to collaborate with him in the future.

I would like to thank my friend and colleague Dr. Kwang-Wook Park for his suggestions and help in scientific issues.

Special thanks to the Faculty and staff at the Centre for Building Studies and especially to Professors Radu Zmeureanu and Ted Stathopoulos for their advice and excellent teaching.

I also thank Mr. Joseph Zilka for his help in technical issues.

Financial support by ASHRAE and NRC is acknowledged with thanks.

Many thanks to the School of Graduate Studies of Concordia University for providing me with valuable scholarships, awards and assistantships during my Ph.D. studies.

I would like to thank all my friends in Montreal and of course my family for their love and psychological support.

Finally, words cannot describe how grateful I am to Panagiota. She stood by me and helped me overcome many difficulties during the last years. She will always be in my heart.

TABLE OF CONTENTS

LIST OF FIGURES.....	xi
LIST OF TABLES.....	xvii
NOMENCLATURE.....	xviii
1. INTRODUCTION.....	1
1.1. Background.....	1
1.2. Motivation.....	2
1.3. Objectives and scope.....	3
1.4. Thesis overview.....	6
2. BACKGROUND AND LITERATURE REVIEW.....	8
2.1. Assessment of building performance	8
2.2. Simulation types and the need for integration.....	9
2.3. Early stage design.....	12
2.4. Daylight.....	14
2.4.1. Why daylighting?.....	14
2.4.2. Daylight assessment.....	17
2.4.3. Methodology for daylighting design.....	19
2.4.4. Advanced methods for processing luminous flux in interior spaces.....	23
2.4.5. Lighting and daylighting software tools.....	27
2.5. Fenestration systems.....	29
2.5.1. Problems associated with daylighting.....	29
2.5.2. Fenestration: the key component.....	29
2.5.3. Advanced glazings.....	30

2.5.4. Daylighting systems.....	32
2.6. Shading devices.....	32
2.6.1. Thermal and daylighting performance of fenestration systems.....	36
2.6.1.1. Venetian blinds.....	37
2.6.1.2. Roller shades.....	45
2.6.2. Airflow windows and double skin facades.....	48
2.7. Integrated daylighting and thermal analysis for commercial buildings.....	49
2.7.1. Coupling daylighting and thermal simulation.....	49
2.7.2. Limitations and problems with existing tools.....	52
2.7.3. Research needs and aim of Thesis.....	54
3. DEVELOPMENT OF AN INTEGRATED THERMAL AND DAYLIGHTING DESIGN METHODOLOGY.....	57
3.1. Simulation in the early design stage.....	57
3.2. Theoretical basis for an integrated thermal and daylighting methodology during the early design stage.....	58
3.2.1. Integrated performance indices.....	61
3.3. The daylighting simulation module.....	65
3.3.1. Incident daylight on a façade.....	65
3.3.2. Calculation of transmitted daylight in a room.....	68
3.3.3. Illuminance distribution on the work plane.....	70
3.3.4. Calculation of Daylight Availability Ratio.....	71
3.4. The thermal simulation module.....	71

3.5. Dynamic links as design parameters in the integrated daylighting and thermal design methodology.....	76
3.5.1. Glazing type and properties.....	76
3.5.2. Window-to-wall ratio.....	77
3.5.3. Shading device type.....	84
3.5.4. Shading device optical and thermal properties.....	84
3.5.5. Shading device control.....	86
3.6. The three-section façade concept as a design solution.....	91
3.7. Comparison of design options on a relative basis.....	93
3.8. Utilization of innovative systems and selection of degree of modeling detail for design analysis purpose.....	96
4. ANALYSIS OF RESULTS AND DISCUSSION.....	100
4.1. Simulation environment.....	100
4.2. Importing weather data and use for simulation.....	101
4.2.1. Calculation of incident solar radiation on a tilted surface.....	105
4.2.2. Calculation of incident illuminance on a tilted surface.....	106
4.3. Selection of window-to-wall ratio (WWR).....	108
4.4. Selection of shading properties and control - exterior roller shade as an example.....	123
4.5. Results for Venetian blinds.....	140
4.6. A case study - application of the three-section façade concept.....	146
4.6.1. Window-to-wall ratio and glazing type.....	148
4.6.2. Analysis for perimeter private offices.....	149

4.7. Comparison of the integrated simulation results.....	165
4.7.1. Daylight Availability Ratio and lighting energy demand.....	165
4.7.2. Heating and cooling load.....	169
5. CONCLUSION.....	171
5.1. Concluding remarks.....	171
5.2. Research contributions.....	174
5.3. Possible extensions and recommendations for future work.....	175
REFERENCES.....	178
APPENDIX A: Calculation of solar geometry, surface geometry and solar incidence angle (MathCad 2001i file).....	197
APPENDIX B: Calculation of incident beam, sky diffuse and ground-reflected irradiance on a tilted surface using Perez et al. (1990) model (MathCad 2001i file).....	199
APPENDIX C: Perez et al. (1990) luminous efficacy model for calculation of horizontal beam and diffuse illuminance from horizontal irradiance data. Calculation of hourly illuminance values on a tilted surface, using Perez et al. (1990) tilted surface model (MathCad 2001i file).....	202
APPENDIX D: Calculation of window optical properties as a function of solar time for effective use in simulation models (MathCad 20001i file).....	207
APPENDIX E: Detailed analytical calculation of view (form) factors between all interior surfaces in a rectangular room with one window (MathCad 2001i file).....	208

APPENDIX F: Detailed analytical calculation of configuration factors between representative points on the work plane surface in a rectangular room with one window (MathCad 2001i file).....	216
APPENDIX G: Calculation of hourly work plane illuminance using the radiosity method (MathCad 2001i file).....	220
APPENDIX H: Calculation of Daylight Availability Ratio (MathCad 2001i file).....	222
APPENDIX I: Coupled thermal simulation using a thermal network approach and solution using an explicit finite difference method (MathCad 2001i file).....	228
APPENDIX J: The TRNSYS 15 input and listing files (in IISiBat interface) for processing solar radiation data imported from Energy Plus TMY “epw” files.....	248
APPENDIX K: The Lightswitch software output file (used for validation).....	254
APPENDIX L: ESP-r output graphs and input file description (used for validation).....	263

LIST OF FIGURES

Figure 2.1. Energy consumption breakdown for commercial buildings in Colorado.....	15
Figure 2.2. Methods designers use for lighting and daylighting design.....	19
Figure 2.3. Surfaces and angles considered for calculation of view factors, with discretization into small rectangle areas.....	24
Figure 2.4. Examples of exterior venetian blinds and roller shades.....	34
Figure 2.5. Between-glazing and exterior venetian blinds.....	37
Figure 2.6. Discretization of venetian blinds in ISO 15099.....	38
Figure 2.7. BTDF parameters for a venetian blind system.....	42
Figure 2.8. Glazing system with two glass layers and an interior shading layer showing variables used in heat balance equations.....	47
Figure 2.9. Example of existing airflow window and schematic.....	49
Figure 3.1. Schematic showing distinction and relation between direct and secondary links in the coupling process.....	60
Figure 3.2. Process of coupled daylighting and thermal simulation and the interaction with dynamic links.....	62
Figure 3.3. Glazing system consisting of N glass layers.....	68
Figure 3.4. Calculation of integrated performance indices considering window-to-wall ratio as a design variable.....	79
Figure 3.5. Expected variation of performance indices as a function of a direct link (window-to-wall ratio), which is considered a design parameter (theoretical graph).....	80

Figure 3.6. Simulation flowchart that summarizes the integrated design analysis. The interactions between daylighting and thermal performance are described using shading properties and control links as design variables.....	88
Figure 3.7. Expected variation of integrated performance measures as a function of direct shading links which are considered design variables. Selection of shading properties and control for each orientation can be determined based on the information shown.....	90
Figure 3.8. Schematic of three-section façade.....	92
Figure 3.9. Interior, between-glazing and interior roller shade configurations.....	95
Figure 3.10. Interior, between-glazing and interior venetian blind configurations.....	95
Figure 4.1. Preparation of hourly weather data for use in simulation.....	103
Figure 4.2. Hourly beam horizontal irradiance for Montreal.....	103
Figure 4.3. Hourly diffuse horizontal irradiance for Montreal.....	104
Figure 4.4. Direct normal irradiance for Montreal.....	104
Figure 4.5. Hourly dry-bulb temperature for Montreal.....	105
Figure 4.6. Illuminance distribution on the work plane for three different window-to-wall ratios (south façade, June 30 th , 2pm).....	110
Figure 4.7. DAR as a function of window-to-wall ratio for each orientation in Montreal.....	112
Figure 4.8. The impact of window-to-wall ratio on annual electricity demand for lighting for different orientations. No control refers to the passive lighting control.....	115
Figure 4.9. Correlation between two performance indices for a south-facing perimeter space of the base case, assuming active on/off electric lighting control.....	116
Figure 4.10. Thermal network used for the base case.	117

Figure 4.11. Integrated performance indices as a function of WWR for a south-facing perimeter space of the base case, assuming active on/off electric lighting control.....	119
Figure 4.12. Impact of electric lighting control on monthly lighting energy demand....	120
Figure 4.13. Impact of electric lighting control on monthly cooling energy demand.....	121
Figure 4.14. Impact of electric lighting control on monthly heating energy demand....	121
Figure 4.15. The overall impact of electric lighting control on annual energy demand..	122
Figure 4.16. Comparison of monthly energy demand for heating, cooling and lighting for the selected case (30% WWR, south-facing, active on/off electric lighting control).....	123
Figure 4.17. Example of roller shade transmittance schedule for modelling shading control (five successive days in February).....	124
Figure 4.18. Annual DAR as a function of exterior shade transmittance for the two different shading control options.....	127
Figure 4.19. Impact of shading transmittance and control on lighting energy demand..	129
Figure 4.20. Hourly internal gains from electric lights during working hours assuming active automatic shading and lighting control.....	130
Figure 4.21. Integrated thermal and lighting performance indices as a function of shade transmittance, assuming active automatic shading and lighting control.....	131
Figure 4.22. The sum of annual cooling and lighting energy demand –a key integrated performance measure- as a function of roller shade transmittance. The curve reaches a minimum for 20% transmittance.....	133
Figure 4.23. Integrated thermal and lighting performance indices (energy consumption) as a function of shade transmittance, assuming active automatic shading and lighting control.....	134

Figure 4.24. The sum of annual cooling and lighting energy consumption –another key integrated performance measure- as a function of roller shade transmittance.....	135
Figure 4.25. Correlations between daylighting, electric lighting and thermal performance indices taking into account the impact of automatic shading and lighting control.....	136
Figure 4.26. Correlation between cooling and lighting energy demand taking into account the impact of automatic shading and lighting control. The respective roller shade transmittance values are shown.....	137
Figure 4.27. Overall annual energy demand considering an exterior roller shade with 20% transmittance and active automatic lighting and shading control.....	137
Figure 4.28. Annual energy consumption breakdown considering an exterior roller shade with 20% transmittance and active automatic lighting and shading control.....	138
Figure 4.29. Comparison between annual heating, cooling, lighting and total energy demand for the base case with passive and active lighting control and the studied roller shade case with selected transmittance and control.....	139
Figure 4.30. Outside south view of the test room with integral Venetian blinds (Unicel window) and schematic of the window system.....	141
Figure 4.31. Visible transmittance of the window-blind system as a function of blind tilt angle for different solar incidence angles. 90^0 is the horizontal blind position.....	141
Figure 4.32. Daily variation of optimum venetian blind tilt angles for representative months 90^0 is the horizontal blind position.....	142
Figure 4.33. Comparison of daily illuminance on a point of work plane surface 4 m from the façade, modelled with motorized blind control and a static blind at 45^0 tilt angle....	143

Figure 4.34. Thermal resistance (centre-of-glass) of the Unice blind-window system as a function of blind tilt angle. 90° is the horizontal blind position, 180° means blind is fully closed.....	143
Figure 4.35. Comparison of average daily cooling energy demand for automated blind control and static blind (passive control) for each month	145
Figure 4.36. Monthly peak thermal loads for a controlled venetian blind.....	146
Figure 4.37. Guy Street facade (SW) of new Engineering building (note the repeating floors with three sections each – spandrel, middle viewing section and upper fritted glass section).....	147
Figure 4.38. Two options of three-section multifunctional facade design considered for private offices.....	151
Figure 4.39. Work plane illuminance on four points for a SW perimeter office during a clear day in winter.....	154
Figure 4.40. Work plane illuminance on four points for a SW perimeter office during a clear day in summer.....	155
Figure 4.41. Available daylight incident on the back window to illuminate adjacent corridors for a clear day of each month at noon. The top part of the three-section facade was simulated as venetian blinds and as a translucent glazing for comparison.....	157
Fig. 4.42. Illuminance distribution in a 4-m wide corridor, adjacent to a SW-facing perimeter office (July 15 th , noon). Natural daylight is transmitted through a window on the top part of the back wall and provides non-perimeter spaces with daylight. A venetian blind as a top part of a three-section facade is a good solution.....	158

Figure 4.43. Average daily lighting energy demand in a SW perimeter office for different lighting control options, taking into account the impact of shading.....	160
Figure 4.44. Peak thermal loads for different shading and lighting control schemes as a function of glazing thermal resistance for a typical floor.....	161
Figure 4.45. Cooling load shape for different lighting and shading control design schemes during a hot clear summer day for a perimeter office on the southwest façade of the building.....	162
Figure 4.46. Annual heating and cooling energy demand for different shading and lighting control schemes as a function of glazing thermal resistance for a typical floor.....	163
Figure 4.47. Distribution of potential energy savings due to reduction in electricity demand for lighting in the building.....	164
Figure 4.48. Comparison of Daylighting Availability Ratio results between Lightswitch and the current daylighting simulation model.....	167
Figure 4.49. Comparison of annual lighting energy demand for the base case assuming passive lighting control. Results are the same for each orientation.....	168
Figure 4.50. Comparison of annual lighting energy demand assuming active lighting control (continuous dimming in Lightswitch and on/off control in the simulation model). Occupancy schedules in Lightswitch are slightly different.....	168
Figure 4.51. Comparison of peak heating and cooling load between ESP-r and thermal simulation results.....	170

LIST OF TABLES

Table 2.1. Overview and comparison of advanced lighting/daylighting software packages.....	28
Table 3.1. Examples of properties that can be used as design variables.	91
Table 4.1. Monthly and annual DAR for each major orientation in Montreal for different window-to-wall ratios.....	111
Table 4.2. Heating and cooling load as a function of WWR for each orientation.....	118
Table 4.3. MRA and RTA results for different WWR and glazing types.....	147
Table 4.4. General evaluation of different shading options for private offices.....	150
Table 4.5. Description of points on work plane surface used in Figures 4.36-4.37.....	151
Table 4.6. Potential annual energy savings from electric lighting control (kWh).....	157

NOMENCLATURE

A	area (m^2)
ab	direct luminous efficacy coefficient (m^2lx/W)
ach	air changes per hour
ad	diffuse luminous efficacy coefficient (m^2lx/W)
Alt	altitude (m)
a_p	horizon brightness coefficient
bb	direct luminous efficacy coefficient (m^2lx/W)
bd	diffuse luminous efficacy coefficient (m^2lx/W)
b_p	horizon brightness coefficient
BRDF	bi-directional reflectance distribution function
BTDF	bi-directional transmittance distribution function
C	thermal capacitance (J)
c	optical atmospheric extinction coefficient
C_1, C_2	correction coefficients for frame effects
C_A	configuration factor for point a
cb	direct luminous efficacy coefficient (m^2lx/W)
cd	diffuse luminous efficacy coefficient (m^2lx/W)
c_p	specific heat (J/kg^0C)
D	transmitted daylight (lx)
DAR	daylight availability ratio
db	direct luminous efficacy coefficient (m^2lx/W)

dd	diffuse luminous efficacy coefficient ($\text{m}^2\text{lx/W}$)
dt	selected time step (s)
E	Illuminance (lx)
E_b	incident beam illuminance (lx)
E_{bh}	beam horizontal illuminance (lx)
E_{bn}	direct normal illuminance (lx)
E_d	total diffuse incident illuminance (lx)
E_{dh}	diffuse horizontal illuminance (lx)
E_{gd}	ground-reflected incident illuminance (lx)
E_h	total horizontal illuminance (lx)
E_L	lighting energy demand (J)
epw	energy plus weather file type
F_ϵ	emissivity factor
F_1	circumsolar anisotropy index
F_{11} - F_{22}	brightness coefficients
f_{11} - f_{33}	perez irradiance and illuminance coefficients
F_2	horizon brightening anisotropy index
F_{i-j}	view factor between surfaces i and j
\tilde{F}	radiation exchange factor
G	transmitted solar energy (J)
H	hour angle (deg)
h	heat transfer coefficient ($\text{W/m}^2\text{C}$)

h_c	convective heat transfer coefficient ($\text{W/m}^2\text{C}$)
h_n	natural convection coefficient ($\text{W/m}^2\text{C}$)
h_o	exterior heat transfer coefficient ($\text{W/m}^2\text{C}$)
h_r	radiative heat transfer coefficient ($\text{W/m}^2\text{C}$)
h_s	sunset hour angle (deg)
I	incident solar radiation (W/m^2)
i	iteration/surface index
I_b	incident beam irradiance (W/m^2)
I_{bh}	beam horizontal irradiance (W/m^2)
I_{bn}	direct normal irradiance (W/m^2)
I_d	total incident diffuse irradiance (W/m^2)
I_{dh}	diffuse horizontal irradiance (W/m^2)
I_{exn}	extraterrestrial normal radiation (W/m^2)
I_g	incident ground-reflected irradiance
I_h	total horizontal irradiance (W/m^2)
I_{sc}	solar constant (W/m^2)
j	iteration/surface index
k	thermal conductivity ($\text{W/m}^0\text{C}$)
kL	extinction coefficient*glazing thickness
L	luminance, latitude (deg), thickness (m)
l	Length (m)
LNG	Longitude (deg)
LSM	local standard meridian

M	luminous exitance (lx)
m_{opt}	relative optical air mass
MRT	mean radiant temperature ($^{\circ}\text{C}$)
n	day number
n_g	refractive index
p	time step index
P_L	installed lighting power density (W/m^2)
Q	heat source, internal gains (W)
R	thermal resistance ($\text{m}^2\text{C}/\text{W}$)
R_f	roughness coefficient
RTA	radiant temperature asymmetry ($^{\circ}\text{C}$)
S	absorbed solar radiation (W)
s	distance (m)
T_{ij}	radiosity matrix
T	Temperature ($^{\circ}\text{C}$)
t	solar time (hr)
T_{air}	room air temperature ($^{\circ}\text{C}$)
T_{dp}	dew-point temperature ($^{\circ}\text{C}$)
T_m	mean temperature ($^{\circ}\text{C}$)
TMY	typical meteorological year
T_o	ambient dry bulb temperature ($^{\circ}\text{C}$)
T_s	surface temperature ($^{\circ}\text{C}$)
t_{ss}	surface sunset time (hr)

t_y	number of working hours in a year
U	conductance ($\text{W}/\text{m}^2\text{C}$)
v	wind speed (m/s)
Vol	Volume (m^3)
V_s	free stream velocity near façade (m/s)
w	earth's spin rate (Hz)
WC	precipitable water content
WWR	window-to-wall ratio
x	thickness, height (m)
z	Solar zenith angle (deg)

Greek letters

α	solar altitude (deg), glazing absorptance
β	inclination angle (deg)
γ	surface solar azimuth (deg)
δ	solar declination (deg)
Δ	sky brightness
Δt	critical time step (s)
ΔT	temperature difference ($^{\circ}\text{C}$)
ε	sky clearness, emissivity
θ	solar incidence angle (deg)
ρ	reflectance
σ	Stefan-Boltzmann constant ($\text{W}/\text{m}^2\text{K}^4$)
τ_b, τ_e	beam (effective) transmittance

τ_d	diffuse transmittance
ϕ	solar azimuth (deg)
ψ	surface azimuth (deg)
ω	solid angle (sr)

Subscripts and superscripts

a, air	air
b	beam
bh	beam horizontal
bn	direct normal
c	convection
d	diffuse
dh	diffuse horizontal
dp	dew-point
e	earth
ex	exterior
f	front
g	ground
h	horizontal
i	of surface i
j	of surface j
L	lighting
m	mean
n	normal
o	outside, initial
p	at time step p
r	radiative
s	surface

t	time
v	interior wall
w	window
y	yearly
z	zenithal

CHAPTER 1. INTRODUCTION

1.1. Background

Building design is a complex process in which critical decisions concerning the different systems related to the building are made during the early stage. At this conceptual stage, building form is not fixed; geometry, envelope and orientation are still being formulated. Since these are important factors in determining building performance, this is possibly the most crucial stage of the design process.

Perimeter spaces play the key role in building energy performance. While accounting for a large part of energy demand, they provide a filter between the indoor environment and outdoors. Building envelope should be designed for protecting the building from continuously changing weather conditions while at the same time offering a comfortable environment for the occupants.

Daylighting is a necessity for commercial buildings. Daylight utilization improves lighting quality, increases occupants' productivity and reduces electricity consumption for lighting. With the growing interest in energy conscious design and solar architecture, the importance attached to daylight utilization has grown. For all these reasons, many innovative fenestration systems have been produced for implementation in commercial buildings. Therefore the building design team has to choose from a wide variety of design options, for many of which the evaluation of overall performance is difficult. Although an experienced designer can create a successful design, the selection of final design solutions often involves many subjective factors.

The domains of heating, cooling and lighting are closely related. For a complete analysis and understanding of building performance, the interactions between the different systems should be taken into account. These interactions are complex and an integrated approach should be followed for estimating building potential performance. The basic link between thermal and lighting performance is fenestration. Fenestration systems determine the impact of exterior thermal and daylighting conditions on the interior environment. Their optical and thermal properties and associated control are critical factors.

1.2. Motivation

Presently, building performance can be accurately predicted using advanced energy simulation programs. Some of them (i.e. ESP-r, Energy Plus) link daylighting and thermal simulation in an integrated manner (Clarke et al., 1998, Crawley et al., 2002). A major problem is that a separation must be made between the processes of analysis and design. An advanced simulation tool can predict the thermal and lighting performance of a perimeter space for a specific fenestration solution. However, it cannot provide useful information on how (and why) to select design alternatives, since all such software require detailed input data to run simulations, and these data are not yet available at the early design stage.

A preliminary simulation-based design study of options for the new Engineering and Computer Science building of Concordia University in Montreal was completed in 2002 to evaluate the impact of different façade design options on the building energy performance (Tzempelikos and Athienitis 2003b). It was shown that fenestration system

properties and control have a high impact on the daylighting and thermal performance of perimeter spaces. Several design alternatives, including glazing type, glass ratio of façades, shading properties and control and electric lighting options were considered in a combined daylighting and thermal simulation analysis. The impact on peak loads and energy consumption was also considered. In the case of a 15-story high atrium facing near south, utilization of an appropriate motorized shading system resulted in peak cooling load reduction of about 300 kW, eliminating one large chiller. The analysis revealed that all parameters form inter-related links between daylighting and thermal performance and that their impact should be considered simultaneously in an integrative manner.

Coupled thermal and daylighting analysis at the early design stage is essentially a systems integration challenge. Building form and orientation, glass ratio of the façade, fenestration system properties and control, electric lighting control options and HVAC components operation are parameters involved in this integration. Currently, there is no systematic methodology for performing an integrated thermal and lighting analysis during the early design stage, when critical decisions with small economic impact could lead to significant energy savings during the lifetime of the building and simultaneous improvement in interior conditions. A general integrated methodology that could provide designers with a process and guidelines for selection of fenestration system properties and dynamic control is currently missing.

1.3. Objectives and scope

The objectives of this work are:

- To develop a general and systematic simulation methodology for integrated daylighting and thermal analysis of facades and perimeter spaces of commercial buildings during the early design stage;
- To calculate generalized performance-based indices from the continuous interaction between daylighting and thermal simulation as a function of key linking parameters for investigating the balance between daylighting benefits and energy performance;
- To provide guidelines for selection of window-to-wall ratio, shading device properties, and control of shading plus electric lighting based on the results of the integrated analysis, using as criteria maximization of daylight utilization, reduction in energy demand for heating, cooling and lighting, as well as improvement of interior conditions;
- To address the need for considering innovative dynamic fenestration systems at the beginning of the design process and compare design options on a relative basis; also to select the required degree of detail in the simulation at this initial stage in order to maintain accuracy but reduce computation time and unnecessary complexity;
- To develop a simulation design support tool prototype that can be used by building designers for providing fenestration design guidelines based on an integrated approach at the early design stage.

The purpose of this work is to provide a design methodology for facades and perimeter spaces of commercial (office, institutional etc) buildings. Although some of the criteria used for selecting design solutions apply also to residential buildings (such as reduction in energy demand), this methodology was not developed for residential buildings. Advanced automated fenestration systems and dynamic building envelope

components are presently not common for residential buildings, since manually operated simpler and cheaper devices can be used. However, this may also change in the future. Already, solaria are available with motorized blinds.

The glazing optical and thermal properties are not explicitly considered as an optimization variable in this work. Detailed analysis of the impact of glazing properties on building energy performance has been extensively studied in the past. Instead, the approach followed here is to use clear glass for daylight maximization and the emphasis is then placed on determining shading device properties and control. However, the methodology is general and it can be applied to any façade type, orientation, location, glazing and shading type. In the simulation, windows are assumed to be placed on the façade. Skylights and atriums are beyond the scope of this thesis.

Shading and lighting control are modeled as fully automated, because the purpose of the methodology is to provide information on how to select the properties and control of shading based on maximized daylight utilization and reduction in energy demand for cooling and lighting. Manual operation is not included in the analysis, since it does not meet the above criteria.

Finally, this work is not intended to produce a building simulation tool for predicting the energy performance of perimeter office spaces. Advanced building simulation software are most appropriate for overall energy simulation of existing buildings. Instead, this work aims to provide a systematic and integrated simulation methodology for detailed evaluation of design alternatives (and recommendations on selecting fenestration systems) at the early design stage of new buildings, using as criteria energy performance indices as well as other performance measures (e.g. daylight utilization).

1.4. Thesis overview

Chapter 2 presents a review of related literature. Methods for assessing building performance and simulation approaches are discussed. Emphasis is placed on daylighting prediction in interior spaces. Fenestration is identified as a key parameter. Current methods for evaluating optical and thermal properties of shading systems are presented. The need for applying an integrated thermal and daylighting approach at the early design stage is justified and limitations using existing tools are analyzed, followed by the identified research needs.

Chapter 3 presents the developed integrated thermal and daylighting methodology. The approach of performing systematic simulation for design at the early design stage is discussed and a theoretical basis for the methodology is presented. The main links for coupling daylighting, lighting and thermal simulation are identified and development of integrated performance indices follows. After a description of the daylighting and the thermal simulation modules, the need to consider dynamic links as design parameters is explained. The main body of the methodology is then presented; by investigating the combined impact of each link on the integrated performance indices, a means for selecting specific design solutions is provided. The three-section façade concept is introduced and finally the need to include innovative systems in the analysis from the early design stage and to compare different options on a relative basis is discussed.

The results of the integrated methodology for perimeter spaces in Montreal are presented in Chapter 4. A base case scenario is assumed and then window-to-wall ratio recommendations are given, following the methodology presented in Chapter 3. A roller shade is used as an example, to apply the integrated daylighting and thermal analysis for

selecting transmittance and control of an exterior shade, in conjunction with electric lighting control. Experimental and simulation results for venetian blinds are presented next. Then, the findings of the preliminary design study for the Concordia University Engineering building -which was a motive for this work- are discussed. Finally, validation of daylighting and thermal simulation results is presented.

CHAPTER 2. BACKGROUND AND LITERATURE REVIEW

2.1. Assessment of building performance

The analysis of physical phenomena in buildings always depended on technical development and scientific knowledge. In the past, building performance assessment often relied on rules of thumb and approximate calculations. During the last decades, a revolution in performance assessment methods and tools has taken place. Currently, different applications range from spreadsheets with simplified calculation methods to advanced software, which allow simulation of transient physical processes based on numerical methods. Various techniques can be used to assess building performance:

- **Scale models.** Scale models are mock-ups of the real building. They can be used when loss of accuracy due to scaling is acceptable compared to studied parameters. They are generally cheap and can be tested under real and artificial conditions. Errors occur due to scaling effects, simulated materials and level of detail. Also, energy performance and environmental impact assessment are not possible when using scale models.
- **Full-scale experiments.** Full-scale measurements were always used to study building performance. The results are based on real conditions and could lead to direct assessment of the parameters tested. They are also the best option if no mathematical/physical model exists and for validation of theoretical models. However, this method is usually time-consuming and expensive, while some measurement error is inevitable.
- **Analytical mathematical models.** Some physical phenomena can be described using complex mathematical models. Under reasonable assumptions, complex equations can be simplified to reach analytical solutions. This is the usually the most accurate method for

analyzing relatively simple processes, for which direct and accurate analytical solutions can be derived. Nevertheless, the interaction of physical phenomena happening in a building is complex; therefore important assumptions are usually made in order to reach an analytical solution.

- **Numerical simulation models.** Numerical computer simulation models are used to analyze complex physical phenomena that do not have analytical solutions, with the aid of numerical methods. In many cases, these models are quite complicated and not easy to use. However, solutions can be reached and the analysis can be simplified based on minor mathematical assumptions. Advances in computer technology have resulted in improvement of numerical simulation processing by orders of magnitude. Thus, it is possible now to perform highly detailed numerical building energy simulations on widely available inexpensive personal computers.

2.2. Simulation types and the need for integration

Rapid advances in building technology during the last twenty years resulted in the need for an integrated approach in building design to effectively combine these technologies - such as advanced fenestration systems- in an optimal building system. The domains of heating, cooling, lighting, ventilation and acoustics are closely related. A complete analysis and understanding of building behavior is possible only if the interactions between the different systems are taken into account. For instance, office buildings with transparent facades are now common. In contrast with traditional heavyweight constructions, an integrated approach to the design of different systems is required, in

order to provide good interior conditions; otherwise, overheating and glare problems will occur.

From the assessment methods presented above, full-scale experiments and computer simulation can integrate complex physical phenomena and address the inter-relations between different systems in a building. Since full-scale experiments are often not possible and also time-consuming and expensive, computer simulation is the most appropriate method for integrated building analysis and design nowadays.

Four categories of programs that offer overall estimation of building performance are identified, according to simulation capability (Citherlet et al., 2001b):

- **Stand-alone programs.** In this approach several unrelated applications are used and the user has to create one model for each application. The disadvantages are that it is time consuming, there may be inconsistency between models and the user has to master each program's interface.
- **Interoperable programs.** In this case, different computer tools can share information. For example, the model can be created using a CAD tool and then exported to each application. Although the interoperable approach may avoid data redundancy, it does not entirely prevent inconsistency and still requires a complex data management system. Finally, it does not allow an interactive data exchange between applications during the simulation process itself. To overturn this weakness, a sequential data exchange can be provided, where the output extracted from one application is used as input in another application. For instance the lighting analysis package ADELINÉ (Erhorn et al., 1998) can generate an output file of illuminance data, which can be used as input by programs such as DOE-2 (Winkelmann et al., 1993) or TRNSYS (Beckman et

al., 1994) to perform energy simulation. But when the physics between the views is tightly connected or when accurate simulation is required, the sequential exchange of data may not be applicable any more and a different approach is required.

- **Coupled (linked) programs.** These programs link applications at run-time in order to exchange information. This is often called “ping-pong coupling”. Generally, one application controls the simulation and calls another application if necessary. In this case, only the simulation engine of the coupled program(s) is required and the front-end interface corresponds to the driving application. For example, the thermal/ventilation application ESP-r (Clarke, 1997) has been coupled (Janak, 1998) with the lighting application RADIANCE (Larson, 1993). The main advantage of the coupled approach is that it supports the exchange of information during simulation. Limitations remain by link consistency that depends on the separate evolution of each coupled application.

- **Integrated programs.** These programs can simulate different systems within the same program. As in the run-time coupling approach, a truly integrated simulation relies on the information exchange throughout the simulation to resolve a set of combined equations that represents the driving process of simultaneously occurring physical phenomena. Integration can also be achieved by merging into a single tool the best capabilities of existing applications such as done in the case of ENERGY Plus (Crawley et al., 1999) where the energy calculation core of DOE-2 (Winkelmann et al., 1993) and the ventilation calculation core of BLAST (Bauman et al., 1983) were merged at the algorithmic level. Even where domains are not physically interacting, the integrated approach has several advantages. Firstly, the evolution of the application is made easier because it does not depend on external applications. No exchange file format is required

and modifications need only be implemented once. Finally, the fact that there is one interface eases the learning process.

There is no doubt that, for estimation of building overall performance, an integrated simulation tool would provide maximum flexibility and the most reliable results. However, such software is difficult to create and requires a tremendous amount of knowledge from different fields of physics, mathematics and engineering. However, the need for exchanging information at every level of the process indicates that the exchange of data should occur both at the initial stage (import/export of CAD models) and at the simulation stage, where important performance parameters are evaluated at each time step. The latter requirement is not always satisfied with the sequential type of simulation, in which one program runs and then gives the available information to other programs to continue, except if link consistency is ensured and accurate models are used. Coupled run-time simulation is possibly the accurate option, but often it is simply too difficult or impossible to effectively link different applications because of the complexity of simultaneous inter-related physical phenomena.

2.3. Early stage design

Presently, the most efficient approach for building design presently is using advanced simulation tools. The purpose of such tools should not only be energy analysis of existing buildings, but also for exploring the alternatives when designing a new building. The International Building Performance Simulators Association (IBPSA) was established to “advance and promote the science of building performance simulation in order to

improve the design, construction, operation and maintenance of new and existing buildings worldwide”.

The conceptual stage of design occurs very early in the design process. This is the time when competing requirements are shaping the initial building form, when geometry, materials and orientation are still being formulated. As these are arguably the three most important determinants of building performance, this is the crucial stage of a project. Conceptual design is an iterative process of generating ideas that then need to be evaluated and tested, for rejection or further refinement. Traditional methods of testing an idea involve quick perspective sketches, simple geometric analysis on a drawing board, or even small hand-calculations. Being able to quickly reject impractical ideas can save significant amounts of time, each newly rejected idea providing one more clue to a more acceptable one. A major part of this testing process is simply experimenting with an idea until it is shown to work or not. The purpose of this is to gain some understanding, both spatially and operationally, of the full requirements of the final form. Using traditional techniques, the range of testing is quite limited.

The problem lies in the fact that a separation must be made between the act of analysis and the act of design when using simulation tools (Marsch, 1997). At the early conceptual stage, even building geometry is fluid and subject to constant change. Therefore analysis with an advanced building simulation package is almost impossible. It is, however, during this initial stage that critical decisions with high impact on energy performance during the lifetime of the building should be made. For instance, by choosing optimum fenestration area and orientation, the size of HVAC equipment could be significantly reduced. Passive solar techniques, daylight utilization and natural

ventilation can minimize energy consumption. Optimization of thermal mass may contribute to better control of the indoor thermal environment.

The major development in building simulation tools has been the accurate simulation of physical phenomena (heat transfer, air flow, lighting, humidity). As a result, they serve as a detailed design validation tool in the final stage of a project. It is therefore necessary to make these tools applicable to the earlier stages of design, where a more informed analysis of possible alternatives could lead to optimal design solutions, resulting in energy and environmental savings. A conceptual design tool should facilitate the process of entering essential input data at the initial stage as an integral part of the design process itself. The feedback, from the initial design stage to the final analysis, would be the key to a successful design.

2.4. Daylighting

2.4.1. Why daylight?

The concept of daylighting is not a new idea. Before the invention of electric light, the incorporation of daylight was a necessity for buildings. After the oil embargo during the 1970s, interest in daylighting and solar energy utilization accelerated. Lately, with concern about energy efficiency, human health, sustainable design and global warming, daylighting in buildings has been again proposed as a solution. The American Society of Heating, Refrigerating and Air-Conditioning Engineers (ASHRAE, 2001) included a section for daylighting in the Handbook-Fundamentals; the Illuminating Engineering Society of North America (IESNA) includes daylighting as an important part of the

annual meeting and seminars (IESNA, 2005). The benefits of daylight use in buildings can be categorized into two main groups:

1. Energy savings and thermal load reduction

- Natural daylight can substitute electric lighting and is ideal for comfort and health. Efficacy of daylight is high (around 47% of solar radiation is in the visible range). Especially for commercial buildings, where generally long hours of daytime occupancy occur, daylighting is an efficient solution. Lighting power demand is still high and the use of daylight could lead to significant energy savings. Figure 2.1 shows the distribution of energy consumption in commercial buildings based on National Renewable Energy Laboratory (NREL) estimations for a base-case building in Golden, Colorado (Hayter et al., 1999). Taking into account that electricity costs will continue to increase at increasing inflation rates, the long-term savings are actually higher.

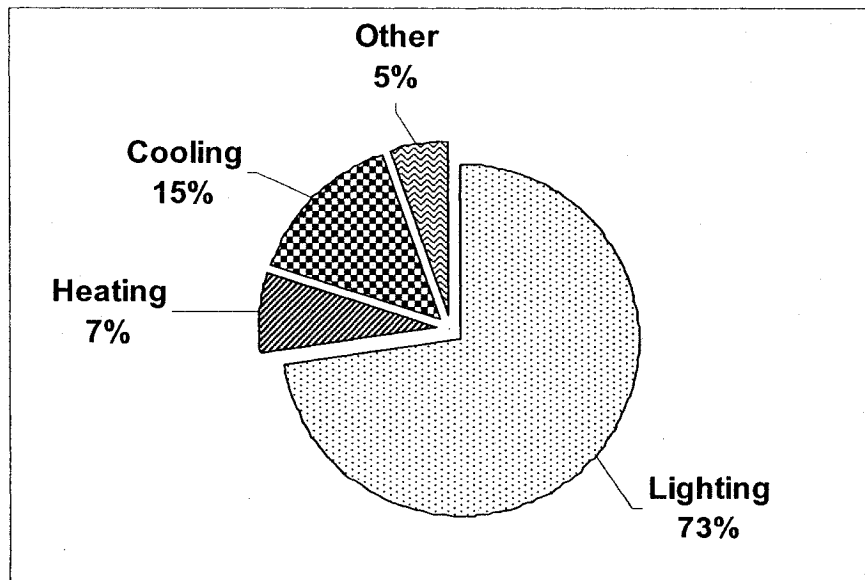


Figure 2.1. Energy consumption breakdown for commercial buildings in Colorado (Hayter et. al., 1999).

About 30% of Canada's energy consumption is for residential and commercial buildings (NRCan 2002); approximately 13% is for commercial/institutional buildings and 30% of this energy is for lighting, which ends up as a cooling load (Natural Resources Canada, Energy Efficiency Trends in Canada (2000)).

- Daylight utilization can reduce building energy consumption for heating and cooling.

The past notion that reducing window area would reduce energy consumption is no longer valid. Utilization of advanced fenestration systems and electric lighting controls has created a potential for reduction in overall building energy requirements.

- Daylight utilization could lead to the control of peak electric demand and load shape. Since peak building loads frequently occur in the afternoon, a daylit building in which the lights are dimmed or turned off would reduce building peak demand (Lee et al., 1998). Moreover, the use of controllable daylighting/shading systems would help in controlling peak demand more effectively, as discussed later.

2. Human comfort, productivity and health

- These include different and important benefits of daylighting. It is now proven that daylight provision improves human performance. Schools incorporating daylighting solutions report better test scores (Heschong, 2002); big-box retail stores with daylight maximize sales; residents in senior-living facilities sleep better and live longer when regularly exposed to natural daylight; even hospital patients located close to windows seem to recuperate more rapidly than those further away from daylight (Garris, 2004).
- The interplay of natural light and building form provides a visually stimulating and productive indoor environment.

- Daylight increases office worker's productivity. The economic benefits of productivity are huge and directly correlated to daylight. A 20% increase in employee productivity pays back the entire cost of a single office construction in the first year, according to recent research studies at Carnegie-Mellon (Loveland, 2004).
- The provision of natural light in the space makes the occupant less dependent on the mechanical systems of a building. For example, in case of a power failure, a worker could continue working with adequate daylight provision.
- Finally, view and visual connection to the outdoors are generally desirable. Other qualitative aspects of daylighting, such as color rendition and visual quality are pleasing to the occupants.

2.4.2. Daylight assessment

Realisation of the significance of daylight utilization in buildings resulted in a large number of daylighting studies. These studies extend from theoretical calculations of sky luminance/illuminance distribution and analytical ways of predicting illuminance level in a closed space to the invention of complex fenestration and daylighting systems for better daylighting performance. In general, there are four main categories of methods for prediction and assessment of the daylighting performance of a building:

- Traditional graphical tools

These “old tools” were used in the past to allow a quick and simplified estimation of the daylighting performance in a space. Almost all of them consist of transparent scales, which are placed on top of window openings. Photometric indices like dots or iso-lux curves determine the average daylight inside the space. The most important methods are

the Waldram diagram method (Waldram, 1950), the Pilkington sky dot method (Pilkington 1969, Lynes 1969) and the BRE overcast sky protractors (Longmore, 1967).

- Scale model photometry

Scale models allow a qualitative and quantitative performance evaluation of the daylight systems used with respect to visual performance only. The designer can evaluate the impact of shading upon the indoor light levels, and also the distribution of daylight inside building spaces, due to the use of daylighting systems. The daylight assessment can be performed either in outdoor conditions (real sky) or under artificial sun/sky simulators (Michel et al., 1995). The disadvantage of scale models is that they can not be used to accurately study transient thermal response of buildings.

- Full-scale measurements

Although scale models and sun/sky simulators can give a good idea of interior lighting conditions, there are also some daylight qualitative parameters (perception of space, visual comfort) that require full-scale measurements. Furthermore, occupant-dependent criteria (assessment of human response to luminous environment) should be investigated by experiments in full-scale rooms.

- Computerized methods

These include all the methods used presently and can model accurately the daylight quantity in a space. Different methods are used to process the luminous flux and some of them require significant amounts of memory and time to converge to a solution as discussed next. These methods can provide the designer with luminance and illuminance images of the interior space and surfaces under different outside daylight conditions.

Figure 2.2 shows techniques used in practice for lighting and daylighting design. Findings from a more recent online survey on the use of daylight simulation programs (Reinhart & Fitz, 2004) indicate that computer lighting simulation software use has increased.

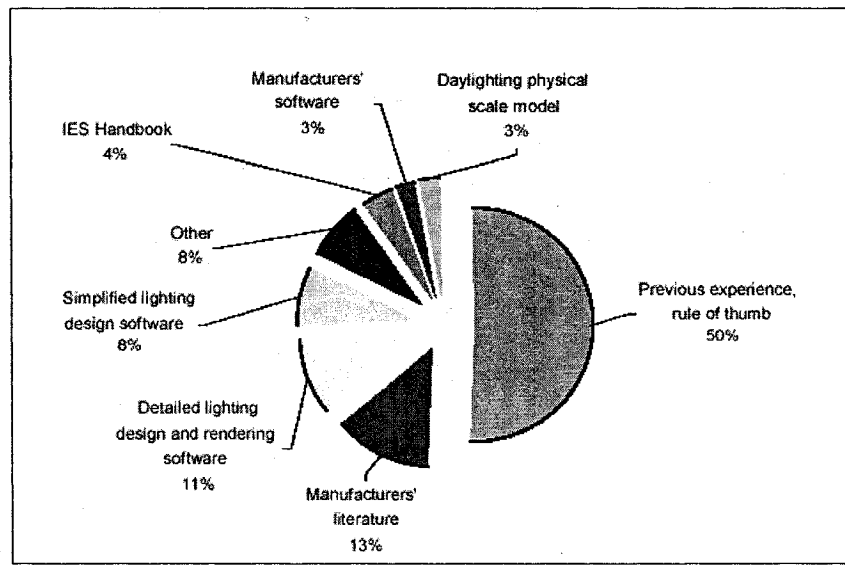


Figure 2.2. Methods designers use for lighting and daylighting design (Citherlet, 2001a).

2.4.3. Methodology for daylighting design

Daylight prediction in closed spaces is not a simple task. For commercial (office) buildings, the detail of accuracy has reached a point where some important parameters- such as working plane illuminance and daylight uniformity in the space- should be determined in order to provide sufficient information to the lighting designer. The general procedure consists of four major steps:

1. Calculation of sky luminance distribution. Typically, this describes the sky conditions. Many researchers have produced different sky luminance models based on measurements and theoretical methods. The easiest and most convenient type is the

uniform overcast sky type, in which the sky is assumed to be fully and uniformly covered by clouds. Moon and Spencer (1942) developed an equation for calculation of sky luminance at different points in the sky (altitude α) as a function of zenith luminance (L_z):

$$L = L_z \cdot \frac{1 + 2 \cdot \sin(\alpha_{point})}{3} \quad (2.1)$$

Practically, this equation requires that the zenith sky luminance is three times higher than the sky luminance at the horizon. CIE adopted this overcast sky model and this is the one still used (Gillette & Kusuda, 1982). For clear sky, the models used are more complicated. The CIE model was based on Kittler's model for clear sky (Kittler, 1965). Other similar models have been produced (Hooper, 1987, Harrison & Coombes, 1988) in which luminance is decreasing as the angular distance from the sun increases. Finally, other models that try to simulate intermediate (partly cloudy) sky conditions have been created. These models are based on the possibility of sunshine (Littlefair, 1992) and the nebulosity index, or they are a combination of a clear and an overcast sky model. The model mostly used is the one proposed by Perez et al. (1993), in which the sky luminance is a function of sky clearness, sky brightness and solar altitude.

2. Illuminance on the earth's surface and on any surface of interest is calculated next. Direct sunlight, diffuse daylight coming from the sky and diffuse reflected light from the ground or from adjacent buildings are computed separately. In the case of overcast sky, there is only diffuse daylight and illuminance is essentially a function of solar altitude. In the case of clear sky, transmission through the atmosphere is taken into account using optical extinction coefficients. Using appropriate equations, the total exterior illuminance

incident on window can be predicted (Kittler, 1981, Gillette & Pierpoint, 1982, Gillette, 1983). The illumination values can also be computed from irradiance values, using the luminous efficacy concept. Perez et al. (1990) and Muneer & Kinghorn (1997) have proposed different luminous efficacy correlations for predicting direct and diffuse horizontal illuminance from the respective irradiance values. The irradiance values are calculated based on existing mathematical and statistical models such as the clearness index model (Liu & Jordan, 1960), further improved by Orgill & Hollands (1977), Collares-Pereira (1979) and Erbs (1982). Then statistical methods are used to compute a series of irradiance values on a horizontal surface (Hollands & Hudget, 1983, Graham & Hollands, 1988, 1990, Gordon & Reddy, 1988, Knight et. al., 1991, Santos et. al., 2003). More recently, horizontal beam and diffuse irradiance values are provided by satellite measurements for many locations around the world (Rigollier et al., 2000). Using these values and one of the available models (Perez et al., 1990) hourly values of irradiance (and illuminance) on a tilted surface can be accurately produced.

3. The third step is calculation of the transmitted daylight through the windows into the space. The process is relatively easy in the case of a simple double-glazed non-shaded window. Direct and diffuse transmission should be treated separately (Brandemuehl & Beckman, 1980). However, if a coating is employed, transmittance could be a function of wavelength. Moreover, if a shading device is used, the situation becomes complicated. For example, the transmission through a venetian blind system is difficult to calculate; it is a function of blind optical properties, sky conditions, blind tilt angle, solar position, wavelength, etc (Andersen et al, 2003, Tzempelikos & Athienitis, 2001, Rosenfeld et al., 2001). These are discussed in a later section.

4. The final step is to process the luminous flux that enters the space. Usually, the objective is to calculate the illuminance on the imaginary surface of the working plane. Simplified methods include the IES method (IES, 1984) and the Lumen method of sidelighting (IES, 1978, Kaufman, 1981). These methods are not accurate, but they can provide the designer with a basic estimation of the average illuminance on the work plane. The main disadvantages of the simplified methods are: (i) they do not apply to the clear sky case, (ii) the space has to be a perfect cube and (iii) fenestration systems cannot be taken into account. Another more detailed procedure has been developed and is widely used in Europe based on the work of many researchers over the past 50 years (Waldram, 1950, Hopkinson, 1966, Bryan, 1981, Robbins, 1984). It is called Daylight Factor method (DF). The daylight factor is expressed as the ratio of the illuminance at a point on a plane inside the room produced by the luminous flux received directly or indirectly at that point from a sky of a given luminance distribution, to the illuminance on a horizontal plane produced by an unobstructed hemisphere of this same sky:

$$DF = (E_i/E_e) \cdot 100\% \quad (2.2)$$

where E_i is the interior illuminance and E_e is the exterior illuminance. In the above definition, direct sunlight is excluded. Thus the daylight factor method has been limited to the cases of the CIE overcast/uniform sky. However, other developments made the method valid for the CIE clear sky also, but they are quite complicated (Bryan, 1981) or based on many assumptions (Alshaibani, 1997). The main disadvantages of the Daylight Factor method are that it applies to overcast sky and cannot model complex fenestration systems. For detailed daylighting calculation, none of the above methods is currently used. The next section presents more advanced methods for predicting interior

illuminance in a space. Usually, the objective is to predict daylight levels on the imaginary work plane surface (desk level where people work) so that poor illumination levels or glare problems can be detected right on the critical points. Nevertheless, the methods described below can be used for calculation of illuminance levels at any surface or point in a room.

2.4.4. Advanced methods for processing luminous flux in interior spaces

- Radiosity model (finite elements)

This method is product of the work of DiLaura (1979) and Siegel (1982), and it was presented as a complete method for the calculation of illuminance values by Goral (1984). The method is based on the principle of energy conservation and it allows the calculation of illuminance distribution on the surfaces of a closed space. Originally developed for energy calculations, the radiosity method was used to determine the energy balance of a set of surfaces exchanging radiant energy. The space is discretized in sub-surfaces and inter-reflections between interior surfaces are computed using form/view factors. The view factor from surfaces A_1 to surface A_2 in Figure 2.3 represents the fraction of diffuse radiation leaving surface A_1 which directly reaches surface A_2 . It is a strictly geometrical quantity equal to:

$$F_{A_i, A_j} = \frac{1}{A_i} \cdot \int_{A_i} \int_{A_j} \delta_{ij} \cdot \frac{\cos \theta_i \cdot \cos \theta_j}{\pi \cdot r^2} \cdot dA_j dA_i \quad (2.3)$$

The final illuminance exitance of each surface can be calculated by:

$$M_i = M_{oi} + \rho_i \cdot \sum_j M_j \cdot F_{i,j} \quad (2.4)$$

where $M_{0,i}$ is the initial luminous exitance of surface (i) and ρ_i is the reflectance of surface (i).

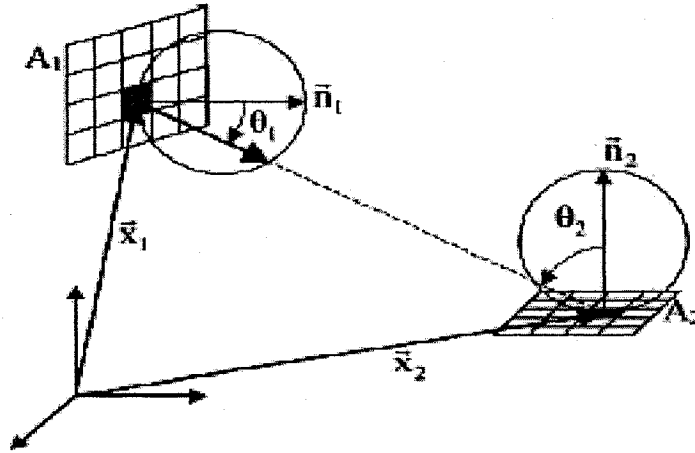


Figure 2.3. Surfaces and angles considered for calculation of view factors, with discretization into small rectangle areas.

Solving for the initial luminous exitances for (n) surfaces, a system of linear equations is created:

$$\begin{aligned}
 M_{0,1} &= M_1 - (\rho_1 \cdot M_1 \cdot F_{1,1} + \dots + \rho_1 \cdot M_7 \cdot F_{1,n}) \\
 M_{0,2} &= M_2 - (\rho_2 \cdot M_1 \cdot F_{2,1} + \dots + \rho_2 \cdot M_7 \cdot F_{2,n}) \\
 &\dots\dots\dots \\
 M_{0,7} &= M_7 - (\rho_n \cdot M_1 \cdot F_{n,1} + \dots + \rho_n \cdot M_n \cdot F_{n,n})
 \end{aligned}
 \tag{2.5}$$

The above system can be written in matrix form (n x n) as:

$$M_0 = (I - T) \cdot M \tag{2.6}$$

where I is the n x n identity matrix and T is a n x n matrix each element of which is equal to $T_{ij} = \rho_i \cdot F_{ij}$. For solution of this system, iterative methods (Jacobi, Gauss-Seidel) have to

be used and convergence is always assured since reflectance and view factor values are always less than unity. The above equation can be written as:

$$M_i = (I - T)^{-1} \cdot M_{oi} \quad (2.7)$$

The inverse matrix may be evaluated using MacLaurin series and the luminous exitance of surface (i) after (k) inter-reflections in the room is calculated from:

$$M_i^{(k)} = T \cdot M_i^{(k-1)} + M_{oi} \quad \text{or} \quad M_i^{(k)} = M_{oi} + \rho_i \sum_{j=1}^n F_{i,j} \cdot M_j^{(k-1)} \quad (2.8)$$

The illuminance on selected points or a grid of points on the work plane can be then calculated using configuration factors (Tzempelikos & Athienitis, 2001). The main limitations of the radiosity method are that all surfaces are assumed Lambertian -no specular reflection or mirror-like surfaces can be processed- (Immel, 1986). However, we can overcome this difficulty with appropriate modifications. The main advantages of the radiosity method are that it is quite accurate -because it does not contain any empirical parameters-, it is not based on sky luminance distribution, and the results are not view-independent. The discretization of the surfaces into smaller elements increases the detail and the accuracy of results. However, the numerical complexity increases exponentially with the number of sub-surfaces. This will be the method primarily used in this work.

▪ Monte Carlo methods and ray-tracing techniques

In the last decade researchers have investigated the potential of the Monte Carlo technique for lighting calculations to overcome some of the drawbacks of the finite element method. The basis of the Monte Carlo method is the tracing of the actual path of

a particle of light from its source to its eventual absorption at a surface. At each change of direction of a particle, caused by reflection or transmission, the new direction is calculated according to statistical probabilities defined by the optical properties of each surface (Tregenza, 1983). The ray tracing approach includes parts of both finite element and Monte Carlo techniques and is capable of modeling a wide range of geometrically complex spaces. The algorithms are based on the “backward ray tracing” technique, in which a ray is traced back from the point of measurement to the source. The ray-tracing technique determines the visibility of surfaces by tracing imaginary rays of light from a viewer’s eye to the objects of a rendered scene (Ward and Rubinstein, 1994). Thanks to the power of new computer algorithms and processors, millions of light rays can be traced to achieve a high-resolution rendered picture. The main advantages of these methods are that they account for every optical process (including specular materials) and can model spaces of extreme complexity. The advances of lighting design methods for non-empty interiors are discussed by Lupton et al. (1996). However, the computation time increases significantly compared with other methods.

- Daylight coefficients

Tregenza & Waters (1983) proposed this method for effectively calculating illuminance values on a point in a room. The sky hemisphere is divided into (145) patches. Mathematical functions (daylight coefficients) that relate sky luminance distribution to the illuminance on a point in a room are computed using matrix algebra. Inter-reflections are taken into account. The main advantage of this method is that once a set of daylight coefficients is determined for a point in a room, the illuminance on the point can be easily calculated for any sky condition.

2.4.5. Lighting and daylighting software tools

In addition to the first generation of simple design tools, several new software products have been recently developed to address the complexity of light propagation into building spaces. These software products can handle tremendous amounts of information and perform lighting calculations in a short period of time. Most of these tools presently work under Windows operating system. Some of them have also been linked to commonly used architectural CAD programs, whose graphical means for entering geometric data are much easier to handle than the conventional numerical input for xyz-coordinate systems used in most of the older stand-alone daylighting tools. Table 1 presents an overview of advanced lighting and daylighting computer design tools.

DAYSIM (Reinhart & Herkel, 2000) is a Radiance-based daylight simulation tool that uses the daylight coefficients approach and the Perez sky luminance model to simulate short-time step indoor illuminances under arbitrary sky conditions. A state-of-the-art comparison with six Radiance-based methods and validation for a test office with external venetian blinds (Reinhart & Walkenhorst, 2001) showed that DAYSIM software is a reliable and accurate tool for daylight simulation. Occupant behavioral models for passive and active manual control of shading devices and electric lighting controls are included in the simulation using the Lightswitch program (Reinhart, 2002). DAYSIM, as well as other recent lighting software, can provide rendered images of the space under different lighting conditions as output so that the designer can visualize directly the results. Moreover, DAYSIM has the advantage of producing not only static values of interior illuminance, but also annual performance indices, as explained in a next section.

Table 2.1. Overview and comparison of advanced lighting/daylighting software packages
(LBL website info)

		ADELIN 3.0	RADIANCE 2.4	SUPERLITE 2.0	LUMEN MICRO 2000
General applications	Indoor Outdoor	✓ ✓	✓ X	✓ X	✓ ✓
Hardware	Operating system System memory required Minimum required processor	<i>Windows 80MB Pentium</i>	<i>Unix/Windows 30MB Any</i>	<i>DOS 1MB Any</i>	<i>Windows 64MB 486</i>
Type of analysis	Horizontal point-by-point illumination Vertical point-by-point illumination Inter-reflection calculations Direct calculations Surface luminance/exittance Zonal cavity method Lumen method Daylighting Visual comfort Economic analysis Unit power density Advanced statistical analysis Image synthesis	✓ ✓ ✓ ✓ ✓ X X ✓ ✓ ✓ X ✓ X ✓ ✓	✓ ✓ ✓ ✓ ✓ X X ✓ ✓ ✓ X X X ✓	✓ ✓ ✓ ✓ ✓ X X X X X X	✓ ✓ ✓ ✓ ✓ ✓ ✓ ✓ ✓ ✓ ✓ X
Special features	Automatic layout Schedules CAD interface Shadowing Interior obstructions Room shape Maximum number of calculation areas	X X ✓ ✓ ✓ ✓ <i>Any Unlimited</i>	X X ✓ ✓ ✓ ✓ <i>Any Unlimited</i>	X X X ✓ ✓ ✓ <i>Any 3</i>	✓ X ✓ ✓ ✓ ✓ <i>Orthogonal Unlimited</i>
User interaction	Tabular entry Graphical entry Metric input/output	✓ ✓ ✓	X X ✓	X X ✓	✓ ✓ ✓
Types of output	Point-by-point Iso-contours Scaled output 3D model view Color output Image visualization	✓ ✓ ✓ ✓ ✓ ✓	✓ ✓ ✓ ✓ ✓ ✓	✓ X X X X X	✓ ✓ ✓ ✓ ✓ ✓
Photometric database	Photometric data manager Photometric graphic viewer Photometric format	X X <i>IESNA</i>	✓ X <i>IESNA</i>	X X X	✓ ✓ <i>LTL-1</i>

2.5. Fenestration systems

2.5.1. Problems associated with daylighting

The utilization of daylight in buildings has many advantages but also creates several problems. The most important are:

- Visual discomfort, high contrast and glare. These can occur if excessive amount of daylight is transmitted in a room. Under clear sky, this is likely to happen. Especially for office buildings, glare has been a major concern according to the Illumination Engineering Society of North America (Hankins & Waters, 2003).
- Daylight is only the visible portion of solar radiation (about 46%). When daylight is transmitted in a space, undesirable parts of solar radiation may also be transmitted. This often results in excessive solar gains and highly varying heating and cooling loads throughout the year, especially when inadequate amounts of thermal mass are present. The amount of available daylight (and solar heat) and the advantages and problems associated with it are totally dependent on one parameter: fenestration.

2.5.2. Fenestration: the key component

ASHRAE (2001) defines fenestration systems as “basic assemblies and components of exterior windows and other openings within the building envelope”. It includes glazing materials, framing, dividers and any type of shading. The (passive) daylighting and thermal performance of perimeter spaces of a building depends on the building envelope design. The area of fenestration in commercial buildings is continuously increasing, driven by the higher demand for buildings with much daylight. Fenestration systems are the critical link between daylighting and thermal performance of perimeter spaces. They

are possibly the component with lowest thermal resistance, but also potentially the most important element in office buildings. They can provide interior spaces with daylight, view and solar heat while at the same time they could be the cause of thermal and visual discomfort, excessive heat gains or heat losses and highly varying heating and cooling loads for perimeter spaces throughout the year.

The balance of positive and negative influence of solar radiation on building energy use and human comfort is something difficult to deal with. Solar radiation accompanies the admission of daylight, which contributes to visual quality and to reduction in electric lighting energy consumption. High solar gains result in increase of cooling load, but also reduction of heating load. Also, appropriate control of electric lights can reduce internal gains and peak cooling load, which is often important in the case of office buildings with high internal gains. Although adequate amounts of daylight is ensured, problems associated with glare and visual discomfort are inevitable if direct solar radiation enters the room. For south-facing facades, extremely high illuminance values result in high contrast and intense glare. In addition, thermal problems arise if no shading is used. Peak cooling load (which is often the highest) may be reduced if the window is well insulated, but still remains high. A solution to the above problem was to utilize a kind of fenestration system, which would be able to admit daylight while at the same time control solar gains. Three major components are used for this purpose: advanced glazings, high-tech daylighting systems and shading devices.

2.5.3. Advanced glazings

Recently, more advanced glazing products have replaced the traditional common double-glazed window. The low emissivity glazing (low-e) has a special coating on one surface

that can dramatically reduce longwave radiation. These glazings can allow high solar gains into a room while minimizing heat losses by radiation to the outside. Variable transmission glasses allow the dynamic use of building envelope, responding to outdoor climate and interior thermal needs. The principle of operation of electrochromic glazing (Cogan, 1986, Hutchins, 2000) is based on the change of the optical properties of certain laminated materials when subjected to an external electric field. An integrated energetic approach for electrochromics recently showed the great potential of this technology (Assimakopoulos et al., 2004). Thermochromic glazing (Lee, 1986) includes a thin tungsten trioxide or vanadium dioxide film. It passively switches between a heat transmitting and heat reflecting state; therefore it can reduce cooling loads and provide solar protection. Translucent glazings have low transmittance and they diffuse daylight; they are suitable for atria and skylights where direct visual communication with the exterior environment is not required. Photochromic glazing has a transmittance inversely proportional to the outdoor illuminance; when the illuminance is low, it acts as a normal glass, while in periods of high illuminance, it behaves like a body-tinted glass (low transmittance and high absorptance). Other gasochromic and thermotropic glazings with a large dynamic range in total solar energy transmittance have also been developed and studied (Wilson, 2000). The IMAGE project (Implementation of Advanced Glazings in Europe) was a big step towards investigating the energy performance of advanced glazing products using the ESP-r simulation engine (Citherlet et al, 2001b). For the thermal performance of the glazings, the WINDOW software was used (Finlayson et al, 1993). A prototype study of an angular selective glazing by Sullivan et al. (1998) for a typical

office showed that peak loads could be reduced by 11% and annual energy consumption by 18%, compared to a conventional double-glazed window.

2.5.4. Daylighting systems

Innovative daylighting components are advanced design features and components that are used to replace or complement window openings with respect to daylighting. They work by redirecting or diffusing sunlight or skylight into a space. These systems aim to increase daylight levels to the rear of deep rooms, improve the daylight uniformity within a space, control direct sunlight so that it can be an effective working light source and at the same time reduce glare and discomfort for the occupants (Littlefair, 2000). Apart from these, they contribute to reduction of energy consumption for electric lighting and cooling. Atria and skylights can be considered such components and they have been used for many years. Traditional light shelves are another important category of daylighting devices. They are used to re-direct light on the ceiling and improve the daylight distribution in the room. More recently, other advanced systems have been developed such as diffuse prismatic panels (Lorenz, 1998), anidolic zenithal openings (Courret, 1994), holographic optical films (Muller, 1994), sun ducts, etc. The most recent complete overview of advanced daylighting systems was presented by Kischkoweit-Lopin (2002).

2.6. Shading devices

The requirement of maximizing natural light in building spaces is, during the summer, in conflict with the need to minimize solar gains in order to reduce energy consumption for cooling. Also, for an office space, it is necessary to avoid glare and high contrast, which cause discomfort to the occupants. Clear sky conditions may result in intense glare,

especially for south-facing facades. Thus, shading provision should be considered as an integral part of fenestration system design. Shading devices can be multi-purpose: block direct sunlight and reduce solar gains during the cooling season, allow the maximum possible amount of daylight (and solar gains) during the heating season, control direct sunlight by diffusing it into the space without causing glare on clear days, while, at the same time, transmit all the available daylight on overcast days. They can eliminate glare and create a pleasant luminous environment. The variety of shading devices is great, but they fall into two main categories: fixed and movable.

Fixed shading devices include overhangs, louvers, vertical fins, awnings and light shelves, whereas movable shading devices are mainly retractable roller shades, shutters, venetian blinds and curtains. Fixed devices are usually employed in the building envelope to exclude solar radiation in the summer (reduction in cooling load) and to admit it in the winter (reduction of heating requirements) (Athienitis & Santamouris, 2002). However, they also block a significant amount of diffuse daylight on clear days and they are not effective under overcast conditions. On the other hand, movable shading devices can be adjusted to account for continuously changing outdoor conditions. These devices can be either manually operated (curtains, shutters, roller shades) or motorized (horizontal louvers/ venetian blinds, retractable roller blinds). Moreover, shading systems can be exterior, interior or intermediate (between glass panes). The most common shading devices used are retractable roller shades and venetian blinds (Figure 2.4).

Roller shades are retractable homogeneous shades used in many commercial buildings. Their transmittance varies from 1% to more than 50%, depending on the material and the number of small holes in the fabric that allow light penetration. They can

be used to ensure privacy and may be left open during overcast days to allow maximum daylight in the room (Tzempelikos & Athienitis, 2004). During clear days, they transmit diffuse daylight in the room, eliminating glare.

Venetian blinds are the other commonly used shading system. They consist of separate, equally spaced horizontal louvers and thus they are a non-homogeneous device. This is why their optical properties are quite complex and they change with the louvers' properties, tilt angle and angle of incidence.

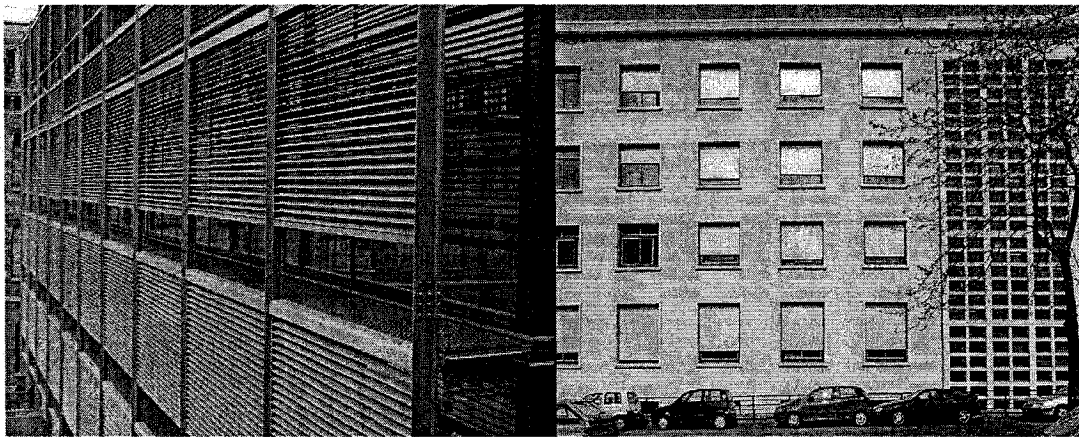


Figure 2.4. Examples of exterior venetian blinds and roller shades

Venetian blinds reflect daylight towards the ceiling and this can be utilized using a ceiling reflector (Tichelen, 2000). Generally, the venetian blind is a multipurpose device: when the sun is present, it can block direct sunlight, protecting the occupants from glare and reducing the cooling load in the summer (Rheault & Bilgen, 1989, Lee & Selkowitz, 1995, Tzempelikos & Athienitis, 2003a); at the same time, it reflects the sunlight and sky light and transmits the reflected light from the ground towards the ceiling, improving the illuminance distribution at the deeper parts of a room. When there is only diffuse

radiation, it can be adjusted to allow the maximum possible amount of daylight in the space and maximize the view field to the outside (Athienitis & Tzempelikos, 2002). During the winter, it can be completely closed at night, minimizing conduction heat losses through the window. Also, it can provide the occupants with the desired degree of privacy at any time. Moreover, it can be even used to serve multiple buildings (when on a south façade): while it provides all the above to an interior space, it reflects sunlight that can be used to illuminate the north facades of neighbouring buildings (Pucar, 2000), just like south-oriented facades reflect daylight onto opposite facades under sunny conditions (Tsangrassoulis et. al., 1999).

Manual operation of shading devices is still being studied. Vine et al. (1998) showed that people prefer to have control of fenestration systems, but complaints about glare and visual discomfort are inevitable on a subjective basis. Love (1998) calculated manual switching probability functions in private offices, based on the work of Hunt (1980). Bulow-Hube (2000) studied the office worker preferences on exterior shading devices, for the case of awnings and Venetian blinds. In this interesting study, the frequency distribution of awning slope and blind tilt angle were plotted based on preference of fifty office workers. Reinhart (2002) has developed a simulation tool (Lightswitch) that predicts the lighting energy performance of manually controlled lighting and blind systems. Probabilistic switching patterns, derived from field data, are used together with annual profiles of user occupancy and work plane illuminance. Within Task 31 (2001-2005), the International Energy Agency has launched subtask A called “user perspectives and requirements”, to investigate current knowledge on human response to the application of daylighting/shading systems and control strategies. The purpose is to

develop a reliable understanding of the role of user perceptions of visual and thermal comfort in the control of daylighting strategies aimed at energy conservation.

2.6.1. Thermal and daylighting performance of fenestration systems

The diurnal and seasonal changes in the sun's position and the sky conditions cause a large and complex variation in the daylight (and solar heat) transmitted through a window system (equipped with a shading device). A major factor in the evaluation of the performance of a complex fenestration system is the determination of its optical and thermal properties. These are usually not provided by manufacturers and there is no standard procedure for measuring the transmittance of shading devices (ISO 15099, 2003). The optical and thermal properties of windows equipped with shading devices depend on (i) the type of glazing(s) used (ii) the type of shading device used and (iii) the location of the shading device with respect to the window glazings. Venetian blinds, roller shades and draperies can be treated as shading layers located parallel to the glazing plane. The shading layer is usually modeled as a one-dimensional layer similar to a pane or film, so the optical properties of the shading system are a function of the device geometry and the position in the assembly. For a complete evaluation of the spatial distribution of daylight, calculations using the full matrix of transmission, forward and backward reflection and absorption at each component for every angle of incidence are required. U-value, solar heat gain coefficients and correlations about convection and radiation coefficients in shading cavities are required for thermal characterization of the system.

2.6.1.1. Venetian blinds

1. Optical properties

Venetian blinds (Figure 2.5) are possibly the most complex type of shading in terms of optical and thermal properties. Most models are based on the pioneer work of Parmelee et al. (1953). In general, the methods and information described in ASHRAE (2001) are not considered a systematic, detailed analysis of venetian blind systems, but provide useful data for estimation of optical and thermal properties of particular venetian blind products (not generalized however). In ISO 15099 (2003) the calculation is done based on three assumptions: (i) the slats are non-specular reflecting (ii) any effects on the window edges are ignored and (iii) slight curving of the slats is ignored. The procedure is to consider two adjacent slats and to subdivide the slats into five equal parts (Figure 2.6).

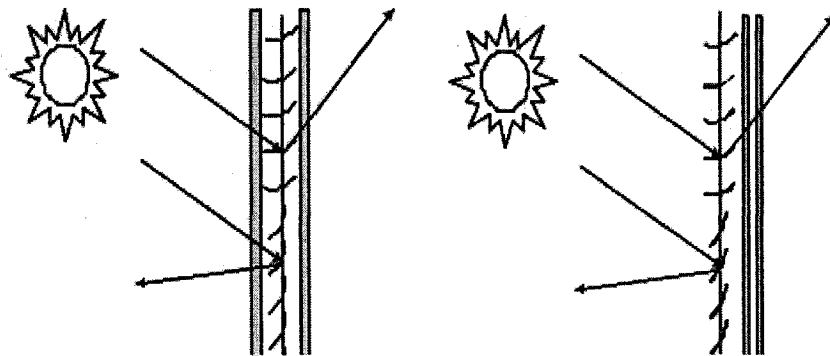


Figure 2.5. Between-glazing and exterior venetian blinds.

Every slat is divided into five elements. Different properties can be assigned to every element, in particular to every side of the slat. The irradiance on each subsurface (f_i) and (b_i), with i from 0 to n (and normally for each spectral interval) is calculated from:

$$E_{f,i} = \sum_k [(\rho_{f,k} + \tau_{b,k})E_{f,k}F_{f,k \rightarrow f,i} + (\rho_{b,k} + \tau_{f,k})E_{b,k}F_{b,k \rightarrow f,i}] \quad (2.9)$$

where F_{p-q} is the view (shape) factor from surface p to surface q .

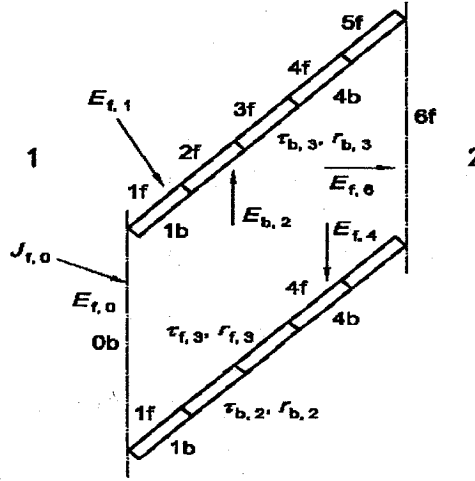


Figure 2.6. Discretization of venetian blinds in ISO 15099 (2003).

The beam radiation passing through the slats without touching can be calculated from the tilt angle and aspect ratio of the slats for any incidence angle, θ . For direct to diffuse transmission and reflection, the parts of the slat (k) directly irradiated are computed for a certain incidence angle, θ . In Energy Plus (2004), the optical properties of the blind are determined by slat geometry (width, separation and angle) and slat optical properties (front-side and back-side transmittance and reflectance). Blind properties for direct radiation are also sensitive to the “profile angle,” which is the angle of incidence in a plane that is perpendicular to the window plane and to the direction of the slats. ISO 15099 and Energy Plus results generally agree within 12%.

Pfrommer et al. (1996) published one of the most significant analytical methods for determining blind solar optical properties. The simulation model calculates effective solar

transmittance values and shading factors for a wide range of different blind systems and control strategies, with corresponding applications in a thermal simulation engine. The method is totally analytical and is derived from fundamental geometrical and physical characteristics of blind systems. WIS (Advanced Window Information System) is a European software tool for the calculation of optical and thermal properties of commercial and innovative window systems, a big part of which is venetian blinds. One of the unique elements in this software is the combination of glazings and shading devices. The way WIS treats the solar optical properties of a “layer type” shading device has been the basis of ISO 15099. A comparison between WIS, Monte Carlo simulation and radiosity results is available by van Dijk (2003). For diffuse to diffuse properties, view factors are calculated based on a three-dimensional model (LAMAS), developed under the European PASCOOL project (Molina et al., 2000).

Another model for the optical properties of venetian blinds was inspired by the fact that, for many cases, the slat reflectance is highly anisotropic, strongly peaked about the specular direction. In this study, Breitenbach et al. (2001) measured the visible and total solar energy transmittance of an integrated venetian blind system using a goniospectrometer, for different slat angles and incidence angles. Then they developed a model as follows: for the light that is diffusely reflected and undergoing two or more inter-reflections, a fraction F of it is assumed to proceed as specular component at each reflection. The fraction $1-F$ is reflected backwards. It retraces its path, having a fraction being absorbed at each reflection on its way back. This model therefore contains one adjustable parameter, F , whose magnitude depends on the degree to which the diffusely reflected light is peaked about the specular direction. The ALTSET project was part of

the European Commission's Standards Measurement and Testing program from 1996 to 1999. Its main objective was to develop procedures to measure the angular dependence of luminous and total solar energy transmittance of complex glazings. Fixed and variable venetian blinds were included in the project. An overview of recent developments in modeling optical and thermal properties of complex windows (Rosenfeld et al., 2000) compares available models with measurements and WIS results.

Due to the complexity of the problem and inaccuracies in the existing models, many researchers work experimentally, obtaining the optical properties of venetian blinds and then use them to create simulation models (Papamichael et al. 2001, Aleo et al., 1994, Tzempelikos & Athienitis, 2001, 2002). The above experimental techniques, although giving an estimation of transmittance values for venetian blind systems, can be used in simulation only if the blind/glazing system is assumed to be a perfect Lambertian surface. However, this is often not the case, since most venetian blinds have a specular component and the spatial distribution of transmitted daylight cannot be modeled accurately. Numerical methods provide a solution to this problem. In some cases, ray-tracing techniques using RADIANCE (Reinhart & Herkel, 2000) or Monte Carlo techniques (Campbell & Whittle, 1997, Andersen, 2001, Tsangrassoulis et al., 1996) were used to predict daylight in rooms equipped with exterior venetian blinds. An accurate evaluation of daylight distribution through complex fenestration systems (such as venetian blinds) requires the knowledge of the effective properties as a function of both incident and emerging directions of light. This was achieved using the concept of Bidirectional Transmission (or reflection) Distribution Functions (BTD[R]F) (Andersen, 2002). These are defined as (Figure 2.7):

$$\text{BTDF}(\theta_1, \theta_2, \phi_1, \phi_2) = \frac{L_2(\theta_1, \theta_2, \phi_1, \phi_2)}{L_1(\theta_1, \phi_1) \cdot \cos \theta_1 \cdot d\omega_1} \quad (2.10)$$

where:

(θ_1, ϕ_1) and (θ_2, ϕ_2) are the polar coordinates of the incoming and transmitted light;

$L_1(\theta_1, \phi_1)$ and $L_2(\theta_1, \phi_1, \theta_2, \phi_2)$ are the luminances of an element of incoming and transmitted light flux;

$d\omega_1$ is the solid angle subtended by incoming light.

Very recently, Andersen et al. (2003) presented the first extensive comparison of BTDF data with ray-tracing simulation. In particular applications for venetian blinds (Andersen et al. 2003, 2005), the inclusion of the specular component in the assessment of BTDF is explained in detail and a state-of-the-art comparison of experimentally measured BTDF and ray-tracing simulation sets the framework for future work on venetian blinds modeling. Using measured or simulated BTDFs, researchers can model the optical properties of venetian blinds and then use one of the available methods for processing transmitted flux with known directional properties. The new version of Energy Plus will incorporate BTDFs in its daylighting simulation engine (Crawley et al., 2002).

2. Thermal properties

In ASHRAE (2001), the so-called “Attenuation Coefficients” are used for all shading devices. These represent the fraction of heat flux that enters the room, some being excluded by the shading. Exterior (EAC), interior (IAC) and between the glazing (BAC) attenuation coefficients are given in tables for medium and light colored venetian blinds respectively, in combination with different glazing systems. In a more detailed attempt,

the solar properties and the SHGC is used, but again the inward flowing fraction is calculated based on approximate values given in tables for particular cases.

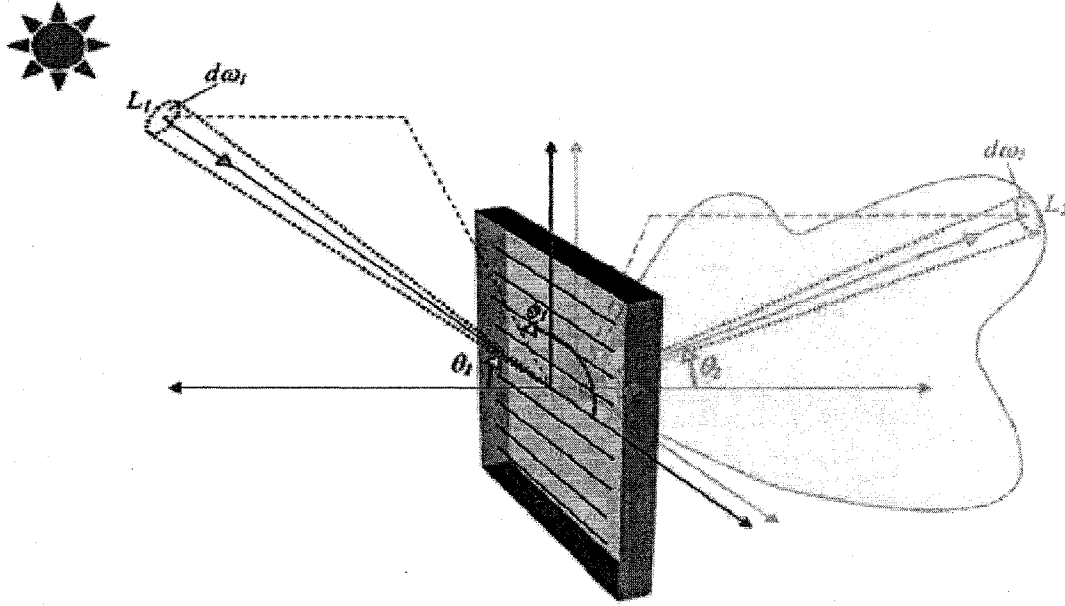


Figure 2.7. BTDF parameters for a venetian blind system (Andersen, 2005).

In a more recent similar experimental study (Fang, 2000), the U-value of interior blinds together with single and double glazing was measured and a model was produced for predicting the U-value of such window systems as a function of slat angle and indoor-outdoor temperature difference:

$$U = C_1 \cdot C_2 \cdot f(\beta) \cdot f(\Delta T) \quad (2.11)$$

where C_1 and C_2 are correction coefficients for frame effects and wind velocity. In a similar experimental study, the R-value of an integrated venetian blind system was measured using a hot box apparatus (Tzempelikos & Athienitis, 2003a). The thermal resistance of the window system varied from $R=0.524 \text{ m}^2 \cdot \text{C/W}$ (for $\beta=120^\circ$) to $R=0.784 \text{ m}^2 \cdot \text{C/W}$ (blinds fully closed, $\beta=180^\circ$).

Rosenfeld et al. (2000) parametrized the secondary inward flow and expressed it as a function of thermal resistances and a parameter (γ) that describes the spatial distribution in the absorption of the glazing/shading system. More precisely, it is the average of the product of the normalized spatial distributions of absorptance and thermal resistance across the glazing/shading system. Its value lies between 0 and 1:

$$\gamma = \int_0^1 \alpha(x) r_s(x) dx \quad (2.12)$$

where x is the distance through the glazing/shading system (perpendicular to its plane), $\alpha(x)$ is the normalized absorptance of the system and $r_s(x)$ is the normalized thermal resistance of the system. This method was initially used to calculate the total solar energy transmittance and absorption distribution function in non-scattering media from the optical and thermal properties of the component layers (Rosenfeld, 1996) and was later extended to more complex systems like integrated venetian blinds.

Most of the detailed research on thermal analysis of venetian blinds systems is conducted in Canada. Rheault & Bilgen (1989) were among the first to perform a detailed heat transfer analysis in an integrated venetian blind window system. A “control volume” was defined as a fictive cavity containing two successive slats separated. An energy balance at outside glazing, inside glazing and slat surface gives a set of non-linear equations that are solved using numerical methods. Klems & Warner (1997) calculated SHGC for venetian blind systems at different tilt angles.

The most complete series of detailed experimental and numerical studies about heat transfer through interior venetian blind systems was performed in three universities in Ontario, Canada (Waterloo, Queen’s and Toronto). The influence of heated, horizontal

venetian blinds on the convective and radiative heat transfer from a vertical isothermal surface including absorption in the venetian blind layer was first demonstrated by Collins et al. (2000). In this study, a steady, laminar two-dimensional conjugate conduction-convection-radiation model was developed and solutions were obtained using a finite element method. The assumptions used in the model were (i) the flow is steady, laminar and two-dimensional (ii) the physical properties are constant, except for fluid density (iii) grey diffuse radiation exchange is considered (Collins et al. 2002). A modified Rayleigh number is expressed as a function of the traditional Rayleigh number and then localized and average “radiation” and “convection” Nusselt numbers are defined. Radiation exchange is modeled using the net radiosity method. Solution of the heat transfer equations is achieved using CFD or finite element methods. Nusselt numbers, convective and radiative heat flux and heat transfer coefficients are evaluated along the cavity for different slat angles, aspect ratios, irradiation levels and indoor-outdoor temperature differences. It was found that the dependence of the results on slat geometry increases with heat flux. Interferometric studies for convection between the interior blind and the glazing were conducted for validation purpose (Collins et. al., 2001, Duarte et. al., 2001), and were in good agreement with the numerical models described above. Convective heat transfer coefficients results were published recently by Collins (2004).

The effect of slat angle and long-wave properties on SHGC was examined using a solar calorimeter by Collins & Harrison (2004a) and a similar to the above numerical model for calculating the thermal gain from a window with interior venetian blinds was produced (Collins & Harrison, 2004b). Overall, from the above studies it was found that the blind has a significant and complex impact on heat transfer through the glazing

system and in many cases the blind layer suppressed boundary layer growth and turbulent transition.

A method for calculation of effective long-wave radiative properties of venetian blinds (Yahoda & Wright, 2004a) was developed by applying net radiation exchange theory in a six-surface fictive enclosure. It was assumed that the slats are opaque and grey surfaces. This study presents results on reflectance, absorptance and transmittance of venetian blinds as a function of slat angle and aspect ratio, and includes modifications about the curvature of slats as opposed to the flat-type approximation. A continuation of this study (Yahoda & Wright, 2004b) allowed a complete heat transfer analysis of integrated venetian blinds, using the radiative properties calculated before and simplified equations for convection heat transfer coefficients across venetian blind layers presented below. Then, U-values for glazing systems with integrated venetian blinds were calculated as a function of slat angle and aspect ratio, and were compared with the experimental results of Garnet et al. (1995).

2.6.1.2. Roller shades

1. Optical properties

Roller shades are maybe the most commonly used shading system, due to its easy operation and low price. They are usually manually controlled to satisfy occupants' needs concerning privacy and glare issues. The optical properties of roller shades are generally assumed to be constant and independent of incidence angle; they are usually considered perfect diffusers. ASHRAE (2001) uses the same methodology as for venetian blinds. For optical properties of interior roller shades, they provide limited data for very few cases of

opaque shades. Most of the time, roller shades are not opaque -they have a certain transmittance. It is mentioned that roller shades (like venetian blinds) are assumed to be perfect diffusers. Surprisingly, there is no different approach in modeling optical properties of roller shades found in literature. Even Energy Plus (2004) models roller shades as perfect diffusers. This means that direct radiation incident on the shade is reflected and transmitted as hemispherically uniform diffuse radiation: there is no direct component of transmitted radiation. It is also assumed that the transmittance, reflectance, and absorptance are the same for the front and back of the shade and are independent of angle of incidence. In published work about modeling transmitted daylight through roller shades (Athienitis & Tzempelikos, 2005a), this same approach was followed. Nevertheless, there are recent indications that the visible and solar optical properties are not equal, and that the shade is not always performing as a perfect diffuser, depending on its construction and material properties.

2. Thermal properties

ISO 15099 (2003) analyses convection heat transfer between glazing layers without referring to roller shades. It is mentioned that, for exterior shading devices, CFD modeling is required. Otherwise, for natural convection the convective coefficient is expressed as a function of Nusselt number and for forced convection a simplified equation can be used:

$$h_{ex} = 4 + 4V_s \text{ [W/m}^2\text{K]} \quad (2.13)$$

where V_s [m/s] is stream velocity near the fenestration surface. For the internal side (natural convection), interior convective heat transfer is again expressed as a function of Nusselt number, which is a function of Rayleigh number depending on window tilt angle.

ASHRAE (2001) follows exactly the same procedure as for venetian blinds, as described in the previous section. Attenuation coefficients are used for exterior, interior and between the glazing roller shades, which are given in tables for some specific products.

In Energy Plus, heat transfer modeling through exterior/interior roller shades and glazing systems is done as follows: a heat balance equation is applied at glazing(s) and shade interior and exterior surfaces (Figure 2.8).

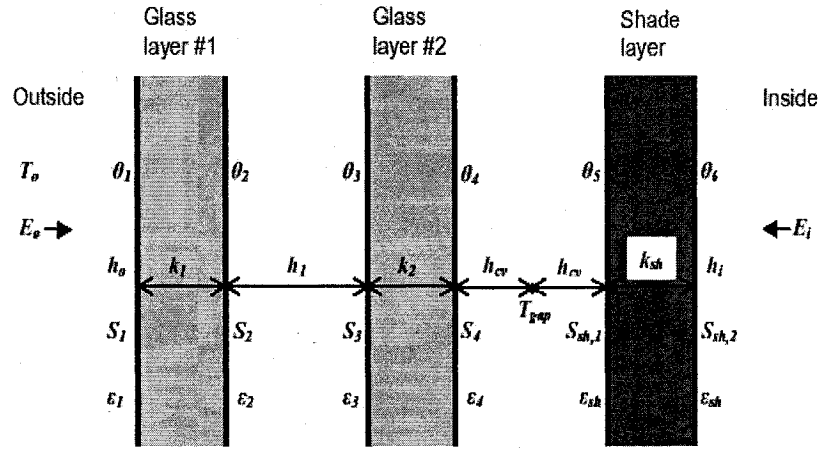


Figure 2.8. Glazing system with two glass layers and an interior shading layer showing variables used in heat balance equations (Energy Plus, 2004).

The heat balance equation for the shading layer surface facing the gap is:

$$\frac{E_i \tau_{sh} \rho_4 \epsilon_{sh}}{1 - \rho_4 \rho_{sh}} + \frac{\sigma \epsilon_{sh}}{1 - \rho_4 \rho_{sh}} \cdot [\epsilon_4 \theta_4^4 - \theta_5^4 (1 - \rho_4 (\epsilon_{sh} + \rho_{sh}))] + k_{sh} (\theta_6 - \theta_5) + h_{cv} (T_{gap} - \theta_5) + S_{sh,1} = 0 \quad (2.14)$$

where ρ is long-wave diffuse reflectance, ϵ is long-wave emissivity, τ is diffuse long-wave transmittance, k_{sh} is the shading layer conductance, S_{sh} is the total radiation (solar +

long-wave) absorbed by the gap-side face of the shading layer and h_{cv} is the convective heat transfer coefficient. A similar equation is written for the shading surface facing inside (zone air). For exterior/interior shades, the convective coefficient and the gap temperature depend on the air velocity in the gap, which is a function of height of shading layer, glass/shading layer separation (gap depth), zone air temperature for interior shading or outside air temperature for exterior shading, and shading layer and glass face temperatures. A pressure balance is used to determine gap air velocity, gap air mean equivalent temperature and gap outlet air temperature according to ISO 15099 (2003).

2.6.2. Airflow windows and double-skin facades

An innovative system that has been initially used in Europe is the airflow window (Figure 2.9). Instead of using sealed double glazing, a flow of room air is introduced in the cavity between the glazing panes. Venetian blinds or roller shades are usually installed in the cavity, to modulate sunlight and daylight. By intercepting direct sunlight, the blinds act as a solar collector surface. The moving air stream transports the thermal gain for redistribution, storage, or rejection (Manz, 2004). Solar gains can be therefore controlled while clear glass is used for its daylighting advantage. More advanced systems are being developed and studied, in which outside air also enters the window cavity, and then it is rejected or used depending on the climate. Creating buffer zones using double facades is a new approach followed in Europe (particularly in Germany). The core space is “protected” from the outside, while the buffer zone can be well used for natural ventilation strategies.

Incorporating photovoltaic panels within the cavity further complicates the problem, but creates a potential for increased thermal and electrical efficiency (Mei et al., 2003, Charron & Athienitis, 2002). Pre-heated air flowing through a double-skin façade can be used by the HVAC system, while at the same time cools the surface of photovoltaic panels, increasing their efficiency.

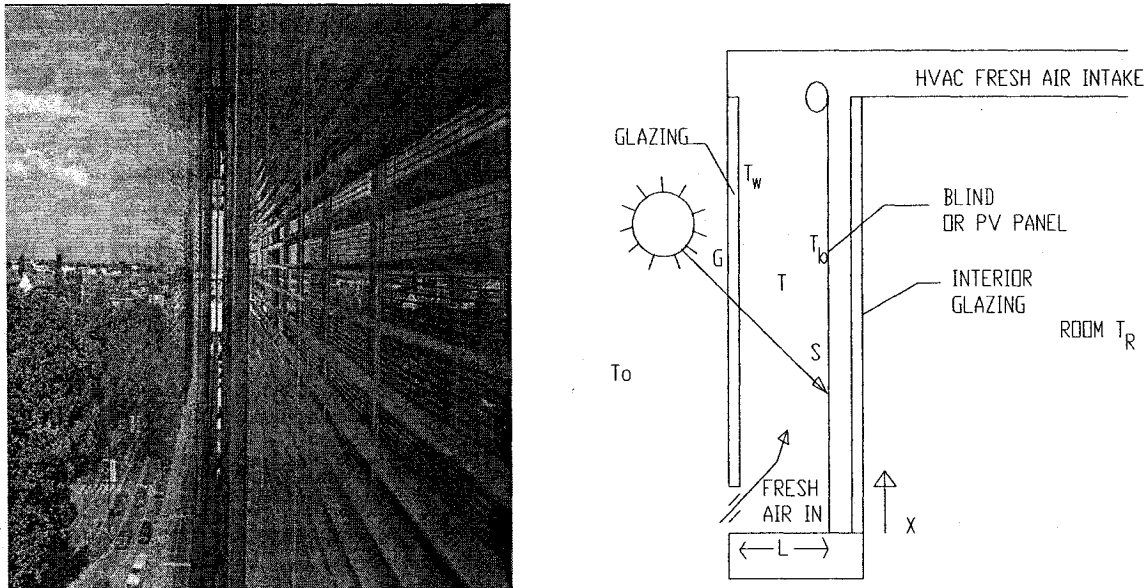


Figure 2.9. Example of existing airflow window and schematic.

2.7. Integrated daylighting and thermal analysis for commercial buildings

2.7.1. Coupling daylighting and thermal simulation

The main focus of building simulation programs has always been the thermal performance of buildings. For this reason, several types of software have been developed, ranging from simple steady-state heat transfer calculations to detailed transient models. The aim of these programs is to predict thermal loads and variation of interior temperatures. An extensive overview of existing models was completed by Balaras

(1996). Advanced methods like the Heat Balance method (Pedersen, 1997), the Radiant Time Series method (Spittler, 1999) and finite difference methods (thermal networks) can predict the dynamic thermal response of commercial buildings with good accuracy.

Developments in dynamic building envelope technologies have created new energy-efficient opportunities to achieve significant savings in building energy, peak demand, and cost, with enhanced occupant satisfaction. Dynamic building envelope technologies include actively controlled shading devices (or advanced glazings), airflow windows and integrated photovoltaic systems. Coupled with electric lighting control systems, dynamic envelope and lighting systems can be actively controlled on a small time step to reduce the largest contributors to commercial building energy consumption: lighting and cooling due to internal gains.

Fenestration systems are the critical link between the daylighting and the thermal performance of perimeter spaces of commercial buildings. The optical and solar properties of fenestration systems determine interior conditions, for a specific amount of thermal mass used. Daylighting is a systems integration challenge, involving building site and orientation, fenestration systems design and control, lighting systems design and control, and dynamic HVAC components operation. Therefore integration of daylighting with thermal simulation is necessary, in order to achieve a successful design.

The first dynamic link of combined daylighting and thermal performance is the glazing optical and thermal characteristics. These have been studied in detail and simulation-based tools for the integrated appraisal of advanced glazings were the outcomes of big projects like IMAGE in Europe (Clarke et al., 1998) and work funded by the U.S. Department of Energy (Johnson et al., 1984). These tools provide designers with

information about selection of glazings and estimation of their overall performance. However, they do not include shading devices and glazing products are imported from existing databases.

The second dynamic link between daylighting and thermal simulation is the shading device. Shading device properties and control should be designed such to satisfy problems inevitably associated with glass usage (glare, overheating) and require a second round of integrated approach in order to reach optimum results. The impact of shading has a significant impact on peak loads, energy consumption, daylighting performance and visual comfort. Fortunately, some studies have considered this problem and applied an evaluation of shading overall performance. Lee et al. (1998) estimated experimentally the thermal and daylighting performance of an existing automated venetian blind system with a dimmable electric lighting system in a full-scale private office at LBNL. Dynamic impacts of blind control on daylight levels and cooling load were identified and measured. Another study discussing blind control strategies and criteria revealed the complexity of the problem (Lee & Selkowitz, 1995). A simulation and experimental study of motorized between-glass venetian blinds (Tzempelikos & Athienitis, 2002) showed the impact of control on overall energy performance.

An effective measure for quantifying the benefits of daylight utilization with respect to energy consumption is the effect on electric lighting usage. A shading device operating in conjunction with controllable lights could lead to minimization of electricity consumption for lighting and possible thermal benefits (Lee et. al. 1995, 1998, Tzempelikos & Athienitis, 2002, 2003b). A simulation study by Herkel (2003) showed that the key between linking electric lighting operation and thermal simulation is the

iterative modeling of the control of the shading device. Recently, an extensive study of the impact of venetian blinds on two types of lighting control for different sky conditions showed the potential for energy savings and the complex dependence on variability of sky conditions (Galasiu et al., 2004).

2.7.2. Limitations and problems with existing tools

Traditionally, the approach followed was to estimate internal gains from lights, which would contribute to space cooling load. However, dynamic operation of shading devices was completely neglected. Recently, with significant architectural developments, the advantages of daylighting have been re-identified and the need for detailed simulation programs integrating thermal and daylighting performance is strong (Selkowitz, 1998). As a result, some researchers have tried to couple daylighting and thermal simulation. However, few have truly realized the key issues and the complexity of the problem - emphasis was given in glazing design optimisation. The number of integration studies including shading device utilization is almost non-existent, according to extensive literature reviews of existing software tools and methods (Zmeureanu, 1997).

The DOE-2 energy simulation engine (Winkelmann et al., 1993) uses the daylighting results from ADELIN software (Erhorn et al., 1998), following a sequential-type approach. Nevertheless, this has an effect on the integration with HVAC system operation (link consistency and data exchange). Moreover, this software uses the concept of the split-flux method, carrying all the resulting disadvantages. More recently, angle-dependent modifiers can help solving some of the problems, but they require significant computational effort and they are not yet standardized.

The dynamic coupling between the widely used and validated tools ESP-r (Clarke, 1997) and RADIANCE (Larson, 1993) by Janak (1998) links daylighting, electric lighting and thermal/airflow simulation. The simulation process is controlled by ESP-r and the lighting engine of RADIANCE is called when required, to perform a detailed ray-tracing-based lighting analysis at each simulation time-step. The problems associated with shading configurations were avoided by using the concept of daylight coefficients and a discussion about photo-sensor controls provided guidelines for integration (Clarke, 2001). The whole process is computationally demanding and requires extensive knowledge of both simulation programs. Recent efforts in coupling Lightswitch (Reinhart, 2002) and ESP-r are very promising (Bourgeois et al., 2004).

ENERGY Plus (Crawley et al., 2002) is a state-of-the-art new generation integrated building simulation software tool. It solves the sequential deficiency of DOE-2 by using integrated techniques at all simulation levels and supports fully integrated simulation for loads, systems and plant. It uses WINDOW 5.0 software (Arasteh, 1994) to handle angular-dependent optical and thermal properties of advanced glazing products, and uses the Perez model (Perez et al., 1990) for calculation of irradiance and illuminance values. The daylighting module can simulate controllable shading devices and produces interior illuminance values, glare indices, and reduced electric lighting operation to be used by the heat balance module. The new release even includes bi-directional transmission functions for complex fenestration products. Despite all improvements, the daylighting engine of DOE-2 is still used and inter-reflection calculations are not simulated accurately. Furthermore, the major disadvantage is that this program does not yet have an interface.

2.7.3. Research needs and aim of Thesis

Except for the disadvantages mentioned above, the main problem is that the latest integrated building simulation software engines (ESP-r, ENERGY Plus and TRNSYS) are used to evaluate the overall energy performance of existing buildings, or in the best case, in the design development stage, when the building form is already determined. The reason for that is that detailed input data is required in order to run even the simplest simulation. ENERGY-10 version 1.6 (BSG, 2002) is a new simulation tool developed specifically for use at conceptual design. Daylighting, passive solar heating, and low-energy cooling strategies are integrated with energy-efficient shell design and mechanical equipment. The program performs hourly simulations for a typical year and was validated using the BESTEST protocol. Thermal analysis uses the California Nonresidential Simulation Engine (CNE) developed by the Berkeley Solar Group, which employs a multizone, thermal-network solution (Wilcox et. al, 1992). However, it is applicable to small buildings and it also uses the split-flux method. Future improvements of this program are very promising. In a comparative study between three simulation programs for calculation of energy savings using energy-efficient measures (Zmeureanu et al., 1995), up to eight different (static) models had to be developed in each software. Other studies (Mahdavi, 2003) try to provide guidelines for selection of shading device type based on traditional optimisation methods, by using objective functions. Unfortunately, many parameters cannot be described in this way (they are just being neglected) and the results are based on subjective values for weighting factors.

In general, a gap between the potential benefits claimed for daylit buildings and the actual achievement in building practice remains. There is no argument that a very

experienced designer is capable of producing a successful design. However, not all designers are very experienced and many of the successful designers do not know how to apply innovative systems and new promising technologies in a new design, based on an integrated approach. In reality, advanced building simulation programs are used to “optimise” design solutions selected on a subjective basis at the conceptual design stage.

Currently, there is no systematic methodology for performing a detailed and dynamic integrated daylighting and thermal analysis of buildings during the early design stage, when critical decisions with small economic impact could lead to significant energy savings during the lifetime of the building and simultaneous improvement in interior conditions. Integrated daylighting and thermal analysis of commercial buildings’ facades in the early design stage should lead to the development of guidelines for selection of fenestration system properties and dynamic control. This should be achieved with objective to lower energy demand for lighting, heating and cooling, while at the same time, maximize daylight utilization for the occupants without creating discomfort problems. Multifunctional facades, which will fulfill all desired requirements for energy efficiency and comfort, would hopefully be the result of this approach, as a recent study revealed (Tzempelikos & Athienitis, 2003b). It is the purpose of this work to address these research needs as follows:

- Develop a systematic methodology for integrated thermal and daylighting analysis for facades and perimeter spaces of commercial buildings during the early design stage, applicable to any location, orientation, glazing type and shading device type;
- Consider fenestration properties as design variables and provide the architect/building designer with appropriate performance-based measures to select form, glass ratio of

façade, shading device properties and control strategies based on an integrated thermal and daylighting simulation-based approach;

- Address the need to consider innovative dynamic fenestration systems from the beginning of the design process and compare fenestration design options on a relative basis for the selection of design solutions;
- Select the required degree of detail in the analysis performed for each component at this initial stage to maintain accuracy but reduce computation time and unnecessary complexity;
- Develop a prototype simulation design support tool that can be used by building designers at the early design stage, to provide fenestration design guidelines based on an integrated daylighting and thermal analysis.

CHAPTER 3. DEVELOPMENT OF AN INTEGRATED THERMAL AND DAYLIGHTING DESIGN METHODOLOGY

3.1. Simulation in the early design stage

During the early design stage, the building geometry, characteristics and materials are still being formulated. Therefore the simulation approach should not be the analysis of a specific design solution, but the systematic exploration of inter-related design alternatives, in order to provide the building designer with a set of efficient design solutions. In general, there is less interest in finding “optimal” design solutions in the strict sense of the word (Mahdavi, 2004). Performance-based design support environments can be used in a flexible, dynamic and iterative manner. Moreover, optimization methods cannot be considered as design support tools, since they only produce optimal values. Design process is not about generation of unique solutions but a multi-level integrated process.

For perimeter spaces, the simulation procedure in this stage should be able to take into account daylighting and thermal parameters, link them in an integrated way, and provide a method for quantitative and qualitative evaluation of design options based on performance-based measures. Since fenestration systems are a key element when designing for daylight, emphasis should be given on the selection and type of analysis of fenestration systems. Driven by technological advances in transparent building facades, design alternatives have shifted to utilizing dynamic fenestration and shading systems for optimal control of daylighting and solar gains. Therefore different building system aspects –daylighting, electric lighting, heating, cooling, shading) have to be considered in

parallel when making early stage decisions. The transition from component-based simulation to a “systems” approach is a key issue for an integrated design process. Components, such as shading devices, can be modeled using one of the methods presented in chapter 2. The effect of variation of the design variables on performance-based parameters could give a more complete picture of design solutions.

The following sections describe the general methodology developed for daylighting and thermal simulation, the coupling between the two and the extraction of useful information based on performance indices generated by the continuous interaction between them. An important requirement is the production of hourly data that will be used for daily, monthly or yearly calculations. The simulation-based approach followed is to create generalized performance indices (at a systems level) as parametric functions of key design parameters (at a component level, such as the glass area of the façade) and then provide the designer with useful information for the selection of the desired value based on the integrated analysis results. The methodology presented in this chapter applies to perimeter spaces of commercial and institutional buildings (particularly private offices) for any location, orientation, glazing type and shading type.

3.2. Theoretical basis for an integrated thermal and daylighting methodology during the early design stage

Early stage design for perimeter spaces is essentially a systems integration challenge, involving all parameters connected to integrated daylighting and thermal performance. The complex interactions between fenestration system design, shading device properties and control, electric lighting control, thermal parameters, human requirements, building

orientation and climatic parameters have to be evaluated from the beginning and provide feedback until the final design stage.

The key issue for coupling the two domains is to determine a set of linking parameters that have an impact on both the thermal and lighting performance of the space. The dynamic interaction between lighting and thermal simulation can then be described by investigating the relationship between these linking parameters and the simultaneous impact on the two domains during the actual simulation process.

Furthermore, a deeper exploration of dynamic links between lighting and thermal performance leads to a distinction between direct and secondary links. Direct links have an immediate impact both on the daylighting and the thermal performance (e.g. amount of transmitted daylight and solar radiation). The following parameters were identified as direct dynamic links between daylighting and thermal simulation:

- Window size
- Window properties
- Shading device type and properties
- Shading device control

Secondary links work like transfer functions. They transfer the dynamic effect of direct links on one domain to the other domain. A secondary dynamic link is the electric lighting control. It is considered a secondary link because, for a given set of direct links, it operates by reading data from the daylighting module and dynamically transfers the effect to the thermal module in the form of resulting internal gains (Figure 3.1).

Finally, linking parameters are separated into continuous and discrete. For example, window size and properties are continuous parameters because simulation could run as a

function of different values. Shading type and control and electric lighting control are discrete parameters because they can take certain values; in a way, they act like interactive boolean operators during the simulation process.

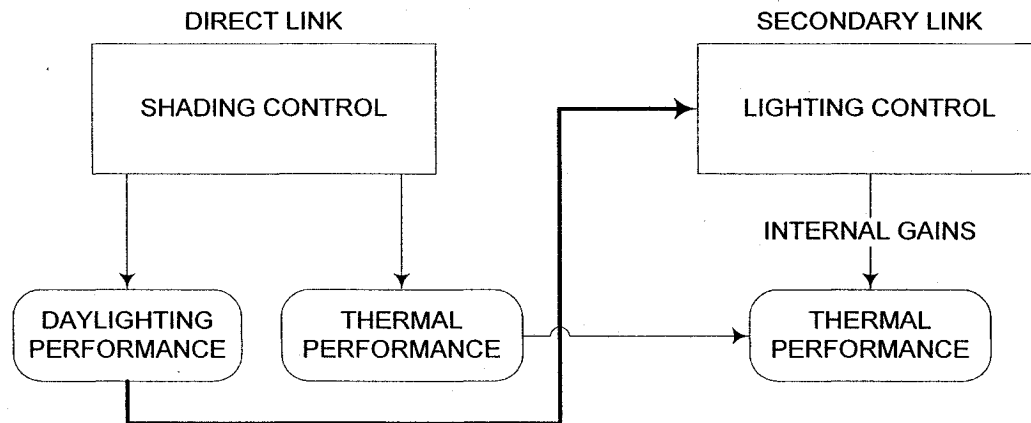


Figure 3.1. Schematic showing distinction and relation between direct and secondary links in the coupling process.

The interaction between the thermal and lighting simulation with the direct and secondary linking parameters is an iterative process. For instance, thermal and lighting simulation will run considering a continuous distribution function of direct continuous links and a set of values for discrete direct links, and values for linking parameters will be selected based on the results of integrated thermal and lighting simulation, taking into account variations in all other links. This iterative sensitivity analysis approach continues until desired values are computed for all parameters, using as measures, correlations between generalized performance indices generated by the continuous interaction between the two domains during the actual simulation process. This dynamic process aims at providing the building designer with significant performance-based measures for

making important decisions during the early design stage, using as basic criteria the following:

- Maximization of daylight utilization for the occupants
- Elimination of glare, and interior illuminance uniformity
- Reduction in peak thermal loads
- Reduction in energy consumption for heating and cooling
- Reduction in electricity consumption for lighting.

Figure 3.2 summarizes the process of coupling and the interactions between linking parameters in the simulation methodology. The last step is computation of correlations between integrated performance-based measures. The details about the individual linking parameters and interactions with the integrated daylighting and thermal simulation design process are described in section 3.5.

3.2.1. Integrated performance indices

The last step of the general methodology is to produce certain “integrated performance indices”. The purpose of these measures is to include useful information to help the designer compare design options on a relative basis. The definition of these parameters implies that the performance indices must have certain characteristics:

- (i) A performance index must be generalized. It has to be a general parameter that includes the impact of climate and building characteristics so that the same unique index can be used to describe the overall performance of perimeter spaces of different form

(e.g., different fenestration) and in different locations, for consistent comparison of measures.

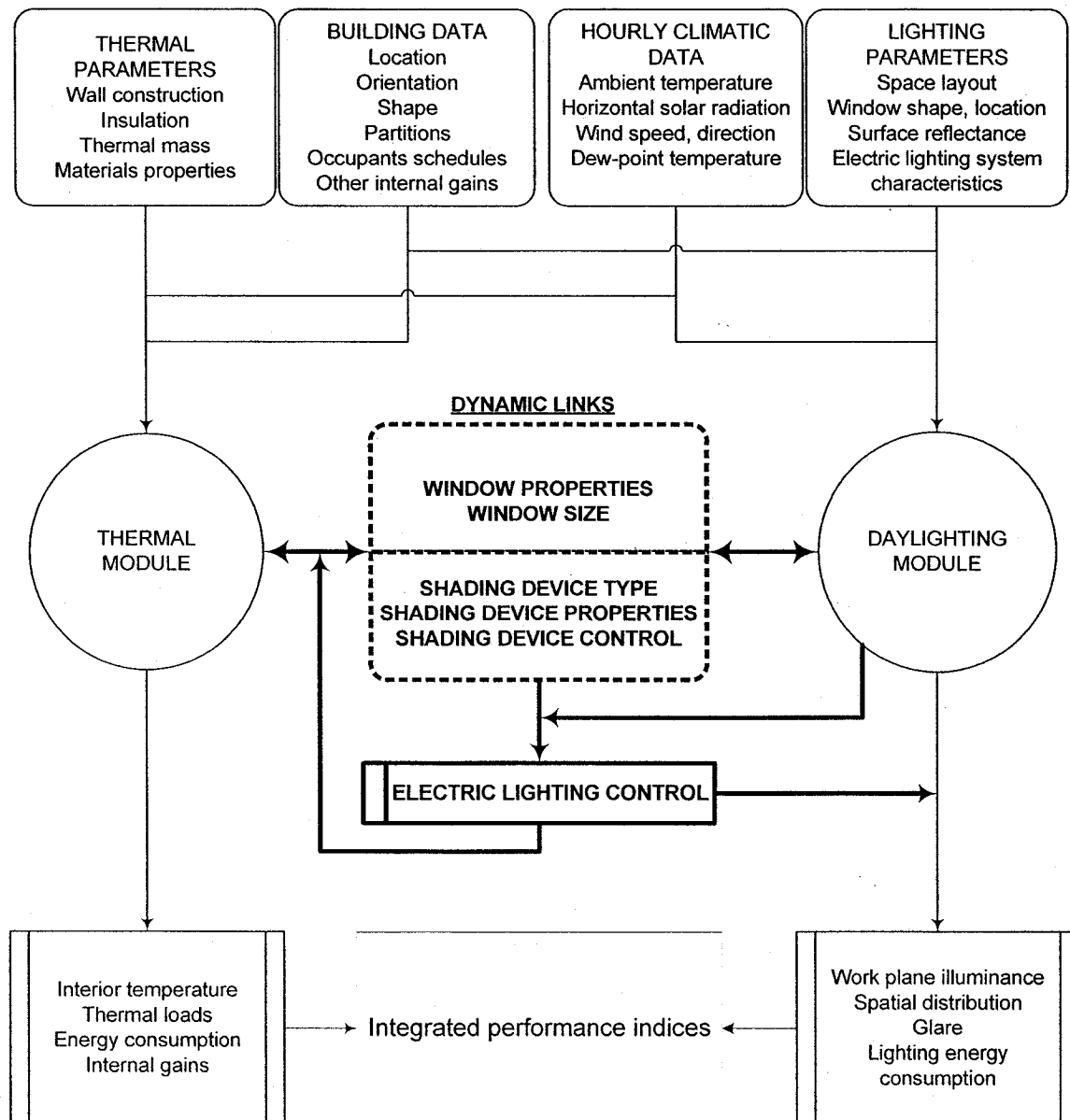


Figure 3.2. Process of coupled daylighting and thermal simulation and the interaction with dynamic links.

(ii) A performance index must preferably be time-independent. Instead of giving a static picture of the thermal/daylighting conditions in a room, it should contain all the necessary

information for sufficient evaluation of the integrated performance of a space. For example, work plane illuminance distribution is not an appropriate performance index since it changes with time. A first step to overcome these problems is to consider annual performance parameters and not values at particular times.

(iii) An integrated performance index is generated by the interactive simulation process and must include the combined effects of linking parameters on daylighting and thermal simulation. Since the links describe interactions between thermal and daylighting domains, a performance index could describe directly one or both domains. Moreover, it must not describe a specific component (or link) but should include their impacts on a systems level.

(iv) For a given set of direct and secondary links, each performance index is represented by a single numerical value. Thus, comparison of integrated performance of spaces could be made simply by comparing single values. However, it is an objective of the current methodology to study the variations of integrated performance indices as a function of linking parameters, so that the designer can make decisions about selection of linking values based on the variation of performance indices. Moreover, correlations between two integrated performance indices could serve the same purpose on a different level, as discussed later.

The above characteristics provide the basis for choosing reliable performance-based measures. The following parameters have been selected as integrated performance indices:

- **Annual heating and cooling energy demand.** These are the most obvious measures, since they contain all the information used in the simulation process and they enclose the combined impact of all linking parameters. This is a general index used by all major simulation software to describe the energy performance of buildings.
- **Peak thermal loads.** Although this index does not characterize the annual energy performance of buildings, it is equally important because (i) during the early design stage it is the measure that determines the HVAC system size (and initial costs) and (ii) study of the dependence of this index on dynamic links for perimeter spaces can provide critical information about load shape and characteristics.
- **Daylight availability ratio (DAR) or daylight autonomy.** There is a need for a generalized index that represents the overall daylighting efficiency in a space. Hourly work plane illuminance profiles are not an appropriate index, since they change continuously. A transformation from hourly values to an annual universal index was achieved using the concept of daylight availability ratio. This is defined as the fraction of time in one year during which sufficient daylight (more than a pre-specified set point) is available on the work plane imaginary surface. The advantages of using this measure are clear: (i) it is a general, time-independent index that fully describes the daylighting availability in a room, taking into account the yearly impact of all fenestration parameters and (ii) it provides the all the necessary information for straight computation of electric lighting energy consumption. None of the existing building simulation software (except for DAYSIM -Reinhart, 2004) provides such a useful index. Instead, tables of work plane illuminances are usually given as output.

- **Energy consumption for electric lighting.** This is also a useful integrated performance index because it includes the impact of all direct linking parameters plus the secondary link of electric lighting control. Electricity consumption for lighting accounts for a large part of total energy consumption,. Also, this index carries one of the impacts of daylighting (on which it depends) on the thermal performance by means of internal gains.

Before analyzing the role of each linking parameter and the interactions between the daylighting and thermal simulation process, the daylighting and thermal simulation modules used in this methodology are presented next with calculation of the above performance-based measures.

3.3. The daylighting simulation module

We refer to daylight as the visible portion of solar radiation in order to separate the daylighting from the thermal effects. The daylighting model consists of three parts: (i) calculation of incident daylight on a window surface (ii) calculation of transmitted daylight in the space and (iii) computation of work plane illuminance distribution. Daylight availability ratio can be then computed.

3.3.1. Incident daylight on a facade

The amount of available daylight incident on a surface can be calculated using the methods described in section 2.4.3. In this work, the following method is used:

Instead of predicting exterior illuminance using one of the available models, that have high uncertainty, available hourly measured values of horizontal solar radiation are used to initially predict horizontal exterior illuminance. Such data are provided for many

locations in the United States and Canada by the US Department of Energy website (<http://www.eere.energy.gov/buildings/energyplus/weatherdata.html>) and for every pixel of satellite maps in Europe by the European database for daylight and solar radiation (www.satellite.net). The latter source also provides illuminance charts, frequency distributions and data so that daylight levels can be directly imported. Usually, the available weather files are Typical Meteorological Year (TMY) files that contain hourly global and direct (or diffuse) horizontal irradiance data for one year. These are measured data, hourly averaged over the last thirty years and provide a reliable source of accurate information. If no such data are available for a particular location, a prediction procedure was summarized in section 2.4.3.

Hourly horizontal beam (E_{bh}) and diffuse (E_{dh}) illuminance values are calculated using the validated Perez et al. (1990) luminous efficacy model. This model is used by all state-of-the-art daylighting and solar radiation simulation software and it is presented in detail in Appendix C. Then the direct (beam) and direct daylight components are treated separately as follows.

- Incident beam daylight on a tilted surface

The solar position is determined by a 3-d angle with spherical coordinates, the solar altitude (α) and the solar azimuth (ϕ). These angles are a function of day number (n) and solar time (t). A major parameter in determining the amount of direct light reaching a surface on earth is the solar incidence angle (θ), which is the angle between the sun's rays and a line normal to the surface, given by (Appendix A):

$$\theta(n, t) = \cos^{-1}[\cos(\alpha(n, t)) \cdot \cos(\phi(n, t) - \psi) \cdot \sin(\beta) - \sin(\alpha(n, t)) \cdot \cos(\beta)] \quad (3.1)$$

where ψ is the orientation of the surface and β the tilt angle of the surface. In Equation (3.1), the solar incidence angle is expressed as a function of day number and solar time, to be used in an hourly basis by the simulation program later. The hourly beam normal illuminance is calculated by:

$$E_{bn}(n, t) = E_{bh}(n, t) / \sin(\alpha(n, t)) \quad (3.2)$$

Then the hourly direct daylight incident on a tilted surface is equal to:

$$E_b(n, t) = E_{bn}(n, t) \cdot \cos(\theta(n, t)) \quad (3.3)$$

- Incident sky diffuse daylight on a tilted surface

The hourly sky diffuse daylight on a tilted surface (E_{sd}) is calculated using the anisotropic diffuse Perez et al. (1990) model (Appendix C). In this model, diffuse radiation is split in three components: (i) isotropic part, received uniformly from all the sky dome (ii) circumsolar diffuse, resulting from forward scattering of solar radiation and concentrated in the part of the sky around the sun and (iii) horizon brightening, concentrated near the horizon, most pronounced in clear skies. Anisotropic sky models have been produced initially by Hay & Davies (1980), and further developed by Reindl et al. (1990). An anisotropy index is used to account for a portion of diffuse radiation which is treated as forward scattered. The Perez et al. model (1990) has been proved to be the most accurate for treating the three parts of diffuse radiation on a tilted surface, although errors are inevitable in some cases (Cucumo et al., 2004).

- Incident ground-reflected daylight on a tilted surface

Another part of incident diffuse daylight comes from reflection on the ground (E_{gd}). This can be approximated by multiplying the total horizontal illuminance with the ground reflectance and a “view factor” between the ground and the surface:

$$E_{gd}(n, t) = [E_{bh}(n, t) + E_{dh}(n, t)] \cdot \rho_g \cdot \frac{1 - \cos(\beta)}{2} \quad (3.4)$$

where ρ_g is the ground reflectance. For a vertical window, the view factor becomes equal to 0.5, since the window sees only “half of the sky”.

The total amount of incident diffuse daylight is equal to:

$$E_d(n, t) = E_{sd}(n, t) + E_{gd}(n, t) \quad (3.5)$$

3.3.2. Calculation of transmitted daylight in a room

Transmitted beam and diffuse daylight are calculated separately. For each component, the amount of transmitted light is equal to the amount of incident daylight multiplied by the window transmittance. The optical properties of windows are usually calculated from the optical properties of the individual glass layers. The three basic quantities: transmittance (τ), front reflectance (ρ^f) and back reflectance (ρ^b) are used and they are a function of wavelength and incidence angle. These properties can be estimated according to ISO 9050 (1998), or using any other standard tool or method with acceptable results.

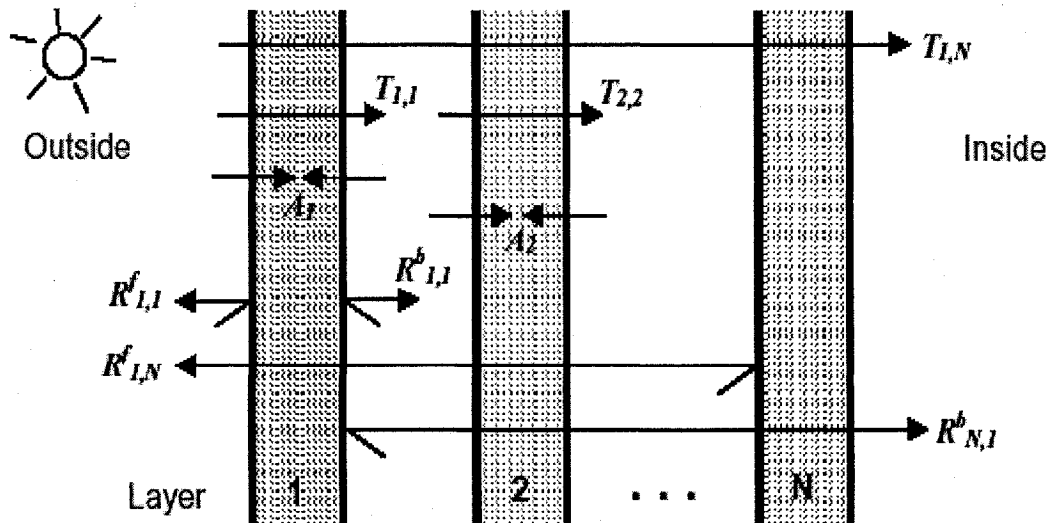


Figure 3.3. Glazing system consisting of N glass layers (e⁺ manual).

Solving the recursion equations between layers (i) and (j), including inter-reflections, yields for the beam component:

$$\tau_{i,j} = \frac{\tau_{i,j-1} \tau_{j,j}}{1 - \rho_{j,j}^f \rho_{j-1,i}^b} \quad \rho_{i,j}^f = \rho_{i,j-1}^f + \frac{\tau_{i,j-1}^2 \rho_{j,j}^f}{1 - \rho_{j,j}^f \rho_{j-1,i}^b} \quad \rho_{j,i}^b = \rho_{j,j}^b + \frac{\tau_{j,j}^2 \rho_{j-1,i}^b}{1 - \rho_{j-1,i}^b \rho_{j,j}^f} \quad (3.6)$$

A detailed explanation of the above may be found in ASHRAE (2001), Hollands et al. (2001), or Rubin et al. (1998). Each property is a function of solar incidence angle and wavelength, thus it could be expressed as a function of time for hourly energy calculations (Appendix D). A large set of glazing and window system properties is available in ASHRAE Handbook (2001). The WINDOW software (2003) uses a very large database of thermal and optical properties of different types of glazings and windows and it can perform a detailed optical and thermal analysis of all kinds of window systems (excluding shading devices). Therefore it is used by most of the advanced building simulation software, to accurately simulate thermal and optical properties of windows. The diffuse window transmittance is equal to the direct transmittance when solar incidence angle equals 60° . The total amount of daylight transmitted into the room is equal to the sum of the product of each transmittance component with the respective amount of incident daylight:

$$D(n, t) = E_d(n, t) \cdot \tau_d(n, t) + E_b(n, t) \cdot \tau_b(n, t) \quad (3.7)$$

where $\tau_d(n, t)$ is the diffuse window transmittance and $\tau_b(n, t)$ is the beam window transmittance expressed as a function of day number and solar time.

If a special selective coating is used, the transmittance is a complicated function of solar incidence angle or wavelength (Karlsson & Roos, 2000, Correa & Almanza, 2004, Wilson, 2000). Angular properties for coated and uncoated glazings are calculated using

optics theory. If a shading device is used, the effective transmittance of the glazing-shading system is calculated as a function of time, based on the type and the optical properties of the shading device. Moreover, shading control schedules are also considered by the daylight simulation model so that the hourly analysis includes the continuous impact of shading properties and control on the interior daylight conditions. In any case, the total effective fenestration transmittance should be evaluated as a function of solar and geometrical angles in an hourly basis, in order to be used for further analysis.

3.3.3. Illuminance distribution on the work plane

The final step is to calculate the illuminance distribution on the work plane (assumed at 0.8 m height from the floor) using one of the advanced methods presented in section 2.4.4. Under overcast skies, the diffuse light entering the space is assumed to be distributed uniformly on all room surfaces, and the radiosity method can be directly applied to calculate luminous exitances of all interior surfaces considering the window as a uniform Lambertian source (Tzempelikos & Athienitis 2002). After computing view factors between interior surfaces, configuration factors are calculated for a selected grid on the work plane area and the final work plane illuminance distribution is determined (Appendix G). For clear sky, a division must be made between the direct and the diffuse part of transmitted light. For the diffuse portion, the same method as for the overcast sky is applied. For direct light, the surface(s) on which it is incident are considered first and their luminous exitances are calculated. Then the method continues as for the overcast sky case, using as light sources the window and the surfaces that are directly illuminated. If there are mirror surfaces or specular reflections in the room, another modified method should be applied. The daylight coefficients method (Tregenza, 1983) can be also applied

for calculation of work plane illuminance under all sky conditions. In this case, daylight coefficients for direct and inter-reflected light are evaluated separately and multiplied by the corresponding patch luminance to obtain hourly illuminance on a point in the room.

3.3.4. Calculation of annual daylight availability ratio

Daylight Availability Ratio (DAR) for a point in the room can be computed from the hourly work plane illuminances. Each value higher than 500 lux (or another target illuminance, if desired) contributes to DAR. Annual DAR is equal to the fraction (%) of the hourly work-plane illuminance values in a year that are higher than 500 lux. This performance index describes the annual daylight efficiency in a room for a certain window system and includes the effect of climate and building characteristics. As explained later, it is a critical factor when selecting window size. A step-by-step description of the overall daylighting simulation process is also presented in chapter 4.

3.4. The thermal simulation module

A thermal network approach is used to simulate thermal performance of considered spaces. Thermal network methods discretize the building into a network of nodes with interconnecting paths, through which energy flows. They can be considered as a refinement of the Heat Balance Method (ASHRAE, 2001). For each heat transfer element, the Heat Balance Method uses one interior surface node and one exterior surface node; the thermal network model may include many additional nodes depending on the accuracy and the detailed desired. Thermal network models can include non-linear heat transfer coefficients and model accurately radiation and convection separately. They

depend on a heat balance at each node to determine the node temperature and energy flow between all connected nodes. A range of techniques may be used to model the energy flow between two nodes. Finite difference models are one of the most efficient techniques used for building simulation (Clarke, 1985). A set of algebraic and differential equations is used and the numerical solution is separated from the model.

In this study, each surface layer is represented by one or more regions. Each region is represented by a node, connected by one or more thermal resistances to other neighboring nodes. The thermal resistances in the network represent the heat flow by conduction, convection and radiation from one node to another. For conduction, the thermal conductivity (k), area (A) and thickness (L) of each material are required. Conduction thermal resistance is then calculated as $R=L/kA$.

Convection and radiation are separated and can be modeled in different degrees of detail, depending on the systems considered. Convection heat transfer coefficients are calculated using the Energy Plus (2004) equations for convection. Convection between interior surfaces and room air is modeled by:

$$h_c = 1.31 \cdot (T_s - T_{air})^{1/3} \quad (3.8)$$

where T_s is the surface temperature and T_{air} is the air temperature. ASHRAE (2001) provides similar equations for heat flow upwards, downwards etc.

Radiation between all interior (and exterior) surfaces is modeled in detail using the radiosity method. Radiation view factors between surfaces are calculated and radiation heat exchange is represented with non-linear heat transfer coefficients (unlike most simulation programs that use simplified radiation models or linearized radiation coefficients). The radiation heat transfer coefficient between two surfaces is equal to:

$$h_{r,i-j} = \frac{\sigma \cdot \tilde{F}_{\epsilon,i-j} \cdot (T_i^4 - T_j^4)}{T_i - T_j} \quad (3.9)$$

where σ is the Stefan-Boltzmann constant, $\tilde{F}_{\epsilon,i-j}$ is the radiation exchange (script F) factor for the two surfaces (a function of view factors and emissivities) and T_i and T_j are the temperatures of surfaces (i) and (j) respectively (in degrees Kelvin).

For the exterior heat transfer coefficient, the advanced Energy Plus approach is followed, which is a combination of the MoWitt and BLAST (DOE-2) detailed convection models. The total exterior coefficient is the sum of the convective and the radiative coefficients. The convective coefficient is calculated as the sum of the natural and forced convective coefficients. The natural convection coefficient is calculated by:

$$h_n = \frac{1.81 \cdot \sqrt[3]{T_s - T_o}}{1.382} \quad (3.10)$$

where T_o is the outside air temperature (in degrees Celsius). The total exterior convective coefficient (including forced convection) is then equal to:

$$h_{co, glass} = \sqrt{h_n^2 + (\alpha \cdot V_0^\beta)^2} \quad \text{for smooth (glass) surfaces and} \quad (3.11)$$

$$h_{co} = h_n + R_f \cdot (h_{co, glass} - h_n) \quad \text{for rough (wall) surfaces} \quad (3.12)$$

where α , β are constant modifiers for forced convection, V_0 is the wind speed at standard conditions and R_f is a surface roughness coefficient (approximately equal to 1.6 for brick/concrete). The radiative exterior coefficient is calculated from the temperature of the sky and the ground and the respective view factors. Linearization in this case is used for simplicity:

$$h_{ro} = 4 \cdot \sigma \cdot \epsilon_s \cdot T_m^3 \quad (3.13)$$

where ϵ_s is the effective emissivity of the exterior surface and T_m is the mean temperature between the sky, the ground and the surface temperature. Then the total exterior heat transfer coefficient is equal to:

$$h_o = h_{co} + h_{ro} \quad (3.14)$$

for each exterior surface. Hourly values of outside temperature are imported from the TMY weather file. Therefore all the heat transfer coefficients (thermal network resistances) are calculated hourly for one year.

Heat storage in walls is modeled by placing one or more thermal capacitances in thermal mass nodes, depending on the material and the desired degree of detail. The value of each thermal capacitance is equal to:

$$C = c_p \cdot \rho \cdot \text{Vol} \quad (3.15)$$

where c_p is the specific heat, ρ is the density and Vol is the volume of each mass element.

Solar gains are calculated in detail in order to accurately model the impact of climate and fenestration on interior conditions of perimeter spaces. Using the hourly horizontal data from a TMY weather file, the Perez irradiance model (Perez et al., 1990) (Appendix B) is used to predict hourly diffuse irradiance, $I_d(n,t)$, on a tilted surface (window). The calculation of incident direct sunlight is done as for the daylight case:

$$I_b(n,t) = I_{bn}(n,t) \cdot \cos(\theta(n,t)) \quad (3.16)$$

where $I_{bn}(n,t)$ is the direct normal irradiance calculated from the beam horizontal irradiance values available in the weather file.

The transmission of solar radiation in the room is done in the same way as for the daylight. Transient hourly values of window solar transmittance are calculated to be used in the thermal simulation model. The amount of heat captured in glazings and released to

room air is also computed. In the case of a shading device, the level of modeling detail depends on the type, location and properties of shading. The shading device solar thermal properties are again estimated as a function of time, to consistently transfer their impact on interior conditions.

Internal gains from lights, appliances and people are also modeled in detail, on an hourly basis. Occupancy and lighting operation schedules and time-based control of shading devices and other systems are all included in the simulation algorithm using an explicit form of the equations. This is a critical characteristic of the simulation process; it will reveal the effect of linking parameters on the integrated performance indices.

An energy balance is applied at each node at regular time steps, to obtain the temperature of the nodes as a function of time. One thermal node is used for room air, except if the mixing of two air masses occurs. When all thermal resistances and heat sources have been calculated, a simulation time-step (Δt) is selected based on a numerical stability criterion. Then all the hourly variables are evaluated for each time step, using a time series method or Fourier transform. The system of simultaneous differential and algebraic non-linear equations can be solved numerically using an explicit finite difference technique, in which we march forward in time from a set of initial conditions. The general form of the explicit finite difference model corresponding to node (i) and time step (p) is (Athienitis, 1994, 1999):

$$T_i^{p+1} = \frac{\Delta t}{C_i} \cdot \left\{ q_i + \sum_j \frac{(T_j^p - T_i^p)}{R_{ij}} \right\} + T_i^p \quad (3.17)$$

where T is temperature, (p+1) indicates next time step, (j) all nodes connected to node (i), R_{ij} is the thermal resistance connecting nodes (i) and (j), C_i the capacitance of node (i), if

any, and q is a heat source at node (i). The only disadvantage of this method is that often small time steps have to be used in order to ensure numerical stability. This may increase computational time but improves the accuracy of results.

Short time-step temperatures of all network nodes and room air are calculated using Eq. (3.17). Heating and cooling load is directly computed using an appropriate proportional control constant that can be calculated using other methods (for example the admittance method, Athienitis et al., 1986). Daily energy demand for heating and cooling is calculated from time integration of thermal loads for the period of one day. Annual heating and cooling demand, which are integrated performance indices that enclose the impact of all linking parameters, are calculated by continuously running the simulation for all 365 days in a typical meteorological year.

3.5. Dynamic links as design parameters in the integrated daylighting and thermal design methodology

3.5.1. Glazing type and properties

Extensive studies on the impact of glazing type and properties on thermal and daylighting performance have been published during the last decade (Citherlet & Scartezzini, 2003, Sullivan et. al., 1998, Clarke et. al., 1998). Even during the 80s, Johnson et al. (1984) realized the need to study the impact of glazing on overall building performance and published a method based on parametric runs of DOE-2 software. The designer can select the desired type of glazing; the approach followed here is to consider primarily clear glass for maximization of daylight utilization, since any other type of glass would reduce daylight availability. Nevertheless, the thermal resistance of the window could vary.

Increase in window thermal resistance will reduce thermal loads without affecting the daylighting performance, if clear glass is still used.

The window itself (without shading) determines the daylight levels in the interior. The type of the window and its optical properties, size, shape, location and orientation are parameters affecting the daylighting performance. Among these, the window sizes vary significantly from building to building, particularly in commercial buildings. Before analyzing the impact of shading, a part of the methodology that aims at helping the designer decide about the glass ratio of a façade is presented next.

3.5.2. Window-to-wall ratio (glass ratio of a façade)

Window size is the most critical direct link affecting both daylighting and thermal performance of a perimeter space. Window size is expressed as window-to-wall ratio (WWR) -or glass ratio- of a façade for generalization of results. The combined effect of window-to-wall-ratio on daylighting and thermal performance of perimeter spaces is investigated by using window area as a continuous design variable: thermal and daylighting modules run using window-to-wall ratio as a continuous variable for each orientation, for different sets of secondary link options (electric lighting control). Then integrated performance indices are computed considering window-to-wall ratio as a design parameter.

Hourly daylighting simulation provides graphs of annual daylight availability ratio for each orientation as a function of window-to-wall ratio. These graphs show the effect of a dynamic link in the first performance index. Electricity consumption for lighting is calculated simultaneously as a function of window-to-wall ratio for different lighting

control strategies. Therefore a second performance index is calculated including the combined effects of a direct and a secondary link. Lighting control options are separated into three categories:

- (i) Passive control, which means electric lights are not controlled but remain on all the time;
- (ii) Active on/off control, which means that electric lights turn off when there is adequate amount of daylight on the work plane, and switch on when additional lighting is required to reach the target level;
- (iii) Active continuous control (dimming), which means that electric lights are always on and the level of intensity is continuously determined as a function of work-plane illuminance detected by a sensor.

The most effective (and expensive) control strategy is the continuous dimming. However, on/off control also reduces significantly electricity consumption for lighting, as shown in previous studies (Tzempelikos & Athienitis, 2002a, 2002b). Daylight availability increases for higher window-to-wall ratios, therefore lighting energy consumption is reduced depending on the control mode. Electricity demand for lighting is calculated directly from the daylight availability ratio as a function of window-to-wall ratio (Tzempelikos & Athienitis, 2004):

$$E_L = P_L \cdot A \cdot t_y \cdot (1 - DAR) \quad (3.18)$$

where P_L is the installed lighting power (W/m^2), A is the total floor area (m^2) and t_y is the total number of working hours in a year. This performance index provides a secondary measure for quantifying the effect of daylight utilization on energy consumption. Reduction in artificial lighting operation results in the reduction in internal gains and thus

a reduction in cooling load and cooling energy demand. Thermal simulation runs simultaneously and plots the remaining performance indices (i.e., heating and cooling loads and demand) as a function of the design variable (window-to-wall ratio), taking into account the impact of electric lighting operation on thermal loads. The procedure is summarized in Figure 3.4.

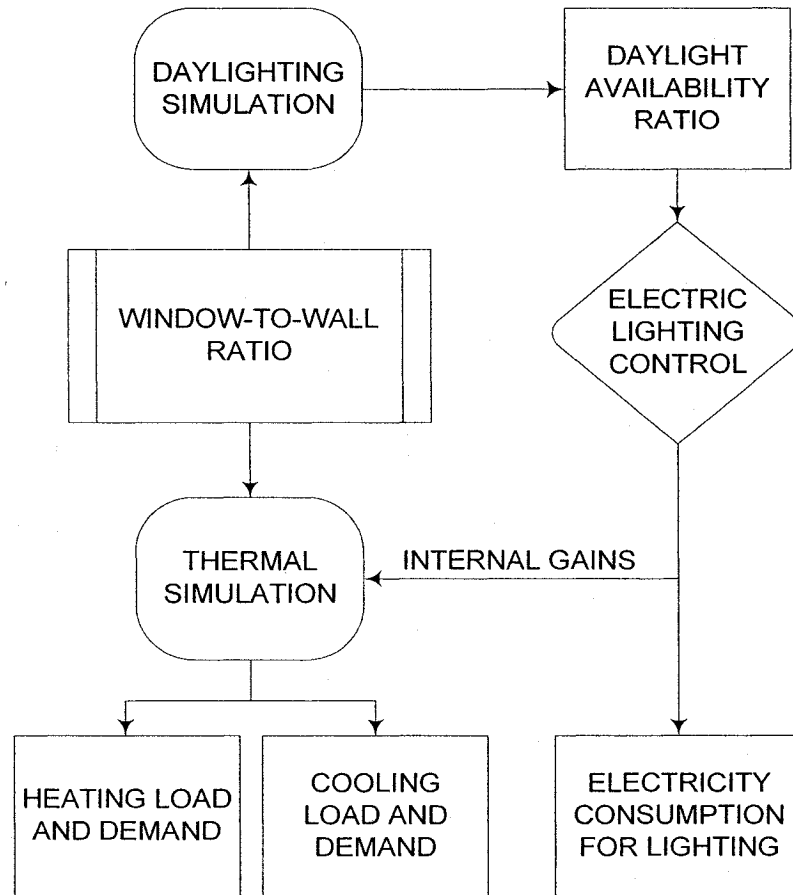


Figure 3.4. Calculation of integrated performance indices considering window-to-wall ratio as a design variable.

A schematic of the expected impact of window-to-wall ratio (a component variable) on the general space performance (i.e., daylighting, lighting and thermal) is possible by plotting integrated performance indices as a function of window-to-wall ratio (Figure 3.5). The building designer can then evaluate the integrated performance characteristics

for the studied design parameter and make recommendations for selecting a value for window-to-wall ratio for each orientation.

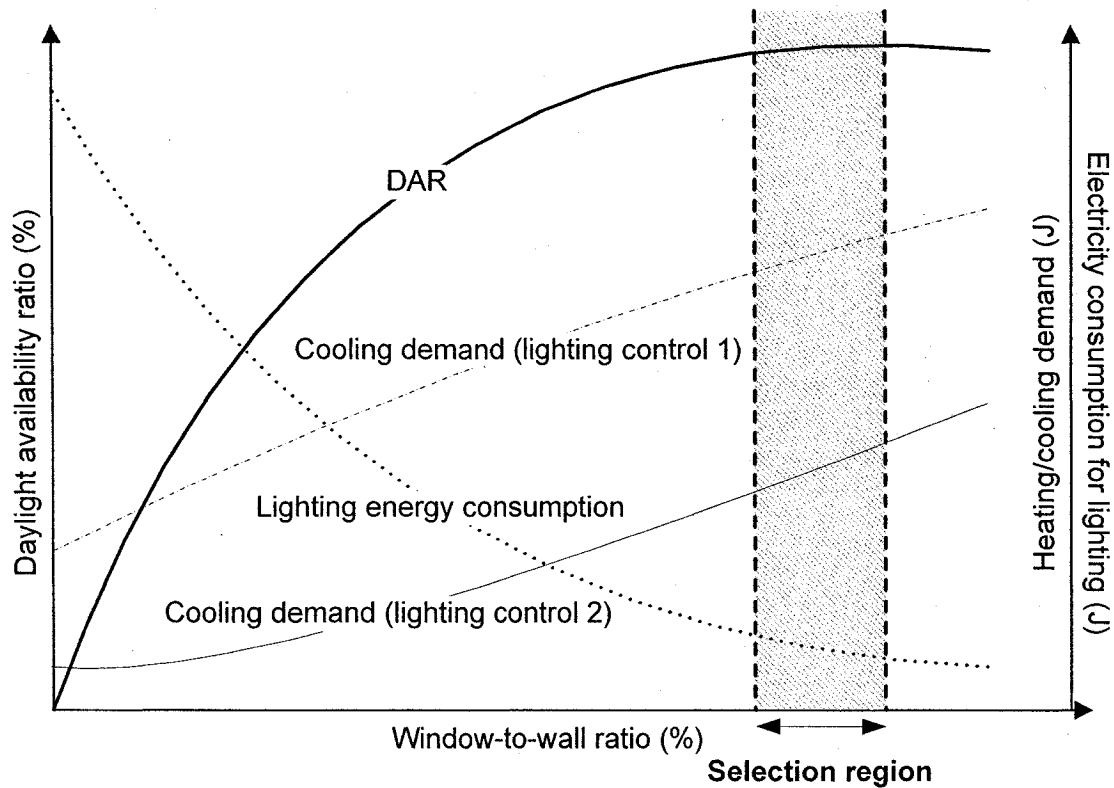


Figure 3.5. Expected variation of performance indices as a function of a direct link (window-to-wall ratio), which is considered a design parameter (theoretical graph).

Daylight Availability Ratio and thermal loads always increase as window-to-wall ratio increases for all orientations. However, the impact of window size on thermal loads (demand) is complicated if the secondary link is included in the analysis. For an active lighting control strategy (control 2 in Figure 3.5), the impact on cooling demand is inverse: the part of cooling load (demand) that results from internal lighting gains decreases for higher window-to-wall ratios because electric lighting operation is reduced

for larger window areas. Yet solar and heat gains are usually higher and this is the reason that cooling load (demand) is likely to increase for larger window areas.

Naturally, daylight availability ratio is higher for larger window areas. However, there is a WWR “region” beyond which further increase in window size does not contribute to daylight availability (shadowed region between the two parallel lines). This is identified as “saturation” of useful daylight (Johnson et al., 1984); If not otherwise requested by the building designer/architect, the initial driving criterion for selection of window-to-wall ratio should be maximization of daylight utilization, without neglecting the thermal performance indices. This means that the maximum window-to-wall ratio for a specific orientation should lie within the “selection region” in Figure 3.5. Choosing a larger window will not result in reduction in electricity consumption for lighting (daylight availability ratio reaches a maximum) neither in reduction of cooling load due to decrease in internal gains from minimized lighting usage. On the contrary, thermal loads would still increase for larger window-to-wall ratios depending on the window thermal properties, which could be increased for reduction in peak loads and energy demand. Moreover, utilization of any kind of shading will significantly reduce daylight availability (and thermal loads as discussed later); thus, maximization of daylight in this stage is desired. Other parameters that should be taken into account when selecting window size, such as glare, thermal comfort, or even aesthetics, are taken into account in the second step of the methodology, when shading devices are also considered in the integrated design process.

The maximum selection region can be described with a mathematical condition:

$$\frac{\partial \text{DAR}}{\partial \text{WWR}} \rightarrow 0 \quad (3.19)$$

The derivative in Eq. (3.19) theoretically never becomes zero; near the saturation region it takes very small values. An exact value for maximum window-to-wall ratio is calculated if a certain small tolerance is used for the derivative value. If, for some reason, the thermal load curves reach a local minimum in the saturation region, the corresponding window-to-wall ratio for that minimum value should be selected, to minimize energy demand within this region:

$$\left. \frac{\partial(\text{load} / \text{demand})}{\partial(WWR)} \right|_{\text{REGION}} = \min \quad (3.20)$$

The designer can evaluate the above information and make recommendations for the window-to-wall ratio of a façade for each orientation. Recent studies started considering the problem (Bulow-Hube, 2004) in a similar way. Ghisi & Tinker (2004) used minimization of annual energy consumption as an index to select optimum window area. Results for Brazil showed that 15%-30% window-to-wall ratio minimizes total energy consumption depending on room shape. However, this ratio does not satisfy daylighting requirements that have an impact on productivity and visual quality and must be taken into account from the early design stage.

In the above first step of analysis, it was assumed that there is no shading provision. Maximization of daylight usage is desired; however, daylight is only the visible portion of solar radiation. High solar gains will increase cooling load, but also reduce heating load during wintertime. Cooling load is an important issue even for heating-dominated climates, especially for south-facing facades (Tzempelikos and Athienitis, 2003b). Unshaded fenestration products become sources of radiant heat by transmitting solar radiation and by emitting longwave radiation to dissipate some of the absorbed solar energy. In winter, glass temperatures usually fall below room air temperature, which may

produce thermal discomfort for occupants near the fenestration. In summer, individuals seated near windows may experience discomfort from both direct solar rays (glare) and long-wave radiation emitted by sun-heated glass.

Shading provision is therefore necessary in order to prevent thermal and visual discomfort as initial motive. Shading devices can control solar gains, block direct sunlight and transmit diffuse daylight in the room; consequently they could eliminate glare and high contrast and create a pleasant visual environment. A wide variety of shading devices are available in the market today and many innovative combined daylighting/shading systems and building envelope elements have been studied and produced in the last decade for the above reasons.

Shading devices are essentially the second direct dynamic link between daylighting and thermal performance of perimeter spaces (Figure 3.2). Shading device type, properties and control have a significant impact on daylighting and thermal interior conditions. Peak thermal loads, energy demand and electricity consumption for lighting strongly depend on shading parameters. A second round of the integrated design methodology is therefore necessary for computation of the general performance-based measures, considering shading variables as design parameters. Due to the complexity of the problem, this approach is not followed by any existing design/simulation software, although the benefits are obvious: the designer is provided with all the required information, taking into account interactions between thermal and daylighting analysis, for selecting appropriate shading system characteristics for each case. As shown in chapter 4, the impact of these characteristics on interior conditions is significant.

3.5.3. Shading device type

The selection of shading system generally depends on the type of building, architectural aesthetics, climate, orientation, functionality and cost. Shading can be placed exterior, interior, or in some cases, inside the window cavity (between glass panes). That would be determined primarily based on climatic conditions. For example, it would be reasonable to assume that in a cooling-dominated climate shading devices should be placed outside in order to reject as much solar heat as possible. More sophisticated systems such as double skin facades or airflow windows with intermediate shading between the two glass panes could be applied to a wide variety of climates.

Utilization of conventional fixed shading devices such as overhangs have disadvantages, as described in section 2.6. Following the technological advancement in building envelopes, movable and controlled shading can be used for better performance. In practice, two main types of shading devices are used in office buildings presently- roller shades and venetian blinds.

3.5.4. Shading device optical and thermal properties

For any kind of shading system, its optical and thermal properties would initially determine the overall impact of shading on the interior. Visible (daylight) and solar transmittance, reflectance and absorptance as well as shading thermal resistance are major parameters that will determine thermal and lighting performance. Orientation, type and location of the shading device affect the selection of shading properties obtained by the integrated daylighting and thermal analysis. If a shading device is present, the transmittance of the shading device should be multiplied with the window transmittance to obtain the total effective transmittance function. Often, manufacturers do not provide

optical and thermal data for their products thus these have to be estimated using one of the methods described in section 2.6. Also, advanced building simulation software can import shading properties from existing databases for certain products (or using measured values) but this approach only allows evaluation of the performance of a specific product with particular characteristics. What the designer needs is a general estimation of the impact of shading properties on performance assessment indices, considering shading as a design parameter.

The basic general methodology for selecting shading device properties is similar to the integrated approach followed for selection of window-to-wall ratio, and the same integrated performance indices are used. However, in this step, the window-to-wall ratio is already determined from the previous step. For each type of shading, integrated performance indices are calculated as a function of shading properties for each orientation during the simulation process. The combined impact of shading optical properties on daylight availability ratio and electricity consumption for lighting is computed in conjunction with the effect of shading solar and thermal properties on heating and cooling demand and peak thermal loads. Furthermore, the secondary link of electric lighting control allows investigation of the impact of shading optical properties on thermal performance indices. Shading properties as design variables provide a means for evaluation of the complex interactions between the thermal and lighting domains of the building system at an advanced level. For a complete analysis, one final basic direct link has to be simultaneously considered: the control of the shading device.

3.5.5. Shading device control

Movable shading devices can be adjusted to changing outdoor conditions. Motorized shading devices can operate based on different criteria: maximization of daylight, minimization of thermal loads, reduction of glare, thermal comfort, etc. Dynamic control of motorized shading devices, fenestration components, electric lighting systems and HVAC system components may lead to minimization of energy consumption for lighting, heating and cooling while maintaining good thermal and visual comfort under continuously changing outside conditions (Lee et al., 1998, Tzempelikos & Athienitis, 2005). There is no standard in selecting control criteria; usually, the shading device is controlled based on glare index values (Lee & Selkowitz, 1995) or transmitted/incident beam radiation (Reinhart & Jones, 2004). Sophisticated methods exist for control of venetian blinds and prediction of indoor illuminances based on correlations between calibrated interior sensors (Park & Athienitis, 2003, 2004).

The selection of control strategy plays a major role in the determination of interior conditions. A shading device can improve the daylighting and thermal performance of a perimeter office space, or may result in increase of electricity consumption for heating, cooling and lighting plus visual discomfort, if not appropriately controlled. For office spaces, it is suggested that direct sunlight is not allowed to enter the room, in order to prevent overheating and glare problems. That means that venetian blinds must rotate to block sun's rays and roller shades must close to allow only diffuse light into the room. Climatic conditions and daylight availability play a major role in the design and control of a shading system. The type and location of the shading also have to be considered simultaneously. For example, for a hot climate, priority could be given in cooling load

reduction. This translates into low effective transmittance and development of a control algorithm for rejection of solar gains. Or, in the case of overcast climates, another strategy should be employed to simultaneously allow daylight maximization.

Furthermore, in order to be consistent with the philosophy of this integrated design methodology, the type of control strategy used has to be decided simultaneously with the selection of its optical and thermal properties for each type of shading device used and for each orientation. This realization is a key point for a successful integrated design. Shading device properties and control (second stage direct dynamic links) are now considered as design variables. Integrated performance indices are computed as a function of shading properties (continuous link) for different options of shading control (discrete link). Shading control has a direct impact on the daylighting and thermal performance, and on electricity consumption for lighting. It also has an indirect impact on thermal conditions, because it affects electric lighting control operation and thus internal gains production. For a holistic approach, electric lighting control and shading control have to be determined together for an integrated solution. The process is summarized in Figure 3.6.

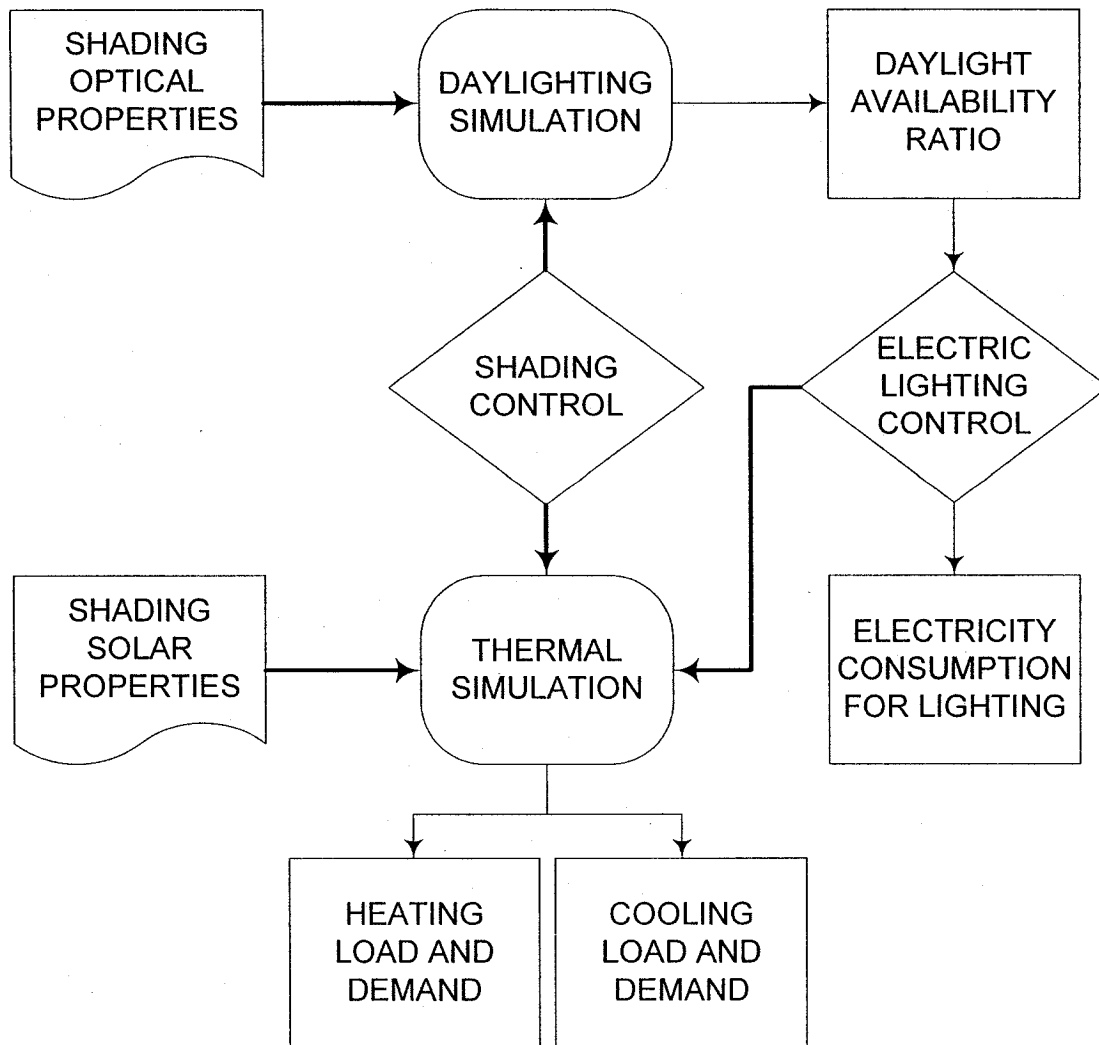


Figure 3.6. Simulation flowchart that summarizes the integrated design analysis. The interactions between daylighting and thermal performance are described using shading properties and control links as design variables.

The variation of integrated performance indices with shading variables (e.g. optical properties) allows extraction of design solutions based on an overall space performance assessment. The designer evaluates the impact of each variable and can make appropriate decisions for each orientation, combining the analysis results with other architectural constraints. Figure 3.7 shows the case for determining shade transmittance, which is

considered a continuous variable in the simulation. The simultaneous impact of different shading control and electric lighting options is shown in the same graph in order to select a matching control strategy at the same time. The curves of Figure 3.7 reveal critical information concerning the integrated space performance. As realised by Johnson et al. (1984), optimum energy performance is achieved when daylighting benefits due to reduced electric lighting operation and also due to reduction in cooling load (due to decreased lighting operation and shading control) exceed the increase in energy demand due to increased solar gains. Therefore a combination between two performance indices was identified as a key indicator: the sum of electricity consumption for lighting and cooling demand (the total energy demand could also be an indicator). For specific shading control strategies, it is possible that this indicator is minimized for certain shading properties, and selection of the respective values is suggested (Eq. 3.21). Maximization of daylight is considered as a criterion in this stage also; the energy performance of shading should not take absolute priority over the daylighting requirements for the occupants. For example, choosing a very low shading transmittance combined with a conservative control would eliminate daylight availability.

$$\left. \frac{\partial(\text{Cooling} + \text{Lighting})}{\partial \tau} \right|_{\text{SELECTION}} = 0 \quad (3.21)$$

Consequently, the condition in Eq. (3.21) is not valid if it is in conflict with the condition in Eq. (3.19) for daylight maximization. A balance between the two is proposed when selecting shading properties and control. The results presented in the next chapter indicate that this is not a problem, since most likely the variable regions described by the conditions of Eqs. (3.19) and (3.21) instinctively overlap.

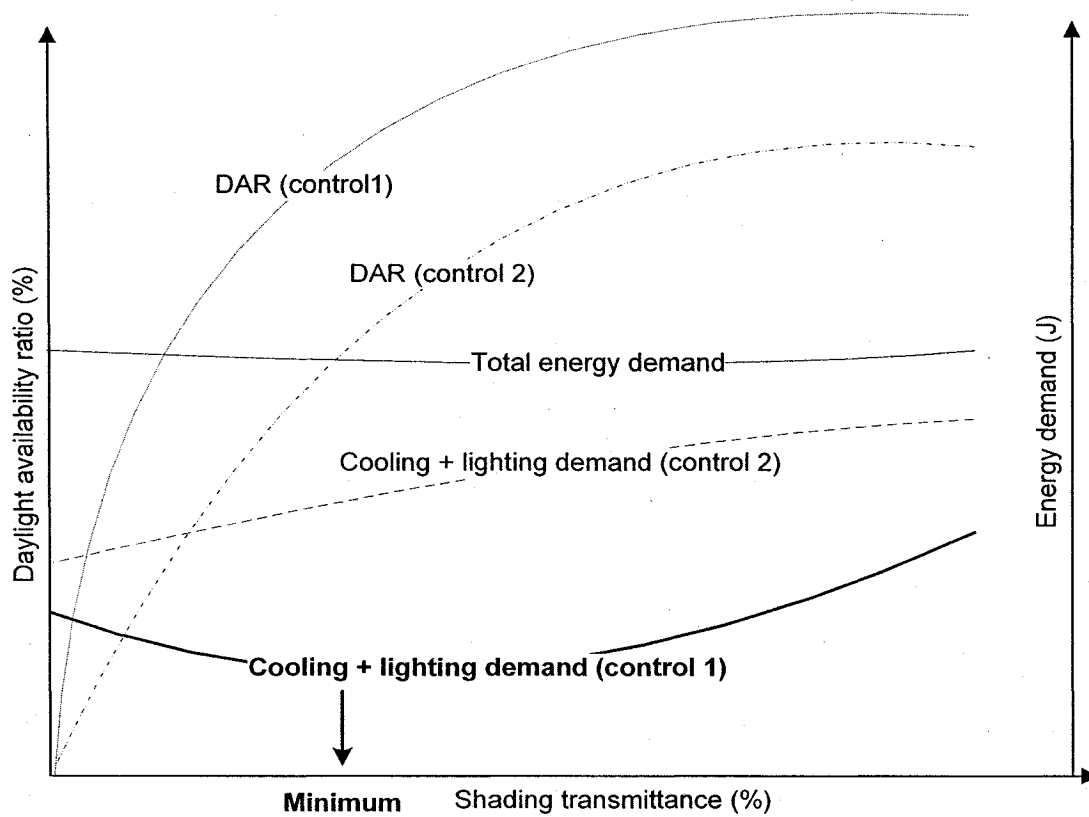


Figure 3.7. Expected variation of integrated performance measures as a function of direct shading links which are considered design variables. Selection of shading properties and control for each orientation can be determined based on the information shown.

The methodology described above is general and can be applied to any type of shading/daylighting device, for any façade, location, orientation, and glazing type (i.e. electrochromic windows). Examples of properties that can be used as design variables in the integrated analysis are shown in Table 3.1 for different shading/daylighting systems. The type of shading control is considered as a separate discrete design variable, wherever applicable.

Table 3.1. Examples of properties that can be used as design variables

Shading/daylighting system	Properties considered as design variables
Exterior roller shade	Transmittance
Interior/intermediate roller shade	Transmittance, absorptance
Exterior venetian blinds	Transmittance, tilt angle
Interior/intermediate venetian blinds	Transmittance, absorptance, tilt angle
Light shelf	Reflectance, dimensions, tilt angle
Exterior awning	Transmittance, dimensions, tilt angle
Prismatic/ translucent glazing	Transmittance, absorptance, thermal resistance

3.6. The three-section façade concept as a design solution

The methodology presented in the previous sections can help the designer make important decisions concerning fenestration and shading characteristics, based on an integrated daylighting and thermal analysis of design options. For example, for a roller shade transmittance equal to 20%, energy demand could be minimized while daylight availability remains at satisfactory levels. However, recent studies have shown that for transmittance values higher than 5%-10%, part of the direct sunlight could penetrate and create glare problems for office workers.

For this reason, a new concept of façade design, motivated by a recent study for the new Concordia University engineering building (Tzempelikos & Athienitis, 2002, 2003b) is proposed. The approach followed is to separate the façade in three parts (for each floor), according to Figure 3.8. The bottom part is opaque and should satisfy thermal resistance requirements for the considered location. The window part is then separated in

a top section, which represents the non-viewing part and a middle section that allows direct view to the outside and should protect the occupants from direct sunlight. The shading properties of the middle part (viewing section) should ensure that direct sunlight is never transmitted inside, to eliminate glare for a seated person. Instead, the shading system must transmit only diffuse light into the room. On the contrary, the top part of the window, if appropriately designed, could allow some beam daylight into the space since it would not create glare problems while it maximizes daylight availability.

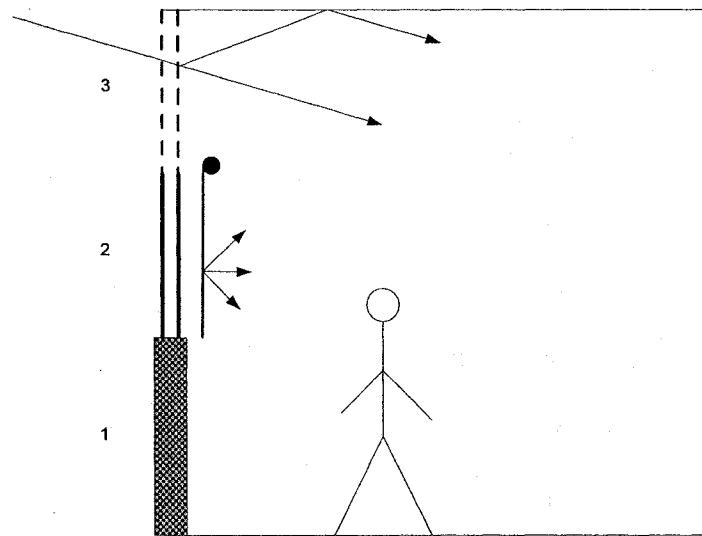


Figure 3.8. Schematic of three-section façade.

Redirecting daylight onto the ceiling is a good solution because it improves daylight uniformity in the space and illuminates the deeper parts, which generally suffer from poor daylighting. Venetian blinds are the most suitable for this task, but also other systems like translucent panels could perform well. Another solution is to use one roller shade for the middle and top sections, but the properties of the shade will differ in each section. For example, the transmittance should be low for the middle section to eliminate glare problems and higher for the top section to maximize daylight availability.

Applying the above methodology to this case results in recommendations for the top part transmittance: a mean transmittance value ($\bar{\tau}$) is determined using the information provided by Figure 3.7. Then a low (5%) transmittance is selected for the middle part and the transmittance of the top part can be determined by solving the following equation for τ_{top} :

$$\bar{\tau} = \frac{\sum (\tau_{bottom} \cdot A_{bottom} + \tau_{top} \cdot A_{top})}{A_{window}} \quad (3.22)$$

where A is the respective area of each section. Moreover, if a roller shade with a continuous transmittance distribution along its height (L) is used for better aesthetics, then the transmittance distribution can be calculated by:

$$\bar{\tau} = \frac{\int_0^L \tau(x) \cdot A(x) dx}{A_{window}} \quad (3.23)$$

where $\tau(x)$ is the shade transmittance at height (x) and $A(x)$ the shade area corresponding to height (x). A real case study using the three-section façade concept involving roller shades and venetian blinds is presented in chapter 4. Other issues, like illuminating adjacent corridors were also considered.

3.7. Comparison of design options on a relative basis

Following the methodology presented above, the designer has enough information to evaluate the integrated performance of a design solution (e.g. for a specific type of shading). However, one needs to know if this is the best design option for a certain case. A comparison of design solutions and configurations should also take place at this early stage, to help the designer select suitable fenestration systems. This comparison must be

made on a relative basis, in order to be able to make subjective decisions about the best option. For instance, the level of modeling detail should be the same when evaluating the integrated performance of two shading systems used for the same case. Also, two different shading systems should be compared for the same climate and orientation, although their properties and control can vary.

Typical cases are shown in Figures 3.9-3.10. A comparison of six different options, using a roller shade and a venetian blind system can be made for each orientation in order to decide which system has the best performance for each case. Considering that different shading device properties can be selected for different orientations, different shading systems can as well result in improved performance. For example, in addition to deciding which of the roller shade configurations in Fig. 3.9 will have better overall performance, the designer has to investigate whether a venetian blind system could result in similar or even better performance, while properties and control can vary for all systems.

Even for heating-dominated climates, cooling is important for office buildings with large glazed areas. Therefore exterior shading is always an option. Placing the shading outside the building is an efficient way to reject solar gains. The thermal properties of the shading device are not important in this case. The optical properties however should be modeled in detail, since they determine the daylighting performance of the space. If a venetian blind is used, daylight uniformity can be improved, since reflection on the ceiling will illuminate areas deeper in the room. However, this always depends on the properties and the control of the device. A disadvantage of exterior shading is the collection of snow and dirt on the device surface, and also maintenance issues. Nevertheless, for cooling-dominated climates exterior shading is perhaps the best option.

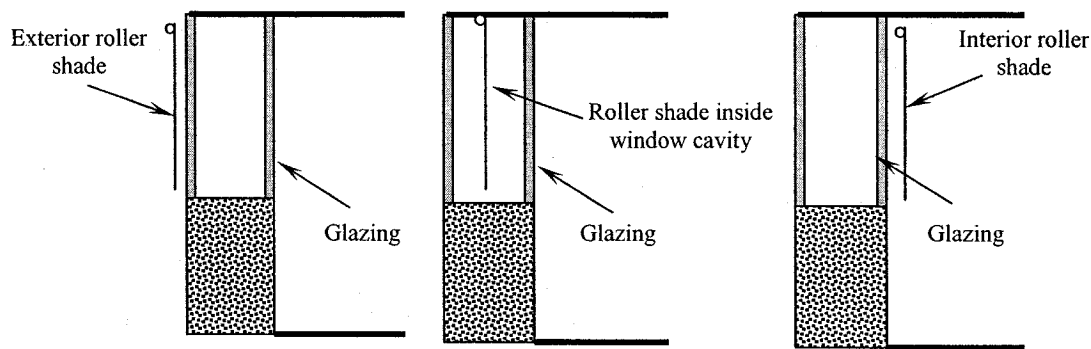


Figure 3.9. Exterior, between-glazing and interior roller shade configurations.

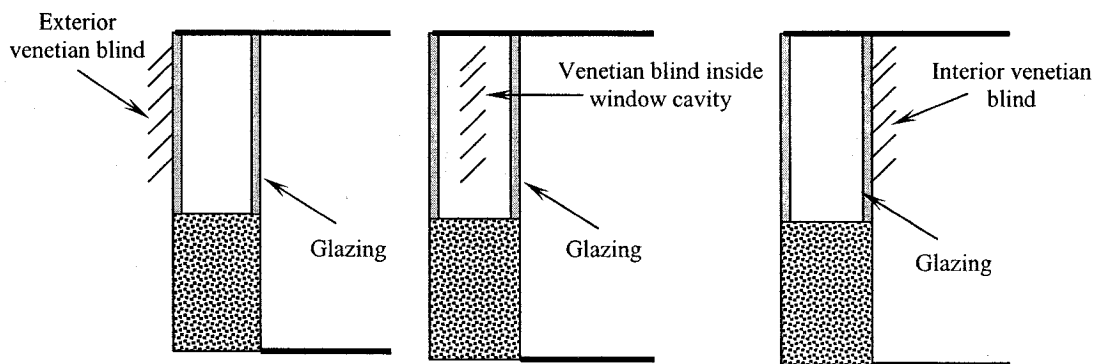


Figure 3.10. Exterior, between-glazing and interior venetian blind configurations.

Placing the shading device in the cavity eliminates the effect of weather conditions. In this case, solar heat is absorbed in the shading device surface, and the temperature of interior glazing increases, exchanging heat by convection with air in the cavity and radiation with the shading device. Therefore shading thermal properties should be considered in the analysis. Light transmission equations change depending on the location of the shading system.

In the case of interior shading, most of the absorbed solar radiation is inevitably transferred into the room. Visible and solar absorptance, transmittance and reflectance are

critical factors in the space performance and should be all considered as design variables in the integrated analysis. Using a transmittance value equal to that for exterior shading, the problem reduces to analyzing the impact of shading absorptance/reflectance on interior conditions. Absorbing shading surfaces should be avoided because all the heat is released to room air by convection and as a result, peak cooling load and energy demand increase. Reflecting materials could reduce solar gains to a small extent.

Other possibilities such as selecting different fenestration systems for different orientations should be also considered. Even for the same façade, the properties of the front and the back surface of the shading layer could be different. In any case, the shading control plays a major role in the system performance and must be simultaneously considered.

3.8. Utilization of innovative systems and selection of degree of modeling detail for design analysis purpose

Innovative daylighting and shading systems are rarely used in new buildings. This happens because designers do not really know how to integrate these systems with other design options and there are not many tools for the evaluation of their overall performance. However, some of these systems are produced to:

- Improve daylighting performance, by diffusing or re-directing light on the ceiling, creating a uniform light distribution on the work plane area and reducing glare
- Improve thermal performance by providing extra thermal resistance to the fenestration system

- Reduce energy consumption for heating or cooling and lighting, if used as “smart” building envelope dynamic elements
- Provide a secure “zone” between the outdoors and the indoor environment, controlling light and heat transfer to the interior

Therefore utilization of such systems is desired. Nevertheless, in order to be used efficiently, an integrated approach should be followed from the early design stage, to evaluate their overall performance and explore the possible benefits from each application. An important case is the double “skin” façade, which includes variations of the airflow window concept. Airflow is introduced in the cavity between the glazing panes. A shading device (usually a roller shade or even venetian blinds) installed in the cavity acts like a solar collector surface. This system can include renewable technologies such as photovoltaic panels between the glazings and several variations of can be used.

By placing the PV modules in the interior of an airflow window (attached to the inner or outer glazing), and passing fresh air through the glazing cavity, the twin objectives of capturing much of the absorbed solar energy that would otherwise be lost as heat, while cooling the PV panels and thereby raising their electrical conversion efficiency are achieved. Thus, the double facade functions as a cogeneration device, which generates both electrical and thermal energy. At the same time, daylight provision is determined by the shading device used in the vision section. Overall evaluation and optimisation of this system is limited by the complexity of the problem, which includes simultaneous consideration of thermal, electrical and daylighting performance. Nevertheless, the benefits of utilizing an optimised form of this multifunctional façade application in commercial buildings are doubtless: in addition to energy savings for heating/cooling and

electric lights as explained before, energy consumption for heating will be drastically reduced when preheated air enters the HVAC system and simultaneous useful power is produced by a renewable technology. Furthermore, the role of the shading device in this case is not only for daylighting, but also to release useful heat to the air flowing through the cavity. Therefore consideration should be given in the selection of shading location and properties.

Semi-transparent photovoltaic panels are another new innovative technology that is multifunctional by nature: they can be used as integrated building envelope elements for electricity production, shading provision and cogeneration of heat if used within a double façade construction. The properties of materials used in semi-transparent photovoltaics, although still under development, could be optimized for specific cases and climates. One example is utilization of translucent semi-transparent panels in the top (non-viewing) part of a three-section façade. This technology is possibly one of the most promising if used appropriately as a multifunctional building envelope component.

The degree of modeling detail when designing at the early design stage differs from application to application. For example, it was found that a 1-D heat transfer model could well describe the basic process happening in the cavity of a double-skin facade (Athienitis et al., 2004). Averaged convective heat transfer coefficients can be used for heat transfer calculations, validated by experimental results. Generally, some detailed modeling should be applied to fenestration systems, since they are the most sensitive elements in determining overall performance (thermal mass is also another important issue, but its impact is smaller). Less detail could be used for simulating the thermal performance of the space; for example linearized heat transfer coefficients would not

result in significant errors in the thermal load prediction. Also, it is necessary to model bidirectional transmittance distribution functions for shading systems that do not have specular-reflecting surfaces (e.g., a roller shade).

For the case of office spaces equipped with a shading device (that is the major case studied in this work), the degree of modeling detail first depends on where the shading device is placed. For exterior shading, enough detail should be used when modeling the optical properties of the shading system, but minimum detail is required for simulation of the thermal characteristics of the shade since the thermal interaction with the interior is negligible. On the contrary, for an interior shade, emphasis will be also given in simulation of the thermal properties of the device, since they have a high impact on convective and radiative heat transfer to the interior. Otherwise errors in estimation of performance indices during the integrated simulation process will result in incorrect selection of the shading device properties and reduced performance. Such an oversight in the early design stage could have significant effects on the energy consumption, cost and indoor comfort conditions during the lifetime of the building.

CHAPTER 4. ANALYSIS OF RESULTS AND DISCUSSION

4.1. Simulation environment

The open environment of MathCad software (version 2001i) was selected for the simulation. In MathCad, the source code is written in the form of mathematical expressions. Equations can be directly inserted in the program, and all kind of advanced mathematical formulations can be used. Boolean operators, symbolic operations, graphs and programming subroutines are available. The advantages of using this environment are: (i) the user can create his own code based on his own algorithm and custom solution method (ii) dynamic changes throughout the program are allowed by adjusting the respective parameters (iii) the visual interface is the program itself and one is not required to go to the source code application to make modifications (iv) improvements in the program can be easily made by adding or modifying equations.

The simulation process is entirely controlled by one program, which is well linked with many available commonly used software packages such as Microsoft Office, Matlab, Visual Basic, AutoCAD and other applications like Labview, data acquisition systems, sound and image file generators, etc. In most cases, information is shared with other applications using components that could be text (ASCII) files, tables, worksheets, images or even subroutines created in a common programming language (C++, Visual Basic, etc). Moreover, for large programs, several smaller files, dynamically linked, can be used in the form of sequential referencing.

Daylighting and thermal simulations are performed simultaneously in MathCAD so that consistency in data exchange and use of the same simulation time step are ensured.

In this way, work plane illuminance levels, thermal loads and energy demand can be simultaneously computed for given outside weather conditions in the same time steps.

4.2. Importing weather data and use for simulation

Weather data are critical inputs for both daylighting and thermal simulation. Emphasis should be given in the accuracy of weather data used for producing simulation results; their impact on interior conditions is significant. As described in chapter 3, the preferred method is to use hourly available weather data from Typical Meteorological Year (TMY) files and not to predict outdoor conditions based on existing models. The Energy Plus website is a good source of free available TMY weather data given in “epw” format. The file can be converted to an ASCII file or can be read by another simulation software (like TRNSYS or ESP-r). The hourly data needed for simulation are: (i) beam horizontal irradiance (ii) diffuse horizontal irradiance (iii) ambient dry-bulb temperature and (iv) humidity ratio or dew-point temperature (to be used in Perez model).

The problem with directly using such hourly data from TMY files is that sometimes estimation of solar radiation data at time intervals other than one hour is required and interpolation is necessary. Linear interpolation has several drawbacks, the most apparent being that positive values of radiation are produced before sunrise and after sunset. The ratio of beam radiation on a tilted surface to that on horizontal becomes very large near sunrise and sunset and, if large values for horizontal radiation are interpolated, the error in predicted radiation on tilted surfaces could be significant. For this reason, solar radiation processors in TRNSYS v. 16 interpolate solar radiation data using the curve for extraterrestrial radiation (TRNSYS, 2003).

In this work, a TMY weather data file for Montreal was used from the Energy Plus TMY weather file database. This file contains hourly values for all climatic parameters including horizontal beam and diffuse irradiances, dry-bulb temperatures, humidity ratios and dew-point temperatures, wind data, precipitation and cloud data etc. The dry-bulb and dew-point temperatures can be directly used (as ASCII files) for simulation. For solar radiation data, a solar radiation processor type 16g was used; it reads weather data from the “epw” weather file and gives as output (ASCII file and graphs) corrected hourly values of horizontal beam and diffuse irradiance, global horizontal irradiance, extraterrestrial horizontal irradiance and solar angles. The TRNSYS input file in IISiBat graphical interface is shown in Appendix J. Hourly beam normal irradiance is calculated from:

$$I_{bn} = \frac{I_{bh}}{\sin \alpha} \quad (4.1)$$

where I_{bh} is the beam horizontal irradiance and α is the solar altitude for the corresponding hour. In order to avoid problems with incorrect values of solar altitude near sunrise/sunset and during the night, TRNSYS type 16 solar radiation processor sets the solar zenith angle equal to 99 degrees before sunrise and after sunset for each day. Hourly solar radiation values are then exported to a Microsoft Excel worksheet for extraction of monthly values and statistics (if necessary). The process of obtaining corrected weather data is summarized in Figure 4.1. After this processing, tables of hourly temperatures and radiation data can be imported in MathCad for use in daylighting and thermal simulation modules. Some of the corrected hourly data for Montreal are shown in Figures 4.2-4.5 below.

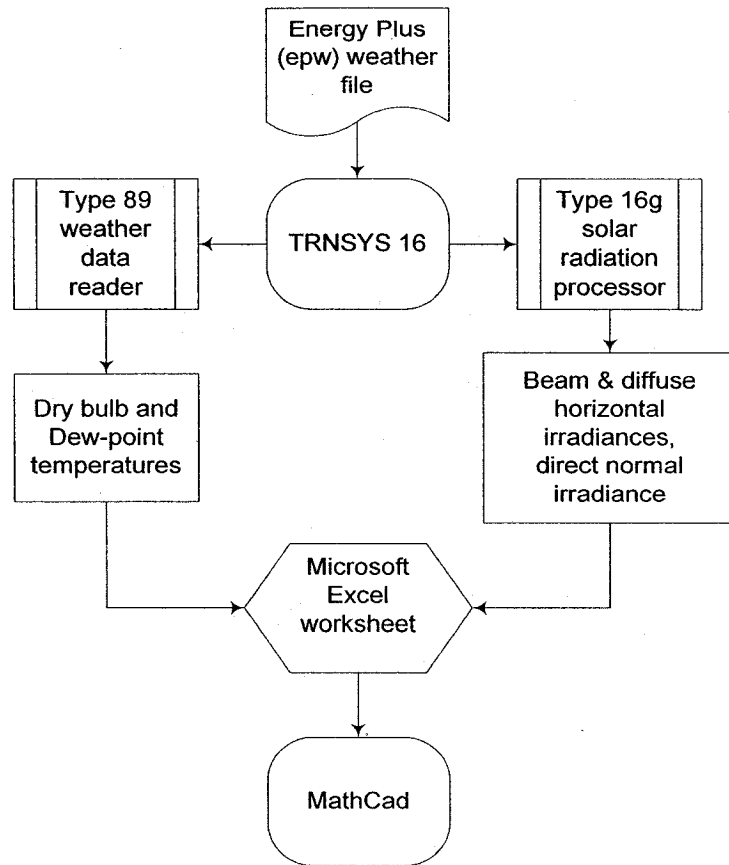


Figure 4.1. Preparation of hourly weather data for use in simulation.

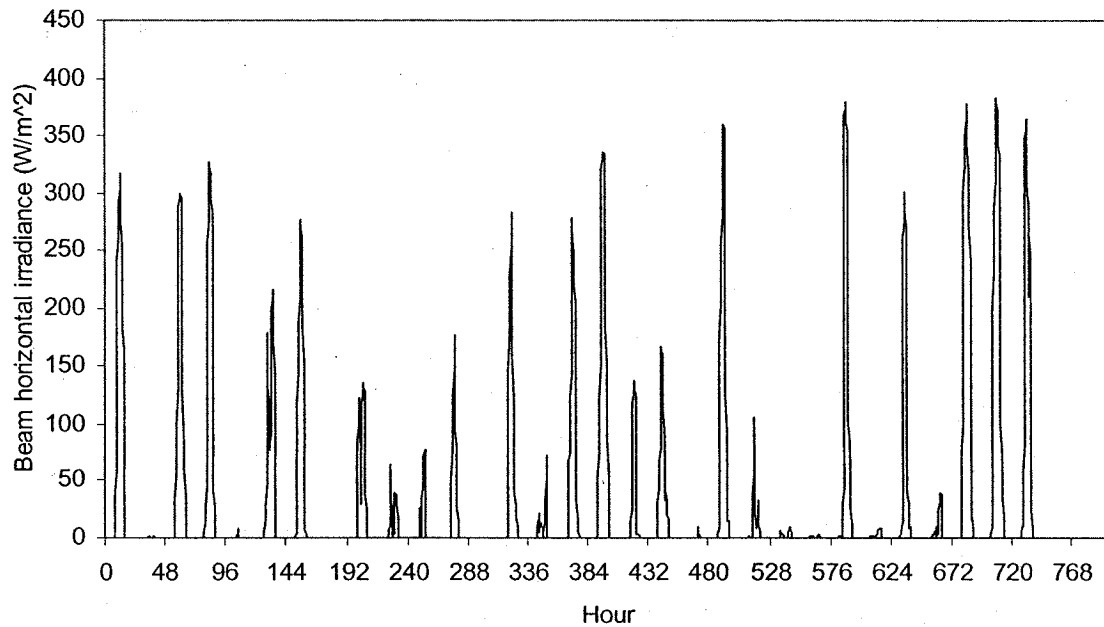


Figure 4.2. Hourly beam horizontal irradiance in January for Montreal.

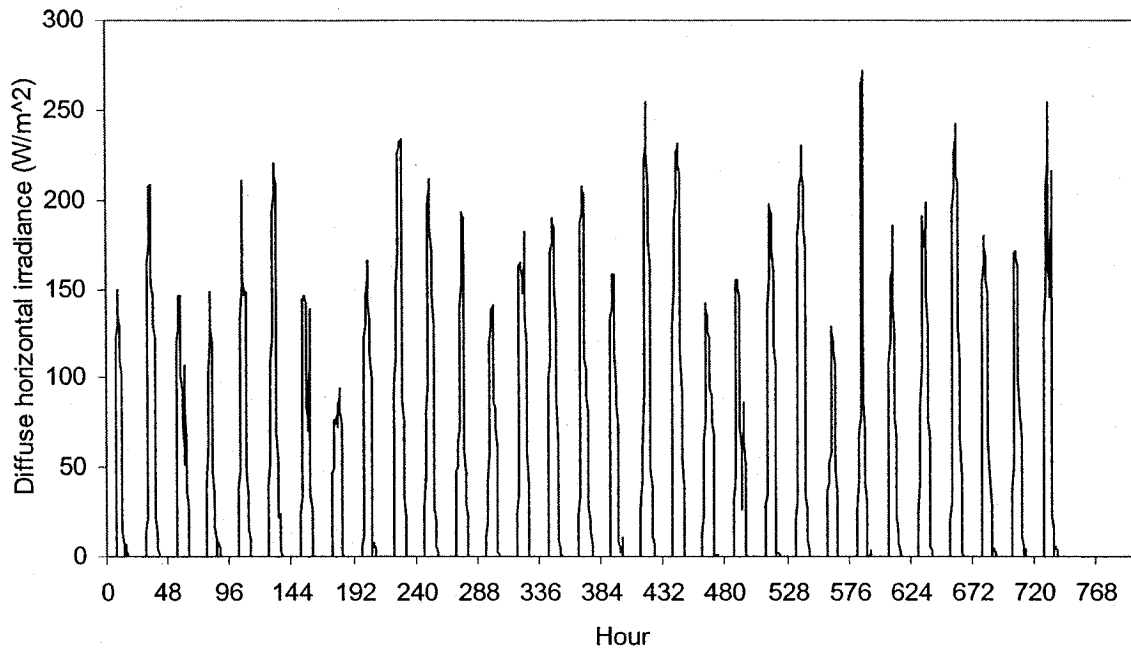


Figure 4.3. Hourly diffuse horizontal irradiance in January for Montreal.

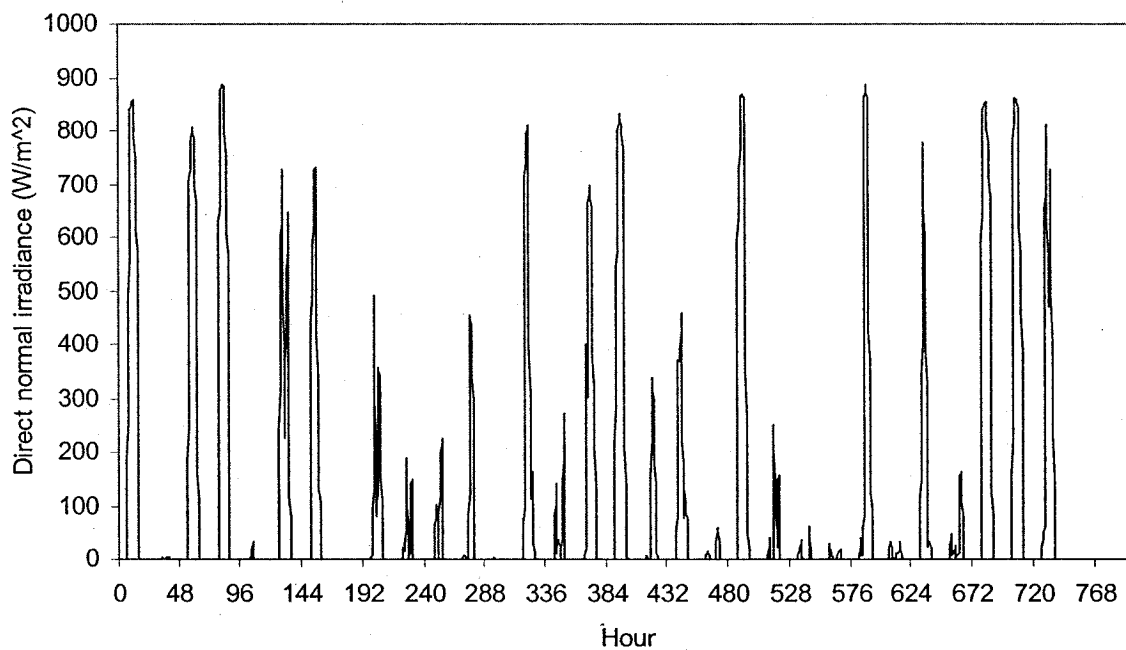


Figure 4.4. Direct normal irradiance in January for Montreal.

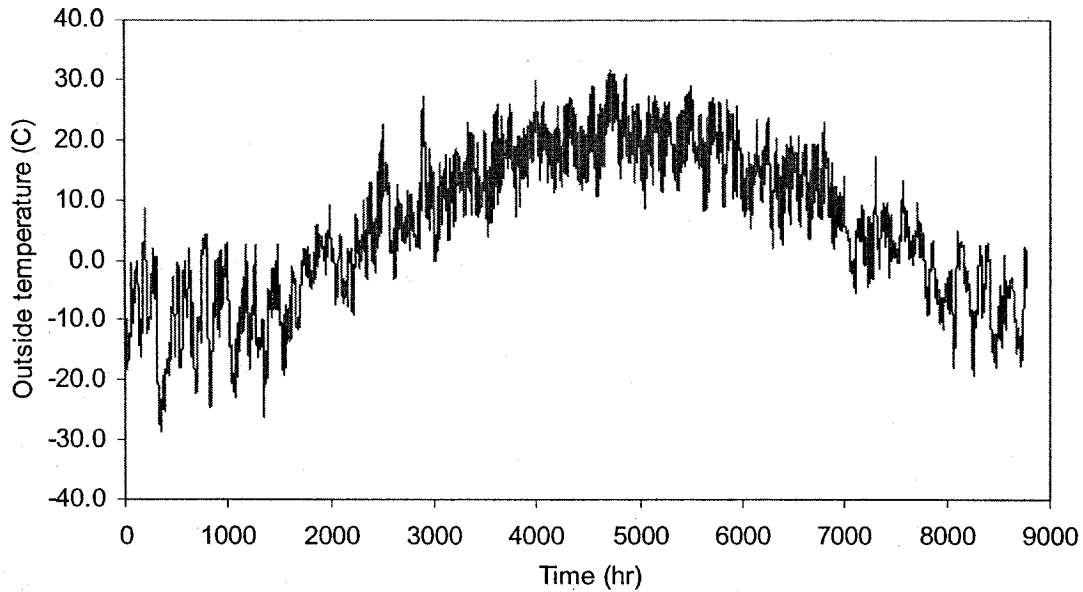


Figure 4.5. Hourly dry-bulb temperature for Montreal.

4.2.1. Calculation of incident solar radiation on a tilted surface

Hourly incident solar radiation on a tilted surface (e.g., window) is calculated from the horizontal irradiance values. All parameters in the simulation are expressed as a function of day number (n) and solar time (t) for effective use in matrix calculations.

- Beam irradiance on a tilted surface is computed from:

$$I_b = I_{bn} \cdot \cos\theta \quad (4.2)$$

where:

θ is the solar incidence angle given in Eq. (3.1), Appendix A;

I_{bn} is the direct normal irradiance;

- Diffuse sky radiation on a tilted surface is calculated using the Perez diffuse model (Perez et al., 1990):

$$I_{ds} = I_{dh} \cdot \left[(1 - F_1) \left(\frac{1 + \cos\beta}{2} \right) + F_1 \cdot \frac{a}{b} + F_2 \sin\beta \right] \quad (4.3)$$

where:

I_{dh} is the sky diffuse horizontal irradiance;

F_1 is the circumsolar brightening coefficient;

F_2 is the horizon brightening coefficient;

β is the tilt angle of the surface;

a is equal to $\max\{0, \cos\theta\}$;

b is equal to $\max\{0.087, \sin\alpha\}$.

The brightening coefficients represent the degree of anisotropy in the sky and they are a function of solar altitude, sky clearness and sky brightness (Appendix B).

▪ The ground-reflected diffuse component is added to the sky diffuse component to obtain the total hemispherical diffuse radiation on a tilted surface. The ground-reflected radiation is equal to:

$$I_{gd} = (I_{bh} + I_{dh}) \cdot \rho_g \cdot \frac{1 - \cos\beta}{2} \quad (4.4)$$

where:

I_{bh} is the beam horizontal irradiance;

I_{dh} is the diffuse horizontal irradiance;

ρ_g is the ground reflectance.

4.2.2. Calculation of incident illuminance on a tilted surface

If horizontal illuminance data are not provided by the weather data file or the solar radiation processor (most likely they are not for North America), the Perez luminous efficacy models (Perez et al., 1990) are used to calculate beam and diffuse (or global)

illuminance values from the horizontal irradiance data. Detailed calculations of all parameters and description of the model can be found in Appendix C.

- Direct normal illuminance is calculated from direct normal irradiance:

$$E_{bn} = \max\{0, I_{bn} \cdot [ab_i + bb_i W + cb_i \cdot e^{5.73 \cdot Z - 5} + db_i \Delta]\} \quad (4.5)$$

where:

ab_i , bb_i , cb_i and db_i are beam luminous efficacy coefficients given in tables by Perez et al. (1990) as a function of sky clearness;

Z is the solar zenith angle ($90^\circ - \alpha$).

The direct illuminance on a tilted surface is then calculated using Eq. (3.3).

- Diffuse horizontal illuminance is calculated from:

$$E_{dh} = I_{dh} \cdot [ad_i + bd_i \cdot W + cd_i \cdot \sin \alpha + dd_i \cdot \ln \Delta] \quad (4.6)$$

where:

ad_i , bd_i , cd_i and dd_i are diffuse luminous efficacy coefficients given in tables by Perez et al. (1990) as a function of sky clearness;

W is the atmospheric precipitable water content (function of dew-point temperature);

Δ is the sky brightness.

Sky diffuse illuminance on a tilted surface is calculated using Eq. (4.3), by replacing illuminance with irradiance values.

- The ground-reflected illuminance is calculated from Eq. (4.4), by replacing illuminance with irradiance values.

The calculated weather data can now be used by the daylighting and thermal simulation modules for extraction of integrated performance indices.

4.3. Selection of window-to-wall ratio (WWR)

The calculated weather data are exported in MathCad to be used as inputs in the simulation modules. 8760 values of incident beam, sky diffuse and ground-reflected incident illuminance and irradiance, as well as dry bulb and dew-point temperatures are used for each orientation. Monthly tables of hourly data can be used in order to reduce computation time (calculations with large matrices require more computation time). Then a room model is developed in MathCad, in which all parameters (dimensions, location, orientation, materials properties, thermal mass, etc) can be adjusted for studying many possible cases of interest. A base case scenario was considered for extraction of results: a 4m x 4m x 3m high typical perimeter office in Montreal, with one exterior wall and one window. Thermal properties of the walls and window are selected based on MNECCB recommendations for Montreal. A common double-glazed window with clear glass was assumed for the base case. Thermal parameters in the basic model are described in Appendix I and lighting parameters are described in Appendices E, F and G.

Following the integrated methodology presented in section 3.5, the effect of the first dynamic link, window-to-wall ratio, is investigated first. The daylighting simulation module calculates the amount of beam and diffuse transmitted daylight into the room for each hour in a year and for each orientation. Window direct transmittance, reflectance and absorptance are calculated as a function of solar incidence angle; therefore they are expressed as a function of day number and solar time for consistent hourly calculations in matrix form (Appendix D). This is a major requirement for any fenestration system in consideration: its effective optical (and thermal) properties have to be calculated as a

function of time (using solar incidence angle dependence equations) so that hourly tables of each property can be used in simulation calculations.

A detailed radiosity method is then applied to compute hourly values of work plane illuminance for one year. Forty-nine view factors between all seven interior surfaces are calculated based on Eq. (2.3) which can be analytically solved for rectangular surfaces. The view factors calculations are presented extensively in Appendix E. Then representative points on the work plane surface are selected and configuration factors between each point and each surface are computed using matrix algebra presented in Appendix F. One to three representative points could determine the daylight availability and the need for artificial lighting. Luminous exitances of interior surfaces are calculated as described in section 2.4.4 after a theoretically infinite number of inter-reflections inside the room solved with the Jacobi numerical method (Appendix G). Final illuminance on a point A on the work plane surface is calculated from:

$$E_A = \sum_i M_i \cdot C_{A-i} \quad (4.7)$$

where:

M_i is the final luminous exitance of surface (i), after inter-reflections;

C_{A-i} is the configuration factor between point A and surface (i).

View factors and configuration factors depend on room geometry and are therefore computed for each window-to-wall ratio. Assuming a working schedule from 9 am to 5 pm, Monday to Friday, 2080 values of work plane illuminance are simulated for each window-to-wall ratio and each orientation. Sample results for work plane illuminance distribution for the base case are shown in Figure 4.6.

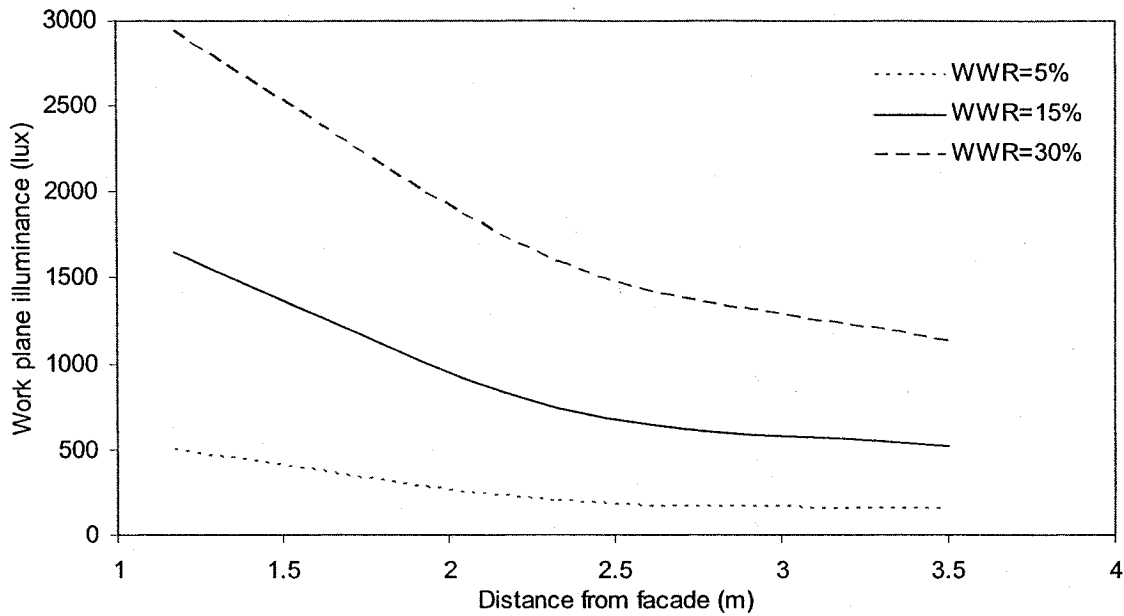


Figure 4.6. Illuminance distribution on the work plane for three different window-to-wall ratios (south façade, June 30th, 2pm).

Daylight Availability Ratio for each case is then calculated by counting the number of hours during which illuminance on the work plane is higher than 500 lux. This is done using advanced automatic matrix operations in MathCad (Appendix H). The daylighting module eventually calculates monthly and annual Daylight Availability Ratio as a function of window-to-wall ratio for each major orientation in Montreal. Some of the results are presented in Table 4.1. This information can be used to characterize the daylighting performance of similar perimeter spaces in Montreal and could be a valuable source to designers/architects who design for daylight.

The effect of window-to-wall-ratio on annual average Daylight Availability Ratio for each orientation in Montreal is shown in Figure 4.7. This is the first performance index studied as a design variable, as described in the methodology, and includes the impact of climate, orientation, room characteristics and fenestration optical properties.

**Table 4.1. Monthly and annual Daylight Availability Ratio for each major orientation in
Montreal for different window-to-wall ratios.**

SOUTH													
WWR	Jan	Feb	Mar	Apr	May	Jun	Jul	Aug	Sep	Oct	Nov	Dec	Annual
5%	0.13	0.05	0	0	0	0	0	0	0	0	0	0.08	0.02
10%	0.33	0.25	0.33	0.4	0.28	0	0	0.2	0.55	0.45	0.2	0.13	0.26
15%	0.53	0.4	0.6	0.65	0.6	0.45	0.68	0.68	0.7	0.6	0.3	0.28	0.54
20%	0.63	0.53	0.65	0.68	0.8	0.78	0.88	0.93	0.8	0.7	0.42	0.35	0.68
30%	0.73	0.58	0.8	0.83	0.9	0.85	0.9	0.94	0.9	0.73	0.5	0.45	0.76
50%	0.8	0.62	0.85	0.9	0.95	0.9	0.93	0.96	0.95	0.77	0.55	0.5	0.81
80%	0.82	0.64	0.88	0.93	0.97	0.94	0.96	0.98	0.97	0.8	0.6	0.55	0.84
NORTH													
5%	0	0	0	0	0	0	0	0	0	0	0	0	0
10%	0	0	0	0	0	0	0	0	0	0	0	0	0
15%	0	0	0	0	0	0	0	0	0	0	0	0	0
20%	0	0	0	0	0	0.05	0.08	0	0	0	0	0	0.02
30%	0	0	0.15	0.08	0.18	0.45	0.68	0.18	0.13	0.05	0	0	0.16
50%	0.28	0.25	0.73	0.73	0.88	0.9	0.9	0.88	0.78	0.53	0.18	0.13	0.6
80%	0.5	0.4	0.82	0.9	0.95	0.95	0.95	0.93	0.85	0.65	0.4	0.3	0.72
EAST													
5%	0	0	0	0	0.08	0.03	0	0	0.02	0	0	0	0.01
10%	0.07	0.03	0.12	0.22	0.45	0.18	0.3	0.27	0.2	0.08	0	0	0.16
15%	0.1	0.07	0.25	0.27	0.51	0.38	0.43	0.47	0.25	0.13	0	0	0.24
20%	0.13	0.17	0.32	0.42	0.55	0.69	0.62	0.56	0.45	0.18	0.03	0.03	0.35
30%	0.2	0.21	0.45	0.52	0.69	0.78	0.85	0.67	0.57	0.45	0.15	0.08	0.47
50%	0.42	0.43	0.77	0.8	0.9	0.9	0.9	0.89	0.84	0.67	0.32	0.24	0.67
80%	0.6	0.6	0.88	0.9	0.91	0.92	0.91	0.9	0.89	0.82	0.53	0.48	0.78
WEST													
5%	0	0	0	0	0.13	0.05	0	0	0.03	0	0	0	0.02
10%	0.1	0.05	0.18	0.33	0.68	0.28	0.5	0.4	0.3	0.13	0	0	0.24
15%	0.15	0.1	0.38	0.4	0.78	0.58	0.65	0.7	0.38	0.2	0	0	0.36
20%	0.2	0.25	0.48	0.63	0.83	0.88	0.9	0.85	0.68	0.28	0.05	0.05	0.5
30%	0.35	0.33	0.6	0.75	0.95	0.95	0.95	0.92	0.8	0.65	0.23	0.13	0.63
50%	0.5	0.5	.8	0.85	0.96	0.96	0.96	0.95	0.9	0.75	0.4	0.3	0.74
80%	0.7	0.68	0.93	0.93	0.93	0.95	0.96	0.95	0.95	0.94	0.6	0.58	0.84

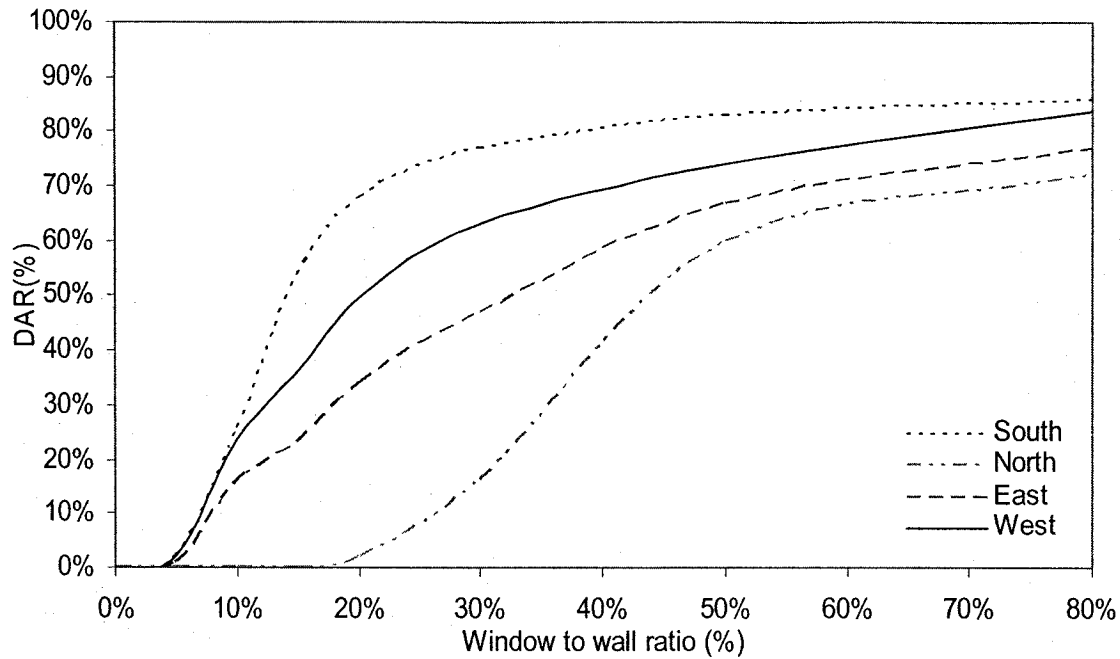


Figure 4.7. DAR as a function of window-to-wall ratio for each orientation in Montreal.

South facades receive more daylight than other orientations and therefore DAR for south facades is higher for any window size. For 30% window-to-wall ratio, natural daylight provides the space with 500 lux on the work plane for 76% of the working time in a year. Increasing window size more than 30% will not result in significant increase in useful daylight in the room (9% more until 80% window-to-wall ratio). Therefore this is identified as the daylighting saturation region for south-facing facades in Montreal and should be taken into account when selecting glass ratio of a south-facing façade for daylight maximization.

The situation is similar for west-facing facades; 40% window-to-wall ratio gives 70% DAR. Choosing 50% of a west façade to be glass only increases daylight availability by 4%. East-facing facades receive less daylight during working hours and only after 50% window-to-wall ratio daylight availability levels are stabilized. However, north-facing

facades suffer from poor daylighting throughout the year; even for 20% window-to-wall ratio, the target work plane illuminance of 500 lux is never met and therefore artificial lighting is required during all the working time. North-facing facades reach a “stable” daylighting condition after 50% window-to-wall ratio, but this is in conflict with thermal requirements as explained later. Non-linear multivariate regression techniques can be used to include all curves of Figure 4.7. in one single equation. In that case, the annual daylighting performance of any similar perimeter space in Montreal could be determined by using only one formula: $DAR = f(WWR, \text{orientation})$. Validation of daylighting results using Lightswitch software (Reinhart, 2002) is shown in section 4.7.

The secondary link of electric lighting control is modelled in order to investigate the effect of window-to-wall ratio on the second performance index: electricity demand for artificial lighting. A typical electric lighting system with T8 fluorescent lamps and 15 W/m² installed lighting power was assumed for the simulation. Two options were considered for electric lighting control:

- (i) passive control (electric lights are always on during working hours) and
- (ii) active on/off control (electric lights turn on and off based on occupancy sensors and work plane illuminance levels). When occupants are in the room and illuminance on work plane is less than 500 lux, lights turn on; in all other cases electric lights are automatically switched off.

For the case of passive control, the annual electricity demand for electric lighting is calculated from (Tzempelikos & Athienitis, 2005b):

$$E_L = P_L \cdot t_y \cdot A \quad (4.8)$$

where:

P_L is the installed lighting power (W/m^2);

t_y is the number of working hours in a year;

A is the floor area (m^2).

The annual electricity demand for lighting is equal to 1800 MJ for the base case with passive lighting control, which corresponds to $112.5 \text{ MJ/m}^2\text{y}$. This value is independent of orientation and window size because electric lights are assumed to be continuously on. For the case of active on/off control, the electricity demand for lighting is directly calculated as a function of window-to-wall ratio for each orientation using the Daylight Availability Ratio results as in Eq. (3.18). The results of passive control are multiplied by the factor $(1-\text{DAR})$ for each case, to account for switching off of electric lights when at least 500 lux are incident on the work plane surface during working hours. Figure 4.8 shows the impact of window-to-wall ratio on the second performance index for different orientations. If active dimming control was used, energy savings would be higher as discussed in a later section.

Following the daylighting simulation results, electricity demand for lighting assuming active control decreases with window-to-wall ratio for all orientations. South-facing facades have higher DAR and therefore less energy is required for lighting the space. For 30% WWR, annual electricity demand for lighting is already reduced by 77% (from 1800 MJ to 413 MJ) compared to passive lighting control and practically it is not further reduced for larger window areas. For north-facing facades, the electricity demand for lighting is 1800 MJ for window-to-wall ratios less than 20% because work plane illuminance never reaches 500 lux.

It is also possible to extract correlations between performance indices when they are calculated as a function of the same design variable (e.g. window-to-wall ratio). For example, Figure 4.9 shows the annual electricity demand for lighting as a function of DAR. The correlation between electricity demand for lighting and DAR for the south-facing case is ($R^2=1$):

$$E_L = -1797.5 \cdot \text{DAR} + 1797.2 \quad (4.9)$$

Designers could consult Table 4.1 for daylighting results and then evaluate the impact of daylighting in electricity demand for lighting using Eq. (4.9). Alternatively, Figures 4.7-4.8 can be used as graphical tools. Validation of electric lighting results is shown in section 4.7.

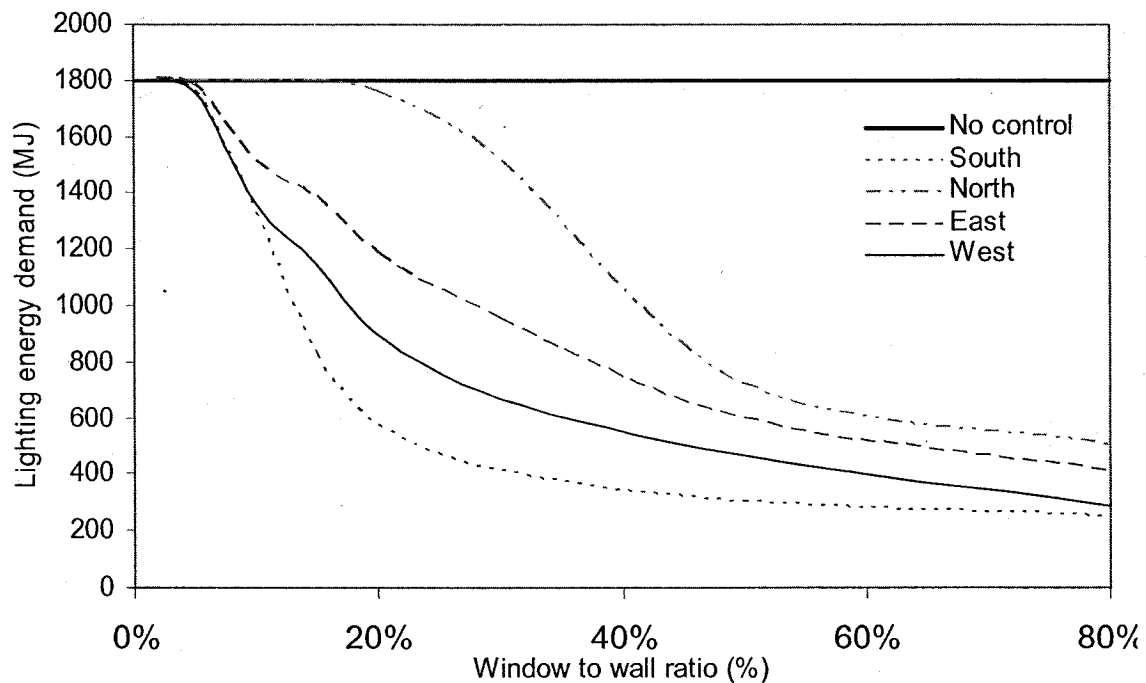


Figure 4.8. The impact of window-to-wall ratio on annual electricity demand for lighting for different orientations. No control refers to the passive lighting control described above.

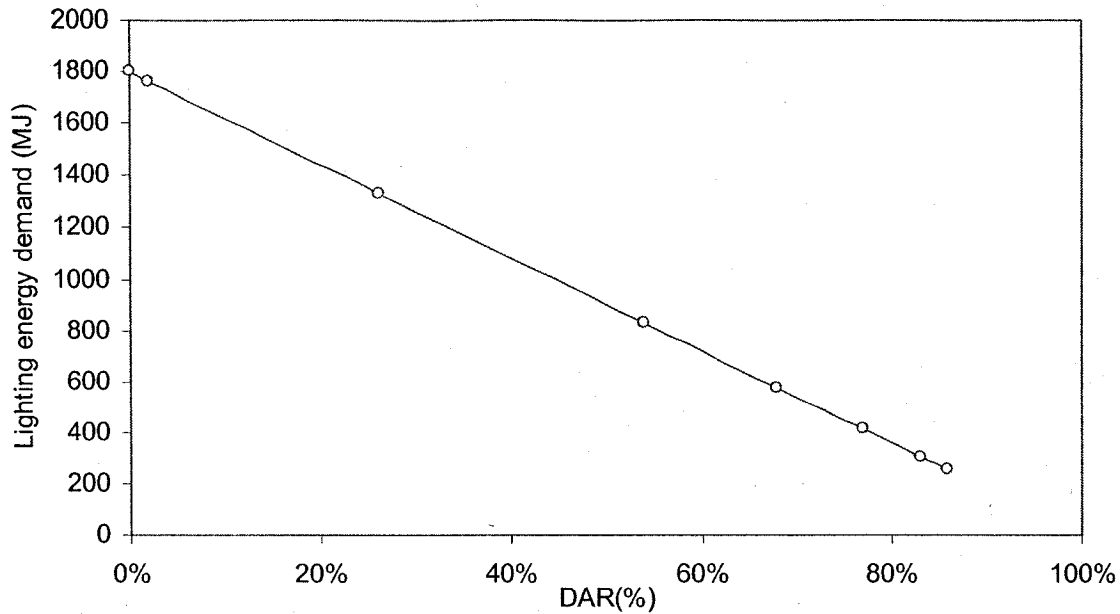


Figure 4.9. Correlation between two performance indices for a south-facing perimeter space of the base case, assuming active on/off electric lighting control.

The thermal simulation module (described in Appendix I) runs simultaneously as a function of window-to-wall ratio. A thermal network for the considered space is constructed and an explicit finite difference method is used to solve the simultaneous nodal energy balance equations, as described in chapter 3. A schematic of the thermal network is shown in Figure 4.10 (explained in Appendix I). Resistances (R) represent heat flow between two nodes (convection, conduction or radiation). Non-linear heat transfer coefficients are used for convection and radiation heat transfer thus network resistances are a function of time (temperature). Sources (S) represent solar radiation absorbed in each layer and capacitances (C) represent heat storage in thermal mass elements. For detailed hourly calculation of solar gains, tables of hourly beam and diffuse incident solar radiation on the façade are used as weather inputs. Then the transmitted part is calculated as for the daylight case and the hourly absorbed radiation by each mass

element is computed for one year. Hourly values of outside temperature are directly used from the TRNSYS type 89 weather data reader output file.

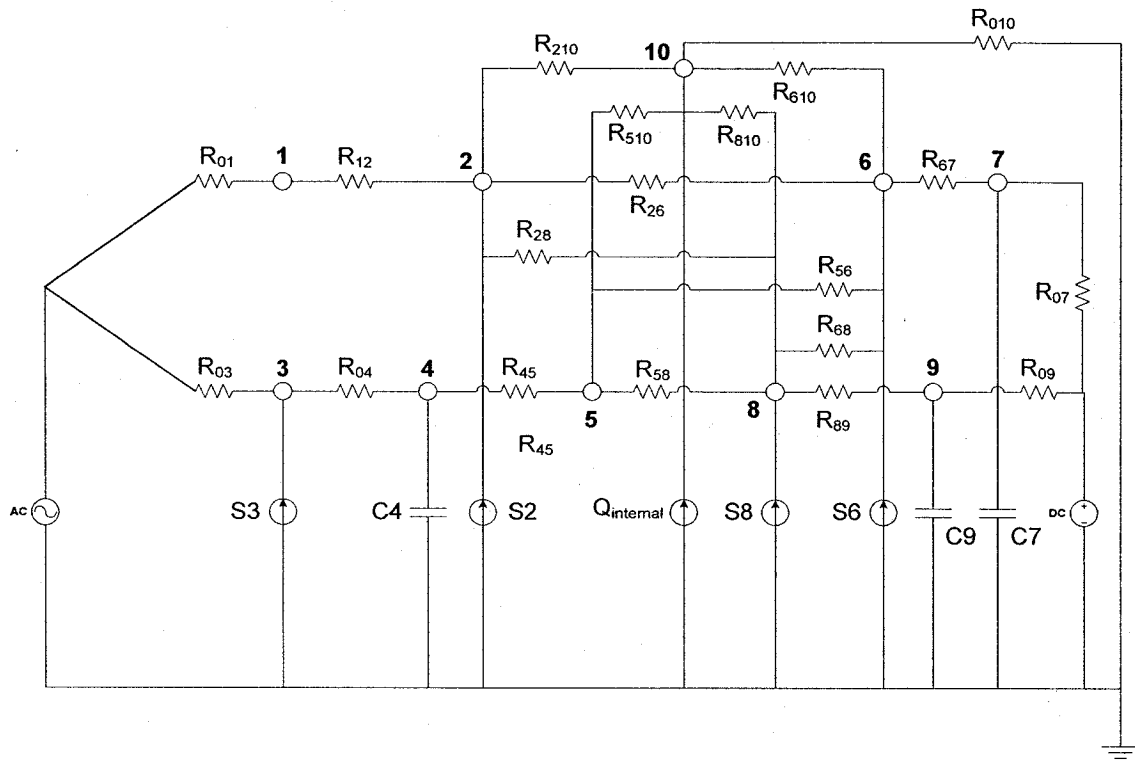


Figure 4.10. Thermal network used for the base case. Node 10 is room air and nodes 6-7 represent the floor (Appendix I).

Window-to-wall ratio is the first dynamic link and therefore its impact on thermal performance indices was studied by running the thermal simulation as a function of WWR. The simultaneous impact of daylighting on thermal performance indices is modelled by consistently passing information from the daylighting and electric lighting simulation to the thermal module on an hourly basis, considering window-to-wall ratio as a design variable. Hourly internal gains from lights and people (Q_{internal}) are modelled as a separate source based on occupancy schedules and reading the daylighting and electric lighting simulation results as a function of window-to-wall ratio.

A simulation time step is selected next based on a numerical stability criterion. For the base case, the maximum time step is five minutes. Thermal simulation must run on a 5-min time step and therefore the values of all simulation parameters must be re-evaluated every 5 min. Transformation from hourly values to 5-min calculations was achieved by modelling of all parameters with discrete Fourier series and then applying an inverse Fourier transform for the new (5-min) time step. The system of simultaneous finite difference heat balance equations is then solved in matrix form in MathCad. Table 4.2 shows peak heating and cooling load results for each orientation.

Table 4.2. Heating and cooling load as a function of WWR for each orientation.

Orient. WWR (%)	South		North		East		West	
	Heating load (W)	Cooling load (W)	Heating load (W)	Cooling load (W)	Heating load (W)	Cooling load (W)	Heating load (W)	Cooling load (W)
0%	220	342	228	317	222	336	223	333
5%	224	348	233	319	227	340	227	339
10%	316	514	342	338	326	464	325	463
15%	365	606	400	358	379	537	378	536
20%	414	698	458	378	432	610	431	608
30%	498	882	574	408	540	756	539	754
40%	610	1067	690	463	648	903	647	902
50%	709	1251	806	508	757	1050	755	1049
60%	808	1436	922	548	866	1197	862	1195
70%	908	1621	1038	598	976	1344	973	1343
80%	1007	1806	1154	648	1085	1491	1082	1489

Heating and cooling energy demand are calculated by integrating thermal loads over time on a daily, monthly or yearly basis. Energy consumption for heating and cooling could be evaluated if a particular HVAC system is selected with a certain COP assumed (e.g. a heat pump). The integrated performance indices are plotted as a function of the considered design variable (window-to-wall ratio) as described in the methodology (chapter 3). Integrated analysis results for a south-facing façade are shown in Figure 4.11.

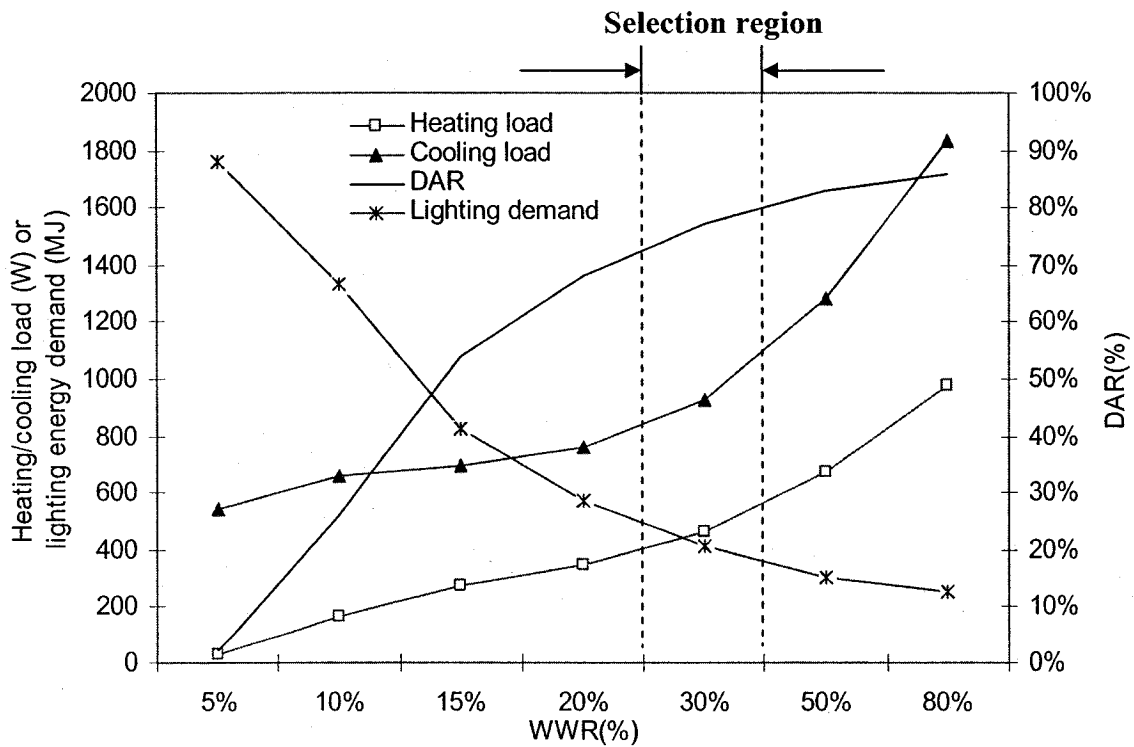


Figure 4.11. Integrated performance indices as a function of WWR for a south-facing perimeter space of the base case, assuming active on/off electric lighting control.

Figure 4.11 provides all the necessary information for the impact of WWR on integrated daylighting and thermal performance and a selection region is identified according to section 3.5. 30% WWR satisfies daylighting requirements (DAR reaches 76%) and the respective effect on thermal performance indices is shown in Fig. 4.11. The above results also indicate that, for south-facing facades in Montreal, larger window areas would only result in higher energy demand for heating and cooling without improving thermal or visual interior conditions and therefore window-to-wall ratios above the selection region should be chosen only for aesthetics purpose according to the overall architectural envelope design of the building. Validation of thermal results is presented in

section 4.7. The results presented next refer to 30% WWR for a south-facing perimeter space. For other window-to-wall ratios, the user has to re-run the program.

The impact of the secondary link (electric lighting control) on monthly cooling, heating and lighting energy demand is separately shown in Figures 4.12-4.17. Lighting energy demand (Figure 4.12) is drastically reduced even during the winter, when daylight availability is low because of snowfall and overcast conditions. This effect is taken into account when calculating monthly cooling and heating energy demand in Figures 4.13-4.14. Cooling energy demand is reduced during the year if active lighting control is used due to reduction in internal gains. On the contrary, heating energy demand is slightly increased (during the winter) when the lights are controlled. Interestingly, Figure 4.13 shows that cooling is required throughout the year, even during the winter season.

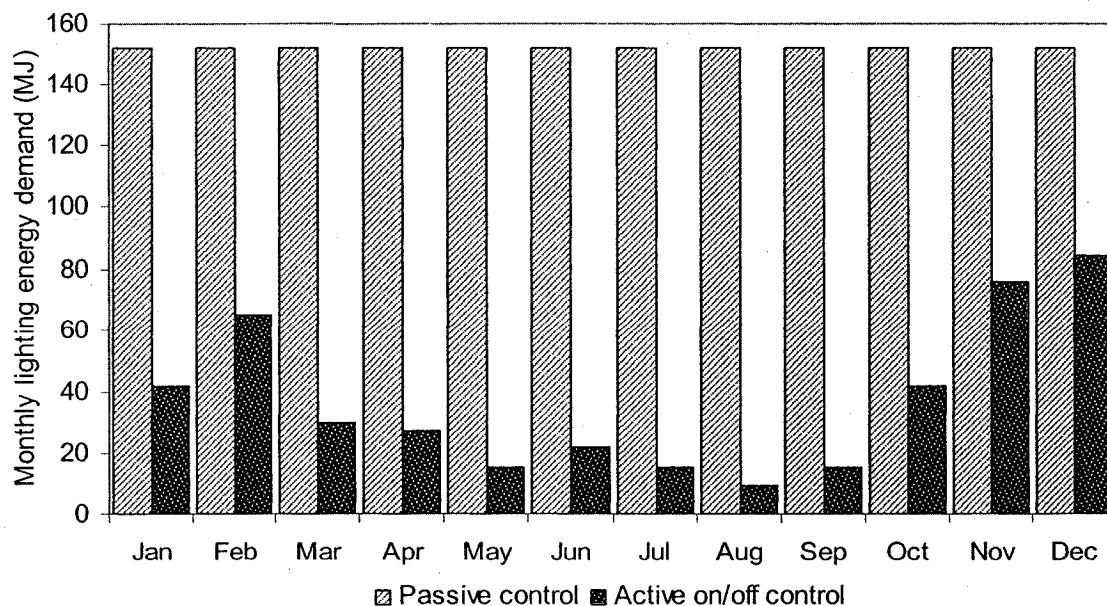


Figure 4.12. Impact of electric lighting control on monthly lighting energy demand.

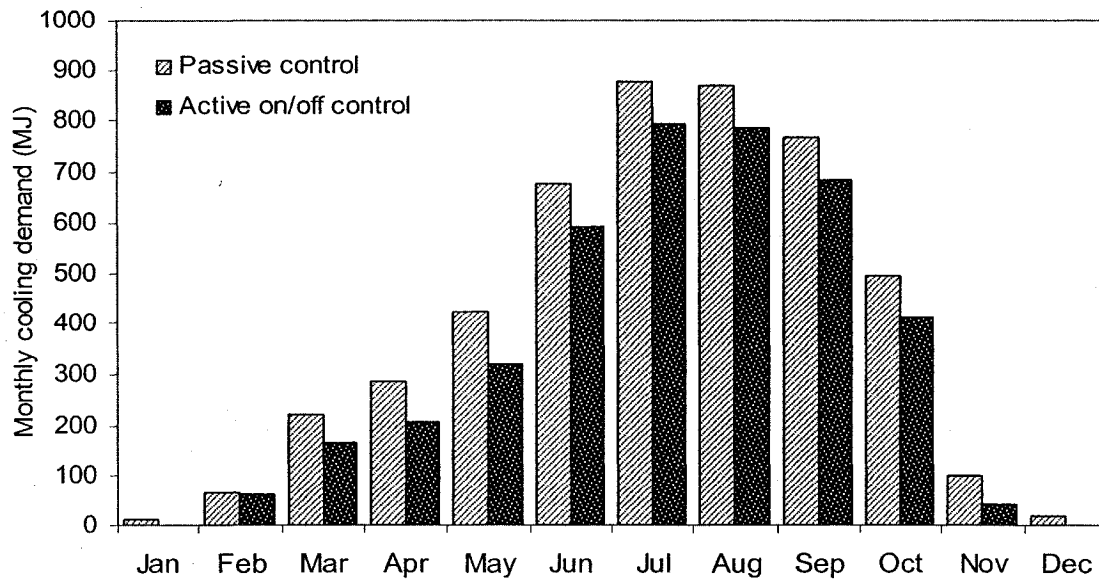


Figure 4.13. Impact of electric lighting control on monthly cooling energy demand.

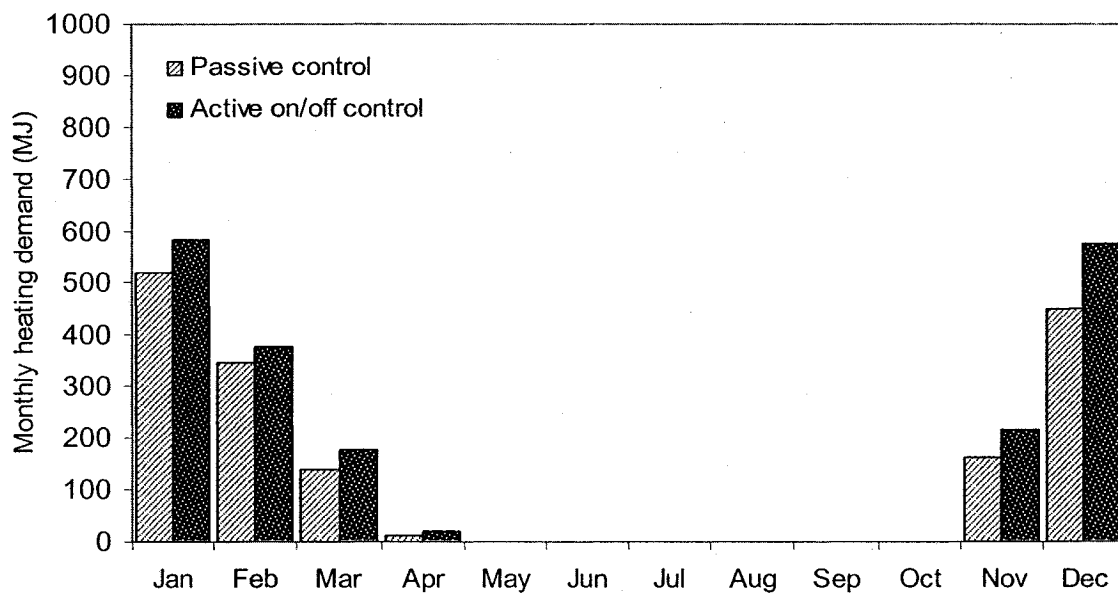


Figure 4.14. Impact of electric lighting control on monthly heating energy demand.

The overall combined impact of daylighting and electric lighting control on annual energy demand for heating, cooling and lighting is shown in Figure 4.15. Active on/off control results in 16% increase in annual heating demand (from 1626 MJ to 1947 MJ),

16% decrease in annual cooling demand (from 4814 MJ to 4060 MJ) and 76% decrease in annual lighting demand. Although the relative percentage of each component change, the total annual energy demand is reduced by 22% (from 8264 MJ to 6449 MJ) if active on/off electric lighting control is enabled.

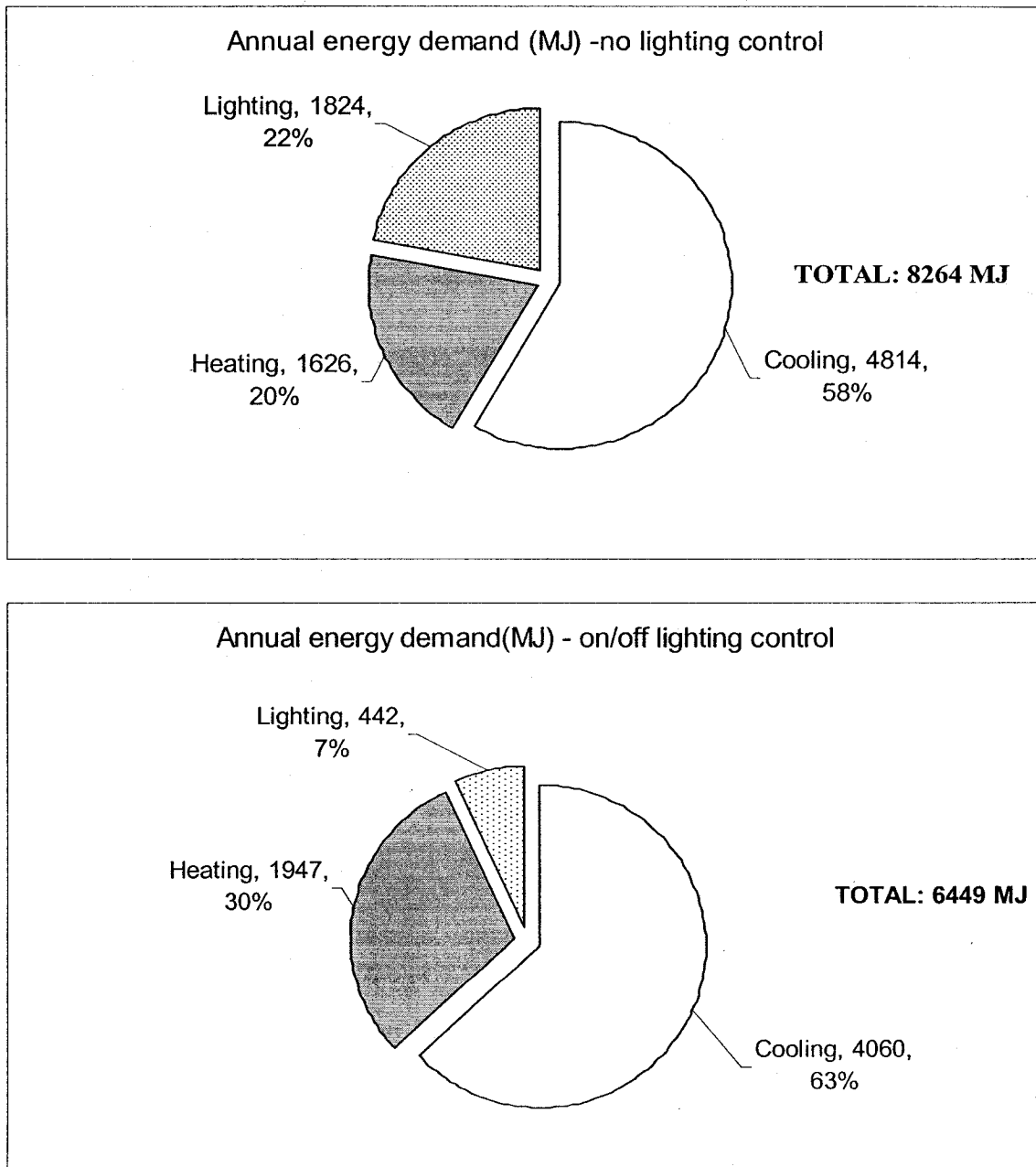


Figure 4.15. The overall impact of electric lighting control on annual energy demand.

Despite the fact that the building is located in Montreal, the perimeter space considered in the integrated analysis is rather cooling-dominated. Monthly comparison of energy demand components for the recommended case is shown in Figure 4.16. For February, March and November both cooling and heating is needed. Energy demand for both heating and cooling could be reduced if a window with higher thermal resistance is used.

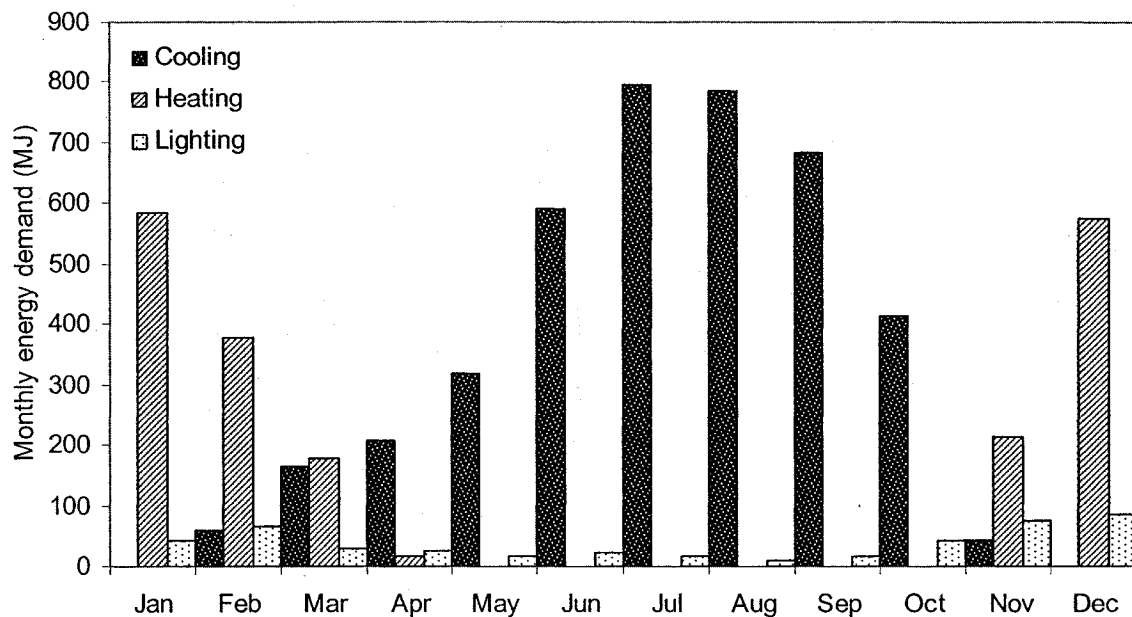


Figure 4.16. Comparison of monthly energy demand for heating, cooling and lighting for the selected case (30% WWR, south-facing, active on/off electric lighting control).

4.4. Selection of shading properties and control - exterior roller shade as an example

The second phase of the integrated daylighting and thermal analysis includes the selection of shading device properties and control, based on their impact on integrated performance indices. As described earlier, shading provision is necessary in order to prevent glare and thermal discomfort, while at the same time reduce cooling energy demand. Since the results presented above show that cooling contributes most to annual

energy demand for the considered space, it is preferred that the shading device is not placed inside, to avoid extra heat gains. Therefore an exterior roller shade was considered as an example. The roller shade solar and optical properties and control are direct links between daylighting and thermal performance and are now considered as design variables. New integrated performance indices will be computed as a function of the design variables, to provide information for selecting shade properties and control. Two types of shading control were considered:

- (i) passive control: roller shade remains closed during working hours to ensure privacy;
- (ii) active automatic control: roller shade is open when beam illuminance on the window is less than 200 lux (or beam solar radiation incident on the window is less than 20 W/m²). For each working hour in the year during which the above condition is satisfied, the roller shade opens automatically for maximization of daylight view to the outside (without causing glare, since there is no direct sunlight).

For an exterior shade, its absorptance and reflectance have negligible effects on interior conditions; the important parameter is the transmittance (visible and solar). It will determine the amount of transmitted daylight into the room and the available solar gains. Daylighting simulation runs therefore as function of shade transmittance for each control option. First, the transmitted amount of beam and diffuse daylight into the room for every hour in a year is calculated by multiplying the beam and diffuse components of window and shading device transmittance respectively. Roller shades are assumed as perfect diffusers with constant transmittance and this assumption was used in this simulation. If (bi)-directional transmission properties for a certain product are available, these can be used as input in the simulation model for a more accurate transmittance characterization.

For example, directional transmittance functions from WIS (van Dijk, 2003) can be used as input in the daylighting simulation model. However, in the early design stage for which this analysis is performed, this degree of detail maybe unnecessary, except if the transmittance of the shading system has a very strong dependence on incident solar angles (even then, after a large number of inter-reflections the error is reduced). The transmitted daylight into the room for each hour in the year is calculated from:

$$D = \frac{E_b \cdot \tau_b + E_d \cdot \tau_d}{1 - \rho_{rs} \cdot \rho_w} \cdot \tau_{rs} \quad (4.10)$$

where:

τ_b is the beam window transmittance;

τ_d is the diffuse window transmittance;

τ_{rs} is the roller shade transmittance;

ρ_w is the window reflectance;

ρ_{rs} is the roller shade reflectance.

All the above parameters are essentially expressed as a function of time (solar incidence angle). The denominator in Eq. (4.10) accounts for inter-reflections between the exterior shade and the window.

The shading control is modelled by modifying the transmittance equations as schedule functions. For passive control, the transmittance of the roller shade is always equal to τ_{rs} . For automatic active shading control, the shade transmittance is set equal to τ_{rs} when beam illuminance on the window is higher than 200 lux and equal to one when no direct sunlight is incident on the window (less than a threshold-200 lux). An example of shading control modelling using transmittance schedules is shown in Figure 4.17 for five

successive days in February. In this case, the transmittance was set to 0.1 (shade closed) if more than 200 lux of beam daylight were incident on the window during working hours (9am-5pm). In all other cases (shade open) it was set equal to one. We can conclude from this figure that the first day is clear and the roller shade is closed to prevent from glare. The second day is cloudy and therefore the shade remains open throughout the day to maximize diffuse daylight utilization. The last day shown is an interesting case; mixed sky conditions occur and the shade is automatically closed for one hour (1pm) because during that time there was beam daylight incident on the window. Then clouds move in front of the sun again and only diffuse daylight is present, thus the shade automatically re-opens.

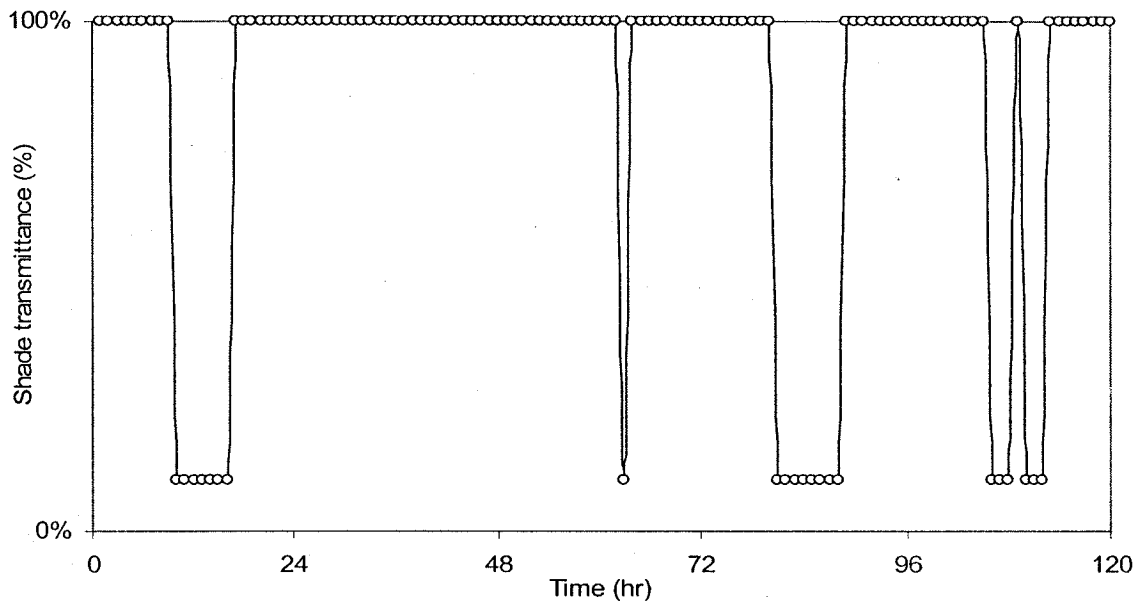


Figure 4.17. Example of roller shade transmittance schedule for modelling shading control (five successive days in February).

Shading control is modelled in the way described above and as a function of shade transmittance (from 5% to 60%). The radiosity method is again employed and hourly

work plane illuminance is computed as a function of roller shade transmittance and control. Daylight availability ratio is calculated in the same way as before, but now it is plotted as a function of shade transmittance for the different control options. The results of the daylighting simulation (Figure 4.18) include the impact of hourly sky conditions and shading control. One of the simultaneous goals is to prevent direct sunlight from entering the space, for glare elimination; however this depends on shade transmittance.

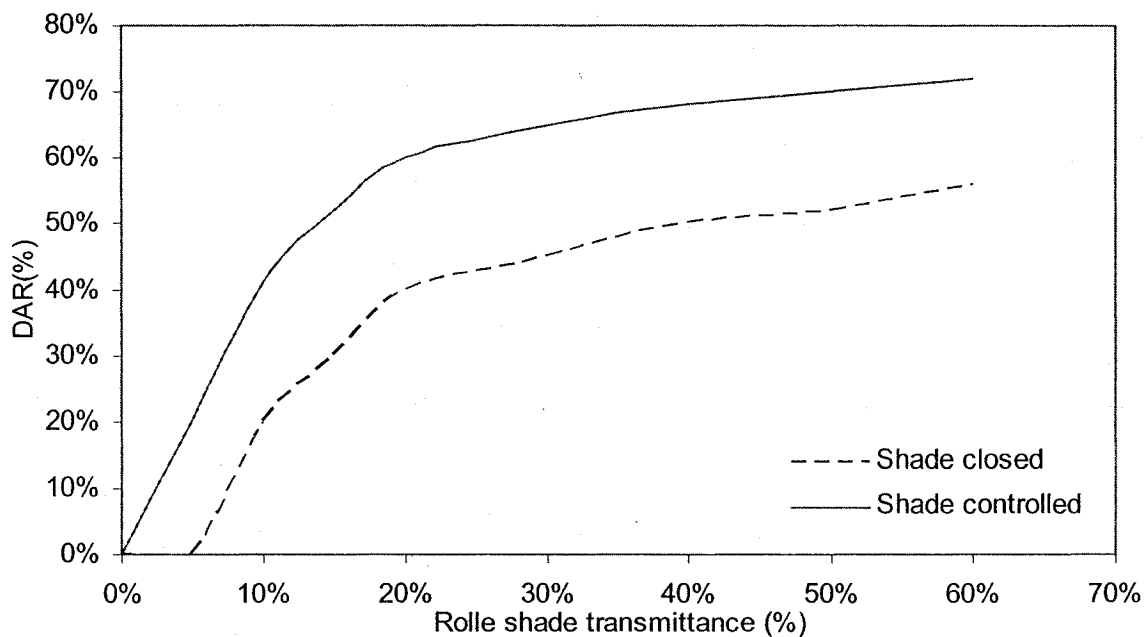


Figure 4.18. Annual DAR as a function of exterior shade transmittance for the two different shading control options.

The impact of control on the daylighting performance index is obvious: passive shading control results in poor daylight availability while simple on/off (open/close) control of the shade during working hours –depending on daylighting conditions– increases annual daylight availability ratio by 20% on average. The variation of the DAR with shade transmittance indicates that the new daylighting saturation region occurs at

about 20% roller shade transmittance for both shading control options. For this transmittance value, active automatic shade control results in exactly 20% more annual DAR (60%) compared to passive shading control (40%). This means that people could perform office tasks (500 lux on work plane) for 20% more time in a year without using artificial lighting (using daylight only). Except for energy savings, this translates in possible increase in productivity (Heschong, 2002).

Shading properties and control also have a direct impact on electricity demand for lighting. Assuming active on/off lighting control (based on previous results), the electricity demand for lighting is calculated from the daylighting analysis results as a function of shade transmittance and control (Figure 4.19). Passive shading control results in higher energy demand for any transmittance value because daylight availability is reduced (Fig. 4.18). Figure 4.19 shows that lighting energy demand is not significantly decreased for shade transmittance higher than 20%. For 20% transmittance, annual electric lighting energy demand is already reduced by 40% for passive shading control and by 60% for active automatic shading control (compared to passive lighting control).

The impact of shading links on the integrated thermal performance indices is studied next. Roller shade transmittance has a direct effect on the solar radiation transmitted into the room and therefore on the thermal performance of the space. Moreover, it has a direct impact on the daylight availability and electric lighting energy demand; therefore it also has an indirect impact on thermal performance indices, expressed with the secondary link of electric lighting control, which determines the variation of internal gains.

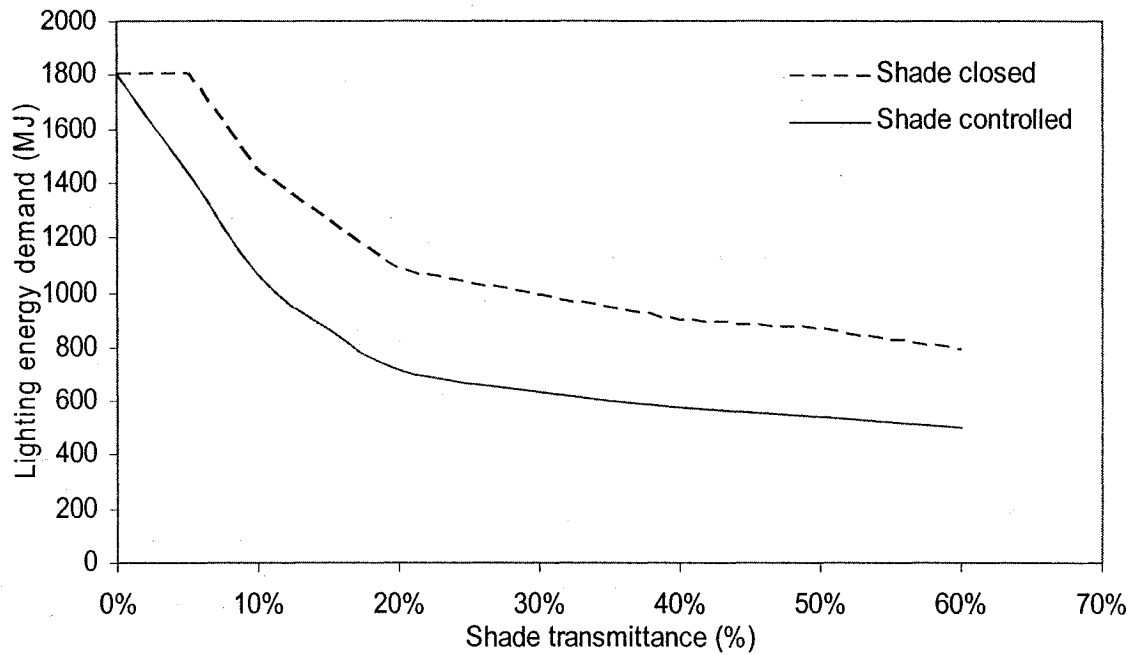


Figure 4.19. Impact of shading transmittance and control on lighting energy demand.

The hourly thermal simulation module runs as a function of shade transmittance and control. The impact of shading control on transmitted solar radiation is modelled with schedule functions of shade transmittance as described above. The secondary impact of shading properties and control on lighting internal gains is modelled using schedule functions for the internal gains source in the thermal network. Based on the daylighting and electric lighting simulation results, hourly information is passed to the thermal simulation file for the same hour in order to include the effect of daylighting on thermal performance as a function of the shading design variables. Internal gains from lights are therefore predicted as a function of roller shade properties for each working hour, taking into account the shading control. Representative results for a day in February are shown in Figure 4.20. In this case, the transmittance of the shade was set to 10% when beam sunlight was incident on the window and active automatic shading control was assumed

in conjunction with on/off lighting control. Mixed sky conditions result in on/off operation of electric lights depending on work plane illuminance values, which eventually depend on shade transmittance and control. The results of Figure 4.20 indicate that at 10am (as well as at 3pm-5pm) electric lights were on, which means that (i) either sky conditions were overcast and there was not enough daylight on the work plane or (ii) that beam daylight was incident and the shade automatically closed so daylight levels dropped below 500 lux and electric lights automatically switched on.

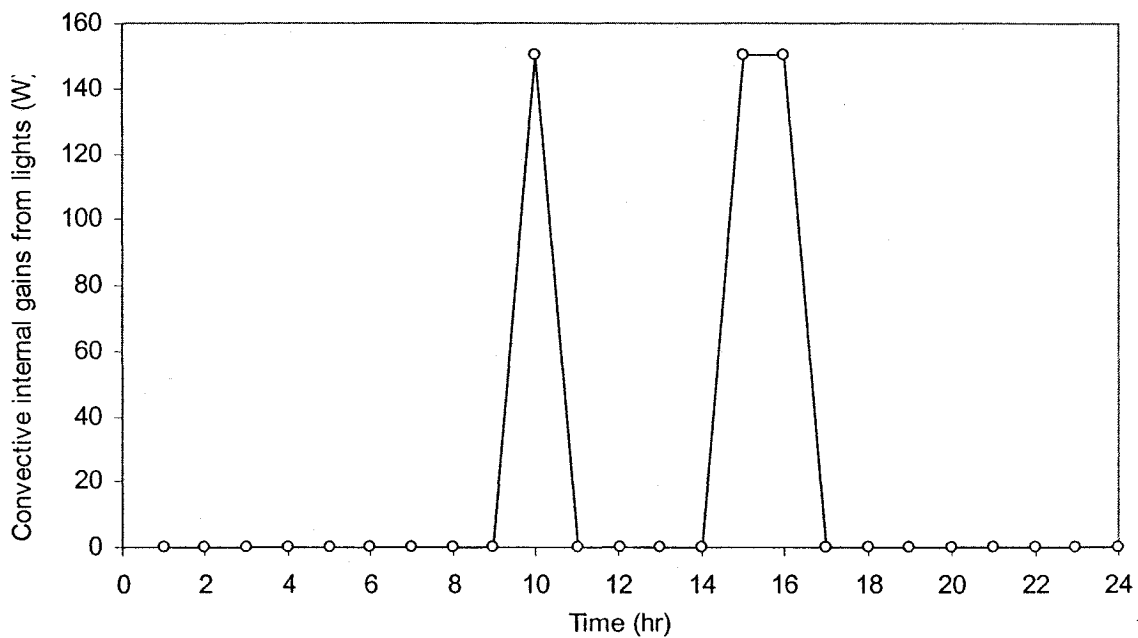


Figure 4.20. Hourly internal gains from electric lights during working hours assuming active automatic shading and lighting control.

Integrated thermal performance indices are calculated and plotted as a function of shade transmittance, taking into account active automatic shading and lighting control. The results are presented in Figure 4.21. Cooling energy demand is slightly reduced for transmittances between 10% and 20% because there is not enough available daylight and

electric lights operate continuously. Then it increases because large solar gains are admitted in the space. Heating energy demand generally decreases with shade transmittance, because higher transmittance values result in higher solar gains. However, heating energy demand is increased for 20% transmittance, because for that value there is enough daylight so on/off control of electric lights results in reduction in internal gains, while at the same time solar gains are not very large yet.

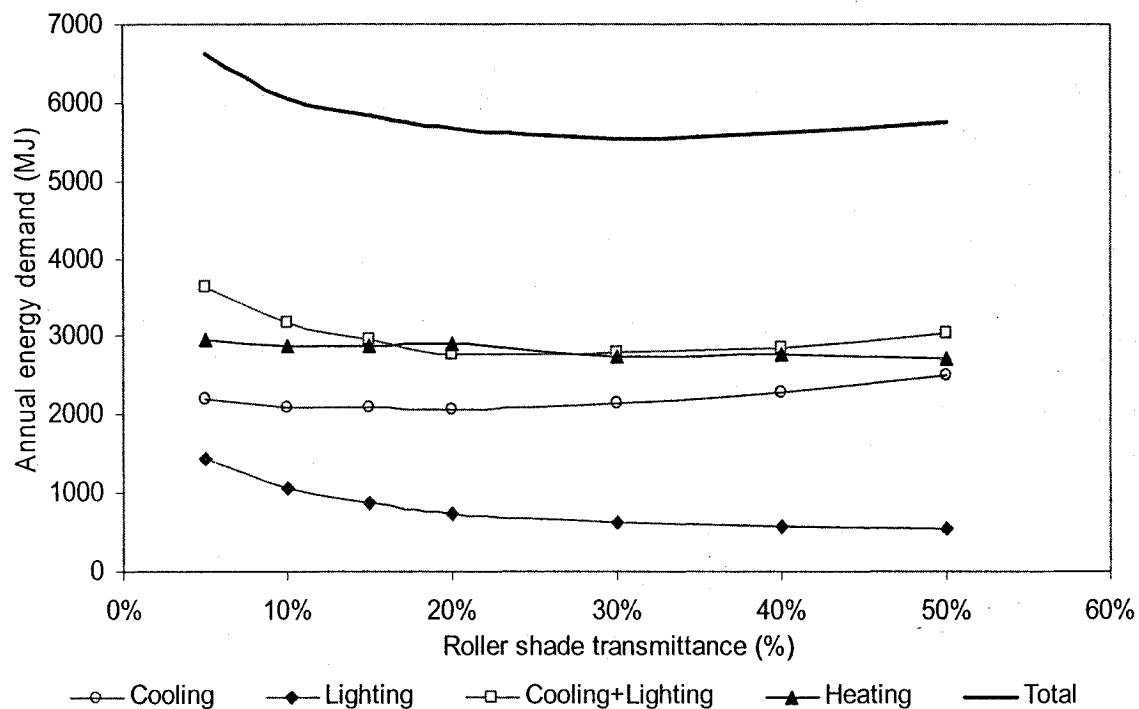


Figure 4.21. Integrated thermal and lighting performance indices as a function of shade transmittance, assuming active automatic shading and lighting control.

The curve that shows the sum of cooling and lighting energy demand is possibly the most important. However it should be noted that lighting is generally the most costly since electricity is directly used and then it also increases cooling load. Since shading is used for reduction in cooling requirements (except for glare), this is the curve that shows

the integrated benefits of daylighting, shading and electric lighting control. This key integrated performance measure, shown separately in Figure 4.22, indicates that optimum energy performance is only achieved if daylighting benefits due to reduced electric lighting operation (and the subsequent reduction in cooling requirements) exceed the increase in energy demand due to increased solar gains, which is always affected by shading control. The variation of this index with shading properties helps in investigating if this region exists (Tzempelikos & Athienitis, 2005a). Figure 4.22 shows that for the considered case it exists and it occurs for 20% roller shade transmittance. For smaller transmittance values, poor daylighting conditions result in large internal gains due to continuous electric lighting operation during working hours; therefore both cooling and lighting demand increase. For higher transmittance values, daylight availability is adequate but excessive solar gains result in an increase of cooling demand which is higher than the reduction due to reduced internal gains. Active automatic shading and lighting control make it possible for this integrated performance index to reach a minimum for a certain roller shade transmittance value (20%) that can be selected from Figure 4.22 and satisfies Eq. (3.21).

Since maximization of daylight utilization is also a criterion when selecting shading properties (and control), we have to examine if the considered region coincides with the saturation region from daylighting simulation results of Figure 4.18. As described in the methodology, the two regions instinctively overlap if the curve of Figure 4.22 really reaches a minimum (which is not always the case). An interesting point is that, although the total annual energy demand shown in Figure 4.21 also reaches a minimum (for $\tau_{rh} = 30\%$), this value does not match exactly with the daylighting saturation region, neither

with the minimization of cooling and lighting energy demand. Furthermore, the annual energy demand is not necessarily minimized for heating-dominated climates, especially for non-south-facing facades (for any type of shading and lighting control). Shading devices are not used for reduction of heating requirements; they are used for rejection of major solar gains -to reduce peak cooling load and cooling energy demand- as well as for glare elimination and possible simultaneous daylight maximization. For the case considered here, a roller shade with 20% transmittance can minimize cooling and lighting energy demand while at the same time daylight availability is maximized if active shading and lighting automatic control is utilized.

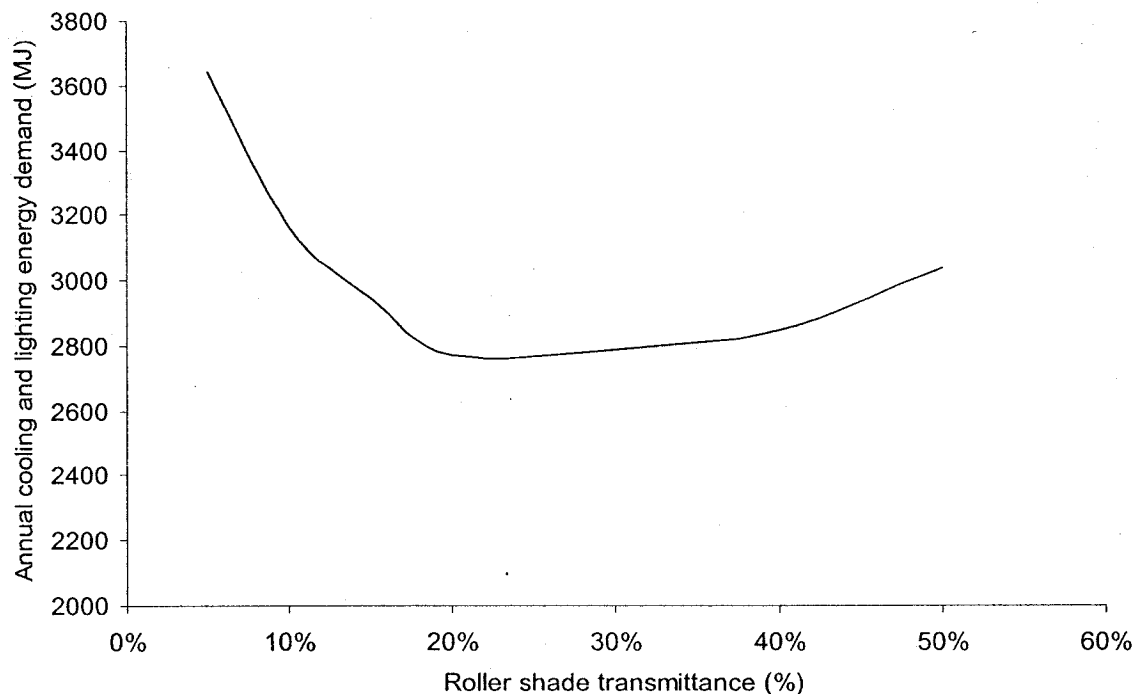


Figure 4.22. The sum of annual cooling and lighting energy demand –a key integrated performance measure- as a function of roller shade transmittance. The curve reaches a minimum for 20% transmittance.

The actual energy consumption can be calculated assuming a typical HVAC system for the climate of Montreal (a heat pump for cooling and a boiler for heating). Using the COP/energy efficiency ratio of the system, the annual energy consumption for heating and cooling can be predicted from the annual energy demand. Figure 4.23 shows the energy consumption results, following the patterns of energy demand presented in Fig. 4.21. The sum of cooling and lighting energy consumption is presented in Fig. 4.24. The minimum has been shifted to the right about 10%, compared with the annual energy demand. For warmer climates, the optimum would shift to the left (smaller transmittance values), since cooling energy would be much higher. Moreover, the total energy consumption could be minimized for cooling-dominated climates.

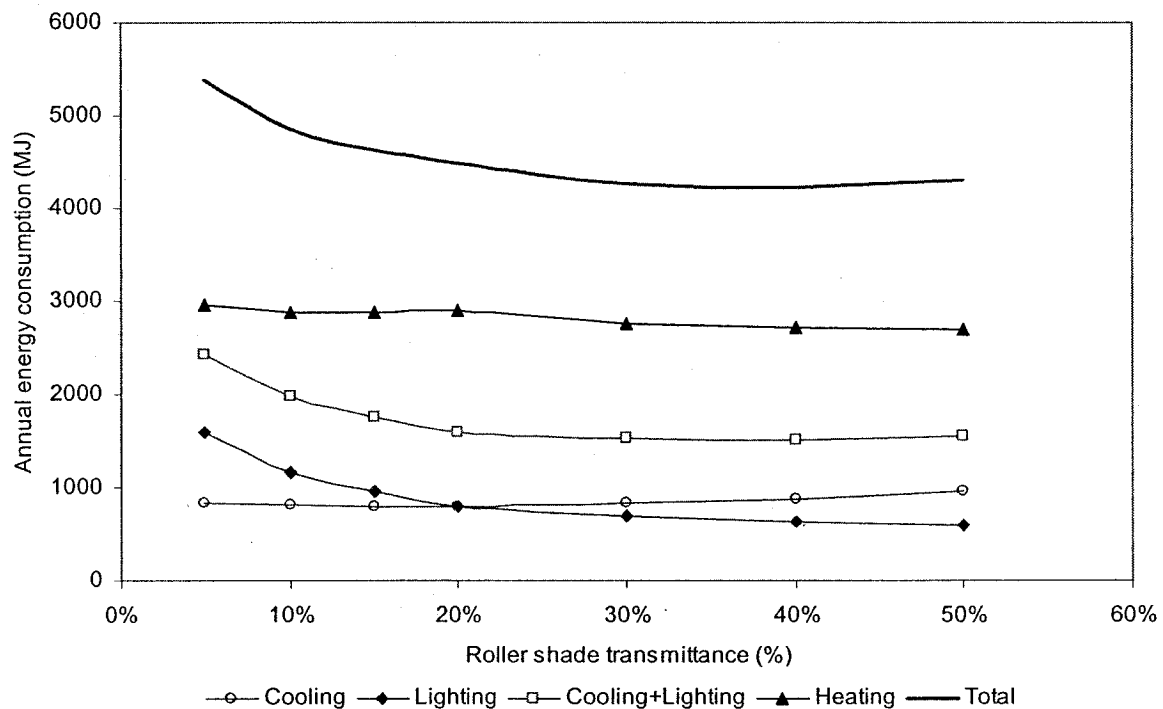


Figure 4.23. Integrated thermal and lighting performance indices (energy consumption) as a function of shade transmittance, assuming active automatic shading and lighting control.

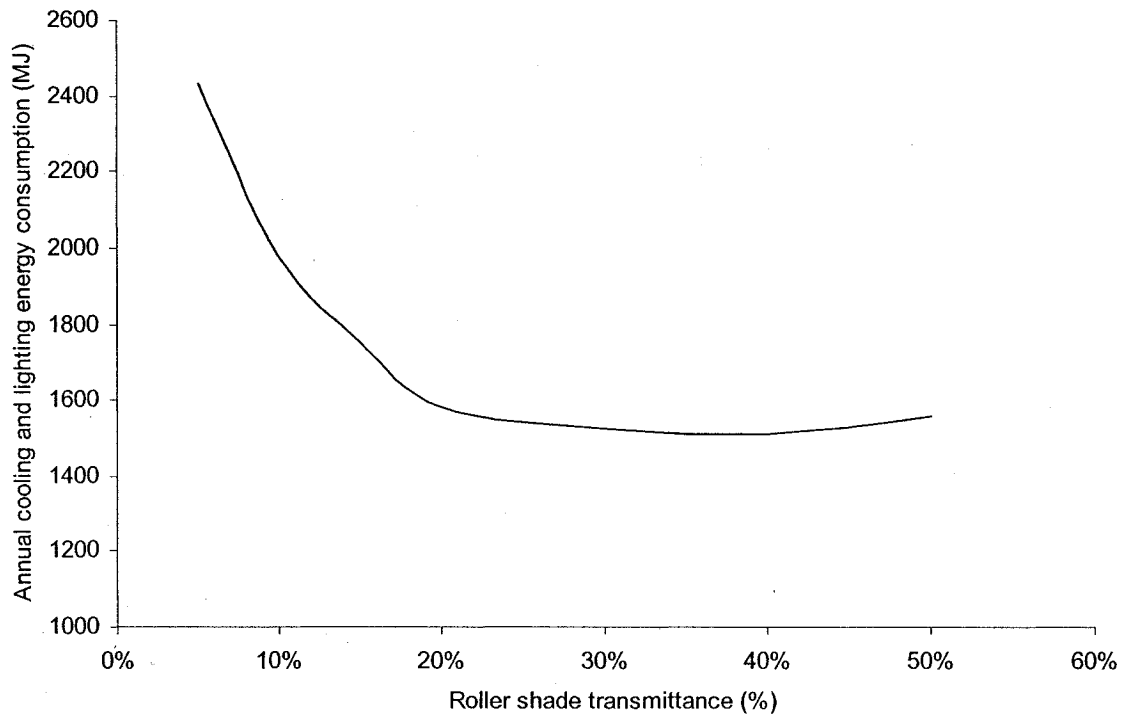


Figure 4.24. The sum of annual cooling and lighting energy consumption –another key integrated performance measure- as a function of roller shade transmittance.

New correlations between integrated performance indices can be found, taking into account the impact of shading control. For example, figure 4.25 shows the variation of lighting and cooling energy demand with Daylight Availability Ratio, for the case of active lighting/shading control. Cooling demand is minimized when Daylight Availability Ratio reaches 60%, because for this condition solar and internal gains are optimally balanced, assuming automatic control. Lighting energy demand decreases when daylight availability is increased (higher transmittance values), and the integrated impact of shading properties and control transforms Eq. (4.10) into a second degree polynomial ($R^2 = 0.9995$):

$$E_L = -868.55 \cdot \text{DAR}^2 - 819.17 \cdot \text{DAR} + 1532.4 \quad (4.11)$$

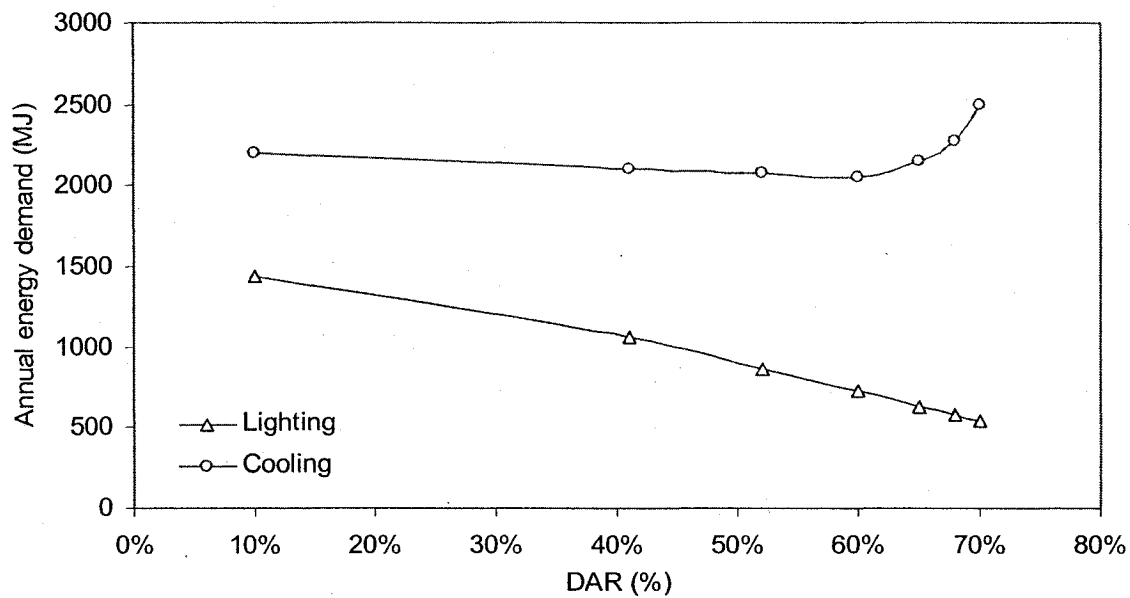


Figure 4.25. Correlations between daylighting, electric lighting and thermal performance indices taking into account the impact of automatic shading and lighting control.

Figure 4.26 presents cooling energy demand as a function of lighting energy demand, assuming lighting and shading automatic control. The respective transmittance values are also shown. For 20% transmittance, which corresponds to 720 MJ lighting energy demand, the impact of shading control results in minimization of cooling demand (2054 MJ) based on the integrated analysis. This value corresponds to 60% DAR, for which solar and internal gains are optimally controlled. Based on the variation of integrated performance indices with shading design variables, it is recommended that 20% transmittance is selected for an exterior roller shade for a south-facing façade with 30% WWR in Montreal, to simultaneously satisfy the thermal and daylighting requirements. The annual energy demand breakdown is shown in Figure 4.27, and energy consumption breakdown is presented in Fig. 4.28. Shading operation results in increased heating demand, which now accounts for 51% of the total, while cooling demand is further reduced to 36% of the total annual energy demand.

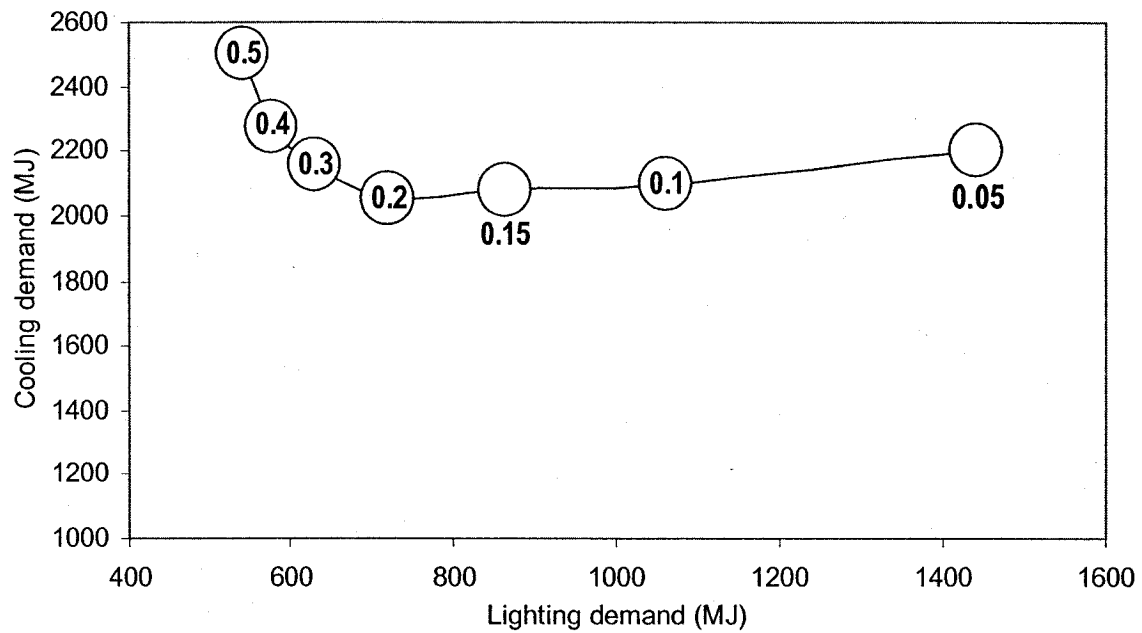


Figure 4.26. Correlation between cooling and lighting energy demand taking into account the impact of automatic shading and lighting control. The respective roller shade transmittance values are shown.

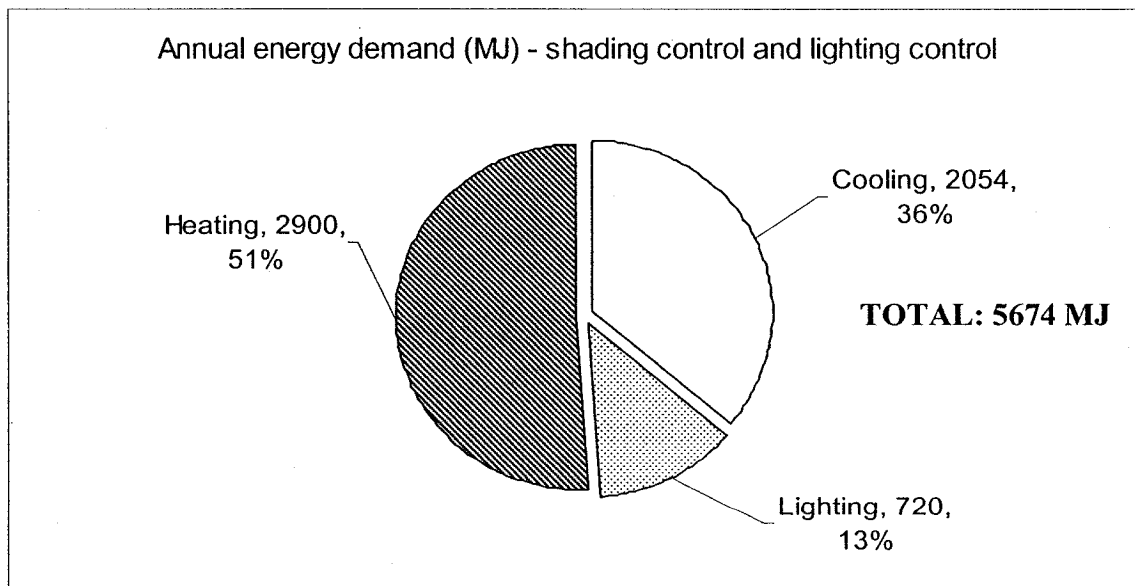


Figure 4.27. Overall annual energy demand considering an exterior roller shade with 20% transmittance and active automatic lighting and shading control.

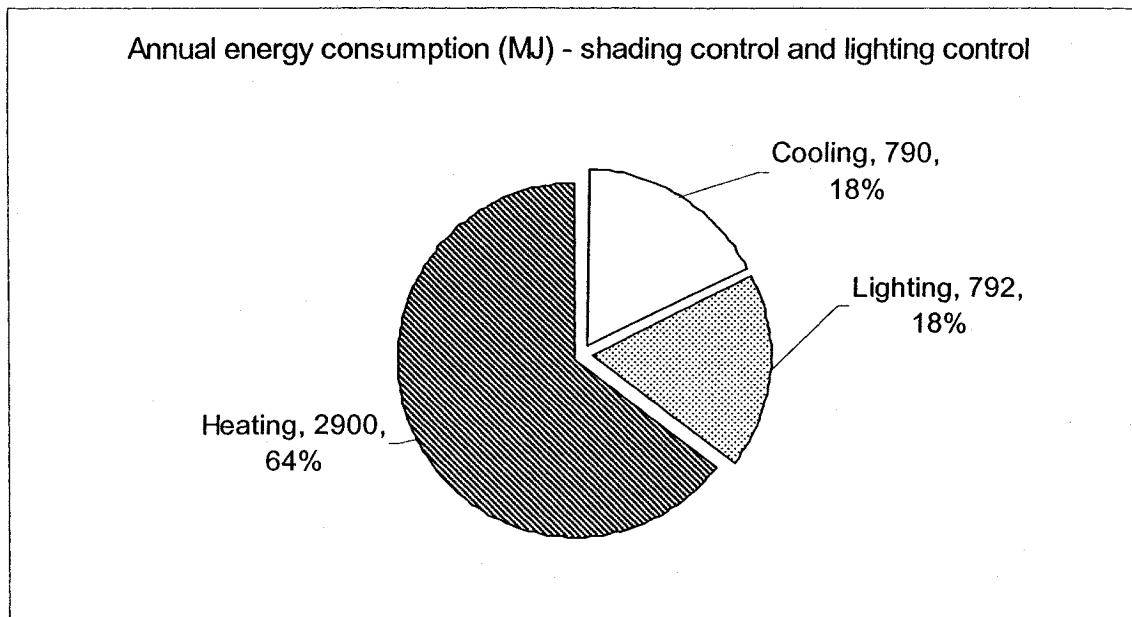


Figure 4.28. Annual energy consumption breakdown considering an exterior roller shade with 20% transmittance and active automatic lighting and shading control.

A general comparison of the integrated daylighting and thermal analysis results (including the shading impact) with the base case (30% window-to-wall ratio) with passive and active electric lighting control is presented in Figure 4.29. Shading control has the highest impact on cooling energy demand; it is dramatically reduced by almost 50% (from 4060 MJ to 2054 MJ) compared to active lighting control without shading. Lighting energy demand is of course affected mostly by lighting control and increases by 38% (from 442 MJ to 720 MJ) if shading is used because of decrease in daylight availability (although shading control takes into account daylight maximization). Heating energy demand is increased by 48% (from 1947 MJ to 2900 MJ) compared to the case of active lighting control without shading because major solar gains are rejected. However, utilization of an exterior shade with 20% transmittance and active automatic control

results in reduction in total annual energy demand by 12% (from 6449 MJ to 5674 MJ).

This happened because:

- (i) cooling is more important than heating for south-facing perimeter spaces;
- (ii) the energy benefits of daylighting with integrated shading and lighting control were higher than the increase of solar gains if the roller shade transmittance was 20% when active automatic shading and lighting control was used and an optimum balance between controlled solar gains and internal gains was achieved (Figure 4.22).

Note that the daylighting criterion for maximization of daylight utilization is satisfied by choosing the right control strategy and selecting the daylight saturation region (Fig. 4.18).

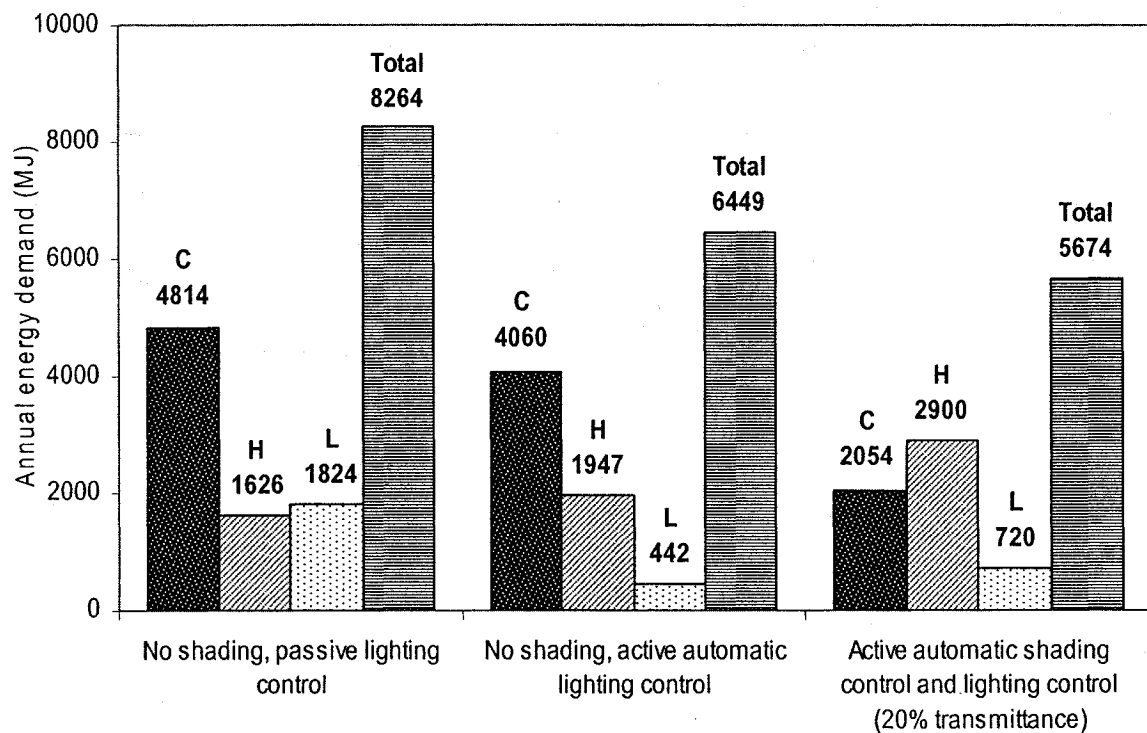


Figure 4.29. Comparison between annual heating, cooling, lighting and total energy demand for the base case with passive and active lighting control and the studied roller shade case with selected transmittance and control.

Results of the integrated daylighting and thermal analysis indicate that the designer should select around 20% transmittance for an exterior roller shade. However, for such a value, part of the direct sunlight will be transmitted and this would still create glare problems. Transmittance values higher than 5% cannot ensure glare elimination. The 20% value should therefore represent the average transmittance of the shading device, which can vary along the height of the shade, as described in section 3.6. A possible solution is to consider a roller shade with variable transmittance- small for the bottom part and high for the top part- following a distribution function presented in Eq. (3.23). Most venetian blind products can overcome this problem because beam daylight is reflected upon the slat surface and it is re-directed towards the ceiling, thus solar rays never reach the occupants sight of vision. Another good solution is the three-section façade concept, a real application of which is described in section 4.6.

4.5. Results for venetian blinds

Thermal and optical properties of a between-glass venetian blind device, installed in an outdoor test room (Fig. 4.30), were measured during 2001-2002. Visible and solar transmittance (Figure 4.31) was calculated as a function of blind tilt angle, solar incidence angle and sky conditions (Tzempelikos & Athienitis, 2001). Transforming the transmittance equations as a function of time using multivariate regression for simulation purpose, an optimization algorithm was developed for automated blind control with respect to daylighting only (Athienitis & Tzempelikos, 2002b), for elimination of glare and simultaneous daylight maximization.

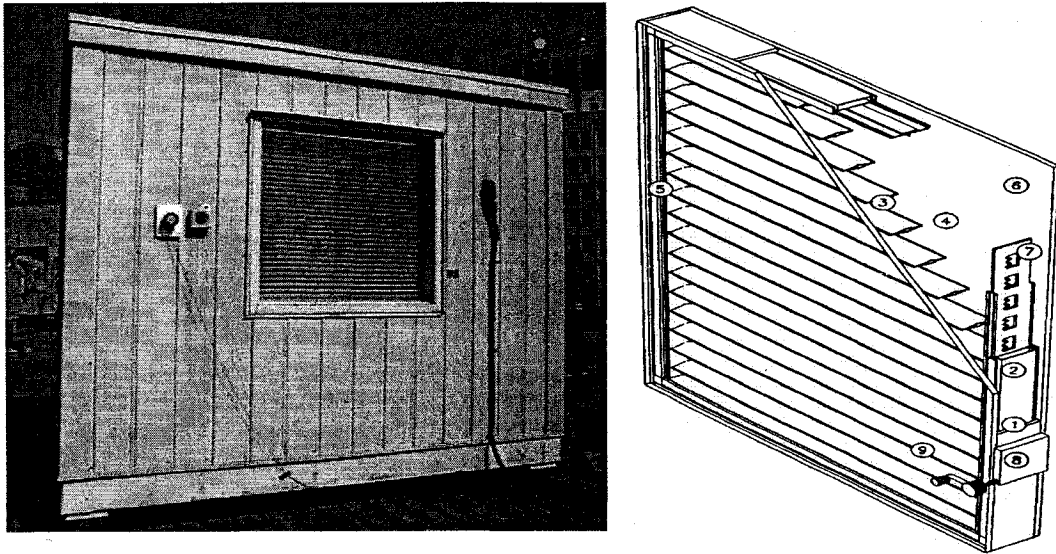


Figure 4.30. Outside south view of the test room with integral Venetian blinds (Unicel window) and schematic of the window system.

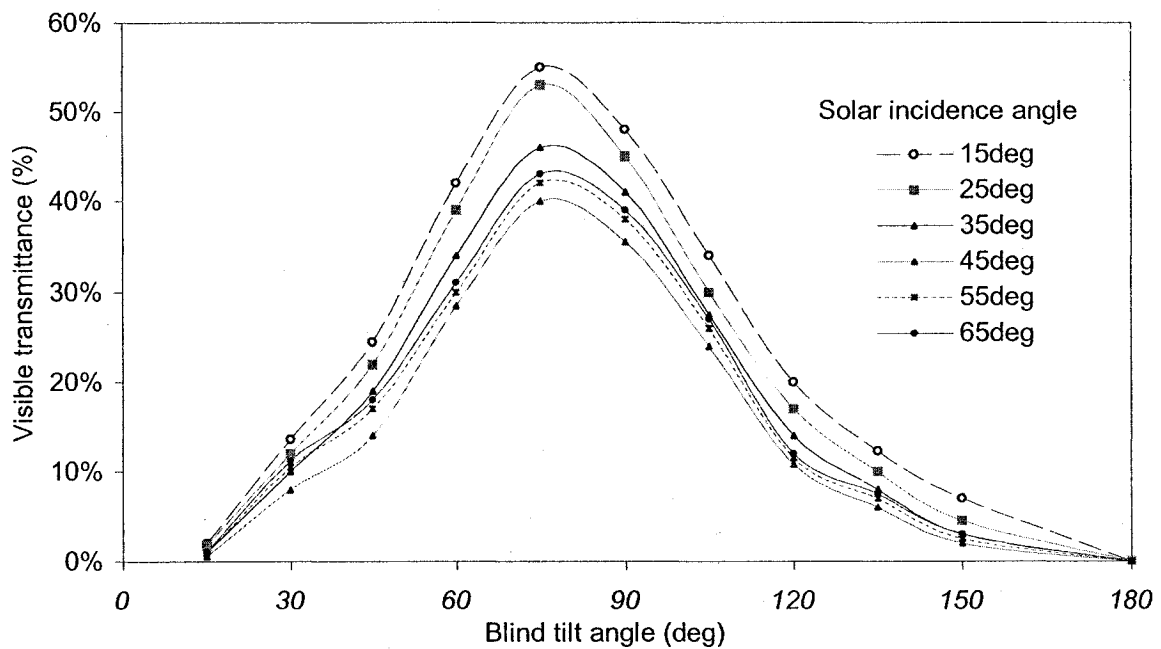


Figure 4.31. Visible transmittance of the window-blind system as a function of blind tilt angle for different solar incidence angles (Tzempelikos & Athienitis, 2001). 90^0 is the horizontal blind position.

Optimum blind tilt angles were calculated for each hour in a year (Figure 4.32) and were then used in the daylighting simulation program to predict work plane illuminance for a considered office space similar to that assumed in the integrated results presented above. A comparison of daylighting results between a fully automated blind (operating according to the algorithm developed for glare elimination) and a static blind revealed the significant impact of venetian blind control (Tzempelikos & Athienitis, 2003a). Figure 4.33 shows the daily illuminance on a point 4 m from the façade for a motorized venetian blind and a static blind. Work plane illuminance is drastically improved with appropriate blind control.

The centre-of-glass thermal resistance of the blind-window system was also measured for use in thermal simulation. Figure 4.34 shows the variation of window thermal resistance with blind tilt angle.

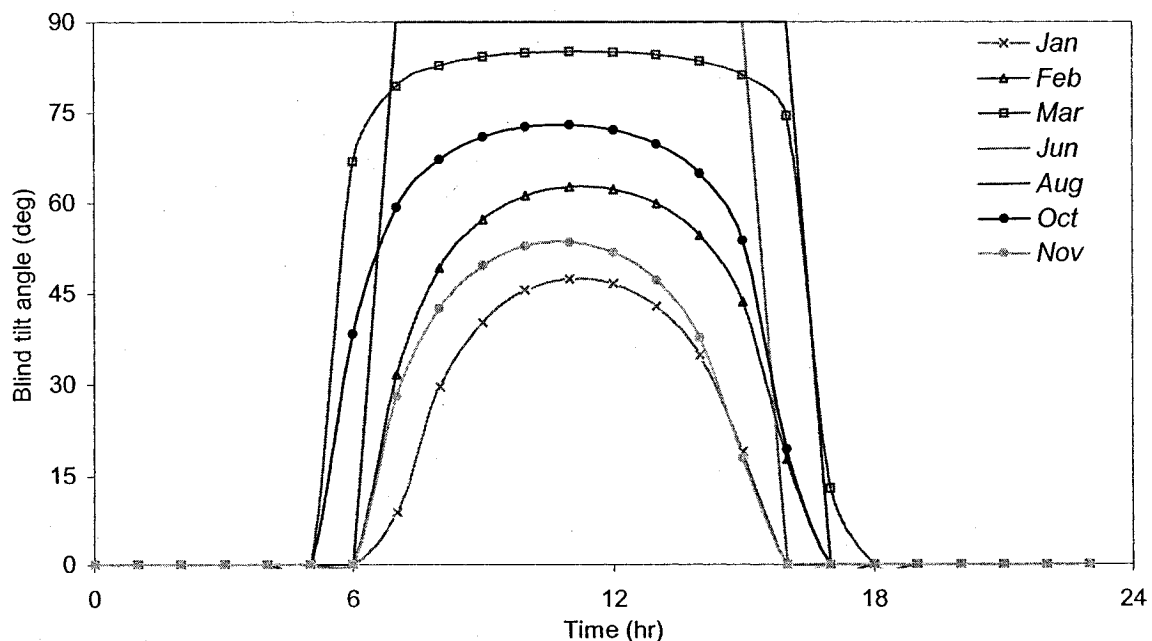


Figure 4.32. Daily variation of optimum venetian blind tilt angles for representative months (Tzempelikos & Athienitis, 2003a). 90^0 is the horizontal blind position.

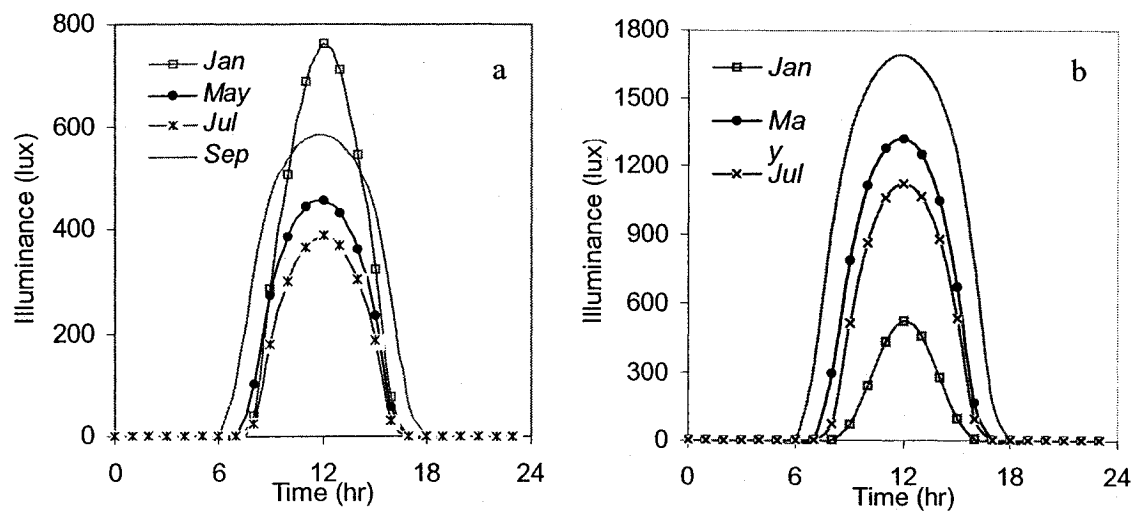


Figure 4.33. Comparison of daily illuminance on a point of work plane surface 4 m from the façade, modelled with motorized blind control (a) and a static blind at 45° tilt angle (b) (Tzempelikos & Athienitis, 2003a).

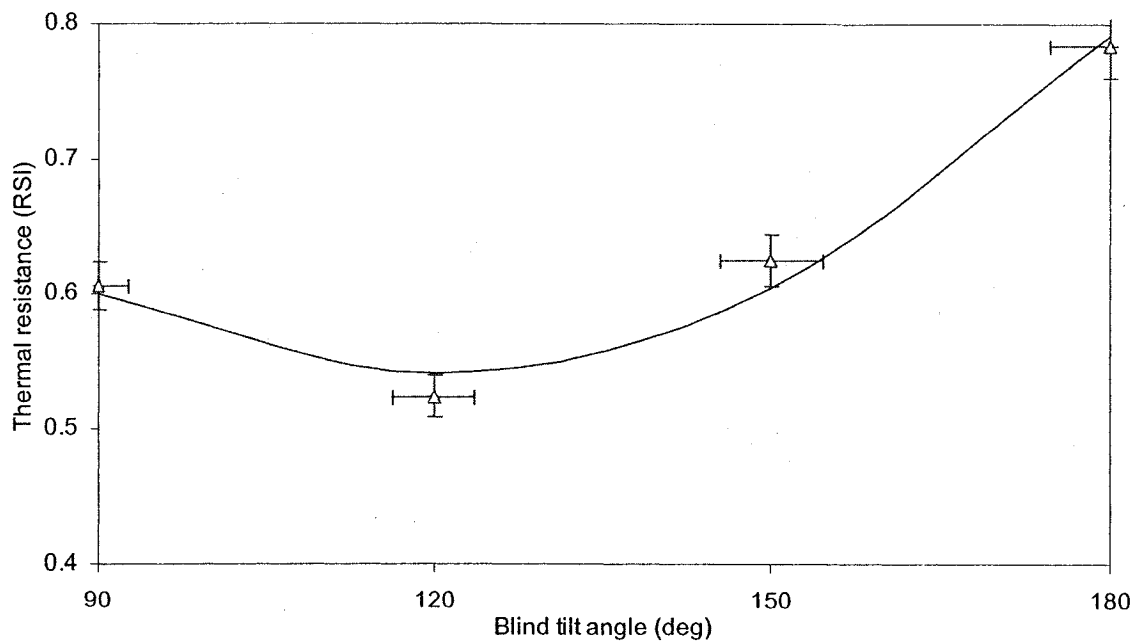


Figure 4.34. Thermal resistance (centre-of-glass) of the Unicel blind-window system as a function of blind tilt angle. 90° is the horizontal blind position, 180° means blind is fully closed.

The thermal resistance of the window system varies from $R=0.524 \text{ m}^2 \cdot ^\circ\text{C}/\text{W}$ (for $\beta=120^\circ$) to $R=0.784 \text{ m}^2 \cdot ^\circ\text{C}/\text{W}$ (blinds fully closed, $\beta=90^\circ$). When the blinds are set horizontal ($\beta=90^\circ$), there is a 23% decrease in thermal resistance ($R=0.606 \text{ m}^2 \cdot ^\circ\text{C}/\text{W}$). As the blind closes, it increasingly blocks the direct exchange of long-wave radiation between the glass panes and in the fully closed position it makes the system almost equivalent to a triple glazed window. In the horizontal position, continuous convection is impeded much more than in the 120° position; thus, for blind tilt angles close to 120° , the thermal resistance is minimized. Practically, for this blind position the net heat transfer due to combined convection and radiation is maximized. The impact of temperature difference (inside-outside) on the window thermal resistance was found to be negligible. The curve of Fig. 4.34 was approximated by a second-degree polynomial ($R^2=0.985$):

$$R(\beta) = \frac{\alpha_2 \cdot (\beta - 90^\circ)^2 + \alpha_1 \cdot (\beta - 90^\circ) + \alpha_0}{1000} \quad [\text{m}^2 \cdot ^\circ\text{C}/\text{Watt}] \quad (4.12)$$

where $\alpha_0=600$, $\alpha_1=-4$, $\alpha_2=0.068$ and β is the blind tilt angle in degrees. The above equation can be used to model the thermal performance of the window system and may be combined with the daylight optimization blind control algorithm developed, for prediction of hourly window thermal resistance in thermal simulations.

Thermal simulations were performed to investigate the effect of variable blind properties and control on peak thermal loads and energy demand. As shown in Figure 4.35, automated blind control for daylight maximization is often in conflict with reduction in energy demand. This is because blinds automatically rotate to reflect beam daylight towards the ceiling (but not reject it) and solar gains are admitted into the space. A static blind could have better energy performance, as seen in Figure 4.35. Nevertheless,

glare problems are always avoided if the automated control is used and at the same time maximization of daylight is achieved. A static blind would results in poor daylighting availability, as shown in Figure 4.33.

Monthly peak thermal loads for the controlled venetian blind are shown in Figure 4.36. The blind rotates in order to block (re-direct) beam solar radiation. During the summer, when the sun is high, the blind can be kept at horizontal position for maximization of view (Fig. 4.32). During spring/fall, the blind moves at a position close to 120° because the sun is lower, so the thermal resistance of the window is minimized (Fig. 4.34) and heat gains are increased. This is why cooling load is high during the spring and fall.

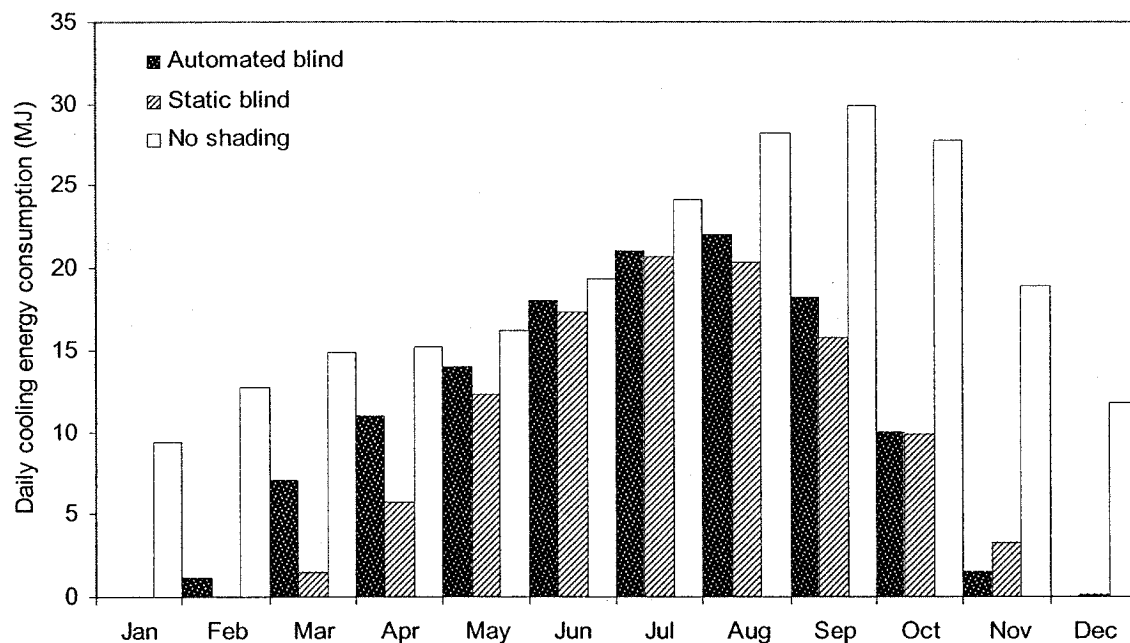


Figure 4.35. Comparison of average daily cooling energy demand for automated blind control and static blind (passive control) for each month (Tzempelikos & Athienitis, 2003a).

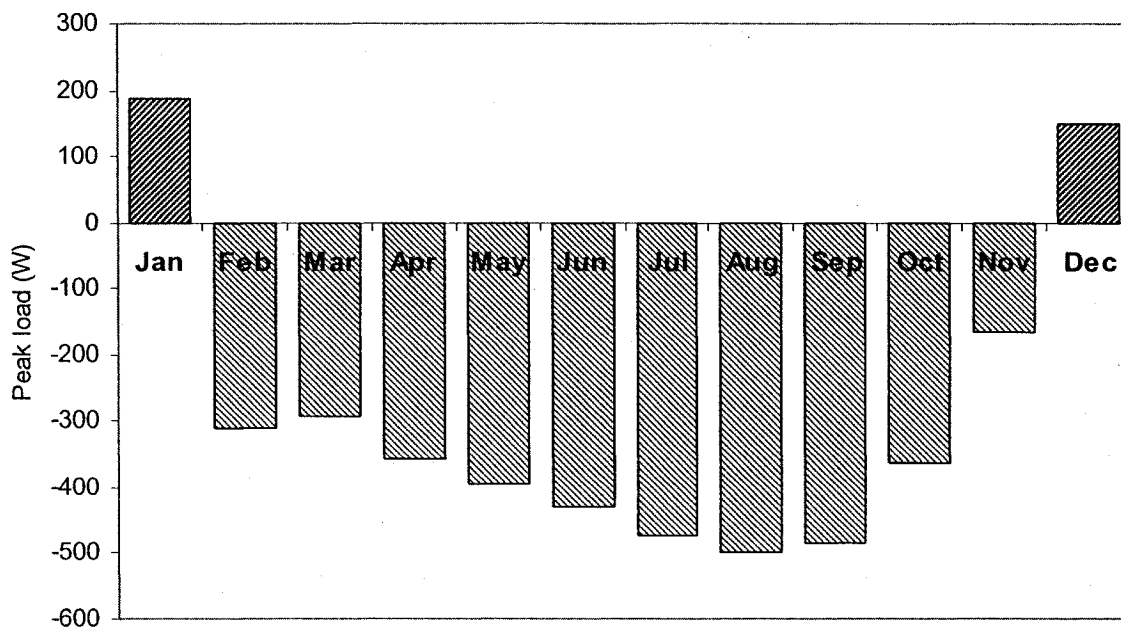


Figure 4.36. Monthly peak thermal loads for a controlled venetian blind (Tzempelikos & Athienitis, 2003a).

4.6. A case study - application of the three-section façade concept

A real design case study was completed for the new Engineering and Computer Science building of Concordia University in 2002. The objective of the design study, which was one of the motivations for the development of this work, was to investigate the integrated daylighting and thermal performance of different façade design schemes. The 17-storey building has just been completed in downtown Montreal (Fig. 4.37) and it has a large perimeter area with two of the main facades facing approximately southwest and southeast. Therefore emphasis was given on optimal control of solar gains using shading devices in conjunction with electric lighting control. The perimeter spaces consist of private offices, labs and a large atrium and separate analysis was done for each case. Daylighting and thermal simulations were performed for the following design variables:

- Window-to-wall ratio;
- Glazing type;
- Shading device type;
- Shading device properties;
- Shading control options;
- Electric lighting control options;

Decisions for each design variable were made based on the following criteria:

- Elimination of perimeter heating;
- Reduction of peak heating and cooling load;
- Reduction in energy demand for heating and cooling;
- Maximization of daylight use;
- Reduction in electricity demand for lighting.

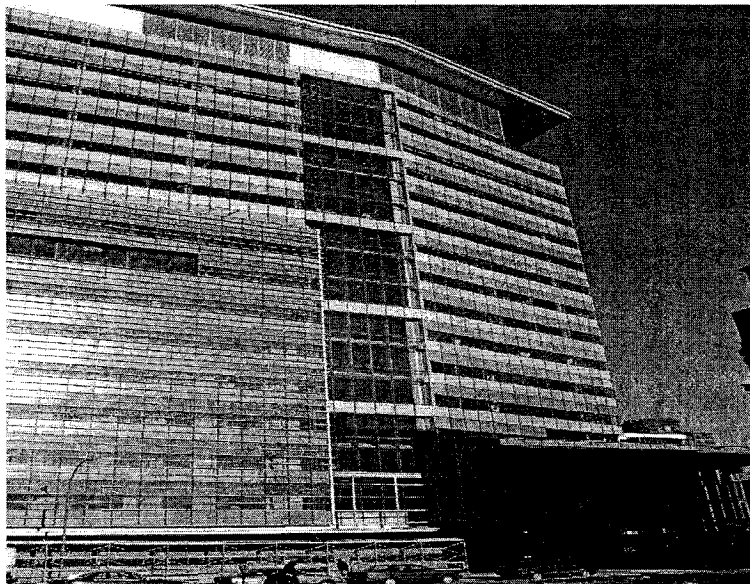


Figure 4.37. Guy Street facade (SW) of new Engineering building (note the repeating floors with three sections each – spandrel, middle viewing section and upper fritted glass section).

4.6.1. Window-to-wall ratio and glazing type

First, an investigation of the impact of window-to-wall ratio and glazing thermal resistance on the overall performance was performed. Three options for WWR were considered: 50%, 60% and 70%. Also, three options for glazing type were simulated:

- clear double-glazed windows with low-emissivity coatings ($R = 0.52 \text{ m}^2\text{K/W}$);
- heat mirror clear glazing ($R = 0.67 \text{ m}^2\text{K/W}$);
- high performance clear glazing ($R = 0.85 \text{ m}^2\text{K/W}$).

Clear glass was preferred in all cases for maximizing daylight penetration. The spandrel section thermal resistance was chosen equal to approximately 3 RSI to meet energy code recommendations for Montreal.

The impact of window size and type on thermal comfort was studied by calculating Mean Radiant temperature and Radiant Temperature Asymmetry for private offices. Normally, perimeter heating is required to raise the temperature of the window interior surfaces to avoid condensation on cold spots and to enable occupants to work near the windows by raising the local mean radiant and operative temperatures. The window interior surface temperature was determined 1 m from the window for a typical office for all three façade glass options with an outside temperature of -24°C and a room air temperature of 22°C . The operative temperature was also calculated. In all three cases, the temperature of the glazing is well above the dew point and no condensation is expected if framing with good thermal break is chosen. Thus, the design parameter is the operative temperature (a function of the temperature of the glass, the other surface temperatures, the air temperature and the radiation view factors between a person and the each surface) and the radiant temperature asymmetry (RTA). The goal was to keep

operative temperature above 20 °C, while keeping RTA less than 10 °C. Table 4.3 shows the results.

The low-e double-glazing (RSI 0.52) would definitely require perimeter heating, while the higher R-value glazings do not require perimeter heating. This translates into capital cost savings and increase of the usable area of the perimeter offices. Daylight availability is ensured for the high window-to-wall ratios considered so the selection of window type and size was based on elimination of perimeter heating and thermal performance. After evaluation of the thermal simulation results (discussed below), a heat mirror clear low-e glazing ($R = 0.67 \text{ m}^2\text{K/W}$) and 60% window-to-wall ratio were selected for perimeter offices and labs.

Table 4.3. MRA and RTA results for different WWR and glazing types

WWR (%)	Glazing R-value (RSI)	Glass Surface temperature, °C	Operative temperature, °C	Mean Radiant Temperature, (MRT) °C	Radiant Temperature Asymmetry (RTA) °C near window
0.6	0.52	10.94	20.76	20.04	11.06
0.6	0.674	13.47	21.04	20.47	8.53
0.6	0.85	15.24	21.24	20.78	6.76
0.7	0.52	10.94	20.62	19.78	11.06
0.7	0.674	13.47	20.93	20.30	8.53
0.7	0.85	15.24	21.15	20.65	6.76

4.6.2. Analysis for perimeter private offices

After determining window-to-wall ratio, an integrated daylighting thermal and daylighting analysis was performed for perimeter private offices. Because for the two major facades high solar gains are expected, shading provision was necessary and the following options were examined for shading:

- (i) motorized venetian blinds integrated in the double-glazed window;
- (ii) interior roller blinds with transmittance in the range 10%-30%;
- (iii) a translucent glazing unit with honeycomb insulation between glazings;
- (iv) different combinations of the above.

Shading control and electric lighting control were studied for each case and the simultaneous impact of each design scheme on the daylighting and thermal performance was simulated. A major goal of the design methodology was to create a multifunctional façade, which could satisfy the different objectives. Two options are shown in Figure 4.38. In the first case, the three-section façade was examined, having the top part shaded by the intermediate venetian blinds studied experimentally (section 4.3 above) and the viewing part shaded by a roller shade. In the second case, a roller shade with variable transmittance was studied. Another option, a combination of a translucent glazing on the top part and a roller shade for the bottom part was also investigated. A general evaluation of the different shading options considering many factors is shown in Table 4.4.

Hourly work plane illuminance was calculated for every perimeter office. Roller shades were controlled like in the integrated methodology (closed when direct sunlight is present) and venetian blinds were controlled based on an algorithm developed for daylight maximization and glare elimination (Athienitis & Tzempelikos, 2002b). Directional transmittance characteristics of venetian blinds were also measured and included in the model (Tzempelikos & Athienitis, 2002), to account for an accurate simulation of work plane illuminance values.

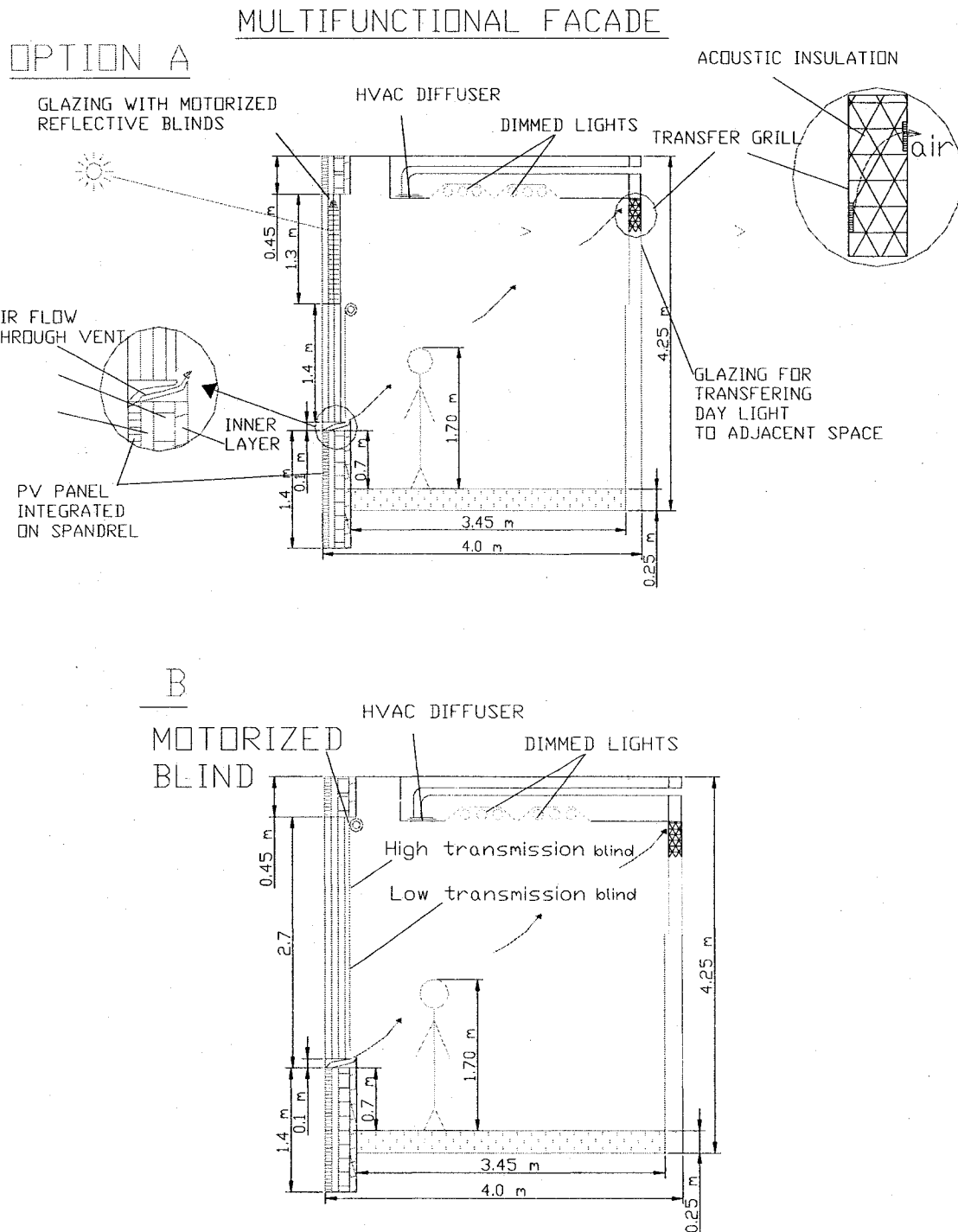


Figure 4.38. Two options of three-section multifunctional façade design considered for private offices.

Table 4.4. General evaluation of different shading options for private offices.

	Roller blind	Venetian blinds	Translucent glazing	Roller blind and venetian blinds	Roller blind and translucent glazing
Shading performance	Good	Good	Not good	Good	Not good
Visual comfort	Good	Excellent	Not good	Excellent	Good
Transmittance	Low	Medium	High	Medium	High
Thermal resistance	Low	Medium	High	Medium	Medium
Privacy	Excellent	Excellent	No	Excellent	Good
Control	Good	Excellent	No	Excellent	Good
Illuminance distribution	Good	Excellent	Not good	Excellent	Good
Reflecting daylight to adjacent spaces	No	Excellent	Good	Excellent	Good
Glare reduction	Excellent	Good	No	Excellent	No
Cooling load reduction	Good	Excellent	No	Excellent	No
User friendliness	Yes	No	No	Yes	Yes
Cost	Low	High	Low	High	Low
Appearance	Good	Not good	Not good	Good	Good
Overall performance	Good	Good	Not good	Excellent	Not good

During the winter, when the sun is low, venetian blinds have to close to prevent glare and interior daylight levels are low. A roller shade with 20% transmittance performs better, but it does not eliminate glare because part of beam sunlight is still transmitted. During the summer, the situation is the opposite. Now the sun is high and venetian blinds can re-direct most of the available daylight on the ceiling, resulting in high interior illuminance values. On the other hand, roller shades must close to prevent glare and therefore work plane illuminance is reduced. A combination of the two, applying the three-section façade concept, solves the glare problem while allows adequate daylight into the room both in winter and summer. Moreover, illuminance distribution in the room

is improved if venetian blinds are used for the top part because, depending on blind tilt angle, most of the transmitted daylight reaches the deepest parts of the perimeter offices, which are not illuminated if a roller shade alone is used. Similar results were produced for labs, which are up to 10 m deep.

Daylighting simulation results for roller shades, venetian blinds and combination for the case of southwest-facing private offices for clear representative days are shown in Figures 4.39 and 4.40 for winter and summer. These Figures show the daily variation of illuminance on four points on the work plane surface, according to Table 4.5. For the case of combination, the room was modelled using a modified radiosity method, as an 8-surface enclosure (six walls and two windows) with two initial luminous sources (the roller shade and the venetian blind). The directional transmission characteristics of the venetian blind system were taken into account when calculating work plane illuminance, by including weighted modifiers in the luminous exitance of respective surfaces.

Table 4.5. Description of points on work plane surface used in Figures 4.39-4.40.

Point	Distance from façade (m)
A	1
B	2
C	3
D	4

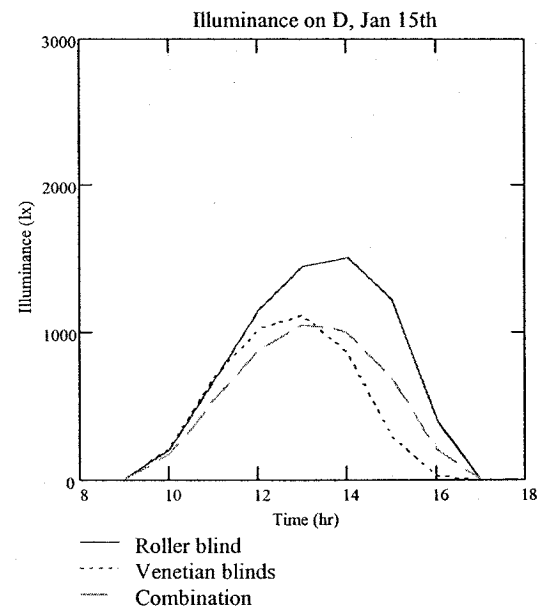
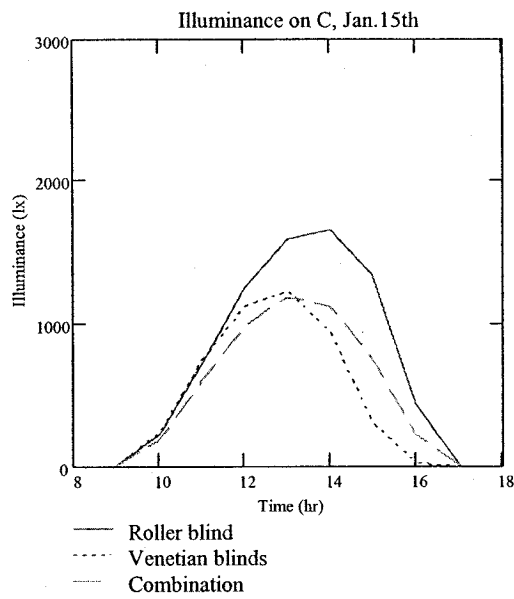
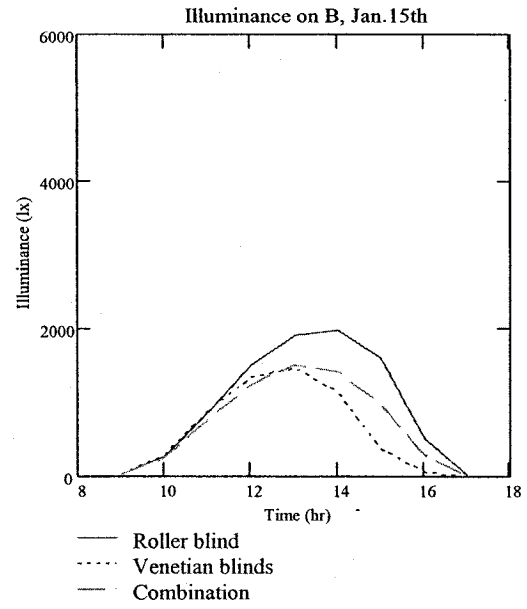
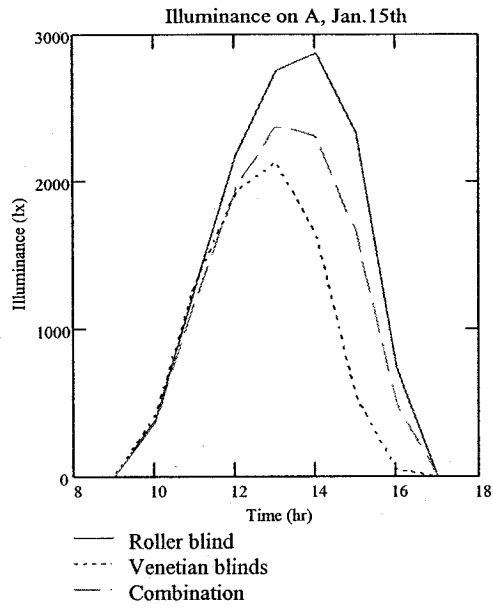


Figure 4.39. Work plane illuminance on four points for a SW perimeter office during a clear day in winter.

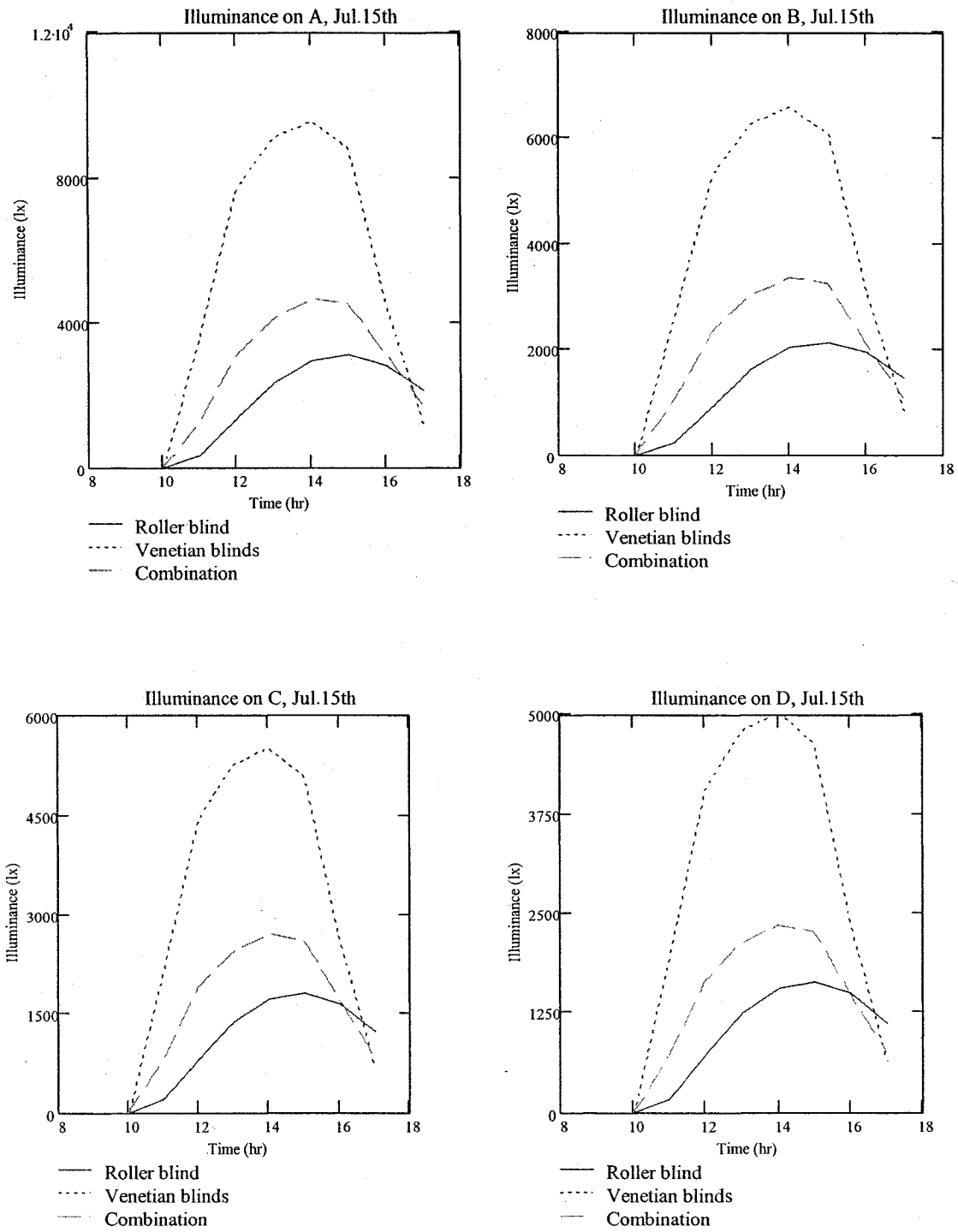


Figure 4.40. Work plane illuminance on four points for a SW perimeter office during a clear day in summer.

Placing motorized venetian blinds on the top part of a three-section façade was found to be serving one extra purpose: illuminating adjacent corridors. Taking advantage of the daylight reflected towards the ceiling and the back wall by the motorized venetian blinds (Fig. 4.38), non-perimeter corridors can be illuminated with natural daylight, thus creating a pleasant visual environment and reducing electricity demand for lighting. Hourly daylighting simulations were performed for this particular case, to calculate the amount of available daylight that can be reflected into the corridors and then predict the illuminance distribution in a 3m wide x 4.25m high corridor at the back of a typical perimeter office of the southwest façade. In this case, the methodology used is the following: first, the amount of daylight incident on the back window of the office was calculated, after computing new view factors between the back window under consideration and the eight interior surfaces of the office (including the two parts of the window- roller shade and venetian blinds). The back windows considered in the simulations were 1.3m high x 4m long (same area as the window with the motorized blinds on the opposite wall), and they were selected single-glazed, to maximize daylight transmission into the corridors. The available amount of daylight incident on the back window was computed for the case of automated venetian blinds and for the case of a translucent glazing (for comparison purpose). A sample of these results is shown in Figure 4.41.

A part of the corridor (4m long, 3m high) exactly behind the office was then considered and simulated as a seven-surface enclosure (like the case of an office with one window). The reflectances of the corridors surfaces were set equal to 60%, except for the two open sides, where the reflectances were set very close to zero (since there is no wall).

The only initial luminous source in this case is the back window. The luminous exitance of each surface and the illuminance distribution in the corridor are then calculated using the standard radiosity method. Results for illuminance distribution on the corridor floor are presented in Figure 4.42. The motorized venetian blinds perform much better than the translucent glazing due to directional reflection upon the slats; in some cases, the amount of daylight during clear days is sufficient even 2.5 m behind the office. Lighting energy demand could therefore be reduced even in non-perimeter spaces if the three-façade concept is applied in innovative ways. Note that the target illuminance in the corridors is 200-250 lux, based on Illuminating Engineering Society of North America recommendations (IESNA, 2005).

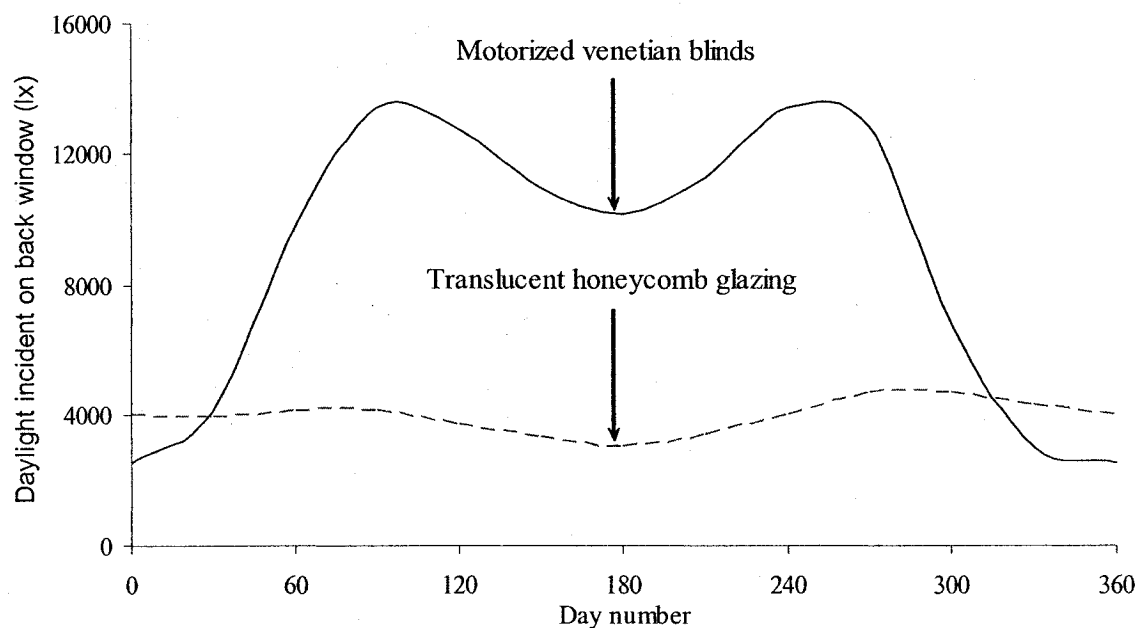


Figure 4.41. Available daylight incident on the back window to illuminate adjacent corridors for a clear day of each month at noon. The top part of the three-section façade was simulated as venetian blinds and as a translucent glazing for comparison (Tzempelikos & Athienitis, 2002).

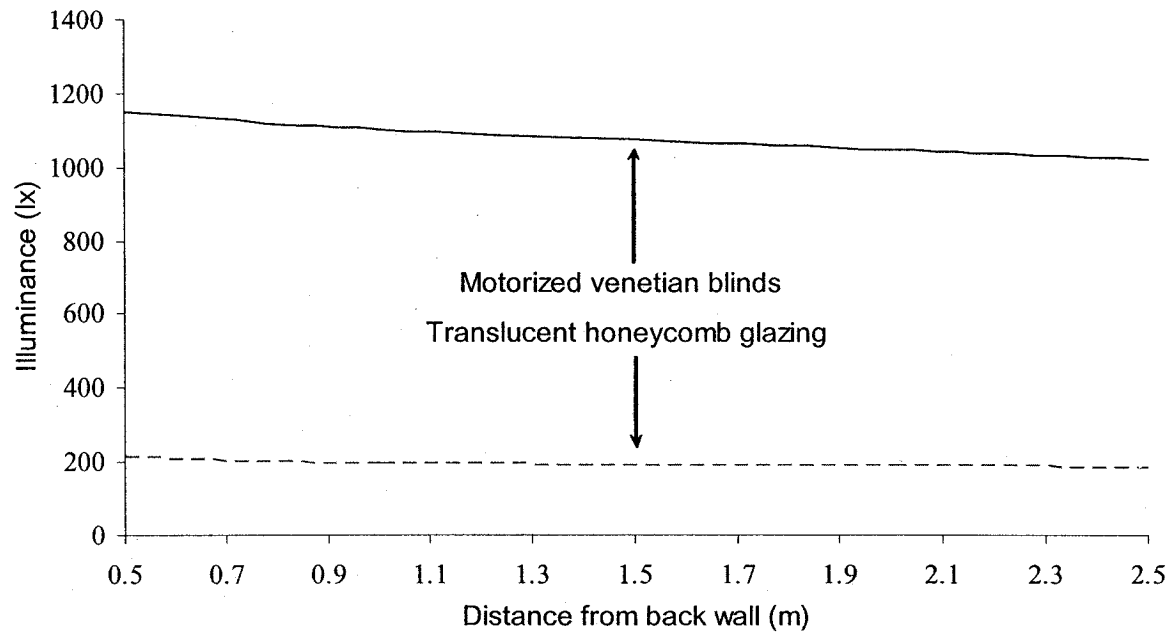


Fig. 4.42. Illuminance distribution in a 4-m wide corridor, adjacent to a SW-facing perimeter office (July 15th, noon). Natural daylight is transmitted through a window on the top part of the back wall and provides non-perimeter spaces with daylight. A venetian blind as a top part of a three-section façade is a good solution (Tzempelikos & Athienitis, 2002).

Three lighting control options were studied in order to evaluate the impact of daylight and shading properties and control on electricity demand for lighting and the integrated impact on thermal performance:

- (i) passive control (lights on);
- (ii) active on/off control (three-level switching of three T8 lamps);
- (iii) active dimming control (continuous dimming of all lamps).

The advantages of dimming control are that, first, better visual quality is ensured (occupants do not realize the change in the light intensity) and second, the energy savings are high because the lamps operate only at the necessary level (for reaching 500 lx on the work plane). However, continuous dimming is expensive. The 3-level lighting option is a

more cost-effective solution that could also result in significant energy savings. One more advantage of on/off control is that the lifetime of electric lamps is increased (compared to continuous dimming) because they turn off when sufficient daylight is present on the work plane- whereas for in the case of continuous dimming, the lamps are always on even if more than 500 lux are available on the work plane.

Simulation of electric lighting operation for all three control options was performed, assuming a three-section façade with venetian blinds on the top part of the window and a roller shade (20% transmittance) on the bottom part. For each working hour in a year, the two shading systems are automatically controlled and work plane illuminance is calculated. Then electric lighting operation is modeled for each lighting control option. Therefore the impact of shading properties and control on electric lighting use is taken into account. Figure 4.43 shows the average daily lighting energy demand of a perimeter office on the SW façade for the different lighting control options. Continuous dimming results in higher energy savings throughout the year for any orientation.

Table 4.6 presents the potential annual energy savings for each facade due to reduction in electric lighting demand for the perimeter offices and labs only, for the two control options (compared to passive lighting control).

Table 4.6. Potential annual energy savings from electric lighting control (kWh)

	Continuous dimming	Active on/off control
SW façade	66000	58000
SE façade	37000	32000
NW façade	17000	12000
NE façade	45000	33000
Total energy in perimeter labs and offices	165000	135000

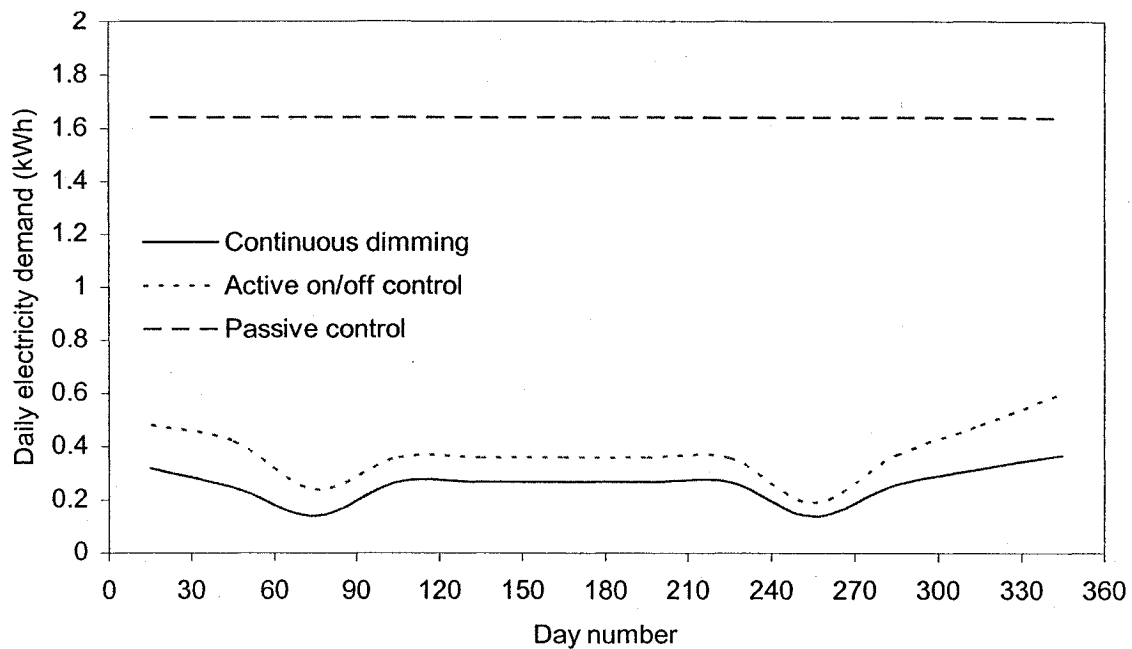


Figure 4.43. Average daily lighting energy demand in a SW perimeter office for different lighting control options, taking into account the impact of shading.

Although continuous dimming minimizes lighting energy demand, the active on/off control (three-level switching) was preferred because the potential savings are also high and the cost is significantly smaller.

An integrated thermal analysis, including the impact of daylighting, was performed for one typical floor of the building. The base case (no shading, passive lighting control) was compared to the proposed design solutions (lighting on/off control and combined shading and lighting control) for a three-section façade with automated venetian blinds and roller shade. The impact of shading-lighting control on internal gains was taken into account, and the combined impact of glazing properties was also examined. Peak heating and cooling load was calculated for the selected design solution for each orientation and the results for the whole floor are shown in Figure 4.44.

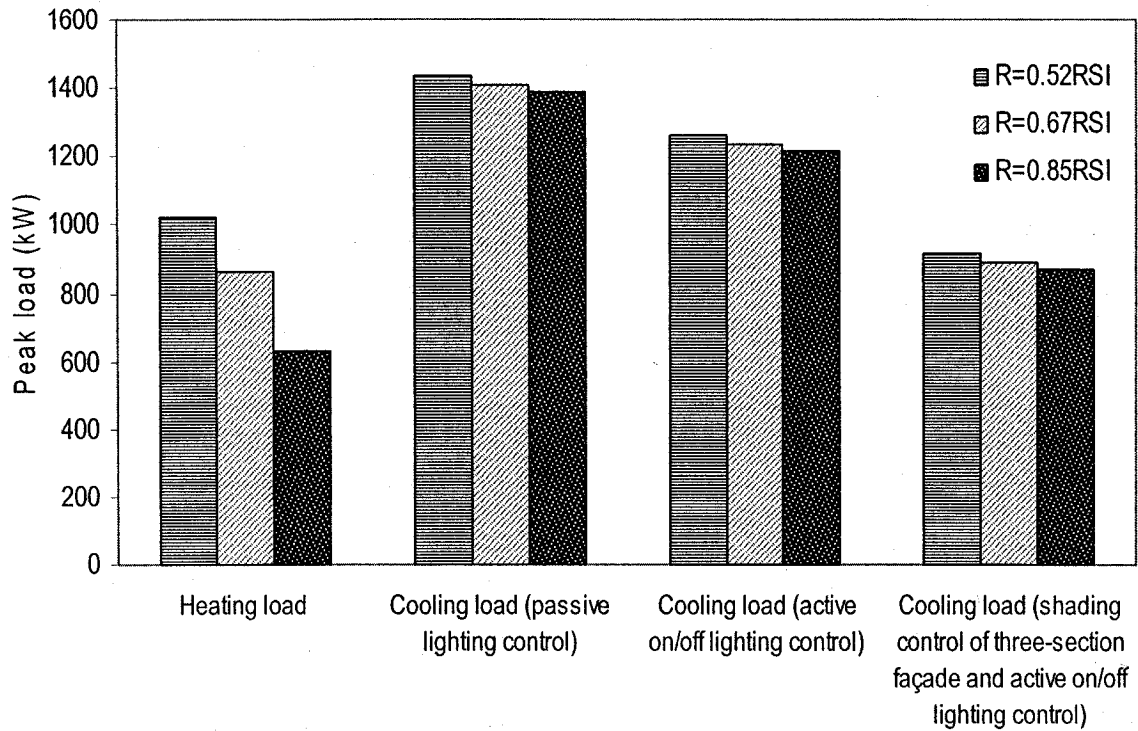


Figure 4.44. Peak thermal loads for different shading and lighting control schemes as a function of glazing thermal resistance for a typical floor.

The impact of glazing thermal resistance is higher for the heating case (selecting heat mirror low-e clear glass can reduce peak heating load by 16%). There is no noticeable reduction in the peak cooling load due to increasing window (or wall) R-value because most of the cooling load is due to solar gains, lighting and other internal gains. Cooling load is the most important because of the big perimeter area of the building and the orientation of the two large facades. For heat mirror glass ($R = 0.67$ RSI), peak cooling load is reduced by 12% if active on/off operation of electric lights is used and (dramatically) by 37% if controlled three-section façades operate in conjunction with on/off lighting control. The significant reduction in peak cooling load for the proposed design solution (513 kW) should be taken into account when sizing the cooling system, so that initial capital costs could be considerably reduced. The impact of lighting and

shading control on the shape of the cooling load curve during a hot clear summer day is shown in Figure 4.45. Different types of shading and lighting control could alter the shape of the cooling load curve and possibly shift the peak if desired.

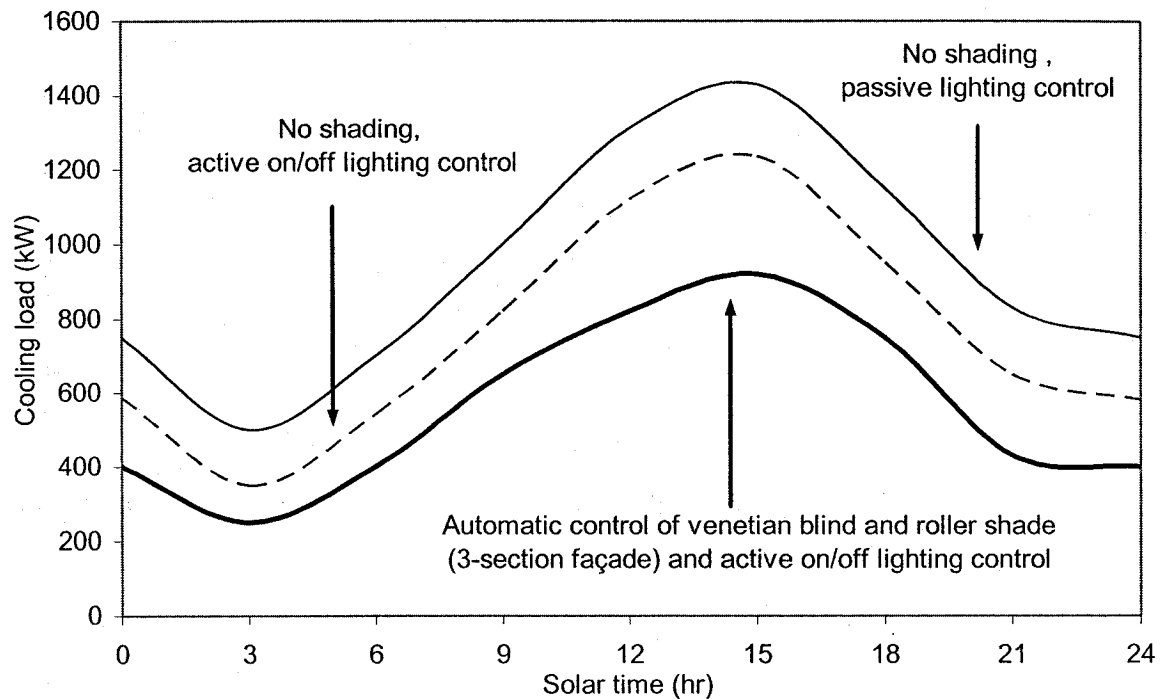


Figure 4.45. Cooling load shape for different lighting and shading control design schemes during a hot clear summer day for a perimeter office on the southwest façade of the building (Tzempelikos & Athienitis, 2003b).

The results for annual cooling and heating energy demand are shown in Figure 4.46. For heat mirror clear glass ($R = 0.67$ RSI), cooling energy demand is reduced by 740 MWh (24%) if electric lights are controlled and by 1540 MWh (51%) if a three-section façade is with automated venetian blinds and roller shade is used. By coincidence, these results match with the integrated analysis results presented in section 4.2 (50% reduction in cooling energy demand), although a different case was considered.

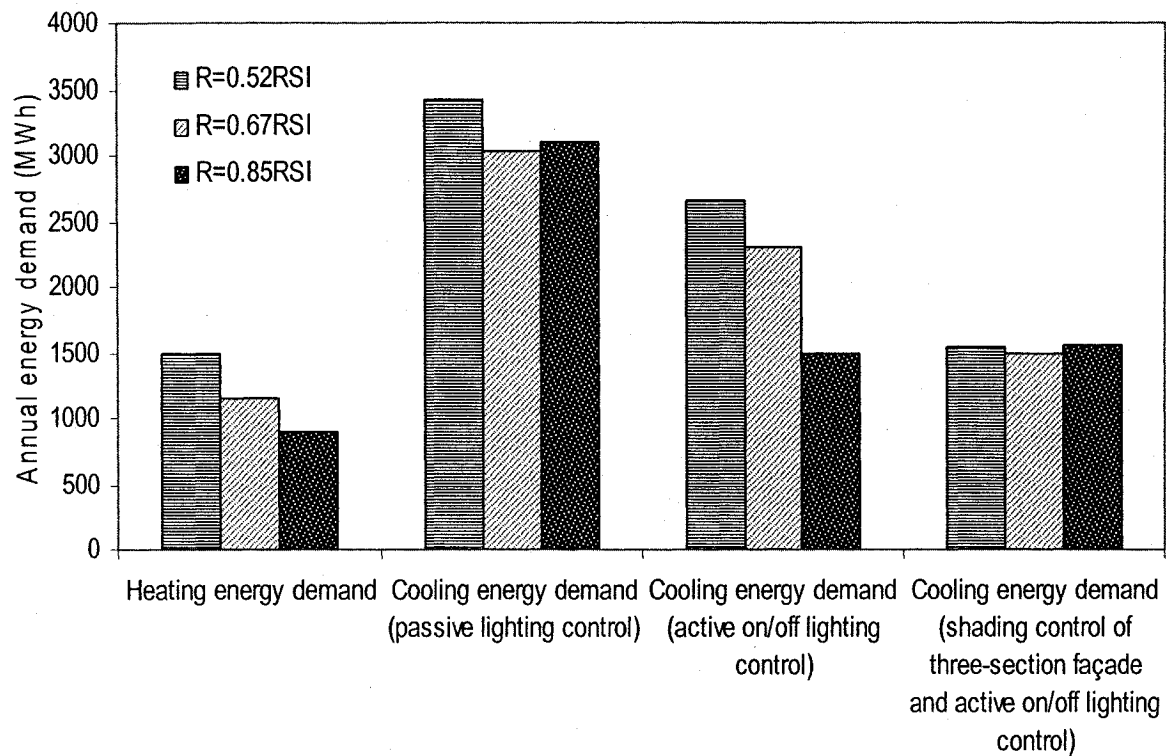


Figure 4.46. Annual heating and cooling energy demand for different shading and lighting control schemes as a function of glazing thermal resistance for a typical floor.

The study also considered a large atrium space on the SW façade of the building. Thermal simulation showed that if this atrium is not provided with appropriate shading, air temperature during hot summer days (especially in August-September) could reach more than 40°C. The cooling load of the building may also rise by about 150 kW if the atrium is unshaded. The shading of the atrium was selected based on:

- Reduction of heating and cooling load;
- Maximization of outside view;
- Architectural aesthetics;
- Illumination of adjacent spaces;
- Other operations (air heating, solar chimneys).

Roller shades, venetian blinds and combinations were again simulated to investigate their impact on thermal and daylighting conditions in the atrium. Glare is not an issue in this case, but rejection of excessive solar gains is necessary, in order to prevent from overheating. An interesting point was the illumination of spaces close to the atrium; useful daylight transmitted in the large atrium penetrates to adjacent spaces and corridors and contributes to further reduction in electricity demand for lighting. Figure 4.47 shows the overall distribution of electric lighting savings in the building. Most potential savings come from the large SW façade. Surprisingly, 13% of the savings is due to illumination of non-perimeter spaces, by using venetian blinds as re-directing devices on a three-section façade. Also, spaces near the atrium could contribute to energy savings by 6%.

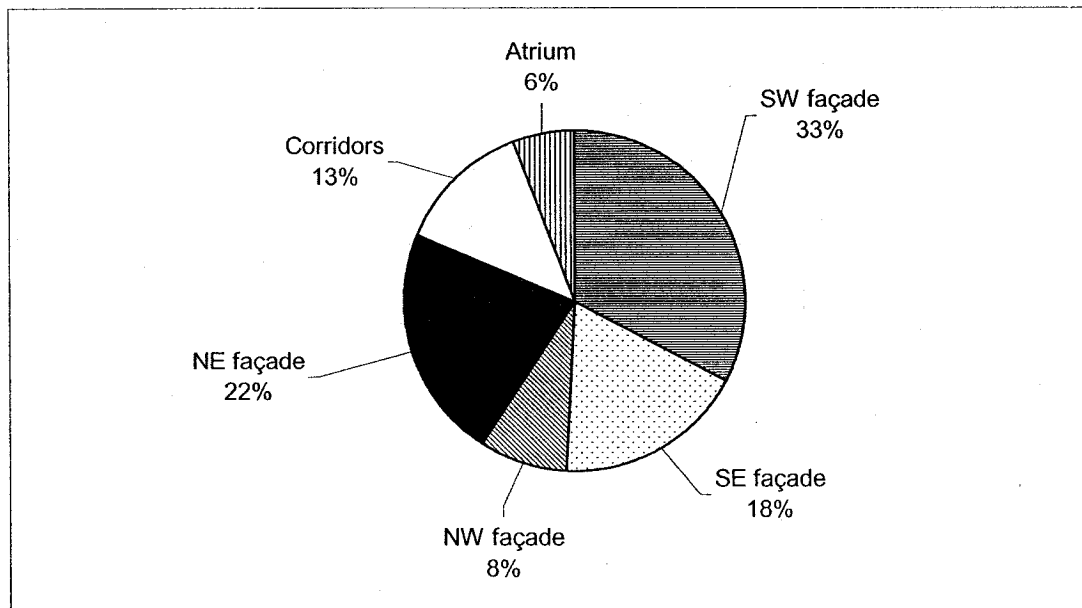


Figure 4.47. Distribution of potential energy savings due to reduction in electricity demand for lighting in the building (Tzempelikos & Athienitis, 2002).

This case study was a motivation for the development of the integrated daylighting and thermal façade design methodology presented in Chapter 3. The design of three-

section multifunctional facades is a promising concept with many objectives: daylight maximization (even in non-perimeter spaces), reduction in peak heating and cooling load, reduction in cooling and heating demand, reduction in lighting energy demand, elimination of perimeter heating, thermal comfort, improvement of daylight uniformity, glare elimination etc. Other concepts, such as natural ventilation and integrated photovoltaic panels can be also considered.

4.7. Comparison of the integrated simulation results

4.7.1. Daylight Availability Ratio and lighting energy demand

For the daylighting results, Lightswitch software (Reinhart, 2002) was used for comparison of the simulation results. Lightswitch is a state-of-the-art lighting and daylighting simulation tool developed in National Research Council of Canada (Institute for Research in Construction) that uses the RADIANCE-based software DAYSIM (Reinhart & Walkenhorst, 2001) to predict work plane illuminance and electric lighting demand. The all-weather Perez sky model (Perez et al., 1993) is used in conjunction with a daylight coefficients approach (Tregenza and Waters, 1983) and a stochastic model to simulate 5-min irradiance data series for better accuracy. Manual and automatic active and passive control of venetian blinds and electric lights can be simulated. This is the only available software package that produces Daylight Availability Ratio (named daylight autonomy) as output. The user has to input information about location, orientation, window size and properties, surface reflectances, working schedule, occupancy sensors, type of shading and lighting control, seating position, target work plane illuminance, installed lighting power, etc. Daylight autonomy, daylight factor

distribution on the work plane and electricity demand for lighting are calculated and given in graphical output format. The free online version offers two options for window-to-wall ratio: 1/3 and 2/3 and shading with a common type of venetian blinds for a limited number of room dimensions. Results were produced for the base case (30% WWR), for a perimeter private office with floor area 18m^2 , to investigate the accuracy of Daylight Availability and electric lighting demand results presented in section 4.3.

Comparison of Daylight Availability Ratio results for each orientation (converted in MJ for the whole floor area) for the base case is shown in Figure 4.48. For south and west orientations, results are in very good agreement (less than 7%). Differences in daylight autonomy for the north and east facades are due to a different approach in modelling transmitted daylight and calculation of work plane illuminance distribution. Comparison of annual lighting energy demand results for the base case assuming passive lighting control is presented in Figure 4.49. The difference was found less than 2%.

Figure 4.50 compares the annual lighting energy demand results for the case of active automatic control. The big difference for north and east-facing offices is because (i) the results depend on the DAR calculations shown in Fig. 4.48 where different methods are used for calculation of work plane illuminance (ii) continuous dimming of electric lights was modelled in Lightswitch (instead of on/off control simulated in the model) and photocell arrangements were included (iii) the occupants schedule is a little different (automatically selected in Lightswitch) from the one used in the simulation model; therefore occupancy sensors modelled in Lightswitch operate based on a slightly different schedule. All the above factors seem to have significant impact on lighting energy demand prediction (higher for north-facing facades). The detailed output of Lightswitch

software for every case is presented in Appendix K. Daylight autonomy, daylight factor distribution on the work plane and lighting energy demand are shown for each orientation and each type of lighting control with a description of the parameters used in the model. The results of the daylighting simulation model can be referenced in section 4.3.

For the considered base case in Montreal, a conservative approach was followed, considering the seating position in the back of the room to ensure that 500 lux are available on every point on the work plane surface (even in the deep part of the room). In reality, results would be a little more optimistic, because the seated person could be seated closer to the window and daylight levels could be higher.

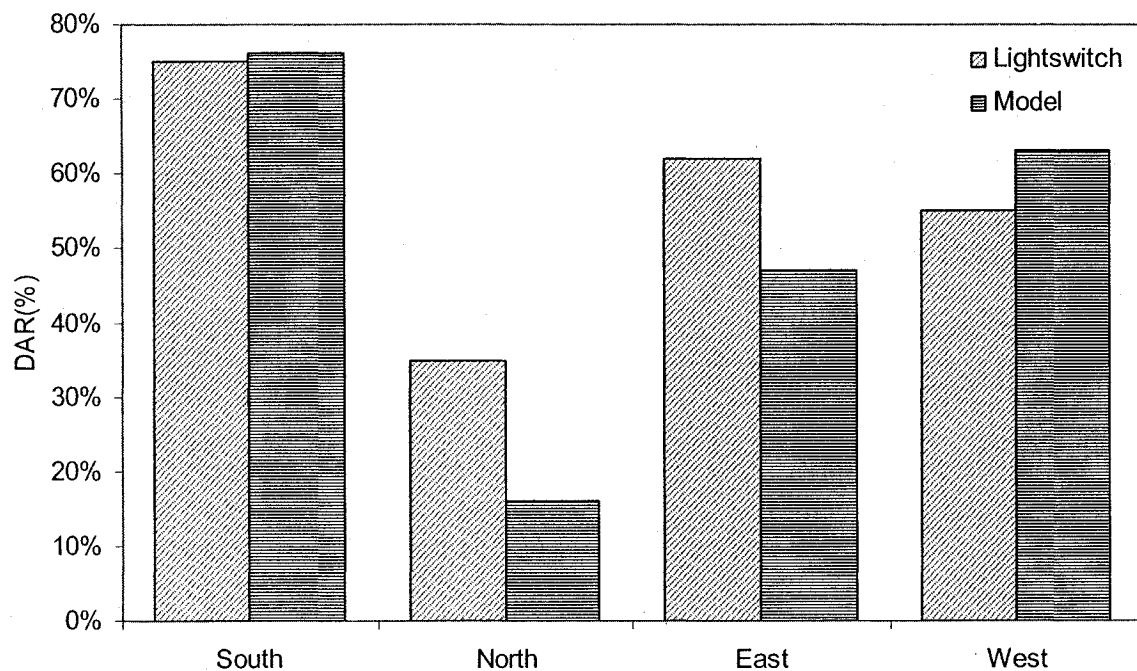


Figure 4.48. Comparison of Daylighting Availability Ratio results between Lightswitch and the current daylighting simulation model.

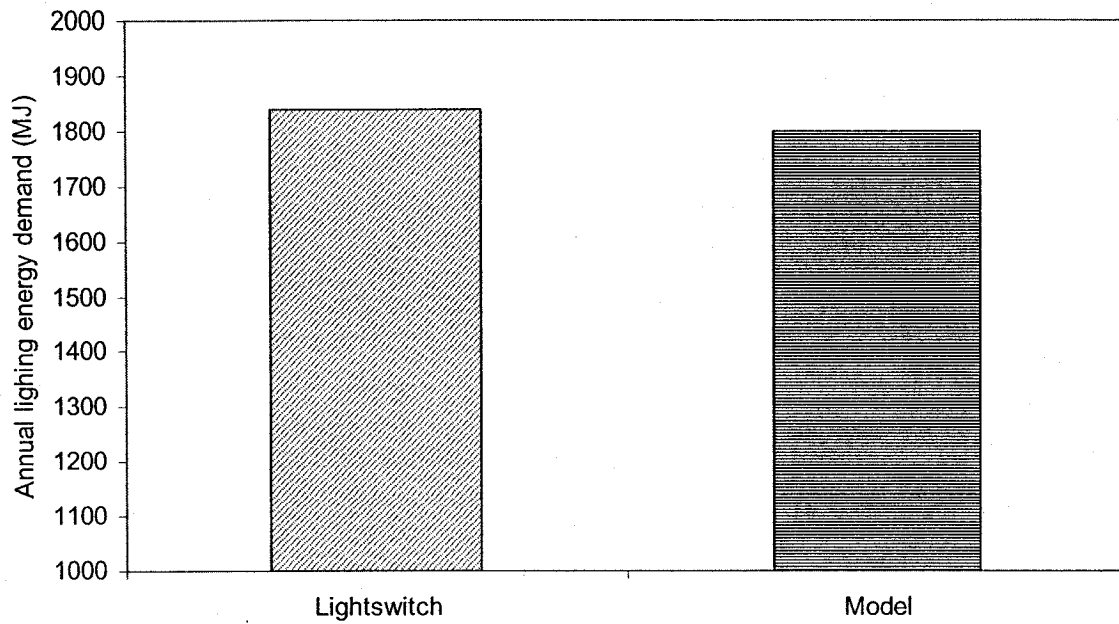


Figure 4.49. Comparison of annual lighting energy demand for the base case assuming passive lighting control. Results are the same for each orientation.

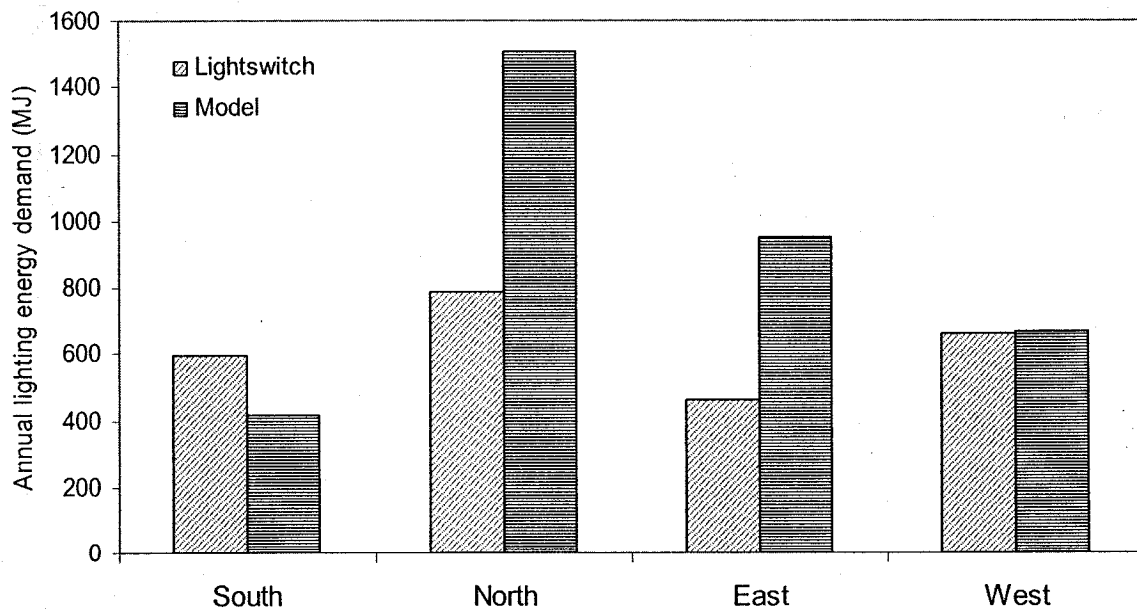


Figure 4.50. Comparison of annual lighting energy demand assuming active lighting control (continuous dimming in Lightswitch and on/off control in the simulation model). Occupancy schedules in Lightswitch are slightly different.

4.7.2. Heating and cooling load

ESP-r software (Clarke, 1997) was selected for validation of thermal simulation results. Integrated simulation between building and HVAC systems is supported. The thermal/ventilation simulation has been coupled with Radiance (Janak, 1998) for integrated daylighting and thermal analysis. For the thermal simulation, ESP-r uses a thermal network approach similar to the one used in this work. Shading and lighting control is possible, and the properties of a large number of fenestration products (imported from WINDOW and WIS) are available. ESP-r is one of the most reliable expert software for building simulation. However, it is not intended for investigating building design options in a systematic way, but for accurate evaluation of specific selected cases.

A complete thermal analysis was done with ESP-r to validate the thermal simulation results for the base case. A south-facing perimeter office in Montreal with 30% window-to-wall ratio was simulated and then hourly heating and cooling load was plotted as a function of time for winter and summer. The peak loads were selected and compared with the respective peak thermal loads from the thermal simulation model used in this work. The comparison is shown in Figure 4.51. Cooling load results agree within 7%, and the difference in peak heating load is 5%. These small differences occur because (i) in ESP-r, a clear double glazing with certain properties is selected from a database whereas in the thermal simulation the optical properties are calculated analytically as a function of solar incidence angle (ii) ESP-r uses different placement of thermal capacitances in thermal mass elements (iii) ESP-r uses linearized radiative heat transfer coefficients, while non-linear coefficients are used in the thermal simulation.

Output graphs of ESP-r together with input file description can be found in Appendix L. Graphs of heating and cooling load are presented for winter and summer respectively, and peak heating and cooling load are plotted for the selected days.

Validation of shading analysis results is not possible because ESP-r uses standard shading products from existing databases and their properties cannot be changed. In Lightswitch, daylight results are available only for a common venetian blind system (with unknown properties).

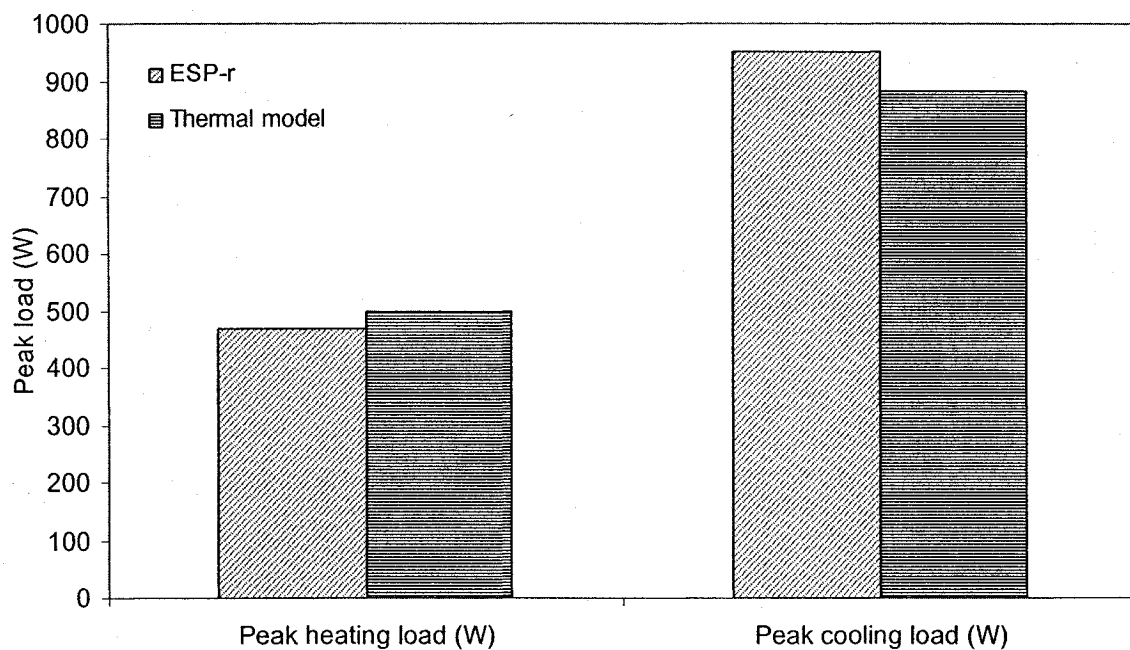


Figure 4.51. Comparison of peak heating and cooling load between ESP-r and thermal simulation results.

5. CONCLUSION

5.1. Concluding remarks

A methodology for integrated thermal-daylighting analysis and design of perimeter zones of commercial buildings was developed. A real case study revealed the impact of fenestration system design and the need to consider the interactions between the thermal and daylighting performance of perimeter spaces from the beginning of the design process for commercial buildings. Critical decisions concerning façade design during the early design stage have a significant impact on both energy performance of the building and human comfort for the occupants. Existing advanced building simulation software, although able to couple daylighting and thermal simulation, cannot provide guidelines for selecting fenestration system characteristics because they require detailed input data to run simulations, and these data are not yet available at the early design stage. Instead, they are mainly use to evaluate specific design solutions or simulate the energy performance of existing buildings. The simulation approach in the design stage should not be analysis for a specific scheme but systematic exploration of design alternatives based on an integrated approach.

Integrated thermal and daylighting analysis for design in the early stage involves systems integration. With the increasing demand for transparent building facades, the objectives of design analysis have shifted to utilizing dynamic fenestration/shading systems for optimal control of solar gains and daylighting benefits. Therefore different building systems (heating, cooling, lighting, and shading) have to be simultaneously

considered from the initial stage of design, taking into account the interactions in the simulation process.

The basic step for developing an integrated and systematic daylighting and thermal design methodology is to consider fenestration properties as design variables in a coupled thermal and daylighting simulation model. The major links between daylighting and thermal performance were identified as (i) window-to-wall ratio (ii) glazing type (iii) shading device optical and thermal properties (iv) shading control and (v) electric lighting control as a secondary link, transferring the impact of daylighting on internal gains. These parameters provide a means for simulating the interactions between daylighting and thermal performance and were used as design variables.

Generalized integrated performance-based measures are then calculated from the coupled daylighting and thermal simulation results. These indices included the impact of climate, fenestration system properties and control and electric lighting control. These enclose the combined effects of linking parameters in the integrated design process. Selection of fenestration systems properties and control was achieved by investigating the variation of integrated performance indices with design variables, using as criteria:

- Maximization of daylight utilization;
- Elimination of glare and improvement of lighting conditions;
- Reduction in peak thermal loads;
- Reduction in energy demand for heating and cooling;
- Reduction in lighting energy demand;

The reduction in energy demand is often in conflict with daylight maximization. Optimum energy performance can be achieved if daylighting benefits, due to the reduction in lighting energy demand and subsequent decrease in cooling load and demand, exceed the increase in energy demand due to increased solar gains. Appropriate selection of shading device properties and control, in conjunction with artificial lighting control can make this possible. At the same time, other benefits of daylighting (e.g. increase of occupant productivity) have to be considered simultaneously, by studying the effect of design variables on the daylighting performance index, named Daylight Availability Ratio, and make decisions based on daylight “saturation” regions. Innovative fenestration systems should be taken into consideration from the early design stage, since they have a potential for satisfying the above requirements.

The integrated thermal and daylighting design methodology for perimeter offices was applied to perimeter office spaces in Montreal. Tables of Daylight Availability Ratio are produced, to guide designers in selecting window-to-wall ratios for each orientation. It was found that a south-facing perimeter office with 30% window-to-wall ratio and clear glass can satisfy the required criteria (increasing glazing R-value would contribute to higher energy savings). In the second phase, the properties and control of an exterior roller shade installed on the façade of the office space were considered as a design variables. The variation of integrated performance indices showed that a roller shade with 20% transmittance could minimize cooling and lighting (and total) energy demand if appropriate automatic shading and lighting control are enabled. At the same time, daylight maximization is achieved and glare problems can be solved using the concept of a three-section façade.

Finally, the significant impact of shading properties and control (and electric lighting control) on the energy performance buildings was shown with a real case study. Using the three-section façade concept (venetian blinds on top and roller shade on bottom), cooling energy demand (which is the most important) is reduced by 50% and peak thermal loads are also reduced, while the load shape could be altered depending on the control strategy followed.

5.2. Research contributions

The contributions of this work can be summarized as follows:

1. A general and systematic simulation methodology for integrated daylighting and thermal analysis of facades and perimeter spaces of commercial buildings during the early design stage was developed; it can be applied for any location, orientation, glazing type and shading device type;
2. To investigate the balance between daylighting benefits and energy performance, generalized performance-based indices were calculated (from the continuous interaction between daylighting and thermal simulation) as a function of fenestration key linking parameters;
 - A method to provide guidelines for the selection of window-to-wall ratio, shading device properties and control and electric lighting control was developed, based on the results of the integrated analysis, using as criteria maximization of daylight utilization, reduction in energy demand for heating, cooling and lighting, as well as improvement of interior conditions;

- The need for considering innovative dynamic fenestration systems from the beginning of the design process was addressed and the three-section façade concept was introduced and used as an example. The required degree of simulation detail in this initial stage could vary, depending on the application, in order to maintain accuracy but reduce computation time and unnecessary complexity;
- A simulation design support tool prototype was developed (in MathCad environment) to provide designers with fenestration design guidelines based on the integrated daylighting and thermal approach at the early design stage.

5.3. Possible extensions and recommendations for future work

In the integrated analysis, it was assumed that shading devices and electric lights are automatically controlled, based on ideal operation of occupancy sensors and photocells. In reality, recent studies have revealed that occupants would rather want to have some control over their luminous environment. Although manual operation of shading would not achieve the goals set in this methodology, it is useful to consider the simulation of manual control of shading and lighting systems for a more realistic representation on the actual perimeter space performance. This would include development of occupant behavioural models (for probabilistic switching functions) and it is one of the current tasks (31-A) of the International Energy Agency. In this framework, Lightswitch software (Reinhart, 2002) was developed for simulating the performance of manually-controlled venetian blinds.

Although the design methodology was implemented as a simulation design tool in MathCad, it is realized that this environment is not practical for building designers

(however, such an open environment is good for research development). A simpler visual interface with graphical output would be more attractive and easy to use. However, the detailed thermal and lighting simulation runs could still be done in MathCad. The new version of MathCad, released in 2005, will provide automatic graphical interface options.

Other extensions include: (i) consideration of double facades with blinds in the cavity, a promising technology for Canada since placing blinds outside faces certain practical problems (ice formation, dirt etc. and difficulty in cleaning exterior glazing) (ii) facades with semitransparent photovoltaic systems (iii) facades with building-integrated photovoltaics and motorized blinds. The combined impact of natural ventilation should be also investigated.

The application of the methodology in warm climates will give more solid results concerning the minimization of cooling and lighting energy demand and consumption. In cooling dominated climates, cooling energy demand and consumption will be higher than heating, and therefore the total energy consumption would be also minimized for smaller values of shade transmittance. Nevertheless, the current analysis showed that, even for heating-dominated climates, buildings with glazed near-south facades and high solar gains could face cooling problems. Considering the cost of electricity, lighting and shading control is important.

Finally, the implementation of the integrated daylighting and thermal design methodology in one of the existing advanced building simulation software packages would create the potential of using these tools for design and not only for simulation. A dual use of an advanced building simulation tool (i.e., for design purpose and for simulation purposes) would fill the gap, still remaining today, in assessing and evaluating

overall building performance from the early design stage. This would result in the design of energy-efficient and healthy buildings.

REFERENCES

- Aleo F., Sciuto S., Viadana R., "Solar transmission measurements in outdoor conditions of non-homogeneous shading devices", Proceedings of the European conference on energy performance and indoor climate in buildings, pp. 1074-1079, Lyon, France, 1994.
- Alshaibani K., "Average daylight factor for clear sky conditions", Lighting Research and Technology, Vol. 29 (4), pp. 192-196, 1997.
- Andersen M., "Light distribution through advanced fenestration systems", Building Research and Information, Vol. 30 (4), pp. 264-281, 2002.
- Andersen M., J.L. Scartezzini, M.D. Rubin, R.C. Powles, "Bi-directional light transmission properties assessment for venetian blinds: computer simulations compared to photogoniometer measurements", Proceedings of ISES Solar World Congress, pp. 187-198, Gotenborg, Sweden, August 2003.
- Andersen M., M.D. Rubin, R.C. Powles, J.L. Scartezzini, "Bi-directional transmission properties of venetian blinds: experimental assessment compared to ray-tracing calculations", Solar Energy, in press, 2005.
- Andersen M., Rubin M., Scartezzini J-L., "Comparison between ray-tracing simulation and bi-directional transmission measurements on prismatic glazing", Solar Energy, Vol. 74 (3), pp. 157-173, 2003.
- Arastheh D.K., Finlayson E.U., Huizenga C., "WINDOW 4.1: Program description", Lawrence Berkeley Laboratory, Berkeley, California, 1994.

- ASHRAE, "ASHRAE Handbook-Fundamentals", Chapter 30. Atlanta: American Society of Heating, Refrigerating and Air-Conditioning Engineers, Inc., 2001.
- ASHRAE, "ASHRAE Handbook-Fundamentals", Chapter 30. Atlanta: American Society of Heating, Refrigerating and Air-Conditioning Engineers, Inc., 1997.
- Assimakopoulos M.N., Tsangrassoulis A., Guarracno G., Santamouris M., "Integrated energetic approach for a controllable electrichromic device", Energy and Buildings, Vol. 36, pp. 415-422, 2004.
- Athienitis A., Tzempelikos A., Poissant Y., "investigation of the performance of a double skin façade with integrated photovoltaic panels", Proceedings of EuroSun '04, Freiburg, Germany, June 2004.
- Athienitis A.K. & Santamouris M., "Thermal analysis and design of passive solar buildings", James and James Ltd., 2002.
- Athienitis A.K. & Tzempelikos A., "Integration of daylighting, lighting control and HVAC system design in Concordia Engineering building", Proceedings of Sustainable Building, September, Oslo, Norway, 2002a.
- Athienitis A.K. and Tzempelikos A., "A methodology for simulation of daylight room illuminance distribution and light dimming for a room with a controlled shading device", Solar Energy, Vol. 72, (4), pp. 271-281, 2002b.
- Athienitis A.K., "Building Thermal Analysis", Electronic MathCAD book, 3rd edition- in Civil Engineering Library, Mathsoft Inc., Boston, USA, 1999.
- Athienitis A.K., "Numerical model for a floor heating system", ASHRAE Transactions, Vol. 100 (1), pp. 1024-1030, 1994.

- Balaras C.A., "The role of thermal mass on the cooling load of buildings-an overview of computational methods", *Energy and Buildings*, Vol. 24, pp. 1-10, 1996.
- Bauman F., Andersson B., Carroll W., Kammerud R. C. and N.E. Friedman, "Verification of BLAST by comparison with measurements of a solar-dominated test cell and a thermally massive building", *ASME Journal of Solar Engineering*, Vol.: 105 (2), pp. 207-216, 1983.
- Beckman W. A., Broman L., Fiksel A., Klein S. A., Lindberg E., "TRNSYS – The Most Complete Solar Energy System Modelling and Simulation Software", *Proceedings of World Renewable Energy Congress*, Reading, United Kingdom, 1994.
- Berkeley Solar Group (BSG), "Energy-10: Program description", 2002.
- Bourgeois D., Hand J., McDonald I., Reinhart C., "Adding sub-hourly occupancy prediction, occupancy sensing control and manual environmental control to ESP-r", *Proceedings of eSim2004*, Vancouver, Canada, June 2004.
- Brandemuehl M.J. & Beckman W.A., "Transmission of diffuse radiation through CPC and flat-plate collector glazings", *Solar Energy*, Vol. 24, pp. 511, 1980.
- Breitenbach J., Rosenfeld J.L.J., Lart S. and Langle I., "Optical and thermal performance of glazing with integral venetian blinds", *Energy and Buildings* 33, pp. 433-442, 2001.
- Bryan H., Clear R., "Calculating daylight illuminance with a programmable hand calculator", *Journal of the Illumination Engineering Society*, Vol. 10 (4), pp. 219, 1981.
- Bulow-Hube H., "Office worker preferences of exterior shading devices: a pilot study", *Proceedings of EuroSun '00*, Copenhagen, Denmark, June 2000.

- Campbell N.S. & J.K. Whittle, "Analyzing radiation transport through complex fenestration systems", Proceedings of 5th IBPSA conference, pp. 173-180, Prague, Czech Republic, 1997.
- Charron R. and Athienitis A.K., "Optimization of the performance of PV-integrated double-façades", Proceedings of 3rd ISES World Congress, Gotenburg, Sweden, 2003.
- Citherlet S & Scartezzini J-L., "Performances of advanced glazing systems based on detailed and integrated simulation", Status Seminar, ETH-Zurich, 2003.
- Citherlet S., "Towards the holistic assessment of building performance based on an integrated simulation approach", Ph.D. Thesis, Swiss Federal Institute of Technology, 2001a.
- Citherlet S., Clarke J.A., Hand J., "Integration in building physics simulation', Energy and Buildings, Vol. 33, pp. 451-461, 2001b.
- Clarke J. A., "Building Performance Simulation Using the ESP-r System", Proceedings of 5th international IBPSA conference, Building simulation '97, Prague, Czech Republic, September 1997.
- Clarke J.A. & Janak M., "Simulating the thermal effects of daylight-controlled lighting", Building Performance, Proceedings of 5th international IBPSA conference, Building simulation '97, Prague, Czech Republic, September 1997.
- Clarke J.A., "Energy Simulation in Building", 1st edition, Adam Hilger, Bristol and Boston, 1985.

Clarke J.A., Janak M., Ruyssevelt P., "Assessing the overall performance of advanced glazings systems", Solar Energy, Vol. 63 (4), pp. 231-241, 1998.

Cogan S., "Optical switching in complementary electrochromic windows", Proceedings of SPIE conference, Vol. 692, San Diego, California, 1986.

Collares-Pereira & Rabl, "The average distribution of solar radiation-correlations between diffuse and hemispherical and between daily and hourly insolation values", Solar Energy, Vol. 22, pp. 155, 1979.

Collins M. & S.J. Harrison, "Calorimetric analysis of the solar and thermal performance of windows with interior louvered blinds", ASHRAE Transactions, Vol. 110 (1), pp. 474-486, 2004a.

Collins M. & S.J. Harrison, "Estimating the solar heat and thermal gain from a window with an interior venetian blind", ASHRAE Transactions, Vol. 110 (1), pp. 486-501, 2004b.

Collins M., Harrison S.J., Naylor D. and Oosthuizen P.H., "An interferometric study of convective heat transfer from an irradiated complex window assembly", Proceedings of IMECE, , pp. 1-13, New York, USA, 2001.

Collins M., S.J. Harrison, D. Naylor and P.H. Oosthuizen, "Heat transfer from an isothermal vertical surface with adjusted heated horizontal louvers: numerical analysis", ASME Transactions, Vol. 124, pp. 1072-1077, 2002

Collins M., S.J. Harrison, D. Naylor and P.H. Oosthuizen, "Numerical modeling of radiative and convective heat transfer from an irradiated complex window assembly", Proceedings of IMECE, pp. 1-12, Orlando, 2000.

- Correa C. & Almanza R., "Copper based thin films to improve glazing for energy savings in buildings", *Solar Energy*, Vol. 76, pp. 111-115, 2004.
- Courret G., Paule B., Scartezzini J. L., "Anidolic zenithal openings", *Proceedings of the European conference on energy performance and indoor climate in buildings*, Lyon, France, 1994.
- Crawley D.B., Lawrie L.K., Pedersen C.O., Liesen R.J., Fisher D.E., "EnergyPlus - A new Generation Building Energy Simulation Program", *Proceedings of 6th International IBPSA Conference (BS '99)*, Kyoto, Japan, pp. 81-88, September 1999.
- Crawley D.B., Lawrie L.K., Pedersen C.O., Strand R.K., Winkelman F.C., Buhl W.F., Huang Y.J., Witte M.J., Henninger R.J., Fisher D.E., Shiery D., "Energy Plus: new, capable and linked", *Proceedings of eSim 2002*, pp. 244-251, Montreal, Canada, June 2002.
- Cucumo M., DeRosa A., Ferraro V., Kaliakatsos D., Marinelli V., "Daylighting measurements and comparisons with calculation methods", *Proceedings of EuroSun '04*, pp. 331-340, Freiburg, Germany, June 2004.
- DiLaura D., "A new technique for interreflected components calculations", *Journal of the Illumination Engineering Society*, Vol. 8, pp. 53-59, 1979.
- Duarte N., D. Naylor, P.H. Oosthuizen, S.J. Harrison, "An interferometric study of free convection at a window glazing with a heated venetian blind", *HVAC & R Research*, Vol. 7 (2), pp. 169-184, 2001.
- Energy Plus Engineering Document: the reference to Energy Plus calculations, United States Department of Energy, 2004.

- Erbs D.G., Klein S.A. & Duffie J.A., "Estimation of the diffuse radiation fraction for hourly, daily and monthly average global radiation", Solar Energy, Vol. 28, 23, 1982.
- Erhorn H., Boer J. d. and Dirksmöller M., "ADELINE - An integrated Approach to Lighting Simulation", Proceedings of Daylighting'98, Ontario, Canada, pp. 21-28, May 1998.
- Fang X.D., "A study of the U-factor of the window with a high-reflectivity venetian blind", Solar Energy, Vol. 68 (2), pp. 207-214, 2000.
- Finlayson E.U., "WINDOW 4.0.:Program description", Lawrence Berkeley Laboratory, Berkeley, California, 1993.
- Galasiu A.D., Atif M.R., McDonald A., "Impact of window blinds on daylight-linked dimming and automatic on/off lighting controls", Solar Energy, Vol. 76, pp. 523-544, 2004
- Garnet J.M., R.A. Fraser, H.F. Sullivan, J.L. Wright, "Effect of internal venetian blinds on window centre-glass U-values", Proceedings of Window Innovations, pp. 273-279, Toronto, Canada, 1995.
- Garris L.B., "The deliberation of daylighting", Buildings magazine, April 2004.
- Ghisi E. and Tinker J.A., "An ideal window area concept for energy efficient integration of daylight and artificial light in buildings", Building and Environment, Vol. 40, pp. 51-61, 2005.
- Gillette G., "A daylight model for building energy simulation", NBS Building Science series 152, Washington, USA, 1983.

- Gillette G., Kusuda T., "A daylighting computation procedure for use in DOE-2", IES Journal, October 1982.
- Gillette G., Pierpoint W., "A general illuminance model for daylighting availability", IES technical conference, Atlanta, USA, 1982.
- Goral C., Greenberg D., Cohen M., "Modelling the interaction of light between diffuse surfaces", Computer Graphics, Vol. 18 (3), 1984.
- Gordon J.M., Reddy T.A., "Time Series analysis of daily horizontal solar radiation", Solar Energy Vol. 41, pp. 215-216, 1988.
- Graham V.A, Hollands K.G.T, Unny T.E., "A time series model for K_t with application to global synthetic weather generation", Solar Energy, Vol, 40, pp. 83-92, 1988.
- Hankins M.L. & Waters C.E., "Glare evaluation systems-a white paper", report submitted to IESNA, May 2003.
- Harrison A., Coombes C., "Angular distribution of clear sky short wavelength radiance", Solar Energy, Vol. 40 (1), pp. 57, 1988.
- Hay J.E. and Davis J.A., "Calculation of the solar radiation incident on an inclined surface", Proceedings of the 1st canadian solar radiation data workshop, Ministry of Supply and Services Canada, 59, 1980.
- Hayter S.J., Torcellini P.A., Judkoff R., "Optimizing building and HVAC systems", ASHRAE journal, pp. 46-49, December 1999.
- Herkel S., "Dynamic link of light and thermal simulation: on the way to integrated planning tools", Proceedings of International Building Simulation conference, Eindhoven, Netherlands, August 2003.

- Heschong L., "Daylighting and human performance", ASHRAE Journal, 44 (8), pp. 65-67, 2002.
- Hollands K.G.T. and Hudget R.G., "A probability density function for the clearness index, with applications", Solar Energy, Vol. 30, pp. 195, 1983.
- Hollands K.G.T., Wright J.L. and Granqvist C.G., "Solar Energy-The state of the art", ISES position papers, Ch. 2: Glazings and coatings, James & James Ltd., 2001.
- Hooper F., Brugner A., Chan C., "A clear sky model of diffuse sky radiance", Trans. of ASME Journal of Solar Energy Engineering, Vol. 109 (1) CIE, 1987.
- Hopkinson R., "Reflected daylight", Architectural Journal, Vol. 19, 1954.
- Hottel H.C., "A simple model for estimating the transmittance of direct solar radiation through clear atmospheres", Solar Energy, Vol. 18, pp. 129-134, 1976.
- Hunt D.R.G., "Predicting artificial lighting use- a method based upon observed patterns of behavior", Lighting Reserch and Technology, Vol. 12 (1), pp. 7-14, 1980.
- Hutchins M.G., Butt N.S., Ageorges P., "Vanadium titanium oxide counter electrodes for variable transmission electrochromic devices", Proceedings of World Renewable Congress VI, pp. 253-258, UK, 2000.
- IES, "Lighting Handbook", Reference Volume, IESNA, New York, 1978.
- IES, "Lighting Handbook", Reference Volume, IESNA, New York, 1984.
- Illuminating Engineering Society of North America (IESNA), Lighting Handbook, 2005.

Immel D., Greenberg D., Cohen M., "A radiosity method for non diffuse environments", Computer graphics, Vol. 20 (4), pp. 133-142, 1986.

International Standard ISO 15099, First Edition: Thermal performance of windows, doors and shading devices: Detailed Calculations, ISO, November 2003.

International Standard ISO 9050, Glass in building — Determination of light transmittance, solar direct transmittance, total solar energy transmittance, ultraviolet transmittance and related glazing factors, ISO, 1998.

Janak M., "The Run Time Coupling of Global Illumination and Building Energy Simulations - Towards an Integrated Daylight-linked Lighting Control Simulation", IDC'98, Ottawa, May 1998.

Johnson R., Sullivan R., Selkowitz S. E., Conner C., Arasteh D., "Glazing energy performance and design optimization with daylighting", Energy & Buildings Vol. 6, pp. 305-317, 1984.

Karlsson J. & Roos A., "Modelling the angular behaviour of the total solar energy transmittance of windows", Solar Energy, Vol. 69 (4), pp. 321-329, 2000.

Kaufman J., Haynes H., "IES lighting handbook", Vol. 1, New York, 1981.

Kischkoweit-Lopin M., "An overview of daylighting systems", Solar Energy Vol. 73 (2), pp. 77-82, 2002.

Kittler R., "Standardization of outdoor conditions for the calculation of daylight factor with clear skies", Proceedings of the CIE Intercessional Conference on Sunlight, Newcastle, Rotterdam, 1965.

Klems J.H. and Warner J.L., "Solar Heat Gain Coefficient of complex fenestrations with as venetian blind for differing slat tilt angles", ASHRAE Transactions, Vol. 103 (1), pp. 1026-1034, 1997.

Knight K.M., Klein S.A., Duffie J.A., "A methodology for the synthesis of hourly weather data", Solar Energy, Vol. 46, pp. 109-20, 1991.

Larson G. W., "The Radiance Synthetic Imaging System", Lawrence Berkeley Laboratory, Berkeley, USA, 1993.

Lee E. & Selkowitz S.E., "The design and evaluation of integrated envelope and lighting control strategies for commercial buildings", ASHRAE Transactions 101 (1), pp. 326-342. 1995.

Lee E.S., DiBartolomeo D.L. and Selkowitz S.E. "Thermal and daylighting performance of an automated venetian blind and lighting system in a full-scale private office", Energy and Buildings 29, pp. 47-63, 1998.

Lee J. et al, "Thermochromic materials research for optical switching", Proceedings of SPIE Conference, Vol. 692, San Diego, California, 1986.

Littlefair P., "Developments in innovative daylighting", BRE-Report CI/SBF N1, April 2000.

Littlefair P., "Modelling daylight illuminances in building environmental performance analysis", IES Journal, Vol. 21, pp. 25, 1992.

Liu B.Y. & Jordan R.C., "The interrelationship and characteristic distribution of direct, diffuse and total solar radiation", Solar Energy, Vol. 4 (3), 1960.

Longmore J., BRS daylight protectors, Garston, Watford, UK, 1967.

- Lorenz W., "Design guidelines for a glazing with seasonally dependent solar transmittance", *Solar Energy*, Vol. 63 (2), pp. 79, 1998.
- Love J.A., "Manual switching patterns in private offices", *Lighting Research and Technology*, Vol. 30 (1), pp. 45-50, 1998.
- Loveland J., in "The deliberation of Daylight", *Buildings magazine*, April 2004.
- Lupton M.J., Leung A.S.M, Carter D.J., "Advances in lighting design methods for non-empty interiors-a review", *Lighting Research and Technology*, Vol. 28 (1), pp. 29-41, 1996.
- Lynes J., "Principles of natural lighting", Elsevier, London, 1969.
- Mahdavi A. & Mahattanatawe P., "Enclosure systems design and control support via dynamic simulation-assisted optimization", *Proceedings of International Building Simulation conference*, pp. 34-41, Eindhoven, Netherlands, August 2003.
- Mahdavi A., "Reflections on computational building models", *Building and Environment*, Vol. 39, pp. 913-925, 2004.
- Manz H., "Total solar energy transmittance of glass double favades with free convection", *Energy and Buildings*, Vol. 36, pp.127-136, 2004.
- Marsch J,A., 1997, "Performance analysis and conceptual design", Ph.D. Thesis, University of Western Australia, 1997
- Matsura K., "Luminance distributions of various reference skies", *CIE Technical Report*, TC3-09, 1988.

- Mei L., Infield D., Eicker U., Fux V., "Thermal modelling of a building with an integrated ventilated PV façade", *Energy and Buildings*, Vol. 35, pp. 605-617, 2003.
- Michel L., Roecker C., Scartezzini J-L., "Performance of a new scanning sky simulator", *Lighting Research and Technology*, Vol. 27 (4), pp. 197, 1995.
- Molina L.J., Maestre R.I., Lindawer E., "A model for predicting the angular dependence of the optical properties of complex windows including shading devices", *Proceedings of PLEA*, pp. 765-770, Cambridge, UK, 2000.
- Moon P., Spencer D., "Illumination from a non-uniform sky", *IES journal*, Vol. 37, pp. 707, 1942.
- Morrison-Beausoleil Ian, "Modelling mixed convection heat transfer at internal building surfaces", *Proceedings of International Building Simulation conference*, Rio de Janeiro, Brazil, August 2001.
- Muller H. O. F., Capelle A., "Transparent shading devices with concentrating holograms and photovoltaics", *World Renewable Energy Congress VI*, Oxford, 2000.
- Muneer T. and Kinghorn D., "Luminous efficacy of solar irradiance: improved models", *Lighting Research and Technology*, Vol. 29 (4), pp. 185-191, 1997.
- Orgill J.F. & Hollands K.G.T., "Correlation equation for hourly diffuse radiation on a horizontal surface", *Solar Energy*, Vol. 19, pp. 357, 1977.
- Papamichael K. and Beltran L., "Simulating the daylight performance of fenestration systems and spaces of arbitrary complexity: the IDC method", *Proceedings of 3rd IBPSA conference*, pp.509-515, Adelaide, 1993.

Park K. and Athienitis A., "Daylight prediction for integrated daylighting control systems with an interior light sensor", Proceedings of SESCO'04, pp. 35-46, Waterloo, Canada, August 2004.

Park K-W. & Athienitis A.K., "Workplane Illuminance Prediction Method for Daylighting Control Systems", Solar Energy, Vol. 75 (4), pp. 277-284, 2003.

Parmelee G.V. and Aubele W.W., "The shading of sunlit glass", ASHVE Transactions, Vol. 58, pp. 377-398, 1952.

Pedersen C.O., Fisher D.E., Liesen R.J., "A heat balance based cooling load calculation procedure", ASHRAE Transactions, Vol. 103 (2), pp. 459-468, 1997.

Perez R., Ineichen P., Seals R., Michalsky J., Stewart R., "Modeling daylight availability and irradiance components from direct and global irradiance", Solar Energy, Vol. 44 (5), pp. 271-289, 1990.

Perez R., Seals R., Michalsky J., "All-weather model for sky luminance distribution-preliminary configuration and validation", Solar Energy, Vol. 50 (3), pp. 235-245, 1993.

Pfrommer P., Lomas K.J. and Kupke C., "Solar radiation transport through slat-type blinds: a new model and its application for thermal simulation of buildings" Solar Energy, Vol. 57 (2), pp. 77-91, 1996.

Pilkington brothers, "Windows and Environment", London, 1969.

Pucar M., "Application of reflecting louvers and convex reflecting parapet for illuminating north sides of neighbouring buildings", World Renewable Energy Congress VI, Oxford, 2000.

- Reindtl D.T., Beckman W.A., Duffie J.A., "Evaluation of hourly tilted surface radiation models", *Solar Energy*, Vol. 45, pp. 9, 1990.
- Reinhart C. F., "Lightswitch-2002: a model for manual and automated control of electric lighting and blinds", *Solar Energy*, Vol. 77, pp. 15-28, 2004.
- Reinhart C.F. & Morrison M., "The lightswitch wizard-reliable daylight simulations for initial design investigation", *Proceedings of International Building Simulation conference*, Eindhoven, Netherlands, August 2003.
- Reinhart C.F. and Fitz A., "Key findings from a online survey on the use of daylight simulation programs", *Proceedings of eSim2004*, pp. 175-182, Vancouver, Canada, June 2004.
- Reinhart C.F. and Herkel S., "The simulation of annual illuminance distributions- a state-of-the-art comparison of six Radiance-based methods", *Energy and Buildings*, Vol. 32 (2), pp. 167-187, 2000.
- Reinhart C.F. and Jones C., "Electric lighting energy savings for an on/off photocell control- a comparative simulation study using DOE 2.1 and DAYSIM", *Proceedings of eSim2004*, pp. 183-189, Vancouver, Canada, June 2004.
- Reinhart C.F. and Walkenhorst O., "Validation of dynamic Radiance-based simulations for a test office with external blinds" *Energy and Buildings* 33, pp. 683-697, 2001.
- Rheault S. and Bilgen E., "Heat transfer analysis in an automated blind window system", *Journal of Solar Energy Engineering*, Vol. 111, pp. 89-95, 1989.
- Rigollier C., Bauer O., Wald L., "On the clear sky model of the ESRA- European Solar Radiation Atlas- with respect to the heliostat method", *Solar Energy*, Vol. 68 (1), pp. 33-48, 2000.

Robins C. & Hunter K., "A method for determining interreflected in clear climates", SERI/TR-254-1845, 1984.

Rosenfeld J.L.J., "On the calculation of the total solar energy transmittance of complex glazings", Proceedings of 8th International meeting on transparent insulation material, pp. 1-6, Freiburg, Germany, June 1996.

Rosenfeld J.L.J., Breitenbach J., Lart S. and Langle I., "Optical and thermal performance of glazing with integral venetian blinds", Energy and Buildings 33, pp. 433-442, 2001.

Rosenfeld J.L.J., W.J. Platzer, H. Van Dijk, A. Maccari, "Modeling the optical and thermal properties of complex glazing: overview of recent developments", Solar Energy, Vol. 69 (6-suppl.), pp. 1-13, 2000.

Rubin M., K. Von Rottkay and R. Powles, "Window Optics", Solar Energy, Vol. 62 (3), pp. 149-161, 1998.

Santos J.M., Pinazo J.M., Canada J., "Methodology for generating daily clearness index values starting from the monthly average daily Kt: determining the daily sequence using stochastic models", Renewable Energy, Vol. 28, pp. 1523-1544, 2003.

Selkowitz S.E., "The elusive challenge of daylighted buildings-a brief review 25 years later", Proceedings of Daylighting'98 Conference, Ottawa, Canada, May 1998

Siegel R. & Howell J., "Thermal radiation Heat Transfer", HPC Publication, 1992.

Spittler J.D. & Fisher D.E., "Development of periodic response factors for use with the radiant time series method", ASHRAE Transactions, Vol. 105 (2), 1999.

Sullivan R., Beltran L.O., Lee E.S., Rubin M.D., Seelkowitz S.E, "Energy and daylight performance of angular selective glazings", Proceedings of Thermal Performance of Exterior Envelopes VII, pp. 319-328, Clear Water, Florida, 1998.

Tichelen P., DeLaet I., Taeymans F., Adams F., "Energy savings from the EE-SYLK daylighting system", Proceedings of World Renewable Congress VI, pp. 657-660, UK, 2000.

Tregenza P.R. and Waters I.M., "Daylight coefficients", Lighting Research and Technology, Vol. 15 920, pp. 65-71, 1983.

Tregenza P.R., "The Monte Carlo method in lighting calculations", Lighting Research and Technology, Vol. 15 (4), pp. 163-170, 1983.

TRNSYS 15 Reference manual, TRANSSOLAR, 2003.

Tsangrassoulis A., Santamouris M., Assimakopoulos D., "Theoretical and experimental analysis of daylight performance for various shading systems", Energy and Buildings, Vol. 24, pp. 223-230, 1996.

Tsangrassoulis A., Santamouris M., Geros V., Wilson M., Asimakopoulos D., "A method to investigate the potential of south-oriented vertical surfaces for reflecting daylight onto oppositely facing vertical surfaces under sunny conditions", Solar Energy, Vol. 66 (6), pp. 439-446, 1999.

Tzempelikos A. & Athienitis A.K., "A methodology for detailed calculation of room illuminance levels and light dimming in a room with motorized blinds integrated in an advance window", Proceedings of 1st eSim National Building Simulation Conference, pp. 77-84, Ottawa, Canada, 2001.

- Tzempelikos A. and Athienitis A.K., "Investigation of lighting, daylighting and shading design options for new Concordia University Engineering building", Proceedings of eSim 2002, pp. 177-184, Montreal, Canada, June 2002.
- Tzempelikos A. & Athienitis A.K., "Modeling and evaluation of a window with integrated motorized venetian blinds", Proceedings of 3rd ISES World Congress, Gotenburg, Sweden, 2003a.
- Tzempelikos A. & Athienitis A.K., "Simulation for façade options and Impact on HVAC system design", Proceedings of International Building Simulation conference, Eindhoven, Netherlands, August 2003b.
- Tzempelikos A. & Athienitis A.K., "Development of a methodology for fenestration design optimization", Proceedings of 3rd eSim National Building Simulation Conference, pp. 101-108, Vancouver, Canada, June 2004.
- Tzempelikos A. & Athienitis A.K., "Integrated thermal and daylighting analysis for design of office buildings", ASHRAE Transactions, Vol. 111 (1), pp. 2005a.
- Tzempelikos A. and Athienitis A.K., "The effect of shading design and control on building cooling demand", Proceedings of 1st International Passive and low energy cooling of buildings, Santorini, Greece, May 2005b.
- Van Dijk D. and H. Oversloot, "WIS, the European tool to calculate thermal and solar properties of windows and window components", Proceedings of the 8th IBPSA conference, pp. 259-266, Eindhoven, Netherlands, August 2003.
- Vine E., Lee E., DiBartolomeo D., Selkowitz S.E., "Office worker response to an automated venetian blind and electric lighting system: a pilot study", Energy and Buildings, Vol. 28, pp. 205, 1998.

Waldram P., "A measuring diagram for daylight illumination", Batsford Pub., London, 1950.

Ward G.J. & Rubinstein F.M., "A new technique for computer simulation of illuminated spaces", Journal of the Illumination Engineering Society, Vol. 17 (1), pp. 777-789, 1994.

WINDOW 5/THERM NFRC simulation manual, Lawrence Berkeley National Laboratory, June 2003.

Winkelmann F. C., Birdsall B. E., Buhl W. F., Ellington K. L., Erdem A. E., "DOE-2, Version 2.1E", Lawrence Berkeley National Laboratory, LBL-34947, 1993.

Yahoda D.S. & J.L. Wright, "Heat transfer analysis of a between-panes venetian blind using effective long-wave radiative properties", ASHRAE Transactions, Vol. 110 (1), pp. 455-463, 2004.

Yahoda D.S. & J.L. Wright, "Methods for calculating the effective long-wave radiative properties of a venetian blind layer", ASHRAE Transactions, Vol. 110 (1), pp. 463-474, 2004.

Zmeureanu R., "Defining the methodology for the next generation HOT2000 simulator", Report submitted to CANMET, July 1997.

Zmeureanu R., Pasqualetto L. and Bilas F., "Comparison of cost and energy savings in an existing large building as predicted by three simulation programs", Proceedings of IBPSA'95, pp. 485-492, Madison, USA, 1995.

APPENDIX A

**Calculation of solar geometry, surface geometry and solar incidence angle
(MathCad 2001i file).**

<u>Input variables:</u>		<u>Range variables:</u>	
Latitude:	$L := 45.5 \cdot \text{deg}$	$n := 0, 1 \dots 364$	Day number
Longitude:	$LNG := 74 \cdot \text{deg}$	$t := 0, 1 \dots 23$	Time index
Local Standard Meridian:	$LSM := 75 \cdot \text{deg}$		
Altitude:	$Alt := 400 \cdot \text{m}$		
Surface azimuth:	$\psi := 0 \cdot \text{deg}$		
Surface tilt angle:	$\beta := 90 \cdot \text{deg}$		
Ground reflectance:	$\rho_g := 0.2$		
<u>Solar and surface geometry:</u>			
Equation of time:	$ET(n) := \left(9.87 \cdot \sin\left(4 \cdot \pi \cdot \frac{n - 81}{364}\right) - 7.53 \cdot \cos\left(2 \cdot \pi \cdot \frac{n - 81}{364}\right) - 1.5 \cdot \sin\left(2 \cdot \pi \cdot \frac{n - 81}{364}\right) \right) \cdot \text{min}$		
Apparent Solar Time:	$AST(n, t) := t \cdot \text{hr} + ET(n) + \frac{(LSM - LNG) \cdot \text{hr}}{15 \cdot \text{deg}}$	$s(n, t) := AST(n, t) - 12 \cdot \text{hr}$	
Solar declination:	$\delta(n) := 23.45 \cdot \text{deg} \cdot \sin\left(360 \cdot \frac{284 + n}{365} \cdot \text{deg}\right)$		
Hour angle:	$H(n, t) := (AST(n, t) - 12 \cdot \text{hr}) \cdot \left(15 \cdot \frac{\text{deg}}{\text{hr}}\right)$		
Sunset hour angle:	$h_s(n) := (\text{acos}(-\tan(L) \cdot \tan(\delta(n))))$		
Sunset time:	$t_s(n) := h_s(n) \cdot \frac{\text{hr}}{15 \cdot \text{deg}}$		
Surface sunset time:	$t_{ss}(n) := \min\left(h_s(n), \text{acos}(-\tan(L - \beta) \cdot \tan(\delta(n)))\right) \cdot \frac{\text{hr}}{15 \cdot \text{deg}}$		

Solar altitude: $\alpha(n,t) := \begin{cases} \arcsin \left[\frac{\cos(L) \cdot \cos(\delta(n)) \cdot \cos(H(n,t)) + \sin(L) \cdot \sin(\delta(n))}{1} \right] & \text{if } \arcsin \left[\frac{\cos(L) \cdot \cos(\delta(n)) \cdot \cos(H(n,t)) + \sin(L) \cdot \sin(\delta(n))}{1} \right] > 2 \cdot \text{deg} \\ 0 \cdot \text{deg} & \text{otherwise} \end{cases}$

Solar azimuth: $\phi(n,t) := \arccos \left(\frac{\sin(\alpha(n,t)) \cdot \sin(L) - \sin(\delta(n))}{\cos(\alpha(n,t)) \cdot \cos(L)} \right) \cdot \frac{H(n,t)}{|H(n,t)|}$

Surface solar azimuth: $\gamma(n,t) := \phi(n,t) - \psi$

The angle of incidence, $\theta(n,t) := \cos(\alpha(n,t)) \cdot \cos(|\gamma(n,t)|) \cdot \sin(\beta) + \sin(\alpha(n,t)) \cdot \cos(\beta)$

$\theta(n,t) := \arccos \left(\frac{\theta(n,t) + |\theta(n,t)|}{2} \right)$ **Solar incidence angle**

APPENDIX B

Calculation of incident beam, sky diffuse and ground-reflected irradiance on a tilted surface using Perez et al. (1990) model (MathCad 2001i file).

➔ Reference: C:\Thanos\PhD Thanos\Solar radiation models\THESIS files\Weather data.mcd(R)

Weather data (horizontal beam and diffuse irradiance and direct normal irradiance) are read from the above reference file, imported as tables after processing in an Excel worksheet.

Extraterrestrial solar radiation (outside the atmosphere):

Solar constant: $I_{sc} := 1367 \cdot \frac{W}{m^2}$

Normal extraterrestrial solar radiation: $I_{exn}(n) := I_{sc} \cdot \left(1 + 0.033 \cdot \cos \left(\frac{360 \cdot n}{365} \cdot \text{deg} \right) \right)$

Hourly average global horizontal irradiance for Montreal:

$$I_h(n, t) := I_{bh}(n, t) + I_{dh}(n, t)$$

Incident beam radiation on an inclined surface:

$$I_b(n, t) := (I_{bn}(n, t) \cdot \cos(\theta(n, t)))$$

Perez diffuse irradiance model:

Diffuse radiation consists of three components:

1. Isotropic part, received uniformly from all the sky dome
2. Circumsolar diffuse, resulting from forward scattering of solar radiation and concentrated in the part of the sky around the sun.
3. Horizon brightening, concentrated near the horizon, most pronounced in clear skies.

Anisotropic sky models have been produced initially by Hay & Davies (1980), and further developed by Reindl et al (1990). An anisotropy index is used to account for a portion of diffuse radiation which is treated as forward scattered. More recently, Perez et al (1988, 1990, 1993) produced more accurate models for treating the three parts of diffuse radiation on a tilted surface.

Horizon brightness coefficients:

$$a_p(n, t) := \max(0, \cos(\theta(n, t))) \quad b_p(n, t) := \max(\cos(85 \text{ deg}), \sin(\alpha(n, t)))$$

Relative optical air mass:

$$m_{\text{opt}}(n, t) := \frac{1}{\sin(\alpha(n, t)) + 0.15 \left(\alpha(n, t) \cdot \frac{\pi}{180 \text{ deg}} + 3.885 \right)^{-1.253}}$$

Sky brightness:

$$\Delta(n, t) := m_{\text{opt}}(n, t) \cdot \frac{I_{\text{dh}}(n, t)}{I_{\text{exn}}(n)}$$

Sky clearness:

$$\varepsilon(n, t) := \begin{cases} \frac{\frac{I_{\text{dh}}(n, t) + I_{\text{bn}}(n, t)}{I_{\text{dh}}(n, t)} + 5.535 \cdot 10^{-6} \cdot (90 \text{ deg} - \alpha(n, t))^3}{1 + 5.535 \cdot 10^{-6} \cdot (90 \text{ deg} - \alpha(n, t))^3} & \text{if } I_{\text{dh}}(n, t) > 0 \cdot \frac{\text{W}}{\text{m}^2} \\ 0 & \text{otherwise} \end{cases}$$

Statistically derived irradiance coefficients for Perez model:

$f_{11}(n, t) := \begin{cases} -0.008 & \text{if } \varepsilon(n, t) \leq 1.065 \\ 0.130 & \text{if } 1.065 < \varepsilon(n, t) \leq 1.23 \\ 0.330 & \text{if } 1.23 < \varepsilon(n, t) \leq 1.5 \\ 0.568 & \text{if } 1.5 < \varepsilon(n, t) \leq 1.95 \\ 0.873 & \text{if } 1.95 < \varepsilon(n, t) \leq 2.8 \\ 1.132 & \text{if } 2.8 < \varepsilon(n, t) \leq 4.5 \\ 1.060 & \text{if } 4.5 < \varepsilon(n, t) \leq 6.2 \\ 0.678 & \text{otherwise} \end{cases}$	$f_{12}(n, t) := \begin{cases} 0.588 & \text{if } \varepsilon(n, t) \leq 1.065 \\ 0.683 & \text{if } 1.065 < \varepsilon(n, t) \leq 1.23 \\ 0.487 & \text{if } 1.23 < \varepsilon(n, t) \leq 1.5 \\ 0.187 & \text{if } 1.5 < \varepsilon(n, t) \leq 1.95 \\ -0.392 & \text{if } 1.95 < \varepsilon(n, t) \leq 2.8 \\ -1.237 & \text{if } 2.8 < \varepsilon(n, t) \leq 4.5 \\ -1.600 & \text{if } 4.5 < \varepsilon(n, t) \leq 6.2 \\ -0.327 & \text{otherwise} \end{cases}$	$f_{13}(n, t) := \begin{cases} -0.062 & \text{if } \varepsilon(n, t) \leq 1.065 \\ -0.151 & \text{if } 1.065 < \varepsilon(n, t) \leq 1.23 \\ -0.221 & \text{if } 1.23 < \varepsilon(n, t) \leq 1.5 \\ -0.295 & \text{if } 1.5 < \varepsilon(n, t) \leq 1.95 \\ -0.362 & \text{if } 1.95 < \varepsilon(n, t) \leq 2.8 \\ -0.412 & \text{if } 2.8 < \varepsilon(n, t) \leq 4.5 \\ -0.359 & \text{if } 4.5 < \varepsilon(n, t) \leq 6.2 \\ -0.25 & \text{otherwise} \end{cases}$
$f_{21}(n, t) := \begin{cases} -0.060 & \text{if } \varepsilon(n, t) \leq 1.065 \\ -0.019 & \text{if } 1.065 < \varepsilon(n, t) \leq 1.23 \\ 0.055 & \text{if } 1.23 < \varepsilon(n, t) \leq 1.5 \\ 0.109 & \text{if } 1.5 < \varepsilon(n, t) \leq 1.95 \\ 0.226 & \text{if } 1.95 < \varepsilon(n, t) \leq 2.8 \\ 0.288 & \text{if } 2.8 < \varepsilon(n, t) \leq 4.5 \\ 0.264 & \text{if } 4.5 < \varepsilon(n, t) \leq 6.2 \\ 0.156 & \text{otherwise} \end{cases}$	$f_{22}(n, t) := \begin{cases} 0.072 & \text{if } \varepsilon(n, t) \leq 1.065 \\ 0.066 & \text{if } 1.065 < \varepsilon(n, t) \leq 1.23 \\ -0.064 & \text{if } 1.23 < \varepsilon(n, t) \leq 1.5 \\ -0.152 & \text{if } 1.5 < \varepsilon(n, t) \leq 1.95 \\ -0.462 & \text{if } 1.95 < \varepsilon(n, t) \leq 2.8 \\ -0.823 & \text{if } 2.8 < \varepsilon(n, t) \leq 4.5 \\ -1.127 & \text{if } 4.5 < \varepsilon(n, t) \leq 6.2 \\ -1.377 & \text{otherwise} \end{cases}$	$f_{23}(n, t) := \begin{cases} -0.022 & \text{if } \varepsilon(n, t) \leq 1.065 \\ -0.029 & \text{if } 1.065 < \varepsilon(n, t) \leq 1.23 \\ -0.026 & \text{if } 1.23 < \varepsilon(n, t) \leq 1.5 \\ -0.014 & \text{if } 1.5 < \varepsilon(n, t) \leq 1.95 \\ -0.001 & \text{if } 1.95 < \varepsilon(n, t) \leq 2.8 \\ 0.056 & \text{if } 2.8 < \varepsilon(n, t) \leq 4.5 \\ 0.131 & \text{if } 4.5 < \varepsilon(n, t) \leq 6.2 \\ 0.251 & \text{otherwise} \end{cases}$

Brightness coefficients:

$$F_1(n, t) := \max \left[0, f_{11}(n, t) + f_{12}(n, t) \cdot \Delta(n, t) + \pi \cdot \frac{(90 \cdot \text{deg} - \alpha(n, t))}{180 \cdot \text{deg}} \cdot f_{13}(n, t) \right]$$

$$F_2(n, t) := \max \left[0, f_{21}(n, t) + f_{22}(n, t) \cdot \Delta(n, t) + \pi \cdot \frac{(90 \cdot \text{deg} - \alpha(n, t))}{180 \cdot \text{deg}} \cdot f_{23}(n, t) \right]$$

Sky diffuse radiation on a tilted surface is calculated by:

$$I_{sd}(n, t) := I_{dh}(n, t) \cdot \left[(1 - F_1(n, t)) \cdot \left(\frac{1 + \cos(\beta)}{2} \right) + F_1(n, t) \cdot \frac{a_p(n, t)}{b_p(n, t)} + F_2(n, t) \cdot \sin(\beta) \right]$$

Ground-reflected radiation on a tilted surface:

$$I_g(n, t) := I_h(n, t) \cdot \rho_g \cdot \frac{1 - \cos(\beta)}{2}$$

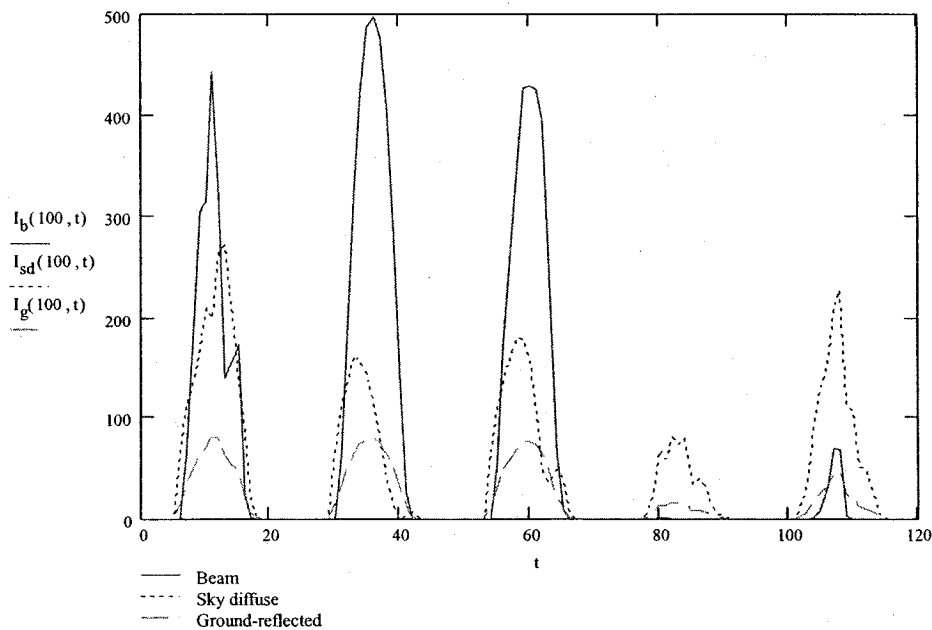
Total diffuse radiation on a tilted surface:

$$I_d(n, t) := I_{sd}(n, t) + I_g(n, t)$$

The total incident solar radiation on a tilted surface is equal to:

$$I(n, t) := I_b(n, t) + I_{sd}(n, t) + I_g(n, t)$$

Graph showing calculated incident beam, sky diffuse and ground-reflected solar radiation on a south-facing facade in Montreal, on April 10th-15th for five successive days, reading horizontal hourly irradiance data from the weather file (referenced on top of the program).



APPENDIX C

Perez et al. (1990) luminous efficacy model for calculation of horizontal beam and diffuse illuminance from horizontal irradiance data. Calculation of hourly illuminance values on a tilted surface, using Perez et al. (1990) tilted surface model (Mathcad 2001i file).

☞ Reference: C:\Thanos\PhD Thanos\Solar radiation models\THESIS files\Perez irradiance model.mcd(R)

This program calculates illuminance values using the Perez et al. (1990) luminous efficacy coefficients. Hourly beam and diffuse horizontal irradiance data and hourly dew-point temperature are read from the file referenced above.

Perez luminous efficacy coefficients:

Direct luminous efficacy:

$ab(n,t) :=$

57.20	if $\varepsilon(n,t) \leq 1.065$
98.99	if $1.065 < \varepsilon(n,t) \leq 1.23$
109.83	if $1.23 < \varepsilon(n,t) \leq 1.5$
110.34	if $1.5 < \varepsilon(n,t) \leq 1.95$
106.36	if $1.95 < \varepsilon(n,t) \leq 2.8$
107.19	if $2.8 < \varepsilon(n,t) \leq 4.5$
105.75	if $4.5 < \varepsilon(n,t) \leq 6.2$
101.18	otherwise

$bb(n,t) :=$

-4.55	if $\varepsilon(n,t) \leq 1.065$
-3.46	if $1.065 < \varepsilon(n,t) \leq 1.23$
-4.90	if $1.23 < \varepsilon(n,t) \leq 1.5$
-5.84	if $1.5 < \varepsilon(n,t) \leq 1.95$
-3.97	if $1.95 < \varepsilon(n,t) \leq 2.8$
-1.25	if $2.8 < \varepsilon(n,t) \leq 4.5$
0.77	if $4.5 < \varepsilon(n,t) \leq 6.2$
1.58	otherwise

$cb(n,t) :=$

-2.98	if $\varepsilon(n,t) \leq 1.065$
-1.21	if $1.065 < \varepsilon(n,t) \leq 1.23$
-1.71	if $1.23 < \varepsilon(n,t) \leq 1.5$
-1.99	if $1.5 < \varepsilon(n,t) \leq 1.95$
-1.75	if $1.95 < \varepsilon(n,t) \leq 2.8$
-1.51	if $2.8 < \varepsilon(n,t) \leq 4.5$
-1.26	if $4.5 < \varepsilon(n,t) \leq 6.2$
-1.10	otherwise

$db(n,t) :=$

117.12	if $\varepsilon(n,t) \leq 1.065$
12.38	if $1.065 < \varepsilon(n,t) \leq 1.23$
-8.81	if $1.23 < \varepsilon(n,t) \leq 1.5$
-4.56	if $1.5 < \varepsilon(n,t) \leq 1.95$
-6.16	if $1.95 < \varepsilon(n,t) \leq 2.8$
-26.73	if $2.8 < \varepsilon(n,t) \leq 4.5$
-34.44	if $4.5 < \varepsilon(n,t) \leq 6.2$
-8.29	otherwise

Diffuse luminous efficacy:

$bd(n,t) :=$	-0.46 if $\varepsilon(n,t) \leq 1.065$	$ad(n,t) :=$	97.24 if $\varepsilon(n,t) \leq 1.065$
	1.15 if $1.065 < \varepsilon(n,t) \leq 1.23$		107.22 if $1.065 < \varepsilon(n,t) \leq 1.23$
	2.96 if $1.23 < \varepsilon(n,t) \leq 1.5$		104.97 if $1.23 < \varepsilon(n,t) \leq 1.5$
	5.59 if $1.5 < \varepsilon(n,t) \leq 1.95$		102.39 if $1.5 < \varepsilon(n,t) \leq 1.95$
	5.94 if $1.95 < \varepsilon(n,t) \leq 2.8$		100.71 if $1.95 < \varepsilon(n,t) \leq 2.8$
	3.83 if $2.8 < \varepsilon(n,t) \leq 4.5$		106.42 if $2.8 < \varepsilon(n,t) \leq 4.5$
	1.90 if $4.5 < \varepsilon(n,t) \leq 6.2$		141.88 if $4.5 < \varepsilon(n,t) \leq 6.2$
	0.35 otherwise		152.23 otherwise

$dd(n,t) :=$	-8.91 if $\varepsilon(n,t) \leq 1.065$	$cd(n,t) :=$	12.00 if $\varepsilon(n,t) \leq 1.065$
	-3.95 if $1.065 < \varepsilon(n,t) \leq 1.23$		0.59 if $1.065 < \varepsilon(n,t) \leq 1.23$
	-8.77 if $1.23 < \varepsilon(n,t) \leq 1.5$		-5.53 if $1.23 < \varepsilon(n,t) \leq 1.5$
	-13.90 if $1.5 < \varepsilon(n,t) \leq 1.95$		-13.95 if $1.5 < \varepsilon(n,t) \leq 1.95$
	-23.74 if $1.95 < \varepsilon(n,t) \leq 2.8$		-22.75 if $1.95 < \varepsilon(n,t) \leq 2.8$
	-28.83 if $2.8 < \varepsilon(n,t) \leq 4.5$		-36.15 if $2.8 < \varepsilon(n,t) \leq 4.5$
	-14.03 if $4.5 < \varepsilon(n,t) \leq 6.2$		-53.24 if $4.5 < \varepsilon(n,t) \leq 6.2$
	-7.98 otherwise		-45.27 otherwise

Precipitable water content:

$$WC(n,t) := e^{0.07 \cdot T_{dp}(n,t) - 0.075}$$

Diffuse horizontal illuminance:

$$E_{dh}(n,t) := I_{dh}(n,t) \cdot \left(ad(n,t) + bd(n,t) \cdot WC(n,t) + cd(n,t) \cdot \sin(\alpha(n,t)) + dd(n,t) \cdot \ln(\Delta(n,t) + 10^{-10}) \right) \cdot lx \frac{m^2}{W}$$

Direct normal illuminance:

$$E_{bn}(n,t) := \max \left[0, I_{bn}(n,t) \cdot \left[ab(n,t) + bb(n,t) \cdot WC(n,t) + cb(n,t) \cdot e^{5.73(90 - \deg - \alpha(n,t)) \frac{\pi}{180 \deg} - 5} + db(n,t) \cdot \Delta(n,t) \right] \cdot lx \frac{m^2}{W} \right]$$

Direct horizontal illuminance:

$$E_{bh}(n,t) := E_{bn}(n,t) \cdot \sin(\alpha(n,t))$$

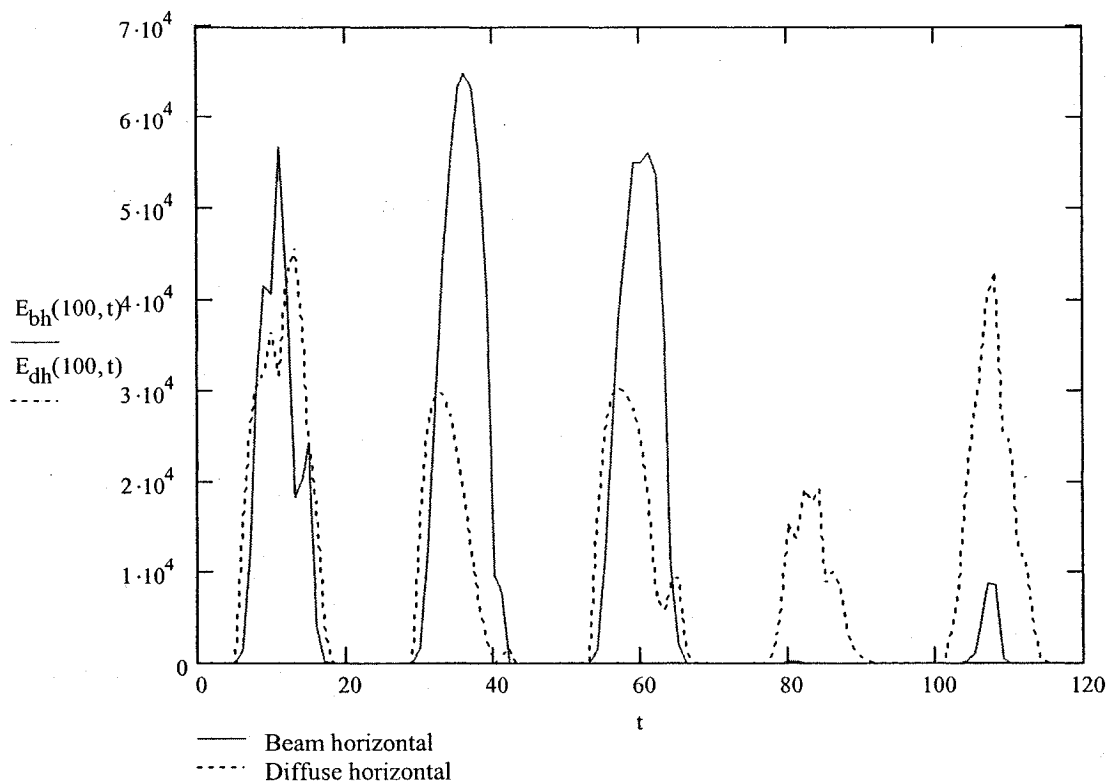
Hourly average global horizontal illuminance:

$$E_h(n,t) := E_{bh}(n,t) + E_{dh}(n,t)$$

Hourly average beam illuminance on a tilted surface:

$$E_b(n,t) := (E_{bn}(n,t) \cdot \cos(\theta(n,t)))$$

The following graph shows hourly beam and diffuse horizontal illuminance , for five successive days (April 10th-April 15th), calculated with the Perez et al. (1990) model.



Statistically derived illuminance coefficients for Perez model:

$f_{11}(n,t) :=$	0.011 if $\varepsilon(n,t) \leq 1.065$ 0.429 if $1.065 < \varepsilon(n,t) \leq 1.23$ 0.809 if $1.23 < \varepsilon(n,t) \leq 1.5$ 1.014 if $1.5 < \varepsilon(n,t) \leq 1.95$ 1.282 if $1.95 < \varepsilon(n,t) \leq 2.8$ 1.426 if $2.8 < \varepsilon(n,t) \leq 4.5$ 1.485 if $4.5 < \varepsilon(n,t) \leq 6.2$ 1.170 otherwise	$f_{12}(n,t) :=$	0.570 if $\varepsilon(n,t) \leq 1.065$ 0.363 if $1.065 < \varepsilon(n,t) \leq 1.23$ -0.054 if $1.23 < \varepsilon(n,t) \leq 1.5$ -0.252 if $1.5 < \varepsilon(n,t) \leq 1.95$ -0.420 if $1.95 < \varepsilon(n,t) \leq 2.8$ -0.653 if $2.8 < \varepsilon(n,t) \leq 4.5$ -1.214 if $4.5 < \varepsilon(n,t) \leq 6.2$ -0.300 otherwise	$f_{13}(n,t) :=$	-0.081 if $\varepsilon(n,t) \leq 1.065$ -0.307 if $1.065 < \varepsilon(n,t) \leq 1.23$ -0.442 if $1.23 < \varepsilon(n,t) \leq 1.5$ -0.531 if $1.5 < \varepsilon(n,t) \leq 1.95$ -0.689 if $1.95 < \varepsilon(n,t) \leq 2.8$ -0.779 if $2.8 < \varepsilon(n,t) \leq 4.5$ -0.784 if $4.5 < \varepsilon(n,t) \leq 6.2$ -0.615 otherwise
$f_{21}(n,t) :=$	-0.095 if $\varepsilon(n,t) \leq 1.065$ 0.050 if $1.065 < \varepsilon(n,t) \leq 1.23$ 0.181 if $1.23 < \varepsilon(n,t) \leq 1.5$ 0.275 if $1.5 < \varepsilon(n,t) \leq 1.95$ 0.380 if $1.95 < \varepsilon(n,t) \leq 2.8$ 0.425 if $2.8 < \varepsilon(n,t) \leq 4.5$ 0.411 if $4.5 < \varepsilon(n,t) \leq 6.2$ 0.518 otherwise	$f_{22}(n,t) :=$	0.158 if $\varepsilon(n,t) \leq 1.065$ 0.008 if $1.065 < \varepsilon(n,t) \leq 1.23$ -0.169 if $1.23 < \varepsilon(n,t) \leq 1.5$ -0.35 if $1.5 < \varepsilon(n,t) \leq 1.95$ -0.559 if $1.95 < \varepsilon(n,t) \leq 2.8$ -0.785 if $2.8 < \varepsilon(n,t) \leq 4.5$ -0.629 if $4.5 < \varepsilon(n,t) \leq 6.2$ -1.892 otherwise	$f_{23}(n,t) :=$	-0.018 if $\varepsilon(n,t) \leq 1.065$ -0.065 if $1.065 < \varepsilon(n,t) \leq 1.23$ -0.092 if $1.23 < \varepsilon(n,t) \leq 1.5$ -0.096 if $1.5 < \varepsilon(n,t) \leq 1.95$ -0.114 if $1.95 < \varepsilon(n,t) \leq 2.8$ -0.097 if $2.8 < \varepsilon(n,t) \leq 4.5$ -0.082 if $4.5 < \varepsilon(n,t) \leq 6.2$ -0.055 otherwise

Brightness coefficients:

$$F_1(n,t) := \max \left[0, f_{11}(n,t) + f_{12}(n,t) \cdot \Delta(n,t) + \pi \cdot \frac{(90 \text{ deg} - \alpha(n,t))}{180 \text{ deg}} \cdot f_{13}(n,t) \right]$$

$$F_2(n,t) := \max \left[0, f_{21}(n,t) + f_{22}(n,t) \cdot \Delta(n,t) + \pi \cdot \frac{(90 \text{ deg} - \alpha(n,t))}{180 \text{ deg}} \cdot f_{23}(n,t) \right]$$

Sky diffuse illuminance on a tilted surface is calculated by:

$$E_{sd}(n,t) := E_{dh}(n,t) \left[\left(1 - F_1(n,t) \right) \cdot \left(\frac{1 + \cos(\beta)}{2} \right) + F_1(n,t) \cdot \frac{a_p(n,t)}{b_p(n,t)} + F_2(n,t) \cdot \sin(\beta) \right]$$

Ground-reflected illuminance on a tilted surface:

$$E_g(n,t) := E_h(n,t) \cdot \rho_g \cdot \frac{1 - \cos(\beta)}{2}$$

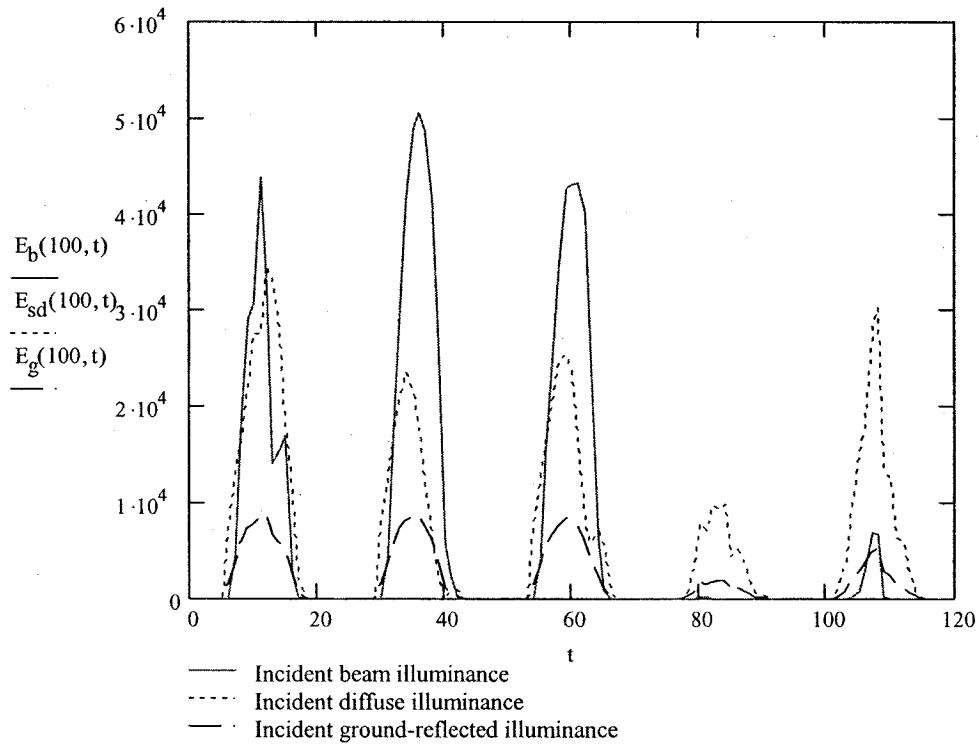
Total diffuse illuminance on a tilted surface:

$$E_d(n,t) := E_{sd}(n,t) + E_g(n,t)$$

The total incident illuminance on a tilted surface is equal to:

$$E(n, t) := E_b(n, t) + E_{sd}(n, t) + E_g(n, t)$$

The following graph shows calculated hourly beam, sky diffuse and ground-reflected illuminance on a south-facing window in Montreal for five successive days in April (April 10th-April 15th).



APPENDIX D

Calculation of window optical properties as a function of solar time for effective use in simulation models (MathCad 2000i file).

Calculation of window properties as a function of solar time (for further hourly simulation) is achieved if the properties of glazing are expressed as a function of solar incidence angle, which is computed as a function of solar time and day number. For any glazing type, transmittance, absorptance and reflectance can be analytically calculated by applying the Fresnel equations and using convergent geometric series.

Glass properties: $kL := 0.04$..extinction coeff.*glazing thickness

$n_g := 1.53$..refractive index

Angle of refraction and component reflectivity:

$$\theta'(n,t) := \arcsin\left(\frac{\sin(\theta(n,t))}{n_g}\right) \quad r(n,t) := \frac{1}{2} \left[\left(\frac{\sin(\theta(n,t) - \theta'(n,t))}{\sin(\theta(n,t) + \theta'(n,t))} \right)^2 + \left(\frac{\tan(\theta(n,t) - \theta'(n,t))}{\tan(\theta(n,t) + \theta'(n,t))} \right)^2 \right]$$

Beam transmittance τ , reflectance ρ_0 and absorptance α , of glazing:

$$a(n,t) := \exp\left[-\frac{kL}{\sqrt{1 - \left(\frac{\sin(\theta(n,t))}{n_g} \right)^2}} \right] \quad \tau(n,t) := \frac{(1 - r(n,t))^2 \cdot a(n,t)}{1 - (r(n,t))^2 \cdot (a(n,t))^2}$$

$$\rho_0(n,t) := r(n,t) + \frac{r(n,t) \cdot (1 - r(n,t))^2 \cdot (a(n,t))^2}{1 - (r(n,t))^2 \cdot (a(n,t))^2} \quad \alpha_s(n,t) := 1 - \tau(n,t) - \rho_0(n,t)$$

For double glazed windows:

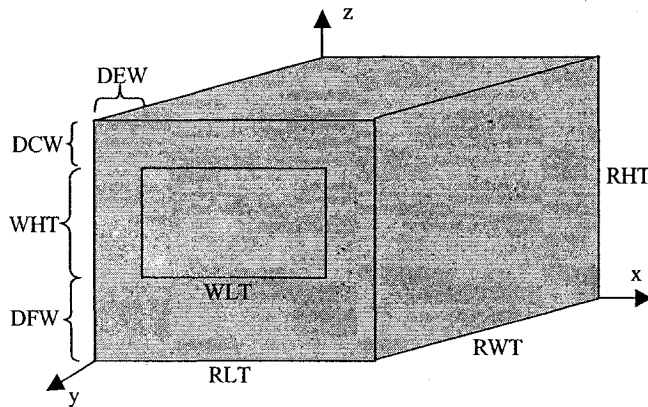
$$\tau_e(n,t) := \frac{(\tau(n,t))^2}{1 - (\rho_0(n,t))^2} \quad \dots \text{effective beam transmittance}$$

$$\alpha_i(n,t) := \alpha_s(n,t) \cdot \frac{\tau(n,t)}{1 - (\rho_0(n,t))^2} \quad \dots \text{interior glazing absorptance}$$

$$\alpha_o(n,t) := \alpha_s(n,t) + \alpha_s(n,t) \cdot \frac{\tau(n,t) \cdot \rho_0(n,t)}{1 - (\rho_0(n,t))^2} \quad \dots \text{exterior glazing absorptance}$$

APPENDIX E

Detailed analytical calculation of view (form) factors between all interior surfaces in a rectangular room with one window (MathCad 2001i file).



Room Dimensions:

RHT := 3-m ...height

RWT := 4-m ...width

RLT := 4-m ...length

Window Dimensions:

WHT := 1.2m ...height

WLT := 1.5m ...length

$$\text{vis} := \frac{\text{WHT} \cdot \text{WLT}}{\text{RHT} \cdot \text{RLT}} \quad \text{vis} = 0.15$$

Distance from Floor to Window: DFW := 0.8m

Distance from Ceiling to Window: DCW := RHT - DFW - WHT DCW = 1m

Distance from Edge to Window:
$$\text{DEW} := \frac{\text{RLT} - \text{WLT}}{2} \quad \text{DEW} = 1.25\text{m} \quad \text{...window located at center}$$

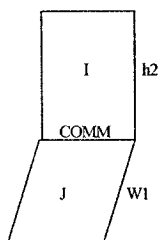
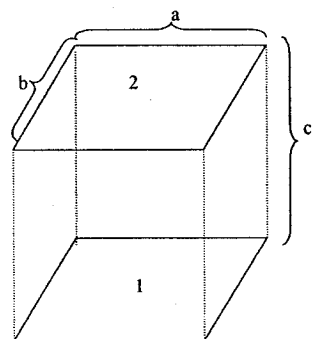
Total number of interior surfaces: nsf := 7 Surfaces indices: i := 0..nsf - 1 j := 0..n

Surface Reflectances:

$\rho :=$	$\begin{pmatrix} 0.05 \\ 0.7 \\ 0.3 \\ 0.8 \\ 0.7 \\ 0.7 \end{pmatrix}$	$\begin{pmatrix} \text{"Window"} \\ \text{"Front Wall"} \\ \text{Floor} \\ \text{Ceiling} \\ \text{"Back Wall"} \\ \text{"Right Wall"} \end{pmatrix}$
-----------	---	---

Surface Areas:

SA :=	$\begin{pmatrix} \text{WLT} \cdot \text{WHT} \\ \text{RLT} \cdot \text{RHT} - \text{WLT} \cdot \text{WHT} \\ \text{RLT} \cdot \text{RWT} \\ \text{RLT} \cdot \text{RWT} \\ \text{RLT} \cdot \text{RHT} \\ \text{RWT} \cdot \text{RHT} \end{pmatrix}$	$\begin{pmatrix} 1.8 \\ 10.2 \\ 16 \\ 16 \\ 12 \\ 12 \end{pmatrix} \text{m}^2$
-------	--	--



The other view factors between the room surfaces are calculated by applying the following principles:

1. Reciprocity: $A_i \cdot F_{i,j} = A_j \cdot F_{j,i}$
2. Symmetry, e.g. $F_{7,5} = F_{7,8}$
3. Energy conservation: $\sum_j F_{i,j} = 1$ (for any surface i)

$$F_{1,1} := 0 \quad F_{2,2} := 0 \quad F_{3,3} := 0 \quad F_{4,4} := 0 \quad F_{5,5} := 0 \quad F_{6,6} := 0 \quad F_{0,0} := 0$$

VIEW FACTORS BETWEEN FLOOR AND CEILING:

$$a := \text{RLT} \quad b := \text{RWT} \quad c := \text{RHT} \quad x := \frac{a}{c} \quad y := \frac{b}{c}$$

$$F_{2,3} := F_{ij}(x,y) \quad F_{2,3} = 0.282733 \quad F_{3,2} := F_{2,3}$$

VIEW FACTORS BETWEEN RIGHT WALL AND LEFT WALL

$$a := \text{RWT} \quad b := \text{RHT} \quad c := \text{RLT} \quad x := \frac{a}{c} \quad y := \frac{b}{c}$$

$$F_{5,6} := F_{ij}(x,y) \quad F_{5,6} = 0.162824 \quad F_{6,5} := F_{5,6}$$

VIEW FACTORS BETWEEN FLOOR AND BACK WALL AND CEILING AND BACK WALL

$$w1 := \text{RWT} \quad h2 := \text{RHT} \quad \text{comm} := \text{RLT} \quad w := \frac{w1}{\text{comm}} \quad h := \frac{h2}{\text{comm}}$$

$$F_{2,4} := F_{12}(w,h) \quad F_{2,4} = 0.179317 \quad F_{4,2} := \frac{F_{2,4}}{SA_4} \cdot SA_2 \quad F_{4,2} = 0.239$$

$$F_{3,4} := F_{2,4} \quad F_{4,3} := F_{4,2} \quad \dots \text{ from symmetry}$$

VIEW FACTORS BETWEEN BACK WALL AND RIGHT/LEFT WALL

$$w1 := \text{RLT} \quad h2 := \text{RWT} \quad \text{comm} := \text{RHT} \quad w := \frac{w1}{\text{comm}} \quad h := \frac{h2}{\text{comm}}$$

$$F_{4,5} := F_{12}(w,h) \quad F_{4,5} = 0.179499$$

$$F_{4,6} := F_{4,5} \quad F_{5,4} := \frac{SA_4}{SA_5} \cdot F_{4,5} \quad F_{5,4} = 0.179 \quad F_{6,4} := F_{5,4}$$

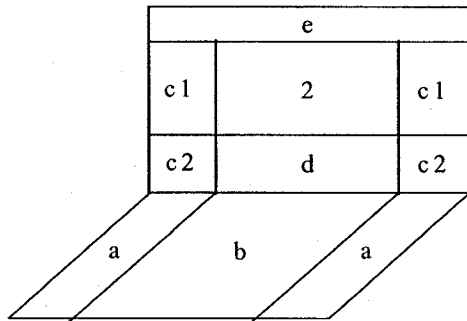
VIEW FACTORS BETWEEN FLOOR AND RIGHT/LEFT WALL AND CEILING AND RIGHT/LEFT WALL

$$w1 := \text{RLT} \quad h2 := \text{RHT} \quad \text{comm} := \text{RWT} \quad w := \frac{w1}{\text{comm}} \quad h := \frac{h2}{\text{comm}}$$

$$F_{2,5} := F_{12}(w,h) \quad F_{2,5} = 0.179317 \quad F_{2,6} := F_{2,5} \quad F_{5,2} := \frac{SA_2}{SA_5} \cdot F_{2,5} \quad F_{6,2} := F_{5,2}$$

$$F_{3,5} := F_{2,4} \quad F_{3,6} := F_{2,5} \quad F_{5,3} := F_{5,2} \quad F_{6,3} := F_{6,2} \quad \dots \text{ from symmetry}$$

$$F_{5,2} = 0.239089 \quad F_{6,2} = 0.239$$



VIEW FACTORS BETWEEN WINDOW AND FLOOR

Now we have to separate the floor in 3 parts and the window wall in 7 parts.

$$\begin{aligned}
 A_a &:= \text{DEW} \cdot \text{RWT} & A_a &= 5 \text{ m}^2 \\
 A_b &:= \text{RWT} \cdot \text{WLT} & A_b &= 6 \text{ m}^2 \\
 A_{c1} &:= \text{WHT} \cdot \text{DEW} & A_{c1} &= 1.5 \text{ m}^2 \\
 A_{c2} &:= \text{DEW} \cdot \text{DFW} & A_{c2} &= 1 \text{ m}^2 \\
 A_d &:= \text{WLT} \cdot \text{DFW} & A_d &= 1.2 \text{ m}^2 \\
 A_2 &:= \text{WLT} \cdot \text{WHT} & A_2 &= 1.8 \text{ m}^2 \\
 A_{ab} &:= A_a + A_b & A_{ab} &= 11 \text{ m}^2
 \end{aligned}$$

$$w1 := \text{RWT} \quad h2 := \text{DFW} + \text{WHT} \quad \text{comm} := \text{WLT} \quad w := \frac{w1}{\text{comm}} \quad h := \frac{h2}{\text{comm}}$$

$$F_{b2d} := F12(w, h) \quad F_{b2d} = 0.103$$

$$w1 := \text{RWT} \quad h2 := \text{DFW} \quad \text{comm} := \text{WLT} \quad w := \frac{w1}{\text{comm}} \quad h := \frac{h2}{\text{comm}}$$

$$F_{bd} := F12(w, h) \quad F_{bd} = 0.062$$

$$w1 := \text{RWT} \quad h2 := \text{DFW} \quad \text{comm} := \text{DEW} \quad w := \frac{w1}{\text{comm}} \quad h := \frac{h2}{\text{comm}}$$

$$F_{ac2} := F12(w, h) \quad F_{ac2} = 0.059$$

$$w1 := \text{RWT} \quad h2 := \text{DFW} + \text{WHT} \quad \text{comm} := \text{DEW} \quad w := \frac{w1}{\text{comm}} \quad h := \frac{h2}{\text{comm}}$$

$$F_{ac1c2} := F12(w, h) \quad F_{ac1c2} = 0.094$$

$$w1 := \text{RWT} \quad h2 := \text{DFW} + \text{WHT} \quad \text{comm} := \text{DEW} + \text{WLT} \quad w := \frac{w1}{\text{comm}} \quad h := \frac{h2}{\text{comm}}$$

$$F_{abc1c2d2} := F12(w, h) \quad F_{abc1c2d2} = 0.131$$

VIEW FACTORS BETWEEN WINDOW AND CEILING

This view factor would have been equal to the one between the window and the floor, if the window is placed in the middle of the wall.

$$Ad := WLT \cdot DCW \quad Ad = 1.5m^2$$

$$Ac2 := DEW \cdot DCW \quad Ac2 = 1.25m^2$$

$$Ab = 6m^2 \quad A2 = 1.8m^2 \quad Ac1 = 1.5m^2 \quad Aa = 5m^2 \quad Aab = 11m^2$$

$$w1 := RWT \quad h2 := DCW + WHT \quad comm := WLT \quad w := \frac{w1}{comm} \quad h := \frac{h2}{comm}$$

$$Fb2d := F12(w, h) \quad Fb2d = 0.107$$

$$w1 := RWT \quad h2 := DCW \quad comm := WLT \quad w := \frac{w1}{comm} \quad h := \frac{h2}{comm}$$

$$Fbd := F12(w, h) \quad Fbd = 0.072$$

$$w1 := RWT \quad h2 := DCW \quad comm := DEW \quad w := \frac{w1}{comm} \quad h := \frac{h2}{comm}$$

$$Fac2 := F12(w, h) \quad Fac2 = 0.067$$

$$w1 := RWT \quad h2 := DCW + WHT \quad comm := DEW \quad w := \frac{w1}{comm} \quad h := \frac{h2}{comm}$$

$$Fac1c2 := F12(w, h) \quad Fac1c2 = 0.097$$

$$w1 := RWT \quad h2 := DCW + WHT \quad comm := DEW + WLT \quad w := \frac{w1}{comm} \quad h := \frac{h2}{comm}$$

$$Fabc1c2d2 := F12(w, h) \quad Fabc1c2d2 = 0.137$$

$$w1 := RWT \quad h2 := DCW \quad comm := DEW + WLT \quad w := \frac{w1}{comm} \quad h := \frac{h2}{comm}$$

$$Fabc2d := F12(w, h) \quad Fabc2d = 0.085$$

$$Fb2 := Fb2d - Fbd \quad Fb2 = 0.035 \quad F2b := \frac{Ab}{A2} \cdot Fb2$$

$$Fa2d := \frac{Aab \cdot Fabc1c2d2 - Aa \cdot Fac1c2 - Ab \cdot Fb2d}{2 \cdot Aa} \quad Fa2d = 0.038$$

$$Fad := \frac{Aab \cdot Fabc2d - Aa \cdot Fac2 - Ab \cdot Fbd}{2 \cdot Aa} \quad Fad = 0.017$$

$$Fa2 := Fa2d - Fad \quad Fa2 = 0.021 \quad F2a := \frac{Aa}{A2} \cdot Fa2 \quad F2a = 0.058$$

$$F_{0,3} := 2 \cdot F2a + F2b \quad F_{0,3} = 0.233405 \quad F_{3,0} := \frac{SA_0}{SA_3} \cdot F_{0,3} \quad F_{3,0} = 0.026258$$

VIEW FACTORS BETWEEN WINDOW AND RIGHT/LEFT WALLS

The view factors between the window and the left wall and between the window and the right wall will be equal because of symmetry.

PART CLOSE TO FLOOR

$$A_b := \text{WHT} \cdot \text{RWT} \quad A_b = 4.8 \text{m}^2$$

$$A_d := \text{WHT} \cdot \text{DEW} \quad A_d = 1.5 \text{m}^2$$

$$A_2 = 1.8 \text{m}^2$$

$$A_{c1} := \text{WLT} \cdot \text{DFW} \quad A_{c1} = 1.2 \text{m}^2$$

$$A_{c2} := \text{DEW} \cdot \text{DFW} \quad A_{c2} = 1 \text{m}^2$$

$$A_a := \text{DFW} \cdot \text{RWT} \quad A_a = 3.2 \text{m}^2$$

$$A_{ab} := A_a + A_b \quad A_{ab} = 8 \text{m}^2$$

$$w_1 := \text{RWT} \quad h_2 := \text{WLT} + \text{DEW} \quad \text{comm} := \text{WHT} \quad w := \frac{w_1}{\text{comm}} \quad h := \frac{h_2}{\text{comm}}$$

$$F_{b2d} := F_{12}(w, h) \quad F_{b2d} = 0.103$$

$$w_1 := \text{RWT} \quad h_2 := \text{DEW} \quad \text{comm} := \text{WHT} \quad w := \frac{w_1}{\text{comm}} \quad h := \frac{h_2}{\text{comm}}$$

$$F_{bd} := F_{12}(w, h) \quad F_{bd} = 0.075$$

$$w_1 := \text{RWT} \quad h_2 := \text{DEW} \quad \text{comm} := \text{DFW} \quad w := \frac{w_1}{\text{comm}} \quad h := \frac{h_2}{\text{comm}}$$

$$F_{ac2} := F_{12}(w, h) \quad F_{ac2} = 0.061$$

$$w_1 := \text{RWT} \quad h_2 := \text{DEW} + \text{WLT} \quad \text{comm} := \text{DFW} \quad w := \frac{w_1}{\text{comm}} \quad h := \frac{h_2}{\text{comm}}$$

$$F_{ac1c2} := F_{12}(w, h) \quad F_{ac1c2} = 0.081$$

$$w_1 := \text{RWT} \quad h_2 := \text{DEW} + \text{WLT} \quad \text{comm} := \text{DFW} + \text{WHT} \quad w := \frac{w_1}{\text{comm}} \quad h := \frac{h_2}{\text{comm}}$$

$$F_{abc1c2d2} := F_{12}(w, h) \quad F_{abc1c2d2} = 0.133$$

$$w_1 := \text{RWT} \quad h_2 := \text{DEW} \quad \text{comm} := \text{DFW} + \text{WHT} \quad w := \frac{w_1}{\text{comm}} \quad h := \frac{h_2}{\text{comm}}$$

$$F_{abc2d} := F_{12}(w, h) \quad F_{abc2d} = 0.09$$

$$F_{b2} := F_{b2d} - F_{bd} \quad F_{b2} = 0.028 \quad F_{2b1} := \frac{A_b}{A_2} \cdot F_{b2} \quad F_{2b1} = 0.075$$

$$F_{a2d} := \frac{A_{ab} \cdot F_{abc1c2d2} - A_a \cdot F_{ac1c2} - A_b \cdot F_{b2d}}{2 \cdot A_a} \quad F_{a2d} = 0.049$$

$$F_{ad} := \frac{A_{ab} \cdot F_{abc2d} - A_a \cdot F_{ac2} - A_b \cdot F_{bd}}{2 \cdot A_a} \quad F_{ad} = 0.026$$

$$F_{a2} := F_{a2d} - F_{ad} \quad F_{a2} = 0.022 \quad F_{2a1} := \frac{A_a}{A_2} \cdot F_{a2} \quad F_{2a1} = 0.039236$$

PART CLOSE TO CEILING

$$Ab = 4.8 \text{ m}^2 \quad Ad = 1.5 \text{ m}^2 \quad A2 = 1.8 \text{ m}^2$$

$$Ac1 := DCW \cdot WLT \quad Ac1 = 1.5 \text{ m}^2$$

$$Ac2 := DEW \cdot DCW \quad Ac2 = 1.25 \text{ m}^2$$

$$Aa := DCW \cdot RWT \quad Aa = 4 \text{ m}^2$$

$$Aab := Aa + Ab \quad Aab = 8.8 \text{ m}^2$$

$$w1 := RWT \quad h2 := DEW + WLT \quad comm := WHT \quad w := \frac{w1}{comm} \quad h := \frac{h2}{comm}$$

$$Fb2d := F12(w, h) \quad Fb2d = 0.103$$

$$w1 := RWT \quad h2 := DEW \quad comm := WHT \quad w := \frac{w1}{comm} \quad h := \frac{h2}{comm}$$

$$Fbd := F12(w, h) \quad Fbd = 0.075$$

$$w1 := RWT \quad h2 := DEW \quad comm := DCW \quad w := \frac{w1}{comm} \quad h := \frac{h2}{comm}$$

$$Fac2 := F12(w, h) \quad Fac2 = 0.069$$

$$w1 := RWT \quad h2 := DEW + WLT \quad comm := DCW \quad w := \frac{w1}{comm} \quad h := \frac{h2}{comm}$$

$$Fac1c2 := F12(w, h) \quad Fac1c2 = 0.093$$

$$w1 := RWT \quad h2 := DEW + WLT \quad comm := WHT + DCW \quad w := \frac{w1}{comm} \quad h := \frac{h2}{comm}$$

$$Fabc1c2d2 := F12(w, h) \quad Fabc1c2d2 = 0.139$$

$$w1 := RWT \quad h2 := DEW \quad comm := WHT + DCW \quad w := \frac{w1}{comm} \quad h := \frac{h2}{comm}$$

$$Fabc2d := F12(w, h) \quad Fabc2d = 0.093$$

$$Fb2 := Fb2d - Fbd \quad Fb2 = 0.028 \quad F2b2 := \frac{Ab}{A2} \cdot Fb2 \quad F2b2 = 0.075446$$

$$Fa2d := \frac{Aab \cdot Fabc1c2d2 - Aa \cdot Fac1c2 - Ab \cdot Fb2d}{2 \cdot Aa} \quad Fa2d = 0.045$$

$$Fad := \frac{Aab \cdot Fabc2d - Aa \cdot Fac2 - Ab \cdot Fbd}{2 \cdot Aa} \quad Fad = 0.024$$

$$Fa2 := Fa2d - Fad \quad Fa2 = 0.021 \quad F2a2 := \frac{Aa}{A2} \cdot Fa2 \quad F2a2 = 0.047$$

$$\text{So } F_{0,5} := F2b1 + F2a1 + F2a2 \quad F_{0,5} = 0.161275 \quad F_{5,0} := \frac{SA_0}{SA_5} \cdot F_{0,5} \quad F_{5,0} = 0.024191$$

$$\text{and } F_{0,6} := F_{0,5} \quad F_{6,0} := F_{5,0} \quad \text{Also } F_{0,1} := 0 \quad F_{1,0} := 0 \quad (\text{on the same wall})$$

VIEW FACTOR FROM WINDOW TO BACK WALL

The sum of the view factors between the window and all surfaces must be equal to one.

$$F_{0,4} := 1 - F_{0,1} - F_{0,2} - F_{0,3} - F_{0,4} - F_{0,5} - F_{0,6}$$

$$F_{0,4} = 0.185365 \quad \text{and} \quad F_{4,0} := \frac{SA_0}{SA_4} \cdot F_{0,4} \quad F_{4,0} = 0.027805$$

OTHER VIEW FACTORS

Now it remains to calculate the view factors between the wall containing the window and all the other surfaces. We calculate these view factors from the energy conservation equation. Since the sum of the view factors between a surface and all the others is equal to one, we have:

$$F_{i,2} = 1 - F_{i,1} - F_{i,3} - F_{i,4} - F_{i,5} - F_{i,6} - F_{i,7}$$

$$F_{0,1} := 0 \quad F_{1,1} := 0$$

$$F_{2,1} := 1 - F_{2,0} - F_{2,2} - F_{2,3} - F_{2,4} - F_{2,5} - F_{2,6}$$

$$F_{3,1} := 1 - F_{3,0} - F_{3,2} - F_{3,3} - F_{3,4} - F_{3,5} - F_{3,6}$$

$$F_{4,1} := 1 - F_{4,0} - F_{4,2} - F_{4,3} - F_{4,4} - F_{4,5} - F_{4,6}$$

$$F_{5,1} := 1 - F_{5,0} - F_{5,2} - F_{5,3} - F_{5,4} - F_{5,5} - F_{5,6}$$

$$F_{6,1} := 1 - F_{6,0} - F_{6,2} - F_{6,3} - F_{6,4} - F_{6,5} - F_{6,6}$$

$$F_{1,0} := 0 \quad F_{1,1} := 0 \quad F_{1,2} := \frac{SA_2}{SA_1} \cdot F_{2,1} \quad F_{1,3} := \frac{SA_3}{SA_1} \cdot F_{3,1} \quad F_{1,4} := \frac{SA_4}{SA_1} \cdot F_{4,1}$$

$$F_{1,5} := \begin{cases} v \leftarrow 0 & \text{if } SA_1 = 0 \\ v \leftarrow \frac{1 - F_{1,2} - F_{1,3} - F_{1,4}}{2} & \text{otherwise} \end{cases} \quad F_{1,6} := F_{1,5}$$

The calculated view factors in matrix form, are:

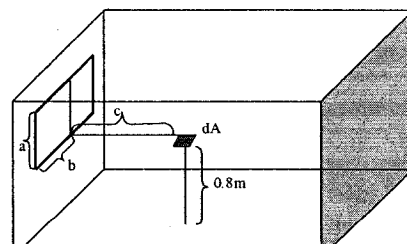
$$F = \begin{pmatrix} 0 & 0 & 0.258679 & 0.233405 & 0.185365 & 0.161275 & 0.161275 \\ 0 & 0 & 0.235632 & 0.240092 & 0.158847 & 0.182715 & 0.182715 \\ 0.029101 & 0.150215 & 0 & 0.282733 & 0.179317 & 0.179317 & 0.179317 \\ 0.026258 & 0.153059 & 0.282733 & 0 & 0.179317 & 0.179317 & 0.179317 \\ 0.027805 & 0.13502 & 0.239089 & 0.239089 & 0 & 0.179499 & 0.179499 \\ 0.024191 & 0.155307 & 0.239089 & 0.239089 & 0.179499 & 0 & 0.162824 \\ 0.024191 & 0.318132 & 0.239089 & 0.239089 & 0.179499 & 0 & 0 \end{pmatrix}$$

The sum of each row must be equal to one (energy conservation)

$$\sum_{i=0}^6 \sum_{j=0}^6 F_{i,j} = 7$$

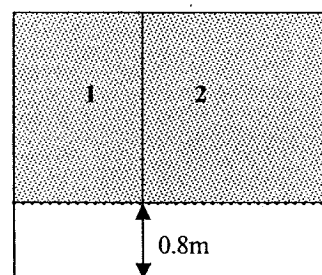
APPENDIX F

Detailed analytical calculation of configuration factors between representative points on the work plane surface in a rectangular room with one window (MathCad 2001i file).



Reference: C:\Thanos\PhD Thanos\Solar radiation model

This quicksheet calculates the configuration factors between the work plane and all the interior surfaces of the room. It also provides the necessary information from the view factors file reference.



3. CONFIGURATION FACTORS BETWEEN A,B,C AND BACK WALL

$$x := \frac{RLT}{2 \cdot m} \quad y := \frac{RHT - WPH}{m} \quad z := \frac{RWT}{m} - S_1 \quad f_{A_4} := 2 \cdot f(x, y, z) \quad f_{A_4} = 0.068$$

$$x = 2 \quad y = 2.2 \quad z := \frac{RWT}{m} - S_2 \quad f_{B_4} := 2 \cdot f(x, y, z) \quad f_{B_4} = 0.158$$

$$x = 2 \quad y = 2.2 \quad z := \frac{RWT}{m} - S_3 \quad f_{C_4} := 2 \cdot f(x, y, z) \quad f_{C_4} = 0.371$$

4. CONFIGURATION FACTORS BETWEEN A,B,C AND CEILING

Now dA is parallel to the surface, so we will use the equation:

$$g(x, y, z) := \frac{1}{2 \cdot \pi} \cdot \left[\left(\frac{y}{\sqrt{y^2 + z^2}} \right) \cdot \text{atan} \left(\frac{x}{\sqrt{y^2 + z^2}} \right) + \frac{x}{\sqrt{x^2 + z^2}} \cdot \text{atan} \left(\frac{y}{\sqrt{x^2 + z^2}} \right) \right]$$

$$x := S_1 \quad y := \frac{RLT}{2 \cdot m} \quad z := \frac{RHT - WPH}{m} \quad g_{A1} := g(x, y, z) \quad g_{A1} = 0.09$$

$$x := \frac{RWT}{m} - S_1 \quad g_{A2} := g(x, y, z) \quad g_{A2} = 0.145$$

$$f_{A_3} := 2 \cdot (g_{A1} + g_{A2}) \quad f_{A_3} = 0.472$$

$$x := S_2 \quad g_{B1} := g(x, y, z) \quad g_{B1} = 0.136$$

$$x := \frac{RWT}{m} - S_2 \quad g_{B2} := g(x, y, z) \quad g_{B2} = 0.115$$

$$f_{B_3} := 2 \cdot (g_{B1} + g_{B2}) \quad f_{B_3} = 0.502$$

$$x := S_3 \quad g_{C1} := g(x, y, z) \quad g_{C1} = 0.153$$

$$x := \frac{RWT}{m} - S_3 \quad g_{C2} := g(x, y, z) \quad g_{C2} = 0.043$$

$$f_{C_3} := 2 \cdot (g_{C1} + g_{C2}) \quad f_{C_3} = 0.394$$

Since dA does not see the floor (we are interested in horizontal illuminance coming from upwards), it is :

$$f_{A_2} := 0 \quad f_{B_2} := 0 \quad f_{C_2} := 0$$

It remains to calculate the configuration factors between the wall containing the window and points A,B,C. These will be again calculated from the energy conservation equation:

$$f_{A_1} := 1 - f_{A_0} - f_{A_2} - f_{A_3} - f_{A_4} - f_{A_5} - f_{A_6} \quad f_{A_1} = 0.143$$

$$f_{B_1} := 1 - f_{B_0} - f_{B_2} - f_{B_3} - f_{B_4} - f_{B_5} - f_{B_6} \quad f_{B_1} = 0.076$$

$$f_{C_1} := 1 - f_{C_0} - f_{C_2} - f_{C_3} - f_{C_4} - f_{C_5} - f_{C_6} \quad f_{C_1} = 0.037$$

The configuration factors between points A,B,C and all the interior surfaces are, respectively:

$$f_{A_i} = \begin{pmatrix} 0.088 \\ 0.143 \\ 0 \\ 0.472 \\ 0.068 \\ 0.115 \\ 0.115 \end{pmatrix} \quad f_{B_i} = \begin{pmatrix} 0.02 \\ 0.076 \\ 0 \\ 0.502 \\ 0.158 \\ 0.122 \\ 0.122 \end{pmatrix} \quad f_{C_i} = \begin{pmatrix} 6.976 \times 10^{-3} \\ 0.037 \\ 0 \\ 0.394 \\ 0.371 \\ 0.096 \\ 0.096 \end{pmatrix}$$

Energy conservation check:

$$\sum_{i=0}^6 f_{A_i} = 1 \quad \sum_{i=0}^6 f_{B_i} = 1 \quad \sum_{i=0}^6 f_{C_i} = 1$$

APPENDIX G

Calculation of hourly work plane illuminance using the radiosity method (MathCad 2001i file).

➤ Reference: C:\Thanos\PhD Thanos\Solar radiation models\THESIS files\View factors in a rectangular room.mcd

➤ Reference: C:\Thanos\PhD Thanos\Solar radiation models\THESIS files\Configuration factors in a room.mcd

➤ Reference: C:\Thanos\PhD Thanos\Solar radiation models\THESIS files\Perez illuminance model.mcd

This worksheet uses the radiosity method and the Jacobi solution method to calculate hourly work plane illuminance values. View factors, configuration factors and hourly incident beam and diffuse illuminance are read from the dynamic referenced programs above.

Transmitted daylight:

$$E_{btr}(n, t) := E_b(n, t) \cdot \tau_e(n, t) \quad \text{Beam}$$

$$E_{dtr}(n, t) := E_d(n, t) \cdot \tau_d \quad \text{Diffuse}$$

$$E_{tr}(n, t) := E_{btr}(n, t) + E_{dtr}(n, t) \quad \text{Total}$$

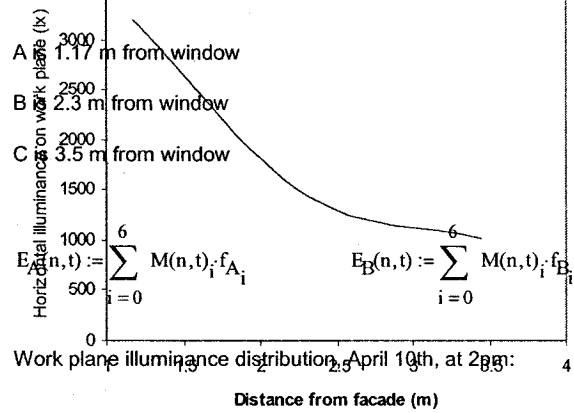
Matrix of initial luminous exitances:

$$M_O(n, t) := \begin{pmatrix} E_{tr}(n, t) \\ 0 \\ 0 \\ 0 \\ 0 \\ 0 \\ 0 \end{pmatrix} \quad M_O(1, 10) = \begin{pmatrix} 2.721 \times 10^4 \\ 0 \\ 0 \\ 0 \\ 0 \\ 0 \\ 0 \end{pmatrix} \text{ lx}$$

$I := \text{identity}(7)$... 7 x 7 identity matrix for delta Cronecker modelling for seven interior surfaces

$TT_{i,j} := \rho_i \cdot F_{i,j}$... form matrix

Work plane illuminance (assume 3 points or more on work plane)



APPENDIX H

Calculation of Daylight Availability Ratio (MathCad 2001i file).

Daylight Availability Ratio is calculated from the matrix of hourly illuminance values. Each value higher than 500 lux on the work plane contributes to DAR. The simulation is done on a monthly basis for reduction in computation time (significant when large matrices are processed). Monthly vectors of hourly illuminances are packed into matrices (columns are day numbers and rows are solar time). Then submatrices are extracted, to account only for working hours (from 9am to 5pm). Finally, an automated location function is used to find out which of the matrix elements are higher than 500 lux and then monthly Daylight Availability Ratio is calculated, together with the average Annual DAR. This is automatically done as a function of window-to-wall ratio and has to be re-calculated for each orientation. The impact of shading devices (if any) is modeled by modifying transmittance equations using schedule equations as a function of shading transmittance.

$$EJAN_t := E_C(1, t) \quad EFEB_t := E_C(45, t) \quad EMAR_t := E_C(75, t) \quad EAPR_t := E_C(105, t)$$

$$EMAY_t := E_C(135, t) \quad EJUN_t := E_C(165, t) \quad EJUL_t := E_C(195, t) \quad EAUG_t := E_C(225, t)$$

$$ESEP_t := E_C(255, t) \quad EOCT_t := E_C(285, t) \quad ENOV_t := E_C(315, t) \quad EDEC_t := E_C(345, t)$$

Pack vectors into arrays for DAR matrix operations:

$$pp := 24 \quad qq := 5$$

$$\text{Pack}(EJAN, pp, qq) := \begin{array}{l} \text{for } jj \in 0..qq-1 \\ \quad \text{for } ii \in 0..pp-1 \\ \quad \quad \left| \begin{array}{l} M_{ii,jj} \leftarrow EJAN_{ii+pp \cdot jj} \text{ if } ii+pp \cdot jj < \text{rows}(EJAN) \\ M_{ii,jj} \leftarrow 0 \text{ otherwise} \end{array} \right. \\ \quad \quad M \end{array}$$

$$\text{Pack}(EFEB, pp, qq) := \begin{array}{l} \text{for } jj \in 0..qq-1 \\ \quad \text{for } ii \in 0..pp-1 \\ \quad \quad \left| \begin{array}{l} M_{ii,jj} \leftarrow EFEB_{ii+pp \cdot jj} \text{ if } ii+pp \cdot jj < \text{rows}(EFEB) \\ M_{ii,jj} \leftarrow 0 \text{ otherwise} \end{array} \right. \\ \quad \quad M \end{array}$$

Pack (EMAR , pp , qq) :=

	for jj \in 0.. qq - 1						
	for ii \in 0.. pp - 1						
	<table border="0"> <tr> <td style="border-right: 1px solid black; padding-right: 10px;"></td> <td>$M_{ii,jj} \leftarrow \text{EMAR}_{ii+pp \cdot jj}$</td> <td>if ii + pp \cdot jj < rows (EMAR)</td> </tr> <tr> <td style="border-right: 1px solid black; padding-right: 10px;"></td> <td>$M_{ii,jj} \leftarrow 0$</td> <td>otherwise</td> </tr> </table>		$M_{ii,jj} \leftarrow \text{EMAR}_{ii+pp \cdot jj}$	if ii + pp \cdot jj < rows (EMAR)		$M_{ii,jj} \leftarrow 0$	otherwise
	$M_{ii,jj} \leftarrow \text{EMAR}_{ii+pp \cdot jj}$	if ii + pp \cdot jj < rows (EMAR)					
	$M_{ii,jj} \leftarrow 0$	otherwise					
	M						

Pack (EAPR , pp , qq) :=

	for jj \in 0.. qq - 1						
	for ii \in 0.. pp - 1						
	<table border="0"> <tr> <td style="border-right: 1px solid black; padding-right: 10px;"></td> <td>$M_{ii,jj} \leftarrow \text{EAPR}_{ii+pp \cdot jj}$</td> <td>if ii + pp \cdot jj < rows (EAPR)</td> </tr> <tr> <td style="border-right: 1px solid black; padding-right: 10px;"></td> <td>$M_{ii,jj} \leftarrow 0$</td> <td>otherwise</td> </tr> </table>		$M_{ii,jj} \leftarrow \text{EAPR}_{ii+pp \cdot jj}$	if ii + pp \cdot jj < rows (EAPR)		$M_{ii,jj} \leftarrow 0$	otherwise
	$M_{ii,jj} \leftarrow \text{EAPR}_{ii+pp \cdot jj}$	if ii + pp \cdot jj < rows (EAPR)					
	$M_{ii,jj} \leftarrow 0$	otherwise					
	M						

Pack (EMAY , pp , qq) :=

	for jj \in 0.. qq - 1						
	for ii \in 0.. pp - 1						
	<table border="0"> <tr> <td style="border-right: 1px solid black; padding-right: 10px;"></td> <td>$M_{ii,jj} \leftarrow \text{EMAY}_{ii+pp \cdot jj}$</td> <td>if ii + pp \cdot jj < rows (EMAY)</td> </tr> <tr> <td style="border-right: 1px solid black; padding-right: 10px;"></td> <td>$M_{ii,jj} \leftarrow 0$</td> <td>otherwise</td> </tr> </table>		$M_{ii,jj} \leftarrow \text{EMAY}_{ii+pp \cdot jj}$	if ii + pp \cdot jj < rows (EMAY)		$M_{ii,jj} \leftarrow 0$	otherwise
	$M_{ii,jj} \leftarrow \text{EMAY}_{ii+pp \cdot jj}$	if ii + pp \cdot jj < rows (EMAY)					
	$M_{ii,jj} \leftarrow 0$	otherwise					
	M						

Pack (EJUN , pp , qq) :=

	for jj \in 0.. qq - 1						
	for ii \in 0.. pp - 1						
	<table border="0"> <tr> <td style="border-right: 1px solid black; padding-right: 10px;"></td> <td>$M_{ii,jj} \leftarrow \text{EJUN}_{ii+pp \cdot jj}$</td> <td>if ii + pp \cdot jj < rows (EJUN)</td> </tr> <tr> <td style="border-right: 1px solid black; padding-right: 10px;"></td> <td>$M_{ii,jj} \leftarrow 0$</td> <td>otherwise</td> </tr> </table>		$M_{ii,jj} \leftarrow \text{EJUN}_{ii+pp \cdot jj}$	if ii + pp \cdot jj < rows (EJUN)		$M_{ii,jj} \leftarrow 0$	otherwise
	$M_{ii,jj} \leftarrow \text{EJUN}_{ii+pp \cdot jj}$	if ii + pp \cdot jj < rows (EJUN)					
	$M_{ii,jj} \leftarrow 0$	otherwise					
	M						

Pack (EJUL , pp , qq) :=

	for jj \in 0.. qq - 1						
	for ii \in 0.. pp - 1						
	<table border="0"> <tr> <td style="border-right: 1px solid black; padding-right: 10px;"></td> <td>$M_{ii,jj} \leftarrow \text{EJUL}_{ii+pp \cdot jj}$</td> <td>if ii + pp \cdot jj < rows (EJUL)</td> </tr> <tr> <td style="border-right: 1px solid black; padding-right: 10px;"></td> <td>$M_{ii,jj} \leftarrow 0$</td> <td>otherwise</td> </tr> </table>		$M_{ii,jj} \leftarrow \text{EJUL}_{ii+pp \cdot jj}$	if ii + pp \cdot jj < rows (EJUL)		$M_{ii,jj} \leftarrow 0$	otherwise
	$M_{ii,jj} \leftarrow \text{EJUL}_{ii+pp \cdot jj}$	if ii + pp \cdot jj < rows (EJUL)					
	$M_{ii,jj} \leftarrow 0$	otherwise					
	M						

Pack (EAUG , pp , qq) :=

	for jj \in 0.. qq - 1						
	for ii \in 0.. pp - 1						
	<table border="0"> <tr> <td style="border-right: 1px solid black; padding-right: 10px;"></td> <td>$M_{ii,jj} \leftarrow \text{EAUG}_{ii+pp \cdot jj}$</td> <td>if ii + pp \cdot jj < rows (EAUG)</td> </tr> <tr> <td style="border-right: 1px solid black; padding-right: 10px;"></td> <td>$M_{ii,jj} \leftarrow 0$</td> <td>otherwise</td> </tr> </table>		$M_{ii,jj} \leftarrow \text{EAUG}_{ii+pp \cdot jj}$	if ii + pp \cdot jj < rows (EAUG)		$M_{ii,jj} \leftarrow 0$	otherwise
	$M_{ii,jj} \leftarrow \text{EAUG}_{ii+pp \cdot jj}$	if ii + pp \cdot jj < rows (EAUG)					
	$M_{ii,jj} \leftarrow 0$	otherwise					
	M						

```

Pack(ESEP,pp,qq) :=
  for jj ∈ 0..qq - 1
    for ii ∈ 0..pp - 1
      Mii,jj ← ESEPii+pp·jj if ii + pp·jj < rows(ESEP)
      Mii,jj ← 0 otherwise
  M

```

```

Pack(EOCT,pp,qq) :=
  for jj ∈ 0..qq - 1
    for ii ∈ 0..pp - 1
      Mii,jj ← EOCTii+pp·jj if ii + pp·jj < rows(EOCT)
      Mii,jj ← 0 otherwise
  M

```

```

Pack(ENOV,pp,qq) :=
  for jj ∈ 0..qq - 1
    for ii ∈ 0..pp - 1
      Mii,jj ← ENOVii+pp·jj if ii + pp·jj < rows(ENOV)
      Mii,jj ← 0 otherwise
  M

```

```

Pack(EDEC,pp,qq) :=
  for jj ∈ 0..qq - 1
    for ii ∈ 0..pp - 1
      Mii,jj ← EDECii+pp·jj if ii + pp·jj < rows(EDEC)
      Mii,jj ← 0 otherwise
  M

```

Monthly matrices of hourly work plane illuminance:

WPIJAN := Pack(EJAN,pp,qq)	WPIFEB := Pack(EFEB,pp,qq)	WPIMAR := Pack(EMAR,pp,qq)
WPIAPR := Pack(EAPR,pp,qq)	WPIMAY := Pack(EMAY,pp,qq)	WPIJUN := Pack(EJUN,pp,qq)
WPIJUL := Pack(EJUL,pp,qq)	WPIAUG := Pack(EAUG,pp,qq)	WPISEP := Pack(ESEP,pp,qq)
WPIOCT := Pack(EOCT,pp,qq)	WPINOV := Pack(ENOV,pp,qq)	WPIDEC := Pack(EDEC,pp,qq)

Extract information for working hours only (9am-5pm) using the submatrix function:

WHJAN := submatrix(WPIJAN,9,16,0,4) WHFEB := submatrix(WPIFEB,9,16,0,4) WHMAR := submatrix(WPIMAR,9,16,0,4)
 WHAPR := submatrix(WPIAPR,9,16,0,4) WHMAY := submatrix(WPIMAY,9,16,0,4) WHJUN := submatrix(WPIJUN,9,16,0,4)
 WHJUL := submatrix(WPIJUL,9,16,0,4) WHAUG := submatrix(WPIAUG,9,16,0,4) WHSEP := submatrix(WPISEP,9,16,0,4)
 WHOCT := submatrix(WPIOCT,9,16,0,4) WHNOV := submatrix(WPINOV,9,16,0,4) WHDEC := submatrix(WPIDEC,9,16,0,4)

Automatic location of elements that contribute to DAR:

Condition the elements must match:

$c(e_l) := e_l > 500\text{lx}$ Target illuminance is set to 500lx.

Automatic calculation of elements greater than setpoint:

Locate(WHJAN,c) := $\left| \begin{array}{l} i \leftarrow 0 \\ L \leftarrow 0 \\ \text{for } m \in 0.. \text{rows}(\text{WHJAN}) - 1 \\ \quad \text{for } n \in 0.. \text{cols}(\text{WHJAN}) - 1 \\ \quad \quad \text{if } c(\text{WHJAN}_{m,n}) = 1 \\ \quad \quad \quad \left| L \leftarrow \begin{pmatrix} m \\ n \end{pmatrix} \\ \quad \quad \quad i \leftarrow i + 1 \end{array} \right. \\ L$

Locate(WHFEB,c) := $\left| \begin{array}{l} i \leftarrow 0 \\ L \leftarrow 0 \\ \text{for } m \in 0.. \text{rows}(\text{WHFEB}) - 1 \\ \quad \text{for } n \in 0.. \text{cols}(\text{WHFEB}) - 1 \\ \quad \quad \text{if } c(\text{WHFEB}_{m,n}) = 1 \\ \quad \quad \quad \left| L \leftarrow \begin{pmatrix} m \\ n \end{pmatrix} \\ \quad \quad \quad i \leftarrow i + 1 \end{array} \right. \\ L$

Locate(WHMAR,c) := $\left| \begin{array}{l} i \leftarrow 0 \\ L \leftarrow 0 \\ \text{for } m \in 0.. \text{rows}(\text{WHMAR}) - 1 \\ \quad \text{for } n \in 0.. \text{cols}(\text{WHMAR}) - 1 \\ \quad \quad \text{if } c(\text{WHMAR}_{m,n}) = 1 \\ \quad \quad \quad \left| L \leftarrow \begin{pmatrix} m \\ n \end{pmatrix} \\ \quad \quad \quad i \leftarrow i + 1 \end{array} \right. \\ L$

Locate(WHAPR,c) := $\left| \begin{array}{l} i \leftarrow 0 \\ L \leftarrow 0 \\ \text{for } m \in 0.. \text{rows}(\text{WHAPR}) - 1 \\ \quad \text{for } n \in 0.. \text{cols}(\text{WHAPR}) - 1 \\ \quad \quad \text{if } c(\text{WHAPR}_{m,n}) = 1 \\ \quad \quad \quad \left| L \leftarrow \begin{pmatrix} m \\ n \end{pmatrix} \\ \quad \quad \quad i \leftarrow i + 1 \end{array} \right. \\ L$

Locate(WHMAY,c) := $\left| \begin{array}{l} i \leftarrow 0 \\ L \leftarrow 0 \\ \text{for } m \in 0.. \text{rows}(\text{WHMAY}) - 1 \\ \quad \text{for } n \in 0.. \text{cols}(\text{WHMAY}) - 1 \\ \quad \quad \text{if } c(\text{WHMAY}_{m,n}) = 1 \\ \quad \quad \quad \left| L \leftarrow \begin{pmatrix} m \\ n \end{pmatrix} \\ \quad \quad \quad i \leftarrow i + 1 \end{array} \right. \\ L$

Locate(WHJUN,c) := $\left| \begin{array}{l} i \leftarrow 0 \\ L \leftarrow 0 \\ \text{for } m \in 0.. \text{rows}(\text{WHJUN}) - 1 \\ \quad \text{for } n \in 0.. \text{cols}(\text{WHJUN}) - 1 \\ \quad \quad \text{if } c(\text{WHJUN}_{m,n}) = 1 \\ \quad \quad \quad \left| L \leftarrow \begin{pmatrix} m \\ n \end{pmatrix} \\ \quad \quad \quad i \leftarrow i + 1 \end{array} \right. \\ L$

```

Locate(WHJUL,c) := | i ← 0
                   | L ← 0
                   | for m ∈ 0..rows(WHJUL) - 1
                   |   for n ∈ 0..cols(WHJUL) - 1
                   |     if c(WHJULm,n) = 1
                   |       | L⟨p⟩ ←  $\binom{m}{n}$ 
                   |       | i ← i + 1
                   | L

```

```

Locate(WHAUG,c) := | i ← 0
                   | L ← 0
                   | for m ∈ 0..rows(WHAUG) - 1
                   |   for n ∈ 0..cols(WHAUG) - 1
                   |     if c(WHAUGm,n) = 1
                   |       | L⟨p⟩ ←  $\binom{m}{n}$ 
                   |       | i ← i + 1
                   | L

```

```

Locate(WHSEP,c) := | i ← 0
                   | L ← 0
                   | for m ∈ 0..rows(WHSEP) - 1
                   |   for n ∈ 0..cols(WHSEP) - 1
                   |     if c(WHSEPm,n) = 1
                   |       | L⟨p⟩ ←  $\binom{m}{n}$ 
                   |       | i ← i + 1
                   | L

```

```

Locate(WHOCT,c) := | i ← 0
                   | L ← 0
                   | for m ∈ 0..rows(WHOCT) - 1
                   |   for n ∈ 0..cols(WHOCT) - 1
                   |     if c(WHOCTm,n) = 1
                   |       | L⟨p⟩ ←  $\binom{m}{n}$ 
                   |       | i ← i + 1
                   | L

```

```

Locate(WHNOV,c) := | i ← 0
                   | L ← 0
                   | for m ∈ 0..rows(WHNOV) - 1
                   |   for n ∈ 0..cols(WHNOV) - 1
                   |     if c(WHNOVm,n) = 1
                   |       | L⟨p⟩ ←  $\binom{m}{n}$ 
                   |       | i ← i + 1
                   | L

```

```

Locate(WHDEC,c) := | i ← 0
                   | L ← 0
                   | for m ∈ 0..rows(WHDEC) - 1
                   |   for n ∈ 0..cols(WHDEC) - 1
                   |     if c(WHDECm,n) = 1
                   |       | L⟨p⟩ ←  $\binom{m}{n}$ 
                   |       | i ← i + 1
                   | L

```

LJAN := Locate(WHJAN,c)	LFEB := Locate(WHFEB,c)	LMAR := Locate(WHMAR,c)	LAPR := Locate(WHAPR,c)
LMAY := Locate(WHMAY,c)	LJUN := Locate(WHJUN,c)	LJUL := Locate(WHJUL,c)	LAUG := Locate(WHAUG,c)
LSEP := Locate(WHSEP,c)	LOCT := Locate(WHOCT,c)	LNOV := Locate(WHNOV,c)	LDEC := Locate(WHDEC,c)

DAYLIGHT AVAILABILITY RATIO:

$$\text{DARJAN} := \frac{\text{cols (LJAN)}}{40} \quad \text{DARJAN} = 0.45$$

$$\text{DARFEB} := \frac{\text{cols (LFEB)}}{40} \quad \text{DARFEB} = 0.425$$

$$\text{DARMAR} := \frac{\text{cols (LMAR)}}{40} \quad \text{DARMAR} = 0.55$$

$$\text{DARAPR} := \frac{\text{cols (LAPR)}}{40} \quad \text{DARAPR} = 0.575$$

$$\text{DARMAY} := \frac{\text{cols (LMAY)}}{40} \quad \text{DARMAY} = 0.6$$

$$\text{DARJUN} := \frac{\text{cols (LJUN)}}{40} \quad \text{DARJUN} = 0.575$$

$$\text{DARJUL} := \frac{\text{cols (LJUL)}}{40} \quad \text{DARJUL} = 0.7$$

$$\text{DARAUG} := \frac{\text{cols (LAUG)}}{40} \quad \text{DARAUG} = 0.675$$

$$\text{DARSEP} := \frac{\text{cols (LSEP)}}{40} \quad \text{DARSEP} = 0.65$$

$$\text{DAROCT} := \frac{\text{cols (LOCT)}}{40} \quad \text{DAROCT} = 0.575$$

$$\text{DARNOV} := \frac{\text{cols (LNOV)}}{40} \quad \text{DARNOV} = 0.375$$

$$\text{DARDEC} := \frac{\text{cols (LDEC)}}{40} \quad \text{DARDEC} = 0.275$$

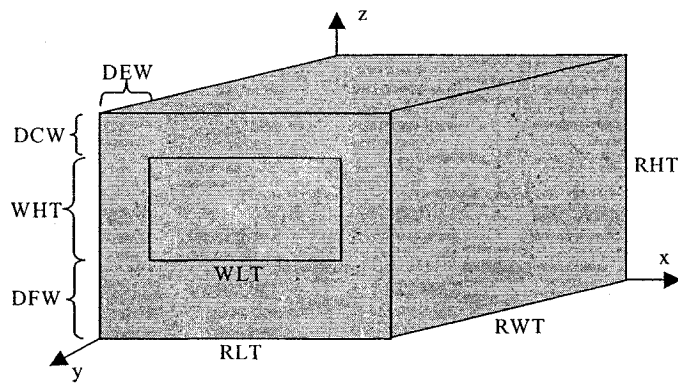
ANNUAL AVERAGE DAR:

$$\text{DAR}_{\text{annual}} := \frac{\text{DARJAN} + \text{DARFEB} + \text{DARMAR} + \text{DARAPR} + \text{DARMAY} + \text{DARJUN} + \text{DARJUL} + \dots + \text{DARAUG} + \text{DARSEP} + \text{DAROCT} + \text{DARNOV} + \text{DARDEC}}{12}$$

$$\text{DAR}_{\text{annual}} = 0.535$$

APPENDIX I

Coupled thermal simulation using a thermal network approach and solution using an explicit finite difference method (MathCad 2001I file).



Walls net areas:

Interior vertical walls: $A_v := 2 \cdot (RWT \cdot RHT) + RHT \cdot RLT + RLT \cdot RHT - A_w$

Ceiling: $A_c := RWT \cdot RLT$

if considered one, add areas

$$A_v := A_v + A_c$$

Floor: $A_f := A_c$

Exterior wall: $A_{ex} := RLT \cdot RHT - A_w$

Infiltration conductance:

$H_i := 2.8 \cdot m$ internal height $Vol := A_f \cdot H_i$ room volume $degC \equiv 1$

$ach := 0.4$ $ach = \text{air changes /hour}$

$c_{pair} \equiv 1000 \cdot \frac{\text{joule}}{\text{kg} \cdot \text{degC}}$ $\rho_{air} \equiv 1.2 \cdot \frac{\text{kg}}{\text{m}^3}$..specific heat and density of air

$U_{inf} := \frac{ach \cdot Vol}{3600 \cdot \text{sec}} \cdot \rho_{air} \cdot c_{pair}$ $U_{inf} = 5.973 \frac{W}{\text{degC}}$ $R_{inf} := \frac{1}{U_{inf}}$

Thermal properties:

Window

Double-glazed window with low-e coating:

$$R_w = \frac{1}{h_{wo}} + \frac{1}{h_{wr} + h_{wc}} + \frac{1}{h_{wi}} \quad h_{wi} := 2 \cdot \frac{W}{m^2 \cdot \text{degC}}$$

The heat transfers coefficients are calculated below as a function of temperatures.

Door

$$R_d := 1m^2 \cdot \frac{\text{degC}}{\text{watt}} \quad R_{door} := \frac{R_d}{A_d}$$

Floor

Concrete blocks: $L_f := 0.05 \cdot \text{m}$ $k_f := 1.7 \cdot \frac{\text{watt}}{\text{m} \cdot \text{degC}}$ $\rho_f := 2200 \cdot \frac{\text{kg}}{\text{m}^3}$

Insulation & plywood: $R_{\text{insf}} := 0.5 \cdot \text{m}^2 \cdot \frac{\text{degC}}{\text{watt}}$ $c_f := 1400 \cdot \frac{\text{joule}}{\text{kg} \cdot \text{degC}}$

$$R_f := \frac{L_f}{k_f} \quad R_f = 0.029 \cdot \text{m}^2 \cdot \frac{\text{degC}}{\text{watt}} \quad R_f := \frac{R_f}{A_f} \quad R_{\text{insf}} := \frac{R_{\text{insf}}}{A_f}$$
$$C_f := c_f \cdot \rho_f \cdot A_f \cdot L_f \quad C_f = 2.464 \times 10^6 \text{ J} \quad \dots \text{ floor thermal capacitance}$$

Interior vertical walls

Gypsum board $L_v := 0.013 \cdot \text{m}$ $\rho_v := 800 \cdot \frac{\text{kg}}{\text{m}^3}$ $k_v := 0.16 \cdot \frac{\text{watt}}{\text{m} \cdot \text{degC}}$ $c_v := 750 \cdot \frac{\text{joule}}{\text{kg} \cdot \text{degC}}$

Siding + sheathing $R_{\text{sidv}} := 0.37 \cdot \text{m}^2 \cdot \frac{\text{degC}}{\text{watt}}$

$$R_v := \frac{L_v}{k_v} \quad R_v = 0.081 \cdot \frac{\text{m}^2}{\text{degC} \cdot \text{W}} \quad R_v := \frac{R_v}{A_v} \quad R_{\text{sidv}} := \frac{R_{\text{sidv}}}{A_v}$$
$$C_v := c_v \cdot \rho_v \cdot A_v \cdot L_v \quad C_v = 4.711 \times 10^5 \text{ J} \quad \dots \text{ interior walls thermal capacitance}$$

Ceiling (if different from walls)

Gypsum board $L_c := L_v$ $k_c := k_v$ $c_c := c_v$ $\rho_c := \rho_v$

Insulation+wood: $R_{\text{insec}} := 0.5 \cdot \text{m}^2 \cdot \frac{\text{degC}}{\text{watt}}$

$$R_c := \frac{L_c}{k_c} \quad R_{\text{insec}} := \frac{R_{\text{insec}}}{A_c}$$
$$C_c := c_c \cdot \rho_c \cdot A_c \cdot L_c \quad C_c = 1.248 \times 10^5 \text{ J} \quad \dots \text{ ceiling thermal capacitance}$$

Exterior wall

Gypsum board $L_{\text{gex}} := L_v$ $k_{\text{gex}} := k_v$ $c_{\text{gex}} := c_v$ $\rho_{\text{gex}} := \rho_v$

Insulation, Siding, sheathing $R_{\text{insex}} := 3 \cdot \text{m}^2 \cdot \frac{\text{degC}}{\text{watt}}$

Face brick: $L_{\text{ex}} := 0.10 \cdot \text{m}$ $k_{\text{ex}} := 1.3 \cdot \frac{\text{watt}}{\text{m} \cdot \text{degC}}$ $\rho_{\text{ex}} := 1800 \cdot \frac{\text{kg}}{\text{m}^3}$ $c_{\text{ex}} := 921 \cdot \frac{\text{joule}}{\text{kg} \cdot \text{degC}}$

$$R_{\text{gex}} := \frac{L_{\text{gex}}}{k_{\text{gex}}} \quad R_{\text{ex}} := \frac{L_{\text{ex}}}{k_{\text{ex}}}$$
$$R_{\text{gex}} := \frac{R_{\text{gex}}}{A_{\text{ex}}} \quad R_{\text{insex}} := \frac{R_{\text{insex}}}{A_{\text{ex}}} \quad R_{\text{ex}} := \frac{R_{\text{ex}}}{A_{\text{ex}}}$$
$$C_{\text{ex}} := c_{\text{ex}} \cdot \rho_{\text{ex}} \cdot A_{\text{ex}} \cdot L_{\text{ex}} \quad C_{\text{ex}} = 1.393 \times 10^6 \text{ J} \quad \dots \text{ exterior wall thermal capacitance}$$

Outdoor temperature:

Average monthly hourly temperatures for Montreal:

$$\begin{aligned} TT1_o(t) &:= T_o(15, t) & TT2_o(t) &:= T_o(45, t) & TT3_o(t) &:= T_o(75, t) & TT4_o(t) &:= T_o(105, t) \\ TT5_o(t) &:= T_o(135, t) & TT6_o(t) &:= T_o(165, t) & TT7_o(t) &:= T_o(195, t) & TT8_o(t) &:= T_o(225, t) \\ TT9_o(t) &:= T_o(255, t) & TT10_o(t) &:= T_o(285, t) & TT11_o(t) &:= T_o(315, t) & TT12_o(t) &:= T_o(345, t) \end{aligned}$$

Incident Solar radiation:

Beam incident:

$$\begin{aligned} I1_b(t) &:= I_b(15, t) & I2_b(t) &:= I_b(45, t) & I3_b(t) &:= I_b(75, t) & I4_b(t) &:= I_b(105, t) & I5_b(t) &:= I_b(135, t) & I6_b(t) &:= I_b(165, t) \\ I7_b(t) &:= I_b(195, t) & I8_b(t) &:= I_b(225, t) & I9_b(t) &:= I_b(255, t) & I10_b(t) &:= I_b(285, t) & I11_b(t) &:= I_b(315, t) & I12_b(t) &:= I_b(345, t) \end{aligned}$$

Diffuse incident:

$$\begin{aligned} I1_d(t) &:= I_d(15, t) & I2_d(t) &:= I_d(45, t) & I3_d(t) &:= I_d(75, t) & I4_d(t) &:= I_d(105, t) & I5_d(t) &:= I_d(135, t) & I6_d(t) &:= I_d(165, t) \\ I7_d(t) &:= I_d(195, t) & I8_d(t) &:= I_d(225, t) & I9_d(t) &:= I_d(255, t) & I10_d(t) &:= I_d(285, t) & I11_d(t) &:= I_d(315, t) & I12_d(t) &:= I_d(345, t) \end{aligned}$$

Total incident:

$$\begin{aligned} I1(t) &:= I1_b(t) + I1_d(t) & I2(t) &:= I2_b(t) + I2_d(t) & I3(t) &:= I3_b(t) + I3_d(t) & I4(t) &:= I4_b(t) + I4_d(t) \\ I5(t) &:= I5_b(t) + I5_d(t) & I6(t) &:= I6_b(t) + I6_d(t) & I7(t) &:= I7_b(t) + I7_d(t) & I8(t) &:= I8_b(t) + I8_d(t) \\ I9(t) &:= I9_b(t) + I9_d(t) & I10(t) &:= I10_b(t) + I10_d(t) & I11(t) &:= I11_b(t) + I11_d(t) & I12(t) &:= I12_b(t) + I12_d(t) \end{aligned}$$

Window transmittance:

Glass properties: $k_L := 0.04$..extinction coeff.*glazing thickness

$n_g := 1.53$..refractive index

Angle of refraction and component reflectivity:

$$\theta'(n, t) := \text{asin}\left(\frac{\sin(\theta(n, t))}{n_g}\right) \quad r(n, t) := \frac{1}{2} \left[\left(\frac{\sin(\theta(n, t) - \theta'(n, t))}{\sin(\theta(n, t) + \theta'(n, t))} \right)^2 + \left(\frac{\tan(\theta(n, t) - \theta'(n, t))}{\tan(\theta(n, t) + \theta'(n, t))} \right)^2 \right]$$

Beam transmittance, τ , reflectance, ρ_o and absorptance, α , of glazing:

$$a(n, t) := \exp \left[- \frac{kL}{\sqrt{1 - \left(\frac{\sin(\theta(n, t))}{n_g} \right)^2}} \right]$$

$$\tau(n, t) := \frac{(1 - r(n, t))^2 \cdot a(n, t)}{1 - (r(n, t))^2 \cdot (a(n, t))^2}$$

$$\rho_o(n, t) := r(n, t) + \frac{r(n, t) \cdot (1 - r(n, t))^2 \cdot (a(n, t))^2}{1 - (r(n, t))^2 \cdot (a(n, t))^2}$$

$$\alpha_s(n, t) := 1 - \tau(n, t) - \rho_o(n, t)$$

For double glazed windows:

$$\tau_e(n, t) := \frac{(\tau(n, t))^2}{1 - (\rho_o(n, t))^2} \quad \dots \text{effective beam transmittance}$$

$$\tau_d(t) := 0.5$$

$$\alpha_d(t) := 0.05$$

$$\alpha_i(n, t) := \alpha_s(n, t) \cdot \frac{\tau(n, t)}{1 - (\rho_o(n, t))^2} \quad \dots \text{interior glazing absorptance}$$

$$\alpha_o(n, t) := \alpha_s(n, t) + \alpha_s(n, t) \cdot \frac{\tau(n, t) \cdot \rho_o(n, t)}{1 - (\rho_o(n, t))^2} \quad \dots \text{exterior glazing absorptance}$$

$\tau_{1e}(t) := \tau_e(15, t)$	$\tau_{2e}(t) := \tau_e(45, t)$	$\tau_{3e}(t) := \tau_e(75, t)$	$\tau_{4e}(t) := \tau_e(105, t)$	$\tau_{5e}(t) := \tau_e(135, t)$	$\tau_{6e}(t) := \tau_e(165, t)$
$\tau_{7e}(t) := \tau_e(195, t)$	$\tau_{8e}(t) := \tau_e(225, t)$	$\tau_{9e}(t) := \tau_e(255, t)$	$\tau_{10e}(t) := \tau_e(285, t)$	$\tau_{11e}(t) := \tau_e(315, t)$	$\tau_{12e}(t) := \tau_e(345, t)$
$\alpha_{1i}(t) := \alpha_i(15, t)$	$\alpha_{2i}(t) := \alpha_i(45, t)$	$\alpha_{3i}(t) := \alpha_i(75, t)$	$\alpha_{4i}(t) := \alpha_i(105, t)$	$\alpha_{5i}(t) := \alpha_i(135, t)$	$\alpha_{6i}(t) := \alpha_i(165, t)$
$\alpha_{7i}(t) := \alpha_i(195, t)$	$\alpha_{8i}(t) := \alpha_i(225, t)$	$\alpha_{9i}(t) := \alpha_i(255, t)$	$\alpha_{10i}(t) := \alpha_i(285, t)$	$\alpha_{11i}(t) := \alpha_i(315, t)$	$\alpha_{12i}(t) := \alpha_i(345, t)$
$\alpha_{1o}(t) := \alpha_o(15, t)$	$\alpha_{2o}(t) := \alpha_o(45, t)$	$\alpha_{3o}(t) := \alpha_o(75, t)$	$\alpha_{4o}(t) := \alpha_o(105, t)$	$\alpha_{5o}(t) := \alpha_o(135, t)$	$\alpha_{6o}(t) := \alpha_o(165, t)$
$\alpha_{7o}(t) := \alpha_o(195, t)$	$\alpha_{8o}(t) := \alpha_o(225, t)$	$\alpha_{9o}(t) := \alpha_o(255, t)$	$\alpha_{10o}(t) := \alpha_o(285, t)$	$\alpha_{11o}(t) := \alpha_o(315, t)$	$\alpha_{12o}(t) := \alpha_o(345, t)$

$\tau_{sh} := 0.2$... roller shade transmittance

Transmitted solar radiation:

Beam:

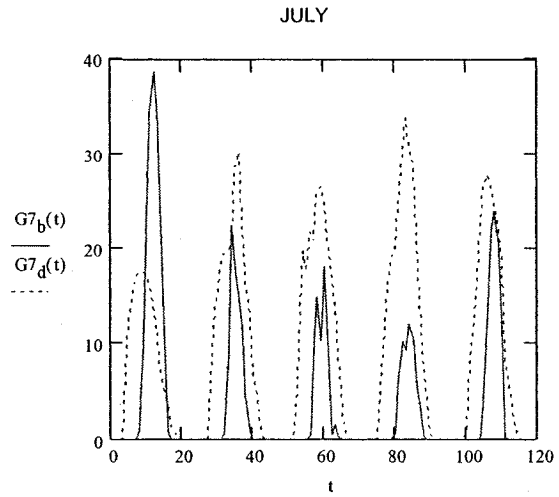
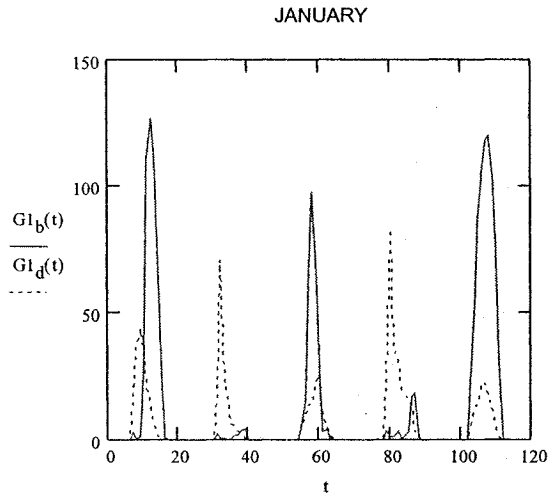
$$\begin{aligned} G1_b(t) &:= I1_b(t) \cdot \tau1_e(t) \cdot 0.2 & G2_b(t) &:= I2_b(t) \cdot \tau2_e(t) \cdot 0.2 & G3_b(t) &:= I3_b(t) \cdot \tau3_e(t) \cdot 0.2 & G4_b(t) &:= I4_b(t) \cdot \tau4_e(t) \cdot 0.2 \\ G5_b(t) &:= I5_b(t) \cdot \tau5_e(t) \cdot 0.2 & G6_b(t) &:= I6_b(t) \cdot \tau6_e(t) \cdot 0.2 & G7_b(t) &:= I7_b(t) \cdot \tau7_e(t) \cdot 0.2 & G8_b(t) &:= I8_b(t) \cdot \tau8_e(t) \cdot 0.2 \\ G9_b(t) &:= I9_b(t) \cdot \tau9_e(t) \cdot 0.2 & G10_b(t) &:= I10_b(t) \cdot \tau10_e(t) \cdot 0.2 & G11_b(t) &:= I11_b(t) \cdot \tau11_e(t) \cdot 0.2 & G12_b(t) &:= I12_b(t) \cdot \tau12_e(t) \cdot 0.2 \end{aligned}$$

Diffuse:

$$\begin{aligned} G1_d(t) &:= I1_d(t) \cdot \tau_d(t) \cdot 0.2 & G2_d(t) &:= I2_d(t) \cdot \tau_d(t) \cdot 0.2 & G3_d(t) &:= I3_d(t) \cdot \tau_d(t) \cdot 0.2 & G4_d(t) &:= I4_d(t) \cdot \tau_d(t) \cdot 0.2 \\ G5_d(t) &:= I5_d(t) \cdot \tau_d(t) \cdot 0.2 & G6_d(t) &:= I6_d(t) \cdot \tau_d(t) \cdot 0.2 & G7_d(t) &:= I7_d(t) \cdot \tau_d(t) \cdot 0.2 & G8_d(t) &:= I8_d(t) \cdot \tau_d(t) \cdot 0.2 \\ G9_d(t) &:= I9_d(t) \cdot \tau_d(t) \cdot 0.2 & G10_d(t) &:= I10_d(t) \cdot \tau_d(t) \cdot 0.2 & G11_d(t) &:= I11_d(t) \cdot \tau_d(t) \cdot 0.2 & G12_d(t) &:= I12_d(t) \cdot \tau_d(t) \cdot 0.2 \end{aligned}$$

Total:

$$\begin{aligned} G1(t) &:= G1_b(t) + G1_d(t) & G2(t) &:= G2_b(t) + G2_d(t) & G3(t) &:= G3_b(t) + G3_d(t) & G4(t) &:= G4_b(t) + G4_d(t) \\ G5(t) &:= G5_b(t) + G5_d(t) & G6(t) &:= G6_b(t) + G6_d(t) & G7(t) &:= G7_b(t) + G7_d(t) & G8(t) &:= G8_b(t) + G8_d(t) \\ G9(t) &:= G9_b(t) + G9_d(t) & G10(t) &:= G10_b(t) + G10_d(t) & G11(t) &:= G11_b(t) + G11_d(t) & G12(t) &:= G12_b(t) + G12_d(t) \end{aligned}$$



Absorbed solar radiation:

Absorbed by floor:

$$\begin{aligned} Sf1(t) &:= 0.7 \cdot G1(t) \cdot A_w & Sf2(t) &:= 0.7 \cdot G2(t) \cdot A_w & Sf3(t) &:= 0.7 \cdot G3(t) \cdot A_w & Sf4(t) &:= 0.7 \cdot G4(t) \cdot A_w \\ Sf5(t) &:= 0.7 \cdot G5(t) \cdot A_w & Sf6(t) &:= 0.7 \cdot G6(t) \cdot A_w & Sf7(t) &:= 0.7 \cdot G7(t) \cdot A_w & Sf8(t) &:= 0.7 \cdot G8(t) \cdot A_w \\ Sf9(t) &:= 0.7 \cdot G9(t) \cdot A_w & Sf10(t) &:= 0.7 \cdot G10(t) \cdot A_w & Sf11(t) &:= 0.7 \cdot G11(t) \cdot A_w & Sf12(t) &:= 0.7 \cdot G12(t) \cdot A_w \end{aligned}$$

Absorbed by walls:

$$\begin{aligned} Sv1(t) &:= 0.1 \cdot G1(t) \cdot A_w & Sv2(t) &:= 0.1 \cdot G2(t) \cdot A_w & Sv3(t) &:= 0.1 \cdot G3(t) \cdot A_w & Sv4(t) &:= 0.1 \cdot G4(t) \cdot A_w \\ Sv5(t) &:= 0.1 \cdot G5(t) \cdot A_w & Sv6(t) &:= 0.1 \cdot G6(t) \cdot A_w & Sv7(t) &:= 0.1 \cdot G7(t) \cdot A_w & Sv8(t) &:= 0.1 \cdot G8(t) \cdot A_w \\ Sv9(t) &:= 0.1 \cdot G9(t) \cdot A_w & Sv10(t) &:= 0.1 \cdot G10(t) \cdot A_w & Sv11(t) &:= 0.1 \cdot G11(t) \cdot A_w & Sv12(t) &:= 0.1 \cdot G12(t) \cdot A_w \end{aligned}$$

Absorbed by exterior wall (outside): $\alpha_{ex} := 0.6$...effective exterior wall absorptance (variable)

$$\begin{aligned} Sex1(t) &:= \alpha_{ex} \cdot I1(t) & Sex2(t) &:= \alpha_{ex} \cdot I2(t) & Sex3(t) &:= \alpha_{ex} \cdot I3(t) & Sex4(t) &:= \alpha_{ex} \cdot I4(t) \\ Sex5(t) &:= \alpha_{ex} \cdot I5(t) & Sex6(t) &:= \alpha_{ex} \cdot I6(t) & Sex7(t) &:= \alpha_{ex} \cdot I7(t) & Sex8(t) &:= \alpha_{ex} \cdot I8(t) \\ Sex9(t) &:= \alpha_{ex} \cdot I9(t) & Sex10(t) &:= \alpha_{ex} \cdot I10(t) & Sex11(t) &:= \alpha_{ex} \cdot I11(t) & Sex12(t) &:= \alpha_{ex} \cdot I12(t) \end{aligned}$$

Exterior heat transfer coefficient:

The *Energy Plus* approach is followed (DOE detailed convection model) which is a combination of the MoWitt and BLAST detailed convection models. The total exterior coefficient is the sum of the convective and the radiative coefficients. The convective coefficient is calculated as the sum of the natural and forced convective coefficients. In the detailed combined model, this is expressed as:

$$h_{c,glass} = \sqrt{h_n^2 + \left[a V_o^b \right]^2} \quad \text{for smooth (glass) surfaces and} \quad h_e = h_n + R_f (h_{c,glass} - h_n) \quad \text{for rough (wall) surfaces}$$

where h_n is the natural convection coefficient given by: $h_n = \frac{1.81 \cdot \sqrt[3]{\Delta T}}{1.382}$ for vertical surfaces and α and b are modifiers

equal to 2.5 and 0.75 respectively (on average) and V_o is the wind speed at standard conditions. R_f is a surface roughness coefficient approximately equal to 1.6 for brick/concrete.

$$R_f := 1.6 \quad \text{.. roughness coefficient for outside surface} \quad V_o := 10 \frac{\text{km}}{\text{hr}}$$

If T_{ex} is the temperature of the exterior wall, then the natural convection coefficient is equal to:
$$h_n = \frac{1.81 \sqrt[3]{T_{ex} - T_o}}{1.382}$$

and the total convective coefficient is given by:
$$h_{glass_{oc}} = \sqrt{h_n^2 + (2.5 V_o^{0.75})^2} \quad \text{and} \quad hex_{oc} = h_n + 1.6(h_{glass_{oc}} - h_n)$$

The radiative exterior coefficient is calculated from the temperature of the sky and the ground and the respective view factors. For simplicity, they can be assumed equal to the outdoor temperature.

$$h_{or} = 4 \cdot \sigma \cdot \epsilon \cdot T_m^3 \quad \text{where } T_m \text{ is the mean temperature in Kelvin:} \quad T_m = \frac{T_o + T_{ex}}{2} + 273$$

Then the exterior combined coefficient is equal to:
$$h_{glass_o} = h_{glass_{oc}} + h_{or} \quad \text{for windows and} \quad hex_o = hex_{oc} + h_{or} \quad \text{for walls}$$

Convection coefficients for internal surfaces:

The following correlation is used for interior convection for all cases:

$$h_{ci} = 1.31 \Delta T^{\frac{1}{3}} \quad \text{where } \Delta T \text{ is the temperature difference between the surface and air temperature.}$$

Radiation heat transfer between internal surfaces:

$$\sigma := 5.67051 \cdot 10^{-8} \frac{W}{m^2 \cdot K^4} \quad \dots \text{ Stefan-Boltzmann constant}$$

$$h_{r_{i,j}} = \frac{\sigma \cdot [(T_i)^4 - (T_j)^4] \cdot F_{\epsilon_{i,j}} \cdot F_{i,j}}{T_i - T_j} \quad \text{where } F_{\epsilon_{i,j}} \text{ is the emissivity factor and } F_{i,j} \text{ is the view factor between surfaces } i,j$$

View factors (pre-calculated):

$F_{wf} := 0.2231 \quad \dots \text{ window-to-floor}$

$F_{wv} := 1 - F_{wf} \quad \dots \text{ window-to-walls}$

$F_{fw} := \frac{A_w}{A_f} \cdot F_{wf} \quad \dots \text{ floor-to-window}$

$F_{fex} := 0.13 \quad \dots \text{ floor-to-exterior wall}$

$F_{fv} := 1 - F_{fw} - F_{fex} \quad \dots \text{ floor-to-walls}$

$F_{vw} := 0.213 \quad \dots \text{ walls-to-window}$

$F_{vex} := 0.489 \quad \dots \text{ walls-to-exterior wall}$

$F_{vf} := 1 - F_{vw} - F_{vex} \quad \dots \text{ walls-to-floor}$

$F_{exf} := 0.246 \quad \dots \text{ exterior wall-to-floor}$

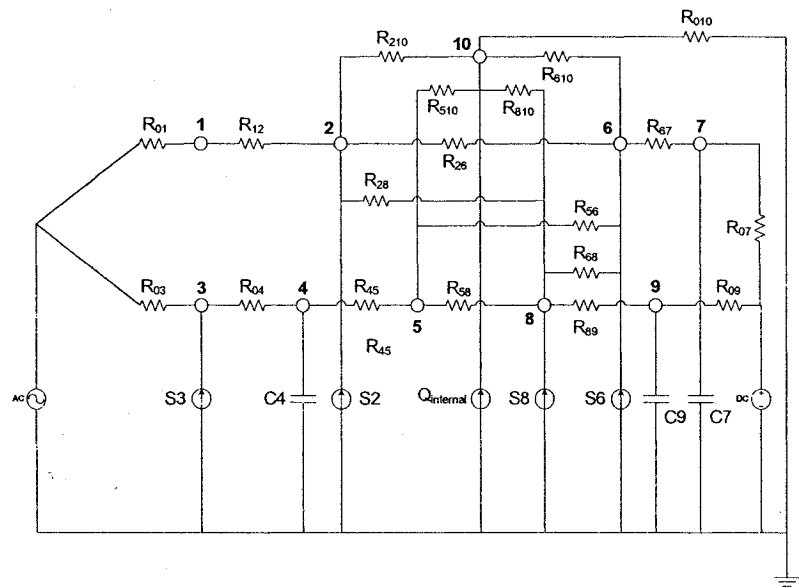
$F_{exv} := 1 - F_{exf} \quad \dots \text{ exterior wall-to-walls}$

Emmissivity factors:

$$F_{\epsilon} := \frac{1}{\frac{1}{0.9} + \frac{1}{0.9} - 1} \quad F_{\epsilon} = 0.818$$

$\epsilon_w := 0.9 \quad \dots \text{ emissivity of window internal surface}$

$\alpha_{ex} := 0.7 \quad \dots \text{ effective exterior wall absorptance}$



CALCULATION OF CONVECTIVE AND RADIATIVE COEFFICIENTS- initial values

Exterior heat transfer coefficient for window surface:

$$h_{ow_0} := \left[\left[\left(\frac{1.81 \cdot \sqrt[3]{T1_0 - TT1_0(1)}}{1.382} \right)^2 + (2.5 \cdot V_o^{0.75})^2 \right] \cdot \frac{W}{m^2 \cdot K} + 4 \cdot \epsilon_w \cdot \sigma \cdot \left[\left(\frac{TT1_0(1) + T1_0}{2} + 273 \right) \cdot K \right]^3 \right] \cdot \frac{K}{degC} \quad h_{ow_0} = 18.504 \frac{W}{m^2 \cdot degC}$$

Exterior heat transfer coefficient for wall surface:

$$h_{oex_0} := \left[\left[\frac{1.81 \cdot \sqrt[3]{T1_0 - TT1_0(1)}}{1.382} + 1.6 \cdot \left[\left(\frac{1.81 \cdot \sqrt[3]{T1_0 - TT1_0(1)}}{1.382} \right)^2 + (2.5 \cdot V_o^{0.75})^2 \right] - \frac{1.81 \cdot \sqrt[3]{T1_0 - TT1_0(1)}}{1.382} \right] \cdot \frac{W}{m^2 \cdot K} + 4 \cdot \epsilon_w \cdot \sigma \cdot \left[\left(\frac{TT3_0(1) + T1_0}{2} + 273 \right) \cdot K \right]^3 \right] \cdot \frac{K}{degC}$$

$$h_{oex_0} = 25.633 \frac{W}{m^2 \cdot degC}$$

Interior convection:

Between window and air:
$$h_{cwa_0} := 1.31 \cdot \left(|T2_0 - T10_0| \right)^{\frac{1}{3}} \cdot \frac{W \cdot degC^{\frac{-4}{3}}}{m^2}$$

Between floor and air:
$$h_{cfa_0} := 1.31 \cdot \left(|T6_0 - T10_0| \right)^{\frac{1}{3}} \cdot \frac{W \cdot degC^{\frac{-4}{3}}}{m^2}$$

Between walls and air:
$$h_{cva_0} := 1.31 \cdot \left(|T8_0 - T10_0| \right)^{\frac{1}{3}} \cdot \frac{W \cdot degC^{\frac{-4}{3}}}{m^2}$$

Between exterior wall and air:
$$h_{cexa_0} := 1.31 \cdot \left(|T5_0 - T10_0| \right)^{\frac{1}{3}} \cdot \frac{W \cdot degC^{\frac{-4}{3}}}{m^2}$$

Network resistances:

Between window-outside: $R_{ow0} := \frac{1}{h_{ow0} \cdot A_w}$ $R_{ow0} = 0.015 \frac{\text{degC}}{W}$

Between wall-outside: $R_{oex0} := \frac{1}{h_{oex0} \cdot A_{ex}}$

Between floor-basement: $R_{bf} := \frac{1}{2 \cdot A_f \cdot \frac{W}{m^2 \cdot \text{degC}}}$ $R_{bf} = 0.031 \frac{\text{degC}}{W}$

Between walls-adjacent rooms: $R_{vb} := R_{bf}$

Convective:

Between exterior wall and air: $R_{exa0} := \frac{1}{h_{cexa0} \cdot A_{ex}}$

Between floor and air: $R_{fa0} := \frac{1}{h_{cfa0} \cdot A_f}$

Between window and air: $R_{wa0} := \frac{1}{h_{cwa0} \cdot A_w}$

Between walls and air: $R_{va0} := \frac{1}{h_{cva0} \cdot A_v}$

Radiative:

Between window and floor: $R_{wfo} := \frac{1}{h_{rwo} \cdot A_w}$

Between window and walls: $R_{wvo} := \frac{1}{h_{rwo} \cdot A_w}$

Between floor and walls: $R_{fvo} := \frac{1}{h_{rfv} \cdot A_f}$

Between exterior wall and floor: $R_{exfo} := \frac{1}{h_{refo} \cdot A_{ex}}$

Between exterior wall and other walls: $R_{exvo} := \frac{1}{h_{rexv} \cdot A_{ex}}$

Window resistance: $R_{w0} := \frac{1}{h_{ow0} \cdot A_w} + \frac{1}{(h_{wi} + h_{rw0}) \cdot A_w} + \frac{1}{h_{cwa0} \cdot A_w}$ $R_{w0} = 0.163 \frac{\text{degC}}{W}$

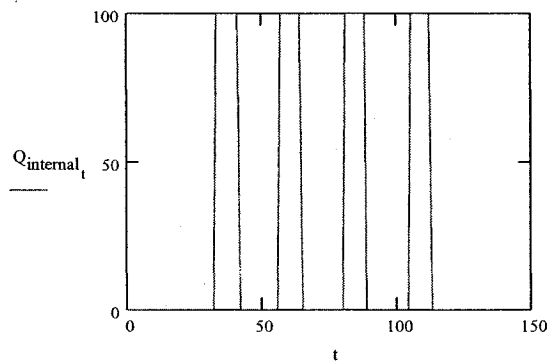
internal gains from lights are modeled as schedule functions, based on passive control. Hourly work plane illuminance is read from the Perez illuminance file and information for the same hour is passed in another file, that calculates electric lighting operation and it can be modeled with on/off automatic control.

Internal gains (people):

$$Q_{\text{people}_t} := \text{if}(33 \leq t \leq 41 \vee 33 \leq t \leq 40 \vee 57 \leq t \leq 64 \vee 81 \leq t \leq 88 \vee 105 \leq t \leq 112, 67 \cdot W, 0 \cdot W)$$

Internal gains (electric lights):

$$Q_{\text{internal}_t} := \text{if}(33 \leq t \leq 41 \vee 33 \leq t \leq 40 \vee 57 \leq t \leq 64 \vee 81 \leq t \leq 88 \vee 105 \leq t \leq 112, 100 \cdot W, 0 \cdot W)$$



Fourier series representation (for change of frequency of inputs):

$$nn := 0, 1..3 \quad j := \sqrt{-1} \quad w_{nn} := \frac{2 \cdot \pi \cdot nn}{24 \cdot \text{hr}}$$

Outside temperature:

$$TT1_{o_{nn}} := \left(\sum_t TT1_o(t) \cdot \frac{\exp(-j \cdot w_{nn} \cdot t \cdot \text{hr})}{24} \right) \quad TT2_{o_{nn}} := \left(\sum_t TT2_o(t) \cdot \frac{\exp(-j \cdot w_{nn} \cdot t \cdot \text{hr})}{24} \right) \quad TT3_{o_{nn}} := \left(\sum_t TT3_o(t) \cdot \frac{\exp(-j \cdot w_{nn} \cdot t \cdot \text{hr})}{24} \right)$$

$$TT4_{o_{nn}} := \left(\sum_t TT4_o(t) \cdot \frac{\exp(-j \cdot w_{nn} \cdot t \cdot \text{hr})}{24} \right) \quad TT5_{o_{nn}} := \left(\sum_t TT5_o(t) \cdot \frac{\exp(-j \cdot w_{nn} \cdot t \cdot \text{hr})}{24} \right) \quad TT6_{o_{nn}} := \left(\sum_t TT6_o(t) \cdot \frac{\exp(-j \cdot w_{nn} \cdot t \cdot \text{hr})}{24} \right)$$

$$TT7_{o_{nn}} := \left(\sum_t TT7_o(t) \cdot \frac{\exp(-j \cdot w_{nn} \cdot t \cdot \text{hr})}{24} \right) \quad TT8_{o_{nn}} := \left(\sum_t TT8_o(t) \cdot \frac{\exp(-j \cdot w_{nn} \cdot t \cdot \text{hr})}{24} \right) \quad TT9_{o_{nn}} := \left(\sum_t TT9_o(t) \cdot \frac{\exp(-j \cdot w_{nn} \cdot t \cdot \text{hr})}{24} \right)$$

$$TT10_{o_{nn}} := \left(\sum_t TT10_o(t) \cdot \frac{\exp(-j \cdot w_{nn} \cdot t \cdot \text{hr})}{24} \right) \quad TT11_{o_{nn}} := \left(\sum_t TT11_o(t) \cdot \frac{\exp(-j \cdot w_{nn} \cdot t \cdot \text{hr})}{24} \right) \quad TT12_{o_{nn}} := \left(\sum_t TT12_o(t) \cdot \frac{\exp(-j \cdot w_{nn} \cdot t \cdot \text{hr})}{24} \right)$$

Absorbed solar energy:

Outer glazing:

$$S1_{wo_{nn}} := \sum_t S1_{wo}(t) \cdot \frac{\exp(-j \cdot w_{nn} \cdot t \cdot hr)}{24}$$

$$S2_{wo_{nn}} := \sum_t S2_{wo}(t) \cdot \frac{\exp(-j \cdot w_{nn} \cdot t \cdot hr)}{24}$$

$$S3_{wo_{nn}} := \sum_t S3_{wo}(t) \cdot \frac{\exp(-j \cdot w_{nn} \cdot t \cdot hr)}{24}$$

$$S4_{wo_{nn}} := \sum_t S4_{wo}(t) \cdot \frac{\exp(-j \cdot w_{nn} \cdot t \cdot hr)}{24}$$

$$S5_{wo_{nn}} := \sum_t S5_{wo}(t) \cdot \frac{\exp(-j \cdot w_{nn} \cdot t \cdot hr)}{24}$$

$$S6_{wo_{nn}} := \sum_t S6_{wo}(t) \cdot \frac{\exp(-j \cdot w_{nn} \cdot t \cdot hr)}{24}$$

$$S7_{wo_{nn}} := \sum_t S7_{wo}(t) \cdot \frac{\exp(-j \cdot w_{nn} \cdot t \cdot hr)}{24}$$

$$S8_{wo_{nn}} := \sum_t S8_{wo}(t) \cdot \frac{\exp(-j \cdot w_{nn} \cdot t \cdot hr)}{24}$$

$$S9_{wo_{nn}} := \sum_t S9_{wo}(t) \cdot \frac{\exp(-j \cdot w_{nn} \cdot t \cdot hr)}{24}$$

$$S10_{wo_{nn}} := \sum_t S10_{wo}(t) \cdot \frac{\exp(-j \cdot w_{nn} \cdot t \cdot hr)}{24}$$

$$S11_{wo_{nn}} := \sum_t S11_{wo}(t) \cdot \frac{\exp(-j \cdot w_{nn} \cdot t \cdot hr)}{24}$$

$$S12_{wo_{nn}} := \sum_t S12_{wo}(t) \cdot \frac{\exp(-j \cdot w_{nn} \cdot t \cdot hr)}{24}$$

Inner glazing:

$$S1_{wi_{nn}} := \sum_t S1_{wi}(t) \cdot \frac{\exp(-j \cdot w_{nn} \cdot t \cdot hr)}{24}$$

$$S2_{wi_{nn}} := \sum_t S2_{wi}(t) \cdot \frac{\exp(-j \cdot w_{nn} \cdot t \cdot hr)}{24}$$

$$S3_{wi_{nn}} := \sum_t S3_{wi}(t) \cdot \frac{\exp(-j \cdot w_{nn} \cdot t \cdot hr)}{24}$$

$$S4_{wi_{nn}} := \sum_t S4_{wi}(t) \cdot \frac{\exp(-j \cdot w_{nn} \cdot t \cdot hr)}{24}$$

$$S5_{wi_{nn}} := \sum_t S5_{wi}(t) \cdot \frac{\exp(-j \cdot w_{nn} \cdot t \cdot hr)}{24}$$

$$S6_{wi_{nn}} := \sum_t S6_{wi}(t) \cdot \frac{\exp(-j \cdot w_{nn} \cdot t \cdot hr)}{24}$$

$$S7_{wi_{nn}} := \sum_t S7_{wi}(t) \cdot \frac{\exp(-j \cdot w_{nn} \cdot t \cdot hr)}{24}$$

$$S8_{wi_{nn}} := \sum_t S8_{wi}(t) \cdot \frac{\exp(-j \cdot w_{nn} \cdot t \cdot hr)}{24}$$

$$S9_{wi_{nn}} := \sum_t S9_{wi}(t) \cdot \frac{\exp(-j \cdot w_{nn} \cdot t \cdot hr)}{24}$$

$$S10_{wi_{nn}} := \sum_t S10_{wi}(t) \cdot \frac{\exp(-j \cdot w_{nn} \cdot t \cdot hr)}{24}$$

$$S11_{wi_{nn}} := \sum_t S11_{wi}(t) \cdot \frac{\exp(-j \cdot w_{nn} \cdot t \cdot hr)}{24}$$

$$S12_{wi_{nn}} := \sum_t S12_{wi}(t) \cdot \frac{\exp(-j \cdot w_{nn} \cdot t \cdot hr)}{24}$$

Floor:

$$Sf1_{nn} := \sum_t Sf1(t) \cdot \frac{\exp(-j \cdot w_{nn} \cdot t \cdot hr)}{24}$$

$$Sf2_{nn} := \sum_t Sf2(t) \cdot \frac{\exp(-j \cdot w_{nn} \cdot t \cdot hr)}{24}$$

$$Sf3_{nn} := \sum_t Sf3(t) \cdot \frac{\exp(-j \cdot w_{nn} \cdot t \cdot hr)}{24}$$

$$Sf4_{nn} := \sum_t Sf4(t) \cdot \frac{\exp(-j \cdot w_{nn} \cdot t \cdot hr)}{24}$$

$$Sf5_{nn} := \sum_t Sf5(t) \cdot \frac{\exp(-j \cdot w_{nn} \cdot t \cdot hr)}{24}$$

$$Sf6_{nn} := \sum_t Sf6(t) \cdot \frac{\exp(-j \cdot w_{nn} \cdot t \cdot hr)}{24}$$

$$Sf7_{nn} := \sum_t Sf7(t) \cdot \frac{\exp(-j \cdot w_{nn} \cdot t \cdot hr)}{24}$$

$$Sf8_{nn} := \sum_t Sf8(t) \cdot \frac{\exp(-j \cdot w_{nn} \cdot t \cdot hr)}{24}$$

$$Sf9_{nn} := \sum_t Sf9(t) \cdot \frac{\exp(-j \cdot w_{nn} \cdot t \cdot hr)}{24}$$

$$Sf10_{nn} := \sum_t Sf10(t) \cdot \frac{\exp(-j \cdot w_{nn} \cdot t \cdot hr)}{24}$$

$$Sf11_{nn} := \sum_t Sf11(t) \cdot \frac{\exp(-j \cdot w_{nn} \cdot t \cdot hr)}{24}$$

$$Sf12_{nn} := \sum_t Sf12(t) \cdot \frac{\exp(-j \cdot w_{nn} \cdot t \cdot hr)}{24}$$

Walls:

$$Sv1_{nn} := \sum_t Sv1(t) \cdot \frac{\exp(-j \cdot w_{nn} \cdot t \cdot hr)}{24}$$

$$Sv2_{nn} := \sum_t Sv2(t) \cdot \frac{\exp(-j \cdot w_{nn} \cdot t \cdot hr)}{24}$$

$$Sv3_{nn} := \sum_t Sv3(t) \cdot \frac{\exp(-j \cdot w_{nn} \cdot t \cdot hr)}{24}$$

$$Sv4_{nn} := \sum_t Sv4(t) \cdot \frac{\exp(-j \cdot w_{nn} \cdot t \cdot hr)}{24}$$

$$Sv5_{nn} := \sum_t Sv5(t) \cdot \frac{\exp(-j \cdot w_{nn} \cdot t \cdot hr)}{24}$$

$$Sv6_{nn} := \sum_t Sv6(t) \cdot \frac{\exp(-j \cdot w_{nn} \cdot t \cdot hr)}{24}$$

$$Sv7_{nn} := \sum_t Sv7(t) \cdot \frac{\exp(-j \cdot w_{nn} \cdot t \cdot hr)}{24}$$

$$Sv8_{nn} := \sum_t Sv8(t) \cdot \frac{\exp(-j \cdot w_{nn} \cdot t \cdot hr)}{24}$$

$$Sv9_{nn} := \sum_t Sv9(t) \cdot \frac{\exp(-j \cdot w_{nn} \cdot t \cdot hr)}{24}$$

$$Sv10_{nn} := \sum_t Sv10(t) \cdot \frac{\exp(-j \cdot w_{nn} \cdot t \cdot hr)}{24}$$

$$Sv11_{nn} := \sum_t Sv11(t) \cdot \frac{\exp(-j \cdot w_{nn} \cdot t \cdot hr)}{24}$$

$$Sv12_{nn} := \sum_t Sv12(t) \cdot \frac{\exp(-j \cdot w_{nn} \cdot t \cdot hr)}{24}$$

Exterior wall:

$$Sex1_{nn} := \sum_t Sex1(t) \cdot \frac{\exp(-j \cdot w_{nn} \cdot t \cdot hr)}{24}$$

$$Sex2_{nn} := \sum_t Sex2(t) \cdot \frac{\exp(-j \cdot w_{nn} \cdot t \cdot hr)}{24}$$

$$Sex3_{nn} := \sum_t Sex3(t) \cdot \frac{\exp(-j \cdot w_{nn} \cdot t \cdot hr)}{24}$$

$$Sex4_{nn} := \sum_t Sex4(t) \cdot \frac{\exp(-j \cdot w_{nn} \cdot t \cdot hr)}{24}$$

$$Sex5_{nn} := \sum_t Sex5(t) \cdot \frac{\exp(-j \cdot w_{nn} \cdot t \cdot hr)}{24}$$

$$Sex6_{nn} := \sum_t Sex6(t) \cdot \frac{\exp(-j \cdot w_{nn} \cdot t \cdot hr)}{24}$$

$$Sex7_{nn} := \sum_t Sex7(t) \cdot \frac{\exp(-j \cdot w_{nn} \cdot t \cdot hr)}{24}$$

$$Sex8_{nn} := \sum_t Sex8(t) \cdot \frac{\exp(-j \cdot w_{nn} \cdot t \cdot hr)}{24}$$

$$Sex9_{nn} := \sum_t Sex9(t) \cdot \frac{\exp(-j \cdot w_{nn} \cdot t \cdot hr)}{24}$$

$$Sex10_{nn} := \sum_t Sex10(t) \cdot \frac{\exp(-j \cdot w_{nn} \cdot t \cdot hr)}{24}$$

$$Sex11_{nn} := \sum_t Sex11(t) \cdot \frac{\exp(-j \cdot w_{nn} \cdot t \cdot hr)}{24}$$

$$Sex12_{nn} := \sum_t Sex12(t) \cdot \frac{\exp(-j \cdot w_{nn} \cdot t \cdot hr)}{24}$$

Internal gains:

$$Q_{intn_{nn}} := \sum_t Q_{internal_t} \cdot \frac{\exp(-j \cdot w_{nn} \cdot t \cdot hr)}{24}$$

$$Q_{peop_{nn}} := \sum_t Q_{people_t} \cdot \frac{\exp(-j \cdot w_{nn} \cdot t \cdot hr)}{24}$$

Selection of time step:

$$TS := \left[\frac{C_{ex}}{\frac{1}{\frac{R_{ex}}{2} + R_{oex0}} + \frac{1}{\frac{R_{ex}}{2} + R_{insex} + R_{gex}}} \quad \frac{C_f}{\frac{1}{\frac{R_f}{2} + R_{insf} + R_{bfr}} + \frac{1}{\frac{R_f}{2}}} \quad \frac{C_v}{\left(\frac{1}{\frac{R_v}{2} + R_{sidv} + R_{vb}} + \frac{1}{\frac{R_v}{2}} \right)} \right]$$

$$TS = (1.253 \times 10^4 \quad 2.232 \times 10^3 \quad 311.371) s$$

$$\Delta t_{critical} := \min(TS) \quad \Delta t_{critical} = 311.371 s \quad \dots \text{critical time step}$$

$$dt := 300 \text{ sec} \quad \dots \text{simulation time step (5 min)}$$

$$120 \frac{\text{hr}}{300 \text{ sec}} = 1.44 \times 10^3$$

$$\text{number of time steps} \quad p := 0, 1.. 1439$$

$$t_p := p \cdot dt \quad \dots \text{times at which simulation will be performed}$$

$$n1 := 1, 2.. 3 \quad \dots \text{new index}$$

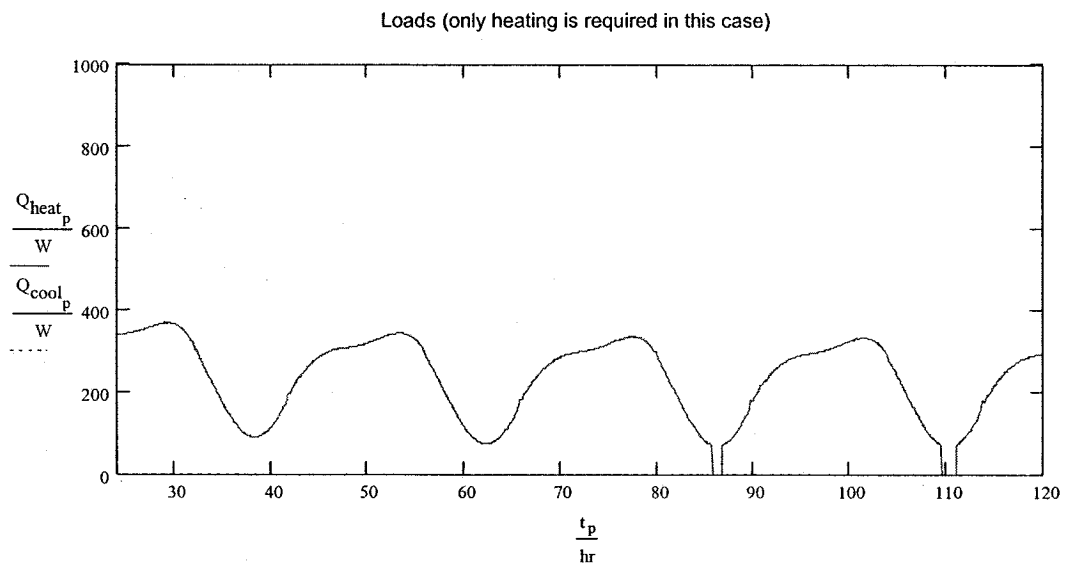
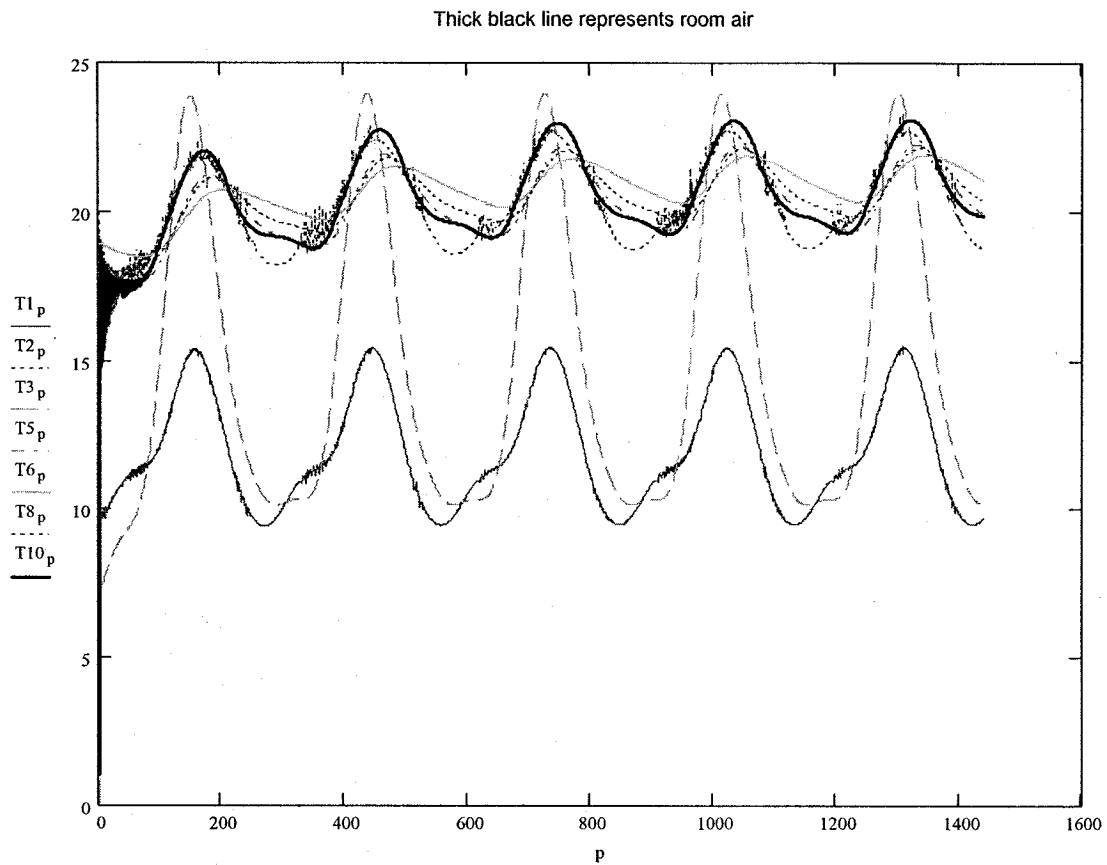
Generation of data for each time step (back to time domain):

$$\begin{aligned} T1_{op} &:= TT1_{o0} + 2 \cdot \left[\sum_{n1} \text{Re} \left[\left(TT1_{on1} \right) \cdot \exp(j \cdot w_{n1} \cdot t_p) \right] \right] & T2_{op} &:= TT2_{o0} + 2 \cdot \left[\sum_{n1} \text{Re} \left[\left(TT2_{on1} \right) \cdot \exp(j \cdot w_{n1} \cdot t_p) \right] \right] \\ T4_{op} &:= TT4_{o0} + 2 \cdot \left[\sum_{n1} \text{Re} \left[\left(TT4_{on1} \right) \cdot \exp(j \cdot w_{n1} \cdot t_p) \right] \right] & T5_{op} &:= TT5_{o0} + 2 \cdot \left[\sum_{n1} \text{Re} \left[\left(TT5_{on1} \right) \cdot \exp(j \cdot w_{n1} \cdot t_p) \right] \right] \\ T7_{op} &:= TT7_{o0} + 2 \cdot \left[\sum_{n1} \text{Re} \left[\left(TT7_{on1} \right) \cdot \exp(j \cdot w_{n1} \cdot t_p) \right] \right] & T8_{op} &:= TT8_{o0} + 2 \cdot \left[\sum_{n1} \text{Re} \left[\left(TT8_{on1} \right) \cdot \exp(j \cdot w_{n1} \cdot t_p) \right] \right] \\ T10_{op} &:= TT10_{o0} + 2 \cdot \left[\sum_{n1} \text{Re} \left[\left(TT10_{on1} \right) \cdot \exp(j \cdot w_{n1} \cdot t_p) \right] \right] & T11_{op} &:= TT11_{o0} + 2 \cdot \left[\sum_{n1} \text{Re} \left[\left(TT11_{on1} \right) \cdot \exp(j \cdot w_{n1} \cdot t_p) \right] \right] \\ T3_{op} &:= TT3_{o0} + 2 \cdot \left[\sum_{n1} \text{Re} \left[\left(TT3_{on1} \right) \cdot \exp(j \cdot w_{n1} \cdot t_p) \right] \right] & T6_{op} &:= TT6_{o0} + 2 \cdot \left[\sum_{n1} \text{Re} \left[\left(TT6_{on1} \right) \cdot \exp(j \cdot w_{n1} \cdot t_p) \right] \right] \end{aligned}$$

$$\begin{aligned}
& \left[\left[\left(\frac{1.81^3 \sqrt{T_1 - T_{10p}}}{1.382} \right)^2 + (2.5V_o^{0.75})^2 \right] \frac{W}{m^2 \cdot K} + 4\epsilon_w \sigma \left[\left(\frac{T_{10p} + T_1}{2} + 273 \right) \cdot K \right]^3 \right] \frac{K}{\text{degC}} \\
& \left[\frac{1.81^3 \sqrt{T_1 - T_{10p}}}{1.382} + 1.6 \left[\left(\frac{1.81^3 \sqrt{T_1 - T_{10p}}}{1.382} \right)^2 + (2.5V_o^{0.75})^2 \right] \frac{1.81^3 \sqrt{T_1 - T_{10p}}}{1.382} \right] \frac{W}{m^2 \cdot K} + 4\epsilon_w \sigma \left[\left(\frac{T_{10p} + T_1}{2} + 273 \right) \cdot K \right]^3 \frac{K}{\text{degC}} \\
& 1.31 \left(T_2 - T_{10p} \right)^{\frac{1}{3}} \frac{W \cdot \text{degC}^{\frac{-4}{3}}}{m^2} \\
& 1.31 \left(T_6 - T_{10p} \right)^{\frac{1}{3}} \frac{W \cdot \text{degC}^{\frac{-4}{3}}}{m^2} \\
& 1.31 \left(T_8 - T_{10p} \right)^{\frac{1}{3}} \frac{W \cdot \text{degC}^{\frac{-4}{3}}}{m^2} \\
& 1.31 \left(T_5 - T_{10p} \right)^{\frac{1}{3}} \frac{W \cdot \text{degC}^{\frac{-4}{3}}}{m^2} \\
& \frac{\sigma \left[\left(T_2 + 273 \right) \cdot K \right]^4 - \left[\left(T_6 + 273 \right) \cdot K \right]^4}{T_2 - T_6} \cdot F_\epsilon \cdot F_{wf} \\
& \frac{\sigma \left[\left(T_2 + 273 \right) \cdot K \right]^4 - \left[\left(T_8 + 273 \right) \cdot K \right]^4}{T_2 - T_8} \cdot F_\epsilon \cdot F_{wv} \\
& \frac{\sigma \left[\left(T_6 + 273 \right) \cdot K \right]^4 - \left[\left(T_8 + 273 \right) \cdot K \right]^4}{T_6 - T_8} \cdot F_\epsilon \cdot F_{fv} \\
& \frac{\sigma \left[\left(T_5 + 273 \right) \cdot K \right]^4 - \left[\left(T_6 + 273 \right) \cdot K \right]^4}{T_5 - T_6} \cdot F_\epsilon \cdot F_{exf} \\
& \frac{\sigma \left[\left(T_5 + 273 \right) \cdot K \right]^4 - \left[\left(T_8 + 273 \right) \cdot K \right]^4}{T_5 - T_8} \cdot F_\epsilon \cdot F_{exv} \\
& \frac{\sigma \left[\left(T_1 + 273 \right) \cdot K \right]^4 - \left[\left(T_2 + 273 \right) \cdot K \right]^4}{T_1 - T_2} \cdot F_\epsilon \\
& \frac{1}{h_{ow} \cdot A_w} \\
& \frac{1}{h_{oex} \cdot A_{ex}} \\
& \frac{1}{h_{cwa} \cdot A_w} \\
& \frac{1}{h_{cfa} \cdot A_f} \\
& \frac{1}{h_{cva} \cdot A_v} \\
& \frac{1}{h_{cexa} \cdot A_{ex}} \\
& \frac{1}{h_{rwf} \cdot A_w} \\
& \frac{1}{h_{rwv} \cdot A_w} \\
& \frac{1}{h_{rfv} \cdot A_f} \\
& \frac{1}{h_{ref} \cdot A_{ex}} \\
& \frac{1}{h_{rexv} \cdot A_{ex}} \\
& \frac{1}{h_{ow} \cdot A_w} + \frac{1}{(h_{wi} + h_{rw}) \cdot A_w} + \frac{1}{h_{cwa} \cdot A_w} \\
& \left(T_{10o} \quad T_2 \quad \right)
\end{aligned}$$

$h_{ow_{p+1}}$
 $h_{oex_{p+1}}$
 $h_{cwa_{p+1}}$
 $h_{cfa_{p+1}}$
 $h_{cva_{p+1}}$
 $h_{cexa_{p+1}}$
 $h_{rwf_{p+1}}$
 $h_{rwv_{p+1}}$
 $h_{rfv_{p+1}}$
 $h_{ref_{p+1}}$
 $h_{rexv_{p+1}}$
 $h_{rw_{p+1}}$
 $R_{ow_{p+1}}$
 $R_{oex_{p+1}}$
 $R_{wa_{p+1}}$
 $R_{fa_{p+1}}$
 $R_{va_{p+1}}$
 $R_{exa_{p+1}}$
 $R_{wf_{p+1}}$
 $R_{wv_{p+1}}$
 $R_{fv_{p+1}}$
 $R_{exf_{p+1}}$
 $R_{exv_{p+1}}$

$\frac{1}{h_{ow} \cdot A_w} + \frac{1}{(h_{wi} + h_{rw}) \cdot A_w} + \frac{1}{h_{cwa} \cdot A_w}$
 $(T_{10o} \quad T_2 \quad)$



Cooling energy demand (due to load only):

$$\sum_{p=0}^{1439} Q_{cool_p} \cdot 300 \text{ sec} = 0 \text{ J}$$

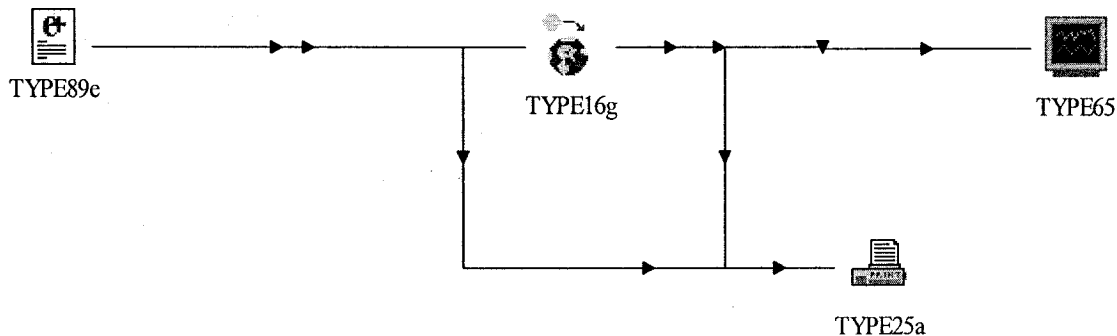
Heating :

$$\sum_{p=0}^{1439} Q_{heat_p} \cdot 300 \text{ sec} = 1.074 \times 10^8 \text{ J}$$

APPENDIX J

The TRNSYS 15 input and listing files (in IISiBat interface) for processing solar radiation data imported from Energy Plus TMY “epw” files.

Type 89 is the weather data reader that reads hourly weather data from a “epw” Energy Plus formatted file. Outdoor dry bulb and dew-point temperatures are exported directly from this file. Type 16g is a solar radiation processor that reads raw solar radiation data and then corrects them (solar radiation values before sunrise and sunset, solar altitude at sunrise and sunset) in order to prevent from predicting wrong radiation values on tilted surfaces in early morning and late evening hours. Type 65 is one online plotter for visualizing data and Type 25a is a printer used for producing output for all data used further in the simulation. Outputs from one component are inputs to another, using configured wiring shown below.



The complete TRNSYS listing file is presented below.

```

1          TRNSYS - A TRANSIENT SIMULATION PROGRAM
          FROM THE SOLAR ENERGY LAB AT THE UNIVERSITY OF WISCONSIN
          VERSION 15 Feb. 2000

```

```

        ASSIGN Thanos montreal.LST

```

```

6

```

```

*****
*****

```

```

    *** Control cards

```

```

*****
*****

```

```

    * START, STOP and STEP

```

```

    CONSTANTS      3

```

```

        START=0

```

```

        STOP=8760

```

```

        STEP=1

```

```

    * User defined CONSTANTS

```

```

    *SIMULATION Start time  End time      Time step

```

```

    SIMULATION      0.000E+00      8.760E+03      1.000E+00

```

```

    *                      Integration Convergence

```

```

    TOLERANCES      1.000E-03      1.000E-03

```

```

    *                      Max iterations      Max warnings      Trace
limit

```

```

    LIMITS          30      30      31

```

```

    *                      TRNSYS numerical integration solver method

```

```

    DFQ      1

```

```

    *                      TRNSYS output file width, number of
characters

```

```

    WIDTH          80

```

```

    *                      NOLIST statement

```

```

    LIST

```

```

    *                      MAP statement

```

```

    MAP

```

```

    *                      Solver statement

```

```

    SOLVER      0

```

```

*****
*****

```

```

    *** Units

```

```

*****
*****

```

```

    * Model "TYPE89e" (Type 89)

```

```

    *

```

```

UNIT 1 TYPE 89 TYPE89e
*$UNIT_NAME TYPE89e
*$MODEL .\Utility\Weather and Other Data Readers\Standard Weather File
Types\EnergyPlus\Simulation Start is first line\TYPE89e.tmf
*$POSITION 110 141
*$LAYER Main
*$$ This component conforms to the format of the TRNSYS TMY and the TMY
data file reader. It is designed
*$$ to read EnergyPlus (*.epw) format weather files.
*$$
*$$
*$$
*$$

PARAMETERS 2
* 1 Mode
* 2 Logical unit
3.000E+00 1.300E+01
*** External files

ASSIGN C:\trnsys15\Weather\EnergyPlus\CAN_PQ_Montreal_CWEC.epw
13
*|? Which file contains the EnergyPlus weather information? |1000
*-----
-----
* Model "TYPE16g" (Type 16)
*

UNIT 2 TYPE 16 TYPE16g
*$UNIT_NAME TYPE16g
*$MODEL .\Physical Phenomena\Radiation Processors\Total Horiz, Direct
Normal Known (Mode=4)\No Radiation Smoothing\TYPE16g.tmf
*$POSITION 383 145
*$LAYER Main
*$$
*$$
*$$

PARAMETERS 9
* 1 Horiz. radiation mode
* 2 Tracking mode
* 3 Tilted surface mode
* 4 Starting day
* 5 Latitude
* 6 Solar constant
* 7 Shift in solar time
* 8 Not used
* 9 Solar time?
4.000E+00 1.000E+00 3.000E+00 1.000E+00 4.500E+01
4.871E+03 0.000E+00 2.000E+00 -1.000E+00

INPUTS 7
* TYPE89e:Global horizontal radiation ->Total radiation on horizontal
surface
* TYPE89e:Direct normal radiation ->Direct normal beam radiation
* TYPE89e:Time of last read ->Time of last data read
* TYPE89e:Time of next read ->Time of next data read
* [unconnected] Ground reflectance
* [unconnected] Slope of surface

```



```

* [unconnected] Azimuth of surface
      1,4          1,3          1,99          1,100          CONST
      CONST          CONST
*** INITIAL INPUT VALUES
      0.000E+00    0.000E+00    0.000E+00    1.000E+00    2.000E-01
      0.000E+00    0.000E+00

```

```

*-----

```

```

* Model "TYPE65" (Type 65)
*

```

```

      UNIT   3      TYPE  65      TYPE65
*$UNIT_NAME TYPE65
*$MODEL .\Output\Online Plotter\TYPE65.tmf
*$POSITION 651 146
*$LAYER Main
*$#
*$#
*$#
*$#
*$#
*$#
*$#
*$#
*$#
*$#

```

```

      PARAMETERS  10
* 1 Nb. of left-axis variables
* 2 Nb. of right-axis variables
* 3 Left axis minimum
* 4 Left axis maximum
* 5 Right axis minimum
* 6 Right axis maximum
* 7 Number of plots per simulation
* 8 X-axis gridpoints
* 9 Shut off Online w/o removing
* 10 Logical Unit for output file
      1.000E+00    1.000E+00    0.000E+00    1.000E+03    0.000E+00
      1.000E+03    1.000E+00    7.000E+00    0.000E+00    -1.000E+00

```

```

      INPUTS      2
* TYPE16g:Beam radiation on horizontal ->Left axis variable
* [unconnected] Right axis variable
      2,05          CONST

```

```

*** INITIAL INPUT VALUES
      Beam          labe      1
      LABELS  5
      KJ\HR\      KJ\HR
      Energy
      Power
      Result

```

```

*-----

```

```

* Model "TYPE25a" (Type 25)
*

```

```

      UNIT   4      TYPE  25      TYPE25a

```

```

*$UNIT_NAME TYPE25a
*$MODEL .\Output\Printer\Print TRNSYS-Supplied Units to
File\TYPE25a.tmf
*$POSITION 547 253
*$LAYER Outputs
*$#
*$#
*$#
*$#
*$#
*$#
*$#
*$#
PARAMETERS 6
* 1 Printing interval
* 2 Start time
* 3 Stop time
* 4 Logical unit
* 5 Print TRNSYS units
* 6 Output format ""normal"" or ""SPREADSHEET""
    1.000E+00    0.000E+00    8.760E+03    1.700E+01    2.000E+00
    0.000E+00
INPUTS 5
* TYPE16g:Beam radiation on horizontal ->Input to be printed-1
* TYPE16g:Horizontal diffuse radiation ->Input to be printed-2
* TYPE89e:Dew point temperature ->Input to be printed-3
* TYPE16g:Solar zenith angle ->Input to be printed-4
* TYPE89e:Dry bulb temperature ->Input to be printed-5
    2,05        2,06        1,09        2,02        1,05
*** INITIAL INPUT VALUES
    Ibh        Idh        Tdp        zenith        Dry
*** External files

ASSIGN MONTREALRESULTS.OUT
17
*|? Which file should contain the printed results? '|1000
*-----
-----

END

```

```

TRANSIENT SIMULATION      STARTING AT TIME = 0.000E+00
                          STOPPING AT TIME = 8.760E+03
                          TIMESTEP = 1
DIFFERENTIAL EQUATION ERROR TOLERANCE = 1.000E-03
ALGEBRAIC CONVERGENCE TOLERANCE = 1.000E-03
1 TRNSYS COMPONENT OUTPUT MAP

```

```

UNIT 1 TYPE 89 UNIT/TYPE/INPUT
OUTPUT 4      2 16 1
OUTPUT 3      2 16 2
OUTPUT 99     2 16 3
OUTPUT100     2 16 4
OUTPUT 9      4 25 3
OUTPUT 5      4 25 5

```

```

UNIT  2 TYPE 16  UNIT/TYPE/INPUT
  OUTPUT  5      3 65  1
              4 25  1
  OUTPUT  6      4 25  2
  OUTPUT  2      4 25  4

```

```

UNIT  3 TYPE 65  UNIT/TYPE/INPUT

```

```

EQUATIONS          UNIT/TYPE/INPUT

```

DIFFERENTIAL EQUATIONS SOLVED BY MODIFIED EULER

***** NOTE *****

```

UNIT  1 TYPE 89 DATA READER (EnergyPlus WEATHER FILE)
LOCATION: Montreal_Mirabel      PQ
TIME ZONE:  5 HOURS W
LATITUDE:   45.68 DEG  LONGITUDE:   74.03 DEG W
ELEVATION:   82 M
HOURS OF E+ DATA ARE IN LOCAL STANDARD TIME, NOT SOLAR TIME.
BE SURE TO PERFORM RADIATION PROCESSING APPROPRIATELY.
SHIFT IN SOLAR TIME HOUR ANGLE (L_STANDARD - L_LOCAL):  0.97 DEG

```

20 STORAGE VARIABLES ALLOCATED FOR UNIT 2, TYPE 16 ENDING AT 21

	HR	:	MIN	:	SEC
Start-Time:	18	:	5	:	4.54
End-Time:	18	:	5	:	8.95
Total Execution Time:	0	:	0	:	4.41

***** WARNING *****

```

UNIT  1 TYPE 89 DATA READER
YOU HAVE EXHAUSTED YOUR DATA. DATA READING RE-STARTED FROM THE
BEGINNING OF FILE.
TIME= 8760.00

```

UNIT	1 WAS CALLED	8762 TIMES
2		8762
3		8763
4		8761

```

*-----*
*  UNIT          # ITERATIVE CALLS          *
*  1 ----- 8762 *
*  2 ----- 8762 *
*
*  Total Iterative Component Calls = 35048 *
*-----*

```

APPENDIX K

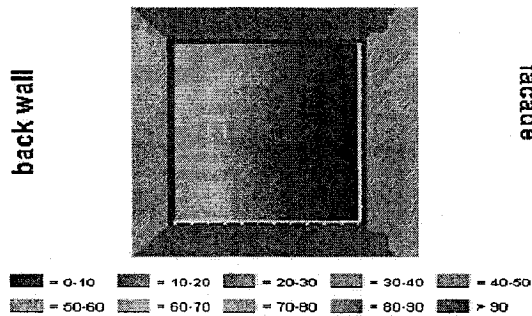
The Lightswitch software output file (used for validation).

Case 1: Comparison of DAR and lighting energy demand between south and north-facing facades, using passive lighting control.

Scenario 1		Scenario 2	
General	Single Office	General	Single Office
<u>Arrival Time</u> 9:00 <u>Departure Time</u> 17:00	<u>Lighting Control</u> Switch on/off occupancy sensor <u>Delay Occupancy Sensor</u> 5 Mins. <u>Blind Control</u> No Blinds <u>Seating Position</u> View <u>Minimum Illuminance Threshold</u> 500 Lux	<u>Building Type</u> single office <u>Country</u> Canada <u>Province</u> Quebec <u>City</u> Montreal <u>External Shading (Due to external objects)</u> no external obstruction <u>Facade Orientation</u> North	<u>User Behavior</u> Lighting Control passive lighting control Blind Control passive blind control <u>Installed Lighting Power</u> 15.00 (Units) W/ft ² W/m ²
<input type="button" value="Run Scenario 1 Simulation"/>		<input type="button" value="Run Scenario 2 Simulation"/>	
Simulation Report: office The predicted annual electric lighting energy use in the office is:		Simulation Report: office The predicted annual electric lighting energy use in the office is:	

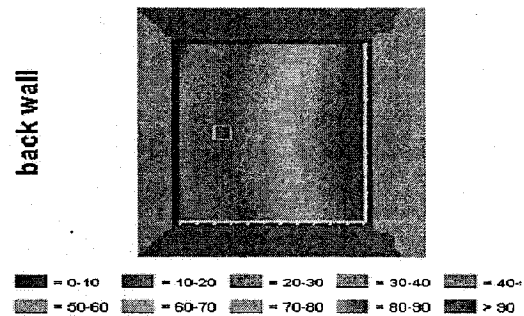
Daylight Autonomy Distribution [%]

MONTREAL Que. min. illuminance office: 500lux, or. South
white square = occupant pos., no blinds, axis unit = 0.31m



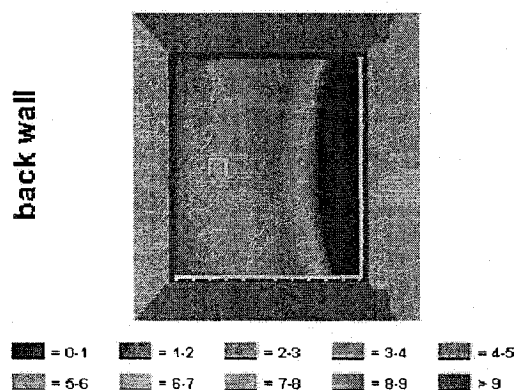
Daylight Autonomy Distribution [%]

MONTREAL Que. min. illuminance office: 500lux, or. North
white square = occupant pos., no blinds, axis unit = 0.31m



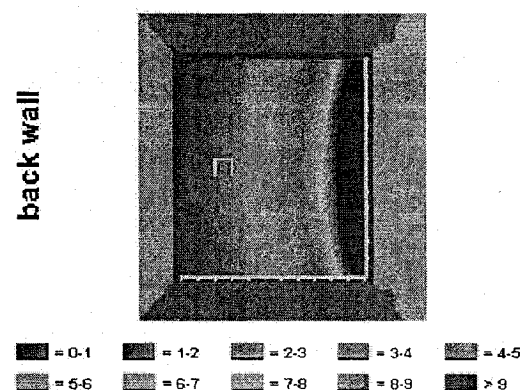
Daylight Factor Distribution [%]

no blinds, axis unit = 0.31m
white square = occupant pos.



Daylight Factor Distribution [%]

no blinds, axis unit = 0.31m
white square = occupant pos.



Site Description

The investigated building is located in MONTREAL Que (N 45°, W 73.75°). Daylight savings time lasts from April 1st to October 31st.

office Description

The office has a facade facing due South. The facade glazing has a visual transmittance of 81.0%. The window unit has a frame proportion of 2.0%. The facade is unobstructed by surrounding buildings or landscape. The office has a floor to ceiling height of 3.05m, is 4.58m wide and 3.97m deep. The diffuse reflectances of the ceiling, walls and floor are 80%, 50%, and 20%, respectively. An elevation of the office facade is shown

Site Description

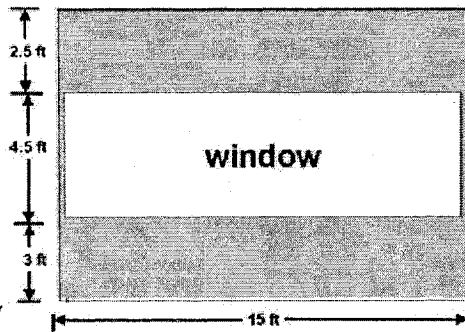
The investigated building is located in MONTREAL Que (N 45°, W 73.75°). Daylight savings time lasts from April 1st to October 31st.

office Description

The office has a facade facing due North. The facade glazing has a visual transmittance of 72.0%. The window unit has a frame proportion of 15.0%. The facade is unobstructed by surrounding buildings or landscape. The office has a floor to ceiling height of 3.05m, is 4.58m wide and 3.97m deep. The diffuse reflectances of the ceiling, walls and floor are 80%, 50%, and 20%, respectively. An elevation of the office facade is shown

below.

Elevation of the investigated facade.



User Description

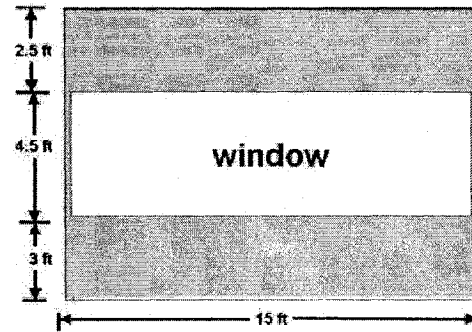
The office is occupied Monday through Friday from 9:00 to 17:00. The occupant leaves the office three times during the day (30 minutes in the morning, 1 hour at midday, and 30 minutes in the afternoon). The occupant performs a task that requires a minimum illuminance of 500 lux. The predicted electric lighting energy use of 24.5 kWh/m² yr is based on a user who keeps the electric lighting on throughout the working day, and keeps the blinds lowered throughout the year to avoid direct sunlight.

Lighting and Blind Control

The electric lighting system has an installed lighting power density of 15.00 W/m² and is automatically controlled via an on/off occupancy sensor with a delay time of 5 minutes. The sensor has a permanent standby power of 3W. The office has no blind system installed.

below.

Elevation of the investigated facade.



User Description

The office is occupied Monday through Friday from 8 to 17:00. The occupant leaves the office three times during the day (30 minutes in the morning, 1 hour at midday, and 30 minutes in the afternoon). The occupant performs a task that requires a minimum illuminance of 500 lux. The predicted electric lighting energy use of 28.4 kWh/m² yr is based on a user who keeps the electric lighting on throughout the working day, and keeps the blinds lowered throughout the year to avoid direct sunlight.

Lighting and Blind Control

The electric lighting system has an installed lighting power density of 15.00 W/m² and is automatically controlled via an on/off occupancy sensor with a delay time of 5 minutes. The sensor has a permanent standby power of 3W. The office has no blind system installed.

Case 2: Comparison of DAR and lighting energy demand between south and north-facing facades, using active lighting control (dimming).

Scenario 1

General
Single Office
User

Arrival Time 9:00 ☐

Departure Time 17:00 ☐

Lighting Control Switch on/off occupancy with aut.dimming ☐

Delay Occupancy Sensor 5 ☐ Mins.

Blind Control No Blinds ☐

Seating Position

Minimum Illuminance Threshold 500 Lux

User Behavior Lighting Control active lighting control ☐

Blind Control passive blind control ☐

Installed Lighting Power 15.00 (Units) ☐ W/ft² ☒ W/m²

Scenario 2

General
Single Office
User

Arrival Time 8:00 ☐

Departure Time 17:00 ☐

Lighting Control Switch on/off occupancy with aut.dimming ☐

Delay Occupancy Sensor 5 ☐ Mins.

Blind Control No Blinds ☐

Seating Position

Minimum Illuminance Threshold 500 Lux

User Behavior Lighting Control active lighting control ☐

Blind Control passive blind control ☐

Installed Lighting Power 15.00 (Units) ☐ W/ft² ☒ W/m²

Simulation Report: office

The predicted annual electric lighting energy use in the office is:

12.2 kWh/m² yr

Daylight Autonomy Distribution [%]
MONTREAL Que. min. illuminance office: 500lux, or. North
white square = occupant pos., no blinds, axis unit = 0.31m

back wall

facade

■ 0-10 ■ 10-20 ■ 20-30 ■ 30-40 ■ 40-50
 ■ 50-60 ■ 60-70 ■ 70-80 ■ 80-90 ■ > 90

■ 0-10 ■ 10-20 ■ 20-30 ■ 30-40 ■ 40-50
 ■ 50-60 ■ 60-70 ■ 70-80 ■ 80-90 ■ > 90

Simulation Report: office

The predicted annual electric lighting energy use in the office is:

9.2 kWh/m² yr

Daylight Autonomy Distribution [%]
MONTREAL Que. min. illuminance office: 500lux, or. South
white square = occupant pos., no blinds, axis unit = 0.31m

back wall

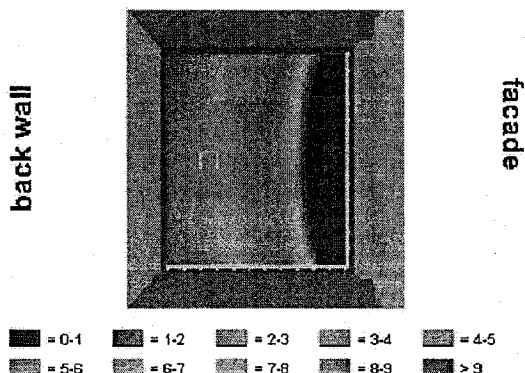
facade

■ 0-10 ■ 10-20 ■ 20-30 ■ 30-40 ■ 40-50
 ■ 50-60 ■ 60-70 ■ 70-80 ■ 80-90 ■ > 90

■ 0-10 ■ 10-20 ■ 20-30 ■ 30-40 ■ 40-50
 ■ 50-60 ■ 60-70 ■ 70-80 ■ 80-90 ■ > 90

Daylight Factor Distribution [%]

no blinds, axis unit = 0.31m
white square = occupant pos.



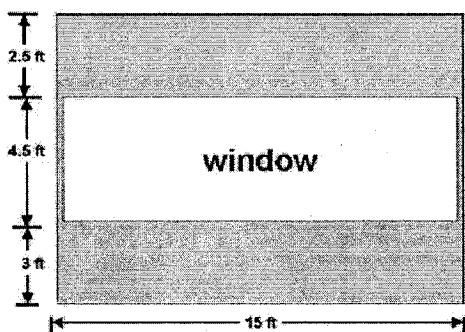
Site Description

The investigated building is located in MONTREAL Que (N 45°, W 73.75°). Daylight savings time lasts from April 1st to October 31st.

office Description

The office has a facade facing due North. The facade glazing has a visual transmittance of 81.0%. The window unit has a frame proportion of 2.0%. The facade is unobstructed by surrounding buildings or landscape. The office has a floor to ceiling height of 3.05m, is 4.58m wide and 3.97m deep. The diffuse reflectances of the ceiling, walls and floor are 80%, 50%, and 20%, respectively. An elevation of the office facade is shown below.

Elevation of the investigated facade.

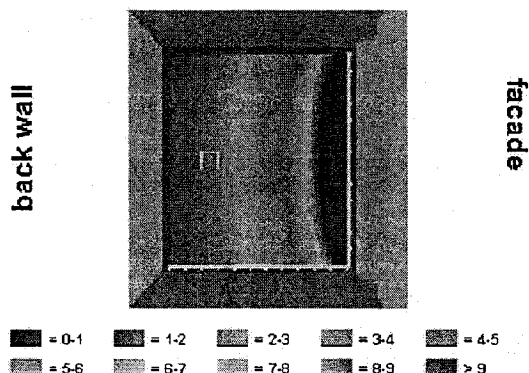


User Description

The office is occupied Monday through Friday from 9:00 to 17:00. The occupant leaves the office three times during the day (30 minutes in the morning, 1 hour at midday, and 30 minutes in the afternoon). The occupant performs a task that requires a

Daylight Factor Distribution [%]

no blinds, axis unit = 0.31m
white square = occupant pos.



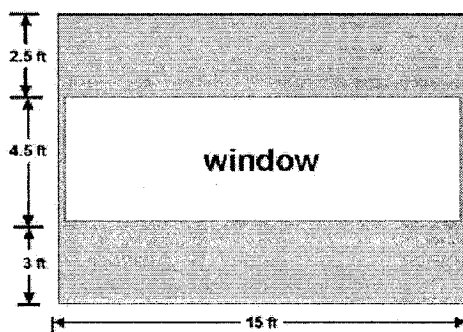
Site Description

The investigated building is located in MONTREAL Que (N 45°, W 73.75°). Daylight savings time lasts from April 1st to October 31st.

office Description

The office has a facade facing due South. The facade glazing has a visual transmittance of 72.0%. The window unit has a frame proportion of 15.0%. The facade is unobstructed by surrounding buildings or landscape. The office has a floor to ceiling height of 3.05m, is 4.58m wide and 3.97m deep. The diffuse reflectances of the ceiling, walls and floor are 80%, 50%, and 20%, respectively. An elevation of the office facade is shown below.

Elevation of the investigated facade.



User Description

The office is occupied Monday through Friday from 8:00 to 17:00. The occupant leaves the office three times during the day (30 minutes in the morning, 1 hour at midday, and 30 minutes in the afternoon). The occupant performs a task that requires a

minimum illuminance of 500 lux. The predicted electric lighting energy use of 12.2 kWh/m² yr is based on a user who operates the electric lighting in relation to ambient daylight conditions, and keeps the blinds lowered throughout the year to avoid direct sunlight.

Lighting and Blind Control

The electric lighting system has an installed lighting power density of 15.00 W/m² and is automatically controlled via an on/off occupancy sensor with a delay time of 5 minutes and a standby power of 3W. The dimming system has an ideally commissioned photocell control. At minimum dim level the lighting system still consumes 15% of its full electric power. The photocell has an additional standby power of 2W. The office has no blind system installed.

minimum illuminance of 500 lux. The predicted electric lighting energy use of 9.2 kWh/m² yr is based on a user who operates the electric lighting in relation to ambient daylight conditions, and keeps the blinds lowered throughout the year to avoid direct sunlight.

Lighting and Blind Control

The electric lighting system has an installed lighting power density of 15.00 W/m² and is automatically controlled via an on/off occupancy sensor with a delay time of 5 minutes and a standby power of 3W. The dimming system has an ideally commissioned photocell control. At minimum dim level the lighting system still consumes 15% of its full electric power. The photocell has an additional standby power of 2W. The office has no blind system installed.

Case 3: Comparison of DAR and lighting energy demand between east and west-facing facades, using active lighting control (dimming).

Scenario 1

General
Single Office
User

Arrival Time 9:00

Departure Time 17:00

Lighting Control Switch on/off occupancy with aut.dimming

Delay Occupancy Sensor 5 Mins.

Blind Control No Blinds

Seating Position View

Minimum Illuminance Threshold 500 Lux

User Behavior

Lighting Control active lighting control

Blind Control passive blind control

Installed Lighting Power 15.00 (Units) W/ft² W/m²

Run Scenario 1 Simulation

Scenario 2

General
Single Office
User

Arrival Time 8:00

Departure Time 17:00

Lighting Control Switch on/off occupancy with aut.dimming

Delay Occupancy Sensor 5 Mins.

Blind Control No Blinds

Seating Position View

Minimum Illuminance Threshold 500 Lux

User Behavior

Lighting Control active lighting control

Blind Control passive blind control

Installed Lighting Power 15.00 (Units) W/ft² W/m²

Run Scenario 2 Simulation

Simulation Report: office

The predicted annual electric lighting energy use in the office is:

7.1 kWh/m² yr

Daylight Autonomy Distribution [%]

MONTREAL Que. min. illuminance office: 500lux, or, East white square = occupant pos., no blinds, axis unit = 0.31m

back wall

facade

= 0-10
 = 10-20
 = 20-30
 = 30-40
 = 40-50

= 50-60
 = 60-70
 = 70-80
 = 80-90
 = > 90

Simulation Report: office

The predicted annual electric lighting energy use in the office is:

10.2 kWh/m² yr

Daylight Autonomy Distribution [%]



MONTREAL Que. min. illuminance office: 500lux, or, West white square = occupant pos., no blinds, axis unit = 0.31m

back wall


facade


= 0-10
 = 10-20
 = 20-30
 = 30-40
 = 40-50


= 50-60
 = 60-70
 = 70-80
 = 80-90
 = > 90


Scenario 1  


General **Single Office** **User**


Arrival Time 9:00 


Departure Time 17:00 


Lighting Control Switch on/off occupancy with aut.dimming 


Delay Occupancy Sensor 5  Mins.

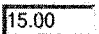


Blind Control No Blinds 

Seating Position **View** 



Minimum Illuminance Threshold 500  Lux

User Behavior Lighting Control active lighting control 


Blind Control passive blind control 


Installed Lighting Power 15.00  (Units)  W/ft²  W/m²


Run Scenario 1 Simulation


Scenario 2  


General **Single Office** **User**


Arrival Time 8:00 

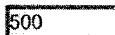
Departure Time 17:00 


Lighting Control Switch on/off occupancy with aut.dimming 


Delay Occupancy Sensor 5  Mins.

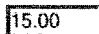


Blind Control No Blinds 

Seating Position **View** 

Minimum Illuminance Threshold 500  Lux

User Behavior Lighting Control active lighting control 

Blind Control passive blind control 

Installed Lighting Power 15.00  (Units)  W/ft²  W/m²

Run Scenario 2 Simulation

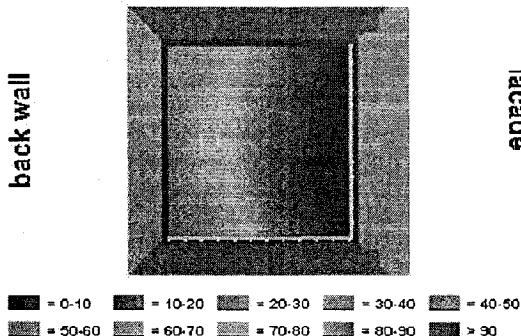
Simulation Report: office

The predicted annual electric lighting energy use in the office is:

7.1 kWh/m² yr

Daylight Autonomy Distribution [%]

MONTREAL Que, min. illuminance office: 500lux, or, East white square = occupant pos., no blinds, axis unit = 0.31m



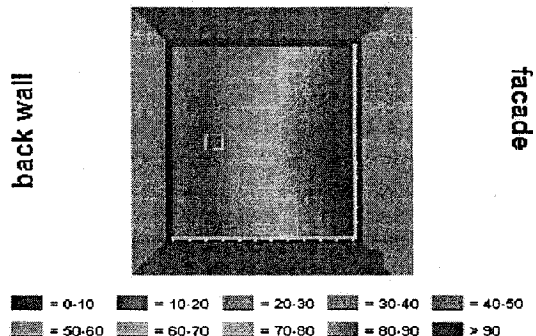
Simulation Report: office

The predicted annual electric lighting energy use in the office is:

10.2 kWh/m² yr

Daylight Autonomy Distribution [%]

MONTREAL Que, min. illuminance office: 500lux, or, West white square = occupant pos., no blinds, axis unit = 0.31m



minimum illuminance of 500 lux. The predicted electric lighting energy use of 7.1 kWh/m² yr is based on a user who operates the electric lighting in relation to ambient daylight conditions, and keeps the blinds lowered throughout the year to avoid direct sunlight.

Lighting and Blind Control

The electric lighting system has an installed lighting power density of 15.00 W/m² and is automatically controlled via an on/off occupancy sensor with a delay time of 5 minutes and a standby power of 3W. The dimming system has an ideally commissioned photocell control. At minimum dim level the lighting system still consumes 15% of its full electric power. The photocell has an additional standby power of 2W. The office has no blind system installed.

minimum illuminance of 500 lux. The predicted electric lighting energy use of 10.2 kWh/m² yr is based on a user who operates the electric lighting in relation to ambient daylight conditions, and keeps the blinds lowered throughout the year to avoid direct sunlight.

Lighting and Blind Control

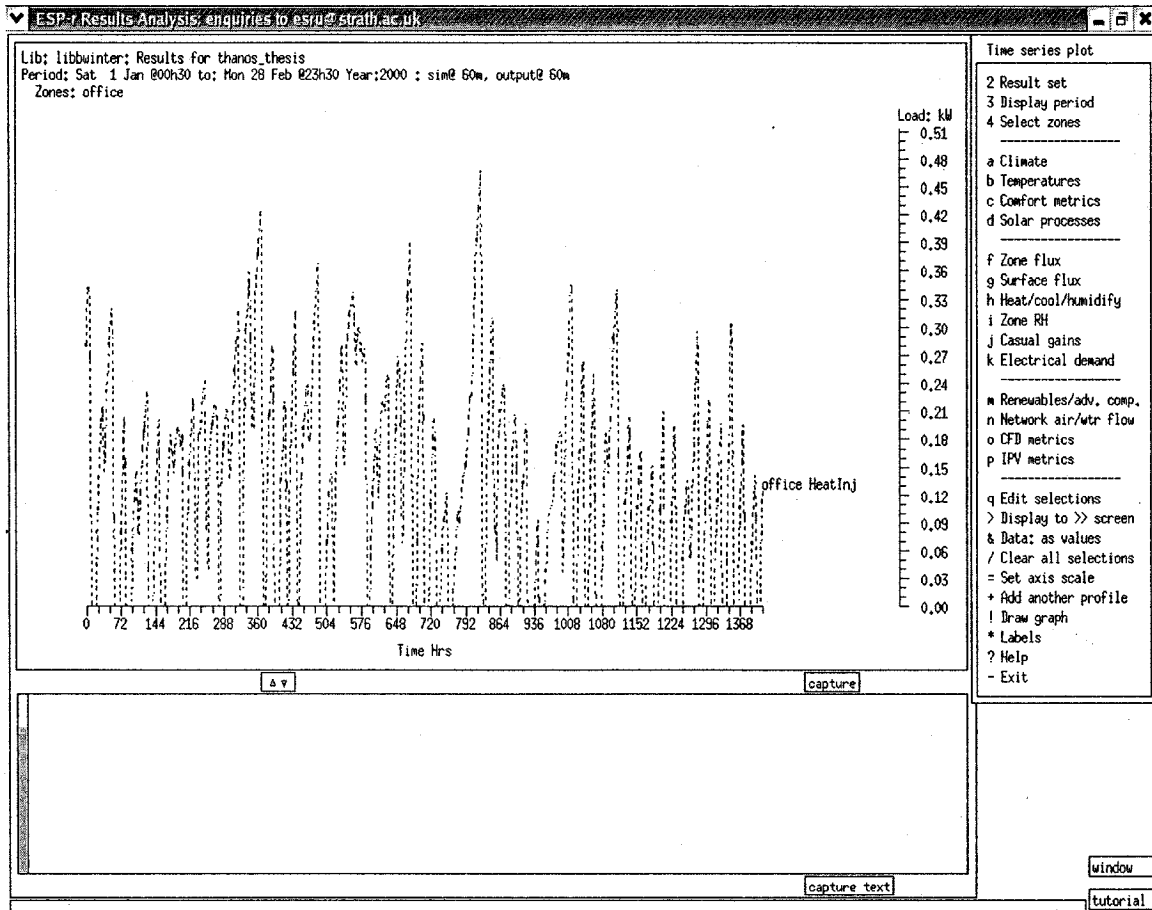
The electric lighting system has an installed lighting power density of 15.00 W/m² and is automatically controlled via an on/off occupancy sensor with a delay time of 5 minutes and a standby power of 3W. The dimming system has an ideally commissioned photocell control. At minimum dim level the lighting system still consumes 15% of its full electric power. The photocell has an additional standby power of 2W. The office has no blind system installed.

APPENDIX L

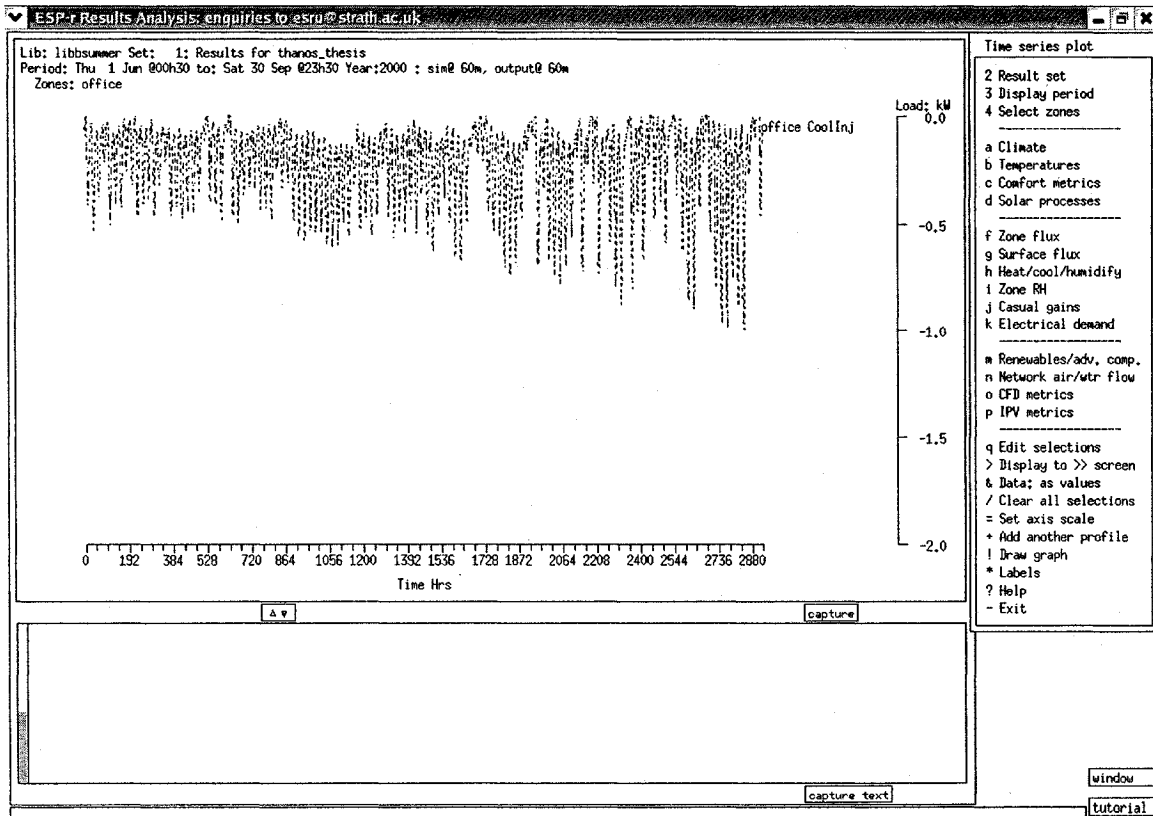
ESP-r output graphs and input file description (used for validation).

1. Hourly heating load for winter, for the base case. Peak heating load reaches 0.47 kW.

The thermal model predicted 0.49kW (5% difference).



2. Cooling load for summer, for the base case. Peak cooling load reaches 0.95 kW. The thermal model predicted 0.88 kW (7% difference).



Input file description:

ID	Zone Name	Volume m ³	No.	Surface Opaque	Transp	-Floor	
1	office	48.0	7	76.2	3.8	16.0	office describes an office...
	all	48.	7	76.	4.	16.	

Control description: proj cntrl

Zones control: no descrip : 1 functions.

The sensor for function 1 senses the temperature of the current zone.
The actuator for function 1 is air point of the current zone
There have been 1 day types defined.

Day type 1 is valid Sat 1 Jan to Sun 31 Dec, 2000 with 1 periods.

Per	Start	Sensing	Actuating	Control law	Data
1	0.00	db temp	> flux	basic control	6000.0 0.0 6000.0

0.0 21.0 21.0 0.0

Zone to control loop linkages:

zone (1) office << control 1

Zone office (1) is composed of 7 surfaces and 12 vertices.

It encloses a volume of 48.0m³ of space, with a total surface area of 80.0m² & approx floor area of 16.0m²

office describes an office...

There is 12.00m² of exposed surface area, 12.00m² of which is vertical.
Outside walls are 51.56 % of floor area & avg U of 0.333 & UA of 2.747
Glazing is 23.44 % of floor & 31.25 % facade with avg U of 0.000 & UA of 0.00

A summary of the surfaces in office(1) follows:

Sur	Area m ²	Azim deg	Elev deg	surface name	geometry type loc	construction name	environment other side
1	8.25	180.	0.	Surf-1	OPAQ VERT	extern_wall	< external
2	12.0	90.	0.	Surf-2	OPAQ VERT	extern_wall	< constant
@ 20dC &	0W rad						
3	12.0	0.	0.	Surf-3	OPAQ VERT	extern_wall	< constant
@ 20dC &	0W rad						
4	12.0	270.	0.	Surf-4	OPAQ VERT	extern_wall	< constant
@ 20dC &	0W rad						
5	16.0	0.	90.	Surf-5	OPAQ CEIL	ceiling	< constant
@ 20dC &	0W rad						
6	16.0	0.	-90.	Surf-6	OPAQ FLOR	floor_1	< constant
@ 20dC &	0W rad						
7	3.75	180.	0.	window	TRAN VERT	d_glz	< external

All surfaces will receive diffuse insolation.

Description: nil_operations

Control: no control of air flow

Number of Weekday Sat Sun air change periods = 0 0 0

Description : nil_operations

Number of Weekday Sat Sun casual gains= 0 0 0

Project floor area is 16.00m2, wall area is 8.250m2, window area is 3.750m2.

Sloped roof area is 0.00m2, flat roof area is 0.00m2, skylight area is 0.00m2.

There is 12.00m2 of outside surface area, 12.00m2 of which is vertical.

Outside walls are 51.56 % of floor area & avg U of 0.333 & UA of 2.747
Glazing is 23.44 % of floor & 31.25 % facade with avg U of 0.000 & UA of 0.00

Multi-layer constructions used:

Details of opaque construction: extern_wall

Layer	Prim	Thick	Conduc-	Density	Specif	IR	Solr	Diffu	R	Descr
	db	(m)	tivity		heat	emis	abs	resis	m^2K/W	
Ext	4	0.1000	0.960	2000.	650.	0.90	0.93	25.	0.10	Outer leaf brick
2	211	0.0810	0.040	250.	840.	0.90	0.30	4.	2.03	Glasswool
3	0	0.0500	0.000	0.	0.	0.99	0.99	1.	0.17	air
Int	107	0.1000	0.190	950.	840.	0.91	0.50	11.	0.53	Gypsum plasterboard

Standardised U value = 0.33

Total area of extern_wall is 44.25

Details of opaque construction: floor_1

Layer	Prim	Thick	Conduc-	Density	Specif	IR	Solr	Diffu	R	Descr
	db	(m)	tivity		heat	emis	abs	resis	m^2K/W	
Ext	214	0.0380	0.030	25.	1000.	0.90	0.30	67.	1.27	EPS
2	32	0.0500	1.400	2100.	653.	0.90	0.65	19.	0.04	Heavy mix concrete
Int	124	0.0500	1.400	2100.	650.	0.91	0.65	19.	0.04	Cement screed

Standardised U value = 0.66

Total area of floor_1 is 16.00

Details of opaque construction: ceiling

Layer	Prim	Thick	Conduc-	Density	Specif	IR	Solr	Diffu	R	Descr
-------	------	-------	---------	---------	--------	----	------	-------	---	-------

	db	(m)	tivity	heat	emis	abs	resis	m ² K/W
Ext	211	0.1000	0.040	250.	840.	0.90	0.30	4. 2.50
Glasswool								
Int	150	0.0100	0.030	290.	2000.	0.90	0.60	8. 0.33 Ceiling
(mineral)								
Standardised U value = 0.33								
Total area of ceiling is 16.00								